THE FUNCTIONAL EFFECTS OF CERAMIDE ON THE MONOCYTE CD36 SCAVENGER RECEPTOR AND NADPH OXIDASE

YINGJUN LUAN

Doctor of Philosophy

The University of Aston in Birmingham

November 2005

Aston University

THE FUNCTIONAL EFFECTS OF CERAMIDE ON THE MONOCYTE CD36 SCAVENGER RECEPTOR AND NADPH OXIDASE

Yingjun Luan

Doctor of Philosophy, 2005

Summary

Atherosclerosis is the principal cause of death in the United States, Europe and much of Asia. During the last decade, inflammation has been suggested to play a key role in the development of atherosclerosis. Reactive oxygen species (ROS) released during inflammation additionally oxidize LDL, which is subsequently taken up in an unregulated way through scavenger receptors on macrophages to form foam cells, the hallmark of atherosclerotic lesions.

Previous work has shown that the lipid ceramide, which is found in aggregated LDL and in atherosclerotic plaques, decreases intracellular peroxide most likely through reducing NADPH oxidase activity. Ceramide is an important component of membrane microdomains called lipid rafts which are important for membrane protein function. Endogenous ceramide enhances lipid raft formation and alters theirs composition. NADPH oxidase membrane subunits cytochrome b558 (which includes gp91) strongly associates with lipid rafts. Therefore present study investigated whether short chain ceramides reduce NADPH oxidase in U937 monocytes by disrupting the membrane component of NADPH oxidase. Results showed that C_2 ceramide alters the distribution of raft marker, flotillin and the raft environment. NADPH oxidase membrane component gp91 *phox* and cytosolic component p47 *phox* were identified in rafts. C_2 ceramide reduces both gp91 and p47 *phox* in rafts, which leads to the decrease of peroxide production by NADPH oxidase.

Ceramide is also an important second messenger involved in many different signaling pathways associated with atherogenesis from the activation of sphingomyelinase (SMase). It has been reported that SMase enhances LDL receptor mediated LDL endocytosis. However, no study has been done to investigate the effect of ceramide on scavenger receptors such as CD36 and oxidized LDL (OxLDL) uptake. CD36 is the major receptor for OxLDL. Reduced CD36 expression results in less foam cell formation and less atherosclerotic lesion without disrupting the clearance of OxLDL from plasma.

This thesis shows that ceramides significantly reduce CD36 surface expression on U937 monocytes, macrophages and human primary monocytes. This effect is seen using both synthetic short chain ceramide and SMase catalysed long chain ceramide treatment. To investigate whether the effect of ceramide on CD36 is functional, OxLDL uptake was measured in ceramide treated cells. Ceramide reduces the uptake of OxLDL by both U937 monocytes and PMA-differentiated macrophages. The mechanism of ceramide reduction of CD36 expression was studied by measuring the surface antigen using flow cytometry and fluorescence microscopy, whole cellular CD36 expression and shedding of CD36 by Western blotting of cell lysates and cell culture supernatants and mRNA level of CD36 using RT-PCR. Ceramide reduces shedding of CD36, activates mRNA expression of CD36 and induces intracellular CD36 accumulation probably through retaining the receptor inside cells.

In summary, ceramides modulate several of the processes involved in LDL oxidation and uptake by CD36 receptors on monocytes/macrophages in a way which may protect against atherosclerosis.

Keywords: U937 cells, monocytes, macrophages, ceramide, CD36, CD11b, oxidized LDL, lipid rafts, reactive oxygen species, NADPH oxidase, and atherosclerosis.

ACKNOWLEDGEMENTS

I would like to thank my supervisor Professor Helen R Griffiths for her support. Also thanks Dr Melissa Grant for her general help through out my PhD research. I would also like to thanks Khujesta Choudhury for her help with checking my English.

I must thank Mum and Dad for their support throught my studies especially the parcels of Chinese food. And my dear housemates Huiying, Linda and Yanli for the family like warm they gave to me.

Most important, I would say thanks to my Heavenly Father.

List of Contents

List of Tables and Figures

Chapter 1 Introduction

1.1 What are reactive oxygen species?

Reactive oxygen species (ROS) are a family of oxidant molecules generated by both environmental sources (e.g. ozone, cigarette smoke) and physiological processes (e.g. inflammatory cells). ROS include the superoxide anion ($O_2^{\cdot-}$), hydrogen peroxide (H_2O_2) and hydroxyl radical ($OH^{\cdot}$). Early research into ROS studied them as destructive agents, targeted against invading pathogens and cellular components. However, more recent research indicates that ROS are important as intracellular signaling molecules in many systems (Poli et al. 2004; Touyz, Tabet, and Schiffrin 2003; Loscalzo 2003; Moran, Gutteridge, and Quinlan 2001; Bauer 2000).

In intracellular signaling systems, ROS can cause the oxidation of proteins, activating redox sensitive transcription factors and lipids, therefore acting as important signaling molecules. Among the different ROS, the superoxide anion radical is a charged molecule, going across biological membranes through anion channels (Lynch and Fridovich 1978). This characteristic of superoxide anion limits its movement, therefore limits its potential role for signaling. The hydroxyl radical is extremely reactive, and usually is depleted at the site of production, therefore is unlikely to be able to mediate specific signals. Hydrogen peroxide, as a small and lipophilic molecule which can cross biological membranes, is the most likely ROS to act as a signaling molecule.

1.2 Different sources of ROS

ROS are generated during normal physiological processes by a number of different mechanisms, such as the activity of NADPH oxidase, mitochondrial electron transport chain, xanthine oxidoreductase and endothelial nitric oxide synthase (eNOS).

1.2.1 NADPH oxidase

NADPH oxidase (NOX) is the earliest reported and most well-characterized source of ROS. As early as 1961, Iyer and his group observed that the increased oxygen uptake of activated phagocytic cells was concomitant with the production of NADPH (Iyer and Islam and Quastel 535-542). The increased oxygen consumption was later reported to be used to produce superoxide anions. A protein complex situated in the plasma membrane, which is now known as NADPH oxidase, catalyses this process. NOX was originally found in neutrophils, but is now described in nearly every cell type in a number of different NOX forms (Suh et al. 1999; Cheng et al. 2001) and is very widely studied (Brandes and Kreuzer 2005; Wolin, Ahmad, and Gupte 2005; Krause 2004).

NADPH oxidase includes two major components. One major component, which is situated in the plasma membrane, is referred to as a flavo-cytochrome. This

cytochrome has anα-band absorbance in the visible spectrum with a maximum absorbance wavelength at 558nm, therefore was named as cytochrome b558. The cytochrome b558 is known to be a heterodimer, containing a small α-subunit, named p22 *phox* and a large β- subunit, gp91 *phox*. The name *phox* was adopted because the components were characterized from a phagocytic cell oxidase. The p22 *phox* has a molecular weight of approximately 22KDa. The large subunit gp91 has a molecular weight of 76-92 KDa and is highly glycosylated. There are two haem groups and one FAD group binding to gp91 *phox*. Other major components are found in the cytosol when the enzyme is non-activated, and binds to the membrane components when activated. These cytosolic components include p47 *phox*, p67 *phox*, p40 *phox* and $p21^{Rac}$ (Griendling, Sorescu, and Ushio-Fukai 2000) (Fig1.1).

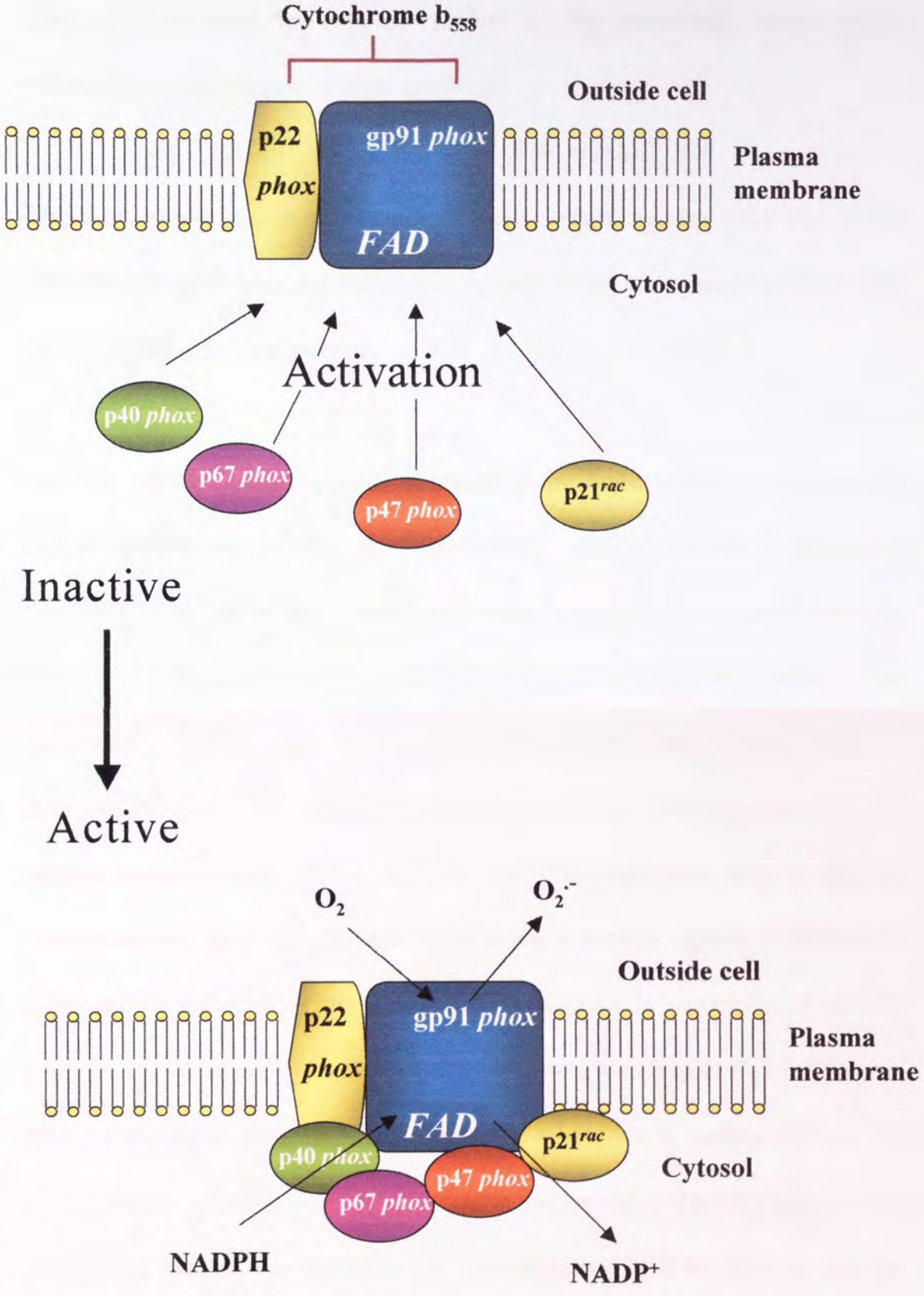

Fig1.1 The mechanism of the NADPH oxidase complex activation by translocation of several cytosolic components to the plasma membrane components.

The ROS produced by NADPH oxidase is the superoxide anion, where intracellular NADPH provides the electrons:

$$2\ O_2 + NADPH \xrightarrow{\text{NADPH oxidase}} 2\ O_2^{\cdot -} + NADP^+ + H^+$$

The electron transfer proceeds from NADPH to oxygen through FAD, then to the haem group of gp91 *phox* and finally onto oxygen. On the other side of the membrane the superoxide anions are released.

NADPH oxidase activation can be triggered by both receptor mediated and receptor-independent mechanisms (Bokoch 1995). NADPH oxidase in phagocytes can be activated by a large number of soluble and particulate factors such as opsonized bacteria, opsonized zymosan, latex particles, complement fragment C5a, formylated peptides such as formyl-methionyl-leucyl-phenylalanine (FMLP), leukotriene B4 (LTB4), platelet-activating factor (PAF), diacylglycerol (DAG), calcium ionophores (ionomycin, A23187), and PKC activators such as phorbol myristate acetate (PMA). LPS from Gram-negative bacteria directly induces ROS production in monocytes (Thiele et al. 2004), whereas in neutrophils it induces priming of NADPH oxidase (DeLeo et al. 1998) through binding to TLR4. There are some other agents, which stimulate superoxide production in neutrophils, such as angiotensin II, the main hormone of the renin-angiotensin system (El Bekay et al. 2003). High glucose also stimulates the production of ROS by NADPH oxidase (Inoguchi et al. 2003).

1.2.2 Mitochondrial electron transport chain

There are some other sources of ROS; mitochondria, for example, can transfer electrons to oxygen, forming superoxide anions. Mitochondria utilize molecular oxygen as a terminal electron acceptor in the metabolism of organic carbon and provide energy. In this respiratory process, the majority of O_2 is reduced by mitochondria, generating ATP, H_2O and carbon dioxide without free radical production. However, there is a small amount of O_2, less than 1% of the total used during electron transport from NADPH to oxygen, which is oxidized to form $O_2^{\cdot-}$ (Beyer 1992; Boveris 1977; Du, Mouithys-Mickalad, and Sluse 1998). The mitochondrial electron transport chain includes four electron-transporting complexes (I-IV) and one H^+ translocating ATP synthetic complex (V) (Fig 2). Two of these complexes are reported to produce superoxide: complex I (the NADH-ubiquinone oxidoreductase) and complex III (the ubiquinol-cytochrome c oxidoreductase (Beyer 1992; Boveris 1977; Takeshige and Minakami 1979). The exact mechanism of superoxide generation by complex I is not fully understood, however, semiquinones generated by complex I were identified as a possible donor for transforming O_2 to $O_2^{\cdot-}$ (Boveris 1977; Du, Mouithys-Mickalad, and Sluse 1998). There are two distinct species of semiquinones on complex I, SQ_{Nf} and SQ_{Ns} (Ohnishi 1998). Superoxide is throught to be produced on one or both sites of semiquinones. On complex III, there are also two species where semiquinones are generated; the cytochrome b_L and

cytochrome b_H (Trumpower 1990). Experiments using inhibitors to these two sites demonstrate cytochrome b_H as a major superoxide producing site (Li, Zhu, and Trush 1999; Li et al. 1995). Superoxide generated by mitochondria can be catalysed to form H_2O_2 by MnSOD in the mitochondrial matrix, which somehow explains why under physiological condition, the production of superoxide by mitochondria is comparatively low (Fig 1.2).

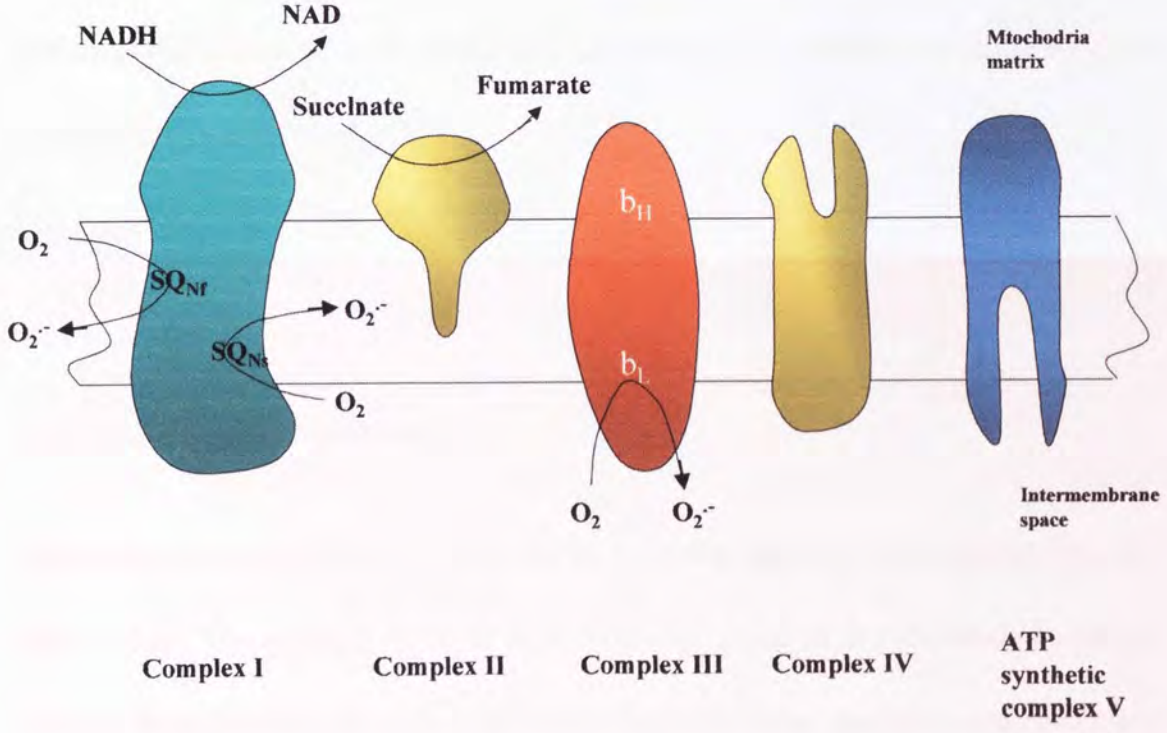

Fig 1.2 The schematic representation of mitochondria electron transport chain complexes.

Complex I inhibitors, rotenone and piericidin increase superoxide and hydrogen peroxide production from mitochondria at complex I, possibly by blocking a site

where semiquinone donates an electron to an acceptor (Pitkanen et al. 1996; Pitkanen and Robinson 1996). Ceramide also induces the production of ROS from mitochondria by targeting the electron transport chain, where the ubiquinone pool is an important site for production of (ROS) (Andrieu-Abadie et al. 2001). Induction of ROS by ceramide results in discrete outcomes, namely growth arrest or apoptosis according to the differences in the magnitude and kinetics of this alteration in cellular redox state (Phillips, Allen, and Griffiths 2002). In an experimental model of diabetes, oxidative damage is eliminated by treatment with rotenone, the inhibitor of mitochondrial complex I, or thenoyltrifluoroacetone, an inhibitor of mitochondrial complex II (Ye et al. 2004).

1.2.3 Reactive nitrogen species

The reactive nitrogen species (RNS) family is another group of biologically relevant free radicals. The primary RNS, NO, was first identified as the endothelial derived relaxing factor (EDRF) (Ignarro et al. 1988; Palmer, Ferrige, and Moncada 1987) and its role in signaling pathways resulting in physiological effects was later established (Gruetter et al. 1979). Nitric oxide is enzymatically produced by nitric oxide synthases (NOS). Several types of NOS have been identified either as inducible or constitutive forms (as reviewed in (Tsutsui 2004).

$$3\ NADPH + 2\ Arginine + 3\ O_2 + H^+ \xrightarrow{\text{Nitric oxide synthase}} 3\ NADP^+ + 2\ Citrulline + 2\ {}^{\cdot}NO + 2\ OH^-$$

The $^{\cdot}NO$ molecule itself is of low chemical reactivity with organic molecules. However, $^{\cdot}NO$ can react with $O_2^{\cdot-}$ forming peroxynitrite, $ONOO^-$, in an extremely rapid reaction ($6.7 \times 10^9\ mol^{-1}\ s^{-1}$) which is determined by the relative amount of $^{\cdot}NO$ and $O_2^{\cdot-}$, their reductive rate by oxyHb and SOD respectively, and the diffusion rate of $^{\cdot}NO$. Therefore, this reaction can only occur in an localized area where $O_2^{\cdot-}$ is released (Wink and Mitchell 1998).

$$^{\cdot}NO + O_2^{\cdot-} \longrightarrow ONOO^-$$

Peroxynitrite can modify the cysteine residues of proteins or glutathione, forming S-nitrosothiols. Subsequently, this allows release of bioavailable $^{\cdot}NO$ that can be exchanged between thiols. Peroxynitrite can also interact with the tyrosine residues, forming 3-nitrotyrosine, which is possibly an irreversible process associated with injury (Kuo et al. 1999). The acid form of peroxynitrite (ONOOH) is very unstable and reactive, and its production is thought to contribute to $^{\cdot}NO$-induced toxicity.

1.2.4 Endothelial NO synthase (eNOS)

Endothelial NO synthase, as named, exists in endothelial cells. Like the other two isoforms of NO synthase family, eNOS has two functional domains: the N-terminal

oxygenase that serve as binding site for haem, BH_4 and L-arginine and the C-terminal reductase that FAD, FMN and NADPH bind to. A calmodulin-binding site links the N-terminal and C-terminal domains together. Calmodulin binds to eNOS in a calcium dependent manner. This binding increases the rate of electron transfer from NADPH to the reductase domain flavins and from the reductase domain to the haem center for the oxidation of the substrate, L-arginine (Palmer, Ashton, and Moncada 1988; Hemmens and Mayer 1998). eNOS can synthesize NO using the electrons received from NADPH, oxygen and L-arginine. Tetrahydrobiopterin (BH_4) is the requisite cofactor for this reaction. If there is not enough BH_4, NOS is inactive for NO generation and instead eNOS generates $O_2^{\cdot-}$ (Wever et al. 1997; Raman et al. 1998; Vasquez-Vivar et al. 1998).

1.2.5 Xanthine oxidoreductase (XOR)

Another source of ROS is from the enzyme xanthine oxidoreductase (XOR). The XOR can either serve as xanthine dehydrogenase that reduces NAD^+ or can serve as a xanthine oxidase that oxidize hypoxanthine to xanthine, and then to uric acid, producing $O_2^{\cdot-}$ and hydrogen peroxide. In cell culture experiments, hypoxanthine and xanthine oxidoreductase are used to promote hydrogen peroxide generation. In endothelial cells, interferon-γ increases XOR expression (Dupont et al. 1992). In the early stages of atherosclerosis in rabbit, the production of $O_2^{\cdot-}$ from the endothelium increases (Ohara, Peterson, and Harrison 1993; White et al. 1996). This phenomenon

is also observed in the aorta and microvessels of spontaneously hypertensive rats (Nakazono et al. 1991; Suzuki et al. 1995). In human cultured endothelial cells, the XOR is identified on the outer surface (Rouquette et al. 1998) and the enzyme displacement from the heparin binding site by heparin infusion promotes the endothelial dependent vasorelaxation (Nakazono et al. 1991; White et al. 1996; Houston et al. 1999). However, the role of XOR in $O_2^{\cdot-}$ production and NO bioavailability in human is still not clear and needs to be elucidated (Guzik et al. 2002).

1.3 Antioxidant defence and redox signaling

The effects of ROS on signaling pathways are usually defined as resulting from oxidative stress, which only happens when there is an imbalance between oxidant exposure and antioxidant protection. There are a number of antioxidant molecules including the enzymes that reduce ROS, such as SOD, catalase and glutathione peroxidase, and the glutathione (GSH/GSSG) and thioredoxin (Trx) systems. In fact, the glutathione (GSH/GSSG) and thioredoxin (Trx) systems play a key role on controlling the redox status of the cells. On GSH and Trx, there are cysteine residues which can be oxidized to form sulfinic acid ($-SO_2H$) or sulfonic acid ($-SO_3H$). The sulfinic and sulfonic acids are irreversible oxidized forms associated with oxidative injury. On the other hand, these cysteine residues can undergo reversible oxidation reaction forming disulfide bonds and protein sulfenic acid moieties, which are

catalysed by several antioxidant enzymes including Trx and glutathione reductase and peroxidase (reactions listed below)(Akerboom and Sies 1981; Bradshaw, Kanarek, and Hill 1967; Bump and Reed 1977; DeLucia et al. 1975; Gilbert 1982; Suzuki et al. 1995). Peroxiredoxins are another family of enzymes that can reduce ROS using thiols (Rhee et al. 1999).

$$H_2O_2 + Trx(SH)_2 \xrightarrow{\text{Thioredoxin peroxidase}} H_2O + TrxS_2$$

$$TrxS_2 + NADPH + H^+ \xrightarrow{\text{Thioredoxin reductase}} Trx(SH)_2 + NADP^+$$

$$2GSH + H_2O_2 \xrightarrow{\text{Glutathione peroxidase}} GSSG + 2H_2O$$

$$GSSG + NADPH + H^+ \xrightarrow{\text{Glutathione reductase}} 2GSH + NADP^+$$

$$2GSH + ONOO^- \xrightarrow{\text{Glutathione peroxidase}} GSSG + ONO^-$$

These reversible thiol-disulfide exchanges make thiols and the associated antioxidant enzymes the mediators of redox signaling (Stamler and Hausladen 1998; Claiborne et al. 1999).

1.4 The effects of ROS on proteins.

The thiol group is a well-described aminoacid target in proteins for ROS. Indeed, H_2O_2 can attack protein thiol moieties resulting in oxidation of the thiol group as described above. This may be the mechanism through which ROS affect the signaling pathways, but not all of the effects are specific to a direct target on protein by ROS.

However, various works indicate that ROS play an important role in regulating a number of signaling pathways. For example, ROS can lead to the activation of transcription factors, such as NF-KB and AP-1, and various cell signaling pathway components including: Mitogen-Activated Protein Kinases (MAP Kinases), extracellular signal regulated kinase (ERK), p38 kinase, PI-3K/Akt and PKC (as reviewed by (Rahman, Marwick, and Kirkham 2004).

NF-κB, includes two subunits P50 and P65, and is reported to regulate the activation of immune and inflammatory genes (Kempe et al. 2005; Wissel et al. 2005). Inactive NF-κB, which localizes in the cytoplasm as a non-DNA binding form, associates with an inhibitory protein, inhibitory κB (IκB) in unstimulated cells. IκB prevents NF-κB from entering the nucleus by masking the nuclear translocation signal. In the NF-κB activation process, it is first phosphorylated on two serine residues. This phosphorylation leads to the targeting of IκB by E3 ubiquitin-ligases, therefore results in ubiquitination of lκB and subsequently degradation by the 26S proteasome. The active NF-κB can then enter the nucleus, binding to the cognate DNA elements (Rahman and MacNee 1998; Rahman and MacNee 2000). A model is proposed, mainly based on studies with antioxidants, which raised the idea that NF-κB is redox-sensitive and its activation is due to the production of ROS by all agonists (Rahman and MacNee 1998; Rahman and MacNee 2000). During oxidative stress, there are more lipid peroxidation products and less glutathione, which leads to rapid phosphorylation and ubiquitination, and subsequently degradation of IκB (Bowie,

Moynagh, and O'Neill 1997; Ginn-Pease and Whisler 1996). Increasing the reducing potential within the cell results in inhibition of IκB phosphorylation, and subsequently decreases NF-κB transcriptional activity in endothelial cells (Cho et al. 1998). Therefore, ROS may activate NF-κB by up-regulating the degradation of NF-κB inhibitory protein IκB. However, this effect appears to be cell type and stimuli specific since some ROS producers such as TNF-α and IL-1β activate NF-κB, whereas diamide, which oxidizes GSH to GSSG and H_2O_2 fails to activate NF-κB in certain cell types (Brennan and O'Neill 1995). The exact mechanism that activates the cascade for ROS-derived activation of NF-κB, is likely to depend on tyrosine phosphorylation of IκB (Janssen-Heininger, Macara, and Mossman 1999) following activation of IκB kinase by H_2O_2 (Kamata et al. 2002).

Activator protein-1 (AP-1) is a transcription factor complex formed by homo- or heterodimerization of members of the Jun and Fos families of proteins. AP-1 is critical for the regulation of stress response genes. UV-irradiation and H_2O_2 initiate the activation of AP-1 through mechanisms that are still largely unknown, although a number of studies have shown that the AP-1 complex is regulated by redox mechanisms. In the basic region of DNA-binding domains of c-Fos and c-Jun, there is a single conserved cysteine residue that needs to be reduced for DNA binding activity (Abate et al. 1990). The direct oxidation of the cysteine residue is not reported, but recent in vitro data indicate that reversible S-glutathiolation of the conserved cysteine may be involved (Klatt et al. 1999). Others mechanisms through which ROS may

regulate AP-1 involve Trx and the nuclear protein Ref-1, which both increase AP-1 binding activity (Schenk et al. 1994; Xanthoudakis and Curran 1992). Direct association between Trx and Ref-1 has been reported (Hirota et al. 1997). In addition, Trx and Ref-1 are both regulated by redox cycling and could be the actual target of ROS/RNS. In particular, there is a suitable target for H_2O_2 on Trx, which leads to a thiolate form of cysteine. The effects of ROS on AP-1 may also alter the capacity for phosphorylation, the activition step for AP-1. Increased binding and transcriptional activation are both signaled by phosphorylation of Fos and Jun (Okazaki and Sagata 1995) by members of the mitogen-activated protein kinases (MAPK) (Cobb 1999). Thus, ROS-controlled activation of AP-1 may occur both in the cytosol and in the nucleus.

1.5 The effect of ROS on gene expression

Intracellular oxidative signals modulate the expression of a selective set of vascular inflammatory genes, which is suggested to be a possible molecular mechanism linking high peroxide level with the early pathogenesis of atherosclerosis (as reviewed in (Kunsch and Medford 1999). H_2O_2-induced monocyte chemoattractant protein-1 (MCP-1) gene expression in endothelial cells is mediated by an AP-1 element in the MCP-1 promoter, which is prevented by *N*-acetylcysteine (NAC) and catalase (Wung et al. 1997). Diverse proinflammatory stimuli activate the expression of vascular inflammatory gene products such as vascular cell adhesion molecule-1 (VCAM-1)

and MCP-1 through a redox-sensitive mechanism involving the redox-regulated transcription factor NF-kB (Marui et al. 1993; Weber et al. 1994; Satriano et al. 1993). Many of the genes that are regulated by NF-kB encode for proteins such as TNFα, IL-1, macrophage colony stimulating factor (CSF), granulocyte CSF, granulocyte-macrophage CSF, MCP-1, tissue factor, VCAM-1, ICAM-1, and E-selectin, which regulate critical processes in atherogenesis. Thus, ROS may act as specific regulators in the signal transduction network to relay environmental and physical signals generated at the cell membrane to nuclear regulatory signals resulting in modulation of inflammatory gene expression.

1.6 Oxidation of lipids

In *vivo*, lipid is enriched in lipid-carrying lipoproteins and cell membranes, therefore lipid peroxidation mainly occurs in these two sites, for example, in polyunsaturated fatty acids within triglycerides in LDL and phospholipids in cell membranes. Lipid peroxidation is observed in nearly all human diseases and appears to be important to atherosclerosis and in worsening the initial tissue injury caused by ischemic or traumatic brain damage.

In the process of lipid peroxidation, 5 steps are essential as shown in Fig 1.3. First, radicals abstract a hydrogen atom from a methylene group next to a double bond in polyunsaturated fatty acids. This radical is transferred to carbon, forming a

carbon-centered radical (2). The double bond is rearranged to stabilize the carbon radical, forming a conjugated diene (3). Owing to the presence of oxygen, the carbon radical can readily react with oxygen, forming the peroxyl radical (4). The peroxyl radical can then react with another phospholipid or triglyceride-linked fatty acid forming a hydroperoxy group (5) and a new carbon-centered radical (2). The new-formed carbon-centered radical can begin a new cycle from reactions 2-5. Whereas the lipid hydroperoxide can further form cyclic peroxide, cyclic endoperoxide and aldehydes, the final peroxidation products.

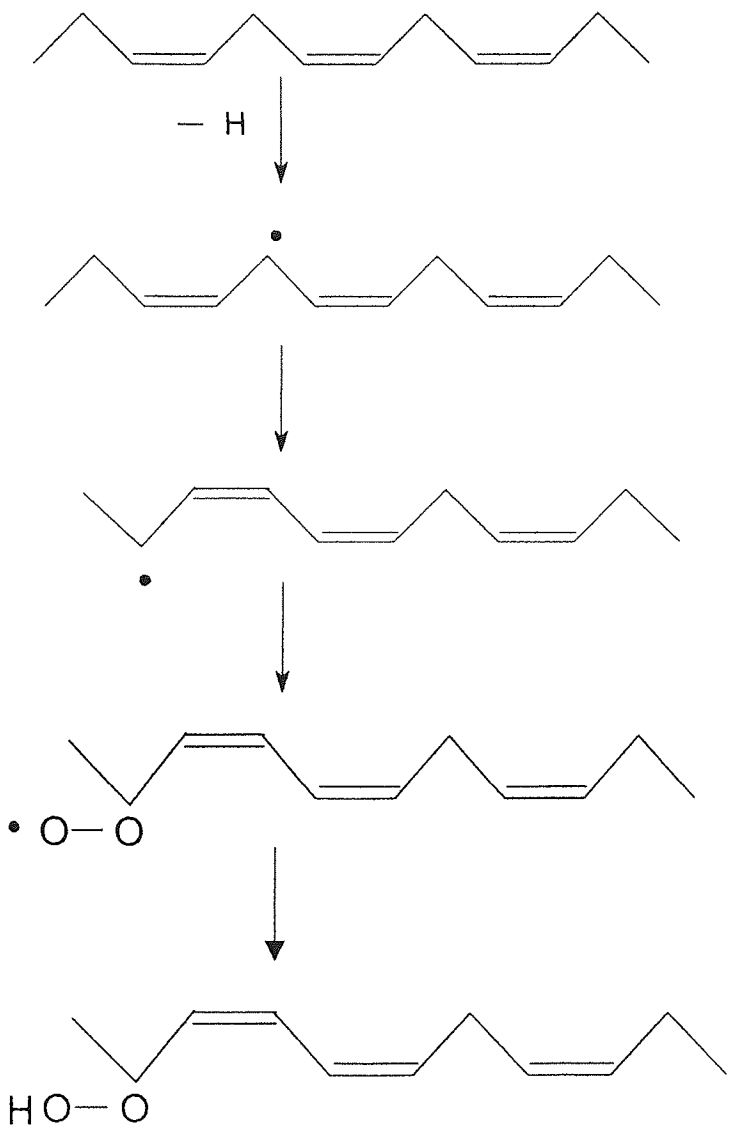

Fig 1.3 Oxidation of lipid

Biomarkers, Helen R.Griffiths, Lennart Moller, Grzegorz Bartosz, etc. 2002. Molecular Aspects of Medicine, 23: 101-108.

These peroxidation products include aldehydes, such as malondialdehyde (MDA) and 4-hydroxynonenal (4-HNE), pentane and ethane, 2,3-*trans*-conjugated dienes, isoprostanes. In particular, MDA and 4-HNE play several important roles in biological environments. For example, these dialdehydes can cross-link with DNA and proteins,

subsequently alter the function or activity of these molecules. Moreover, MDA reacts with amino and thiol groups. The damage caused by aldehydes may extend to more distant sites than free radical generation because of their diffusion ability. MDA and HNE are well-characterized oxidation products of polyunsaturated fatty acids on LDL. Adducts of these compounds have been detected by immunological means in atherosclerotic plaque and have been suggested to serve as biomarkers of lipid modification (Requena et al. 1996).

1.6.1 Lipoxygenase

Lipoxygenases (LOXs) are non-heme iron-containing enzymes that exist in a number of cell types, including reticulocytes, monocytes-macrophages, and certain endothelial cells. LOXs catalyze arachidonate or linoleate oxidation to form linoleate or arachidonate hydroperoxides. LOXs contain a non-heme iron that cycles between Fe^{2+} and Fe^{3+} during turnover. The resting enzyme predominantly exists as Fe^{2+}, requiring oxidation before dioxygenation can occur. In mammalian cells, several LOX isoforms have been discovered, named by their position of oxygen insertion into arachidonate. LOXs are thought to play a key role in cardiovascular disease. They are widely expressed in vascular tissue, with sources including platelets (12-LOX), monocyte/macrophages (15-LOX, 12/15-LOX), neutrophils (5-LOX, 12/15-LOX) and smooth muscle cells (12/15-LOX). LOXs catalyze the oxidation of unsaturated

fatty acids to hydroperoxides and other bioactive metabolites utilizing a non-heme iron active site (Kuhn and Thiele 1999). 12/15-LOX, causes oxidation primarily at C12, but also at C15 forming mainly 12(*S*)- but also some 15(*S*) hydroperoxyeicosatetraenoic acids (HPETE), respectively (Brash 1999; Kuhn and Thiele 1999), whereas 15-LOX forms mainly 15(*S*)HPETE. These hydroperoxides are unstable and are rapidly reduced to 12(*S*)- and 15(*S*) HETEs by cytosolic glutathione peroxidases. Oxidation of arachidonate or linoleate by the ferric enzyme is shown (Fig 1.4).

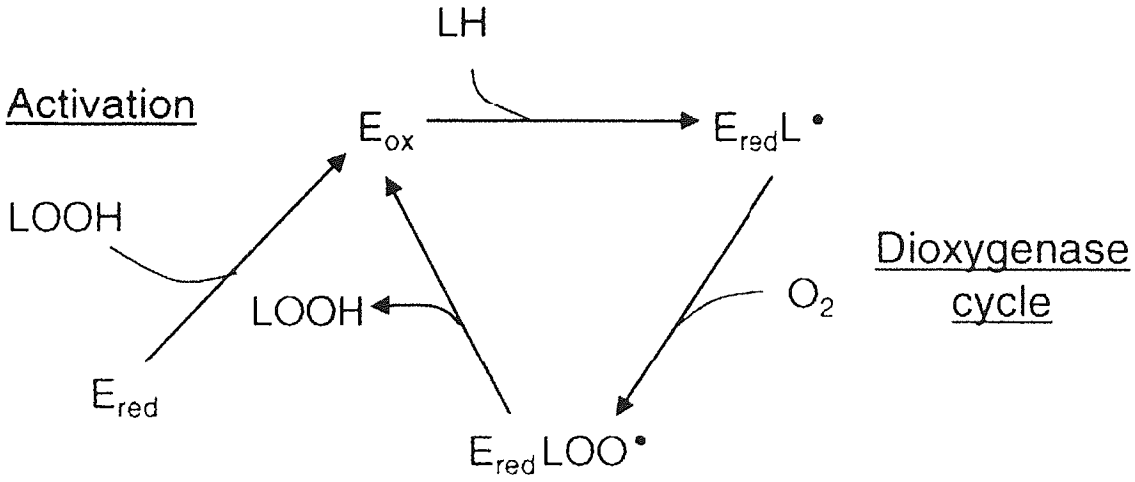

Fig 1.4 Catalytic cycle of lipoxygenases.

Eox: oxidized iron, Ered: reduced iron, LH: arachidonate, L˙: lipid alkyl radical, LOO˙: lipid peroxyl radical, LOOH: lipid hydroperoxide. Activation of the enzyme requires trace hydroperoxide (Rubbo and O'Donnell 2005).

Among these different isoforms, most LOXs, including 5-LOX (leukocytes) and 12-LOX (platelet-type), cause oxidation of free arachidonate substrate, however, the

reticulocyte 15-LOX (human, rabbit), and leukocyte 12/15-LOX (pig, rat, mouse) can oxidize complex lipids including membrane phospholipids and LDL, and also linoleate (Kuhn and Thiele 1999). Several groups propose that LOX is involved in atherosclerosis following observations of specific LOX products in early human and rabbit lesions, the presence of LOX protein and mRNA expression, and that LOX inhibition prevents diet-induced atherosclerosis in rabbits (Belkner, Stender, and Kuhn 1998; Bocan et al. 1998; Folcik et al. 1995; Hiltunen et al. 1995; Kuhn et al. 1994; Sendobry et al. 1997; Yla-Herttuala et al. 1990; Yla-Herttuala et al. 1991; Kuhn et al. 1997). Following from this work, studies were carried out to show that LOXs catalyze the oxidation of LDL, forming a rapidly endocytosed form of LDL, similar to that found in atherosclerotic lesions, This process requires LDL receptor related protein, and can be enhanced by angiotensin II, lipoprotein lipase and secretory phospholipaseA_2 (Scheidegger, Butler, and Witztum 1997; Sigari et al. 1997; Belkner, Stender, and Kuhn 1998; Neuzil et al. 1998; Xu et al. 2003; Zhu et al. 2003). There are a number of ways in which LOX could participate in LDL oxidation. LOX could make LDL more susceptible to oxidation by oxidizing cellular fatty acids, cholesteryl ester, or phospholipid substrates, which can laterally transfer to LDL (Parthasarathy 1987). When in direct contact with LDL, LOX use phospholipid or cholesteryl ester as substrate (Belkner, Stender, and Kuhn 1998), leading to lipid peroxidation. Moreover, LOX products also participate in signal transduction pathways regulating other monocyte-macrophage functions involved in oxidation. In monocyte-macrophage cells, 5-LOX was identified as a participant in LDL oxidation

(Folcik and Cathcart 1993; Jessup et al. 1991). In addition, incubation of LDL with 15-LOX and phospholipase A_2 leads to LDL oxidation in a cell-free system (Sparrow, Parthasarathy, and Steinberg 1988) (Cathcart, McNally, and Chisolm 1991).

1.6.2 Cyclooxygenases (COX)

Cyclooxygenase (COX) is an enzyme that catalyzes the formation of important biological mediators, prostanoids (including prostaglandins, prostacyclin and thromboxane). COX is part of the enzyme complex that catalyzes the production of prostaglandin H_2 (PGH2), the precursor of all prostanoids, from arachidonic acid. The complex consists of a COX isoenzyme and a peroxidase. There are three COX isoenzymes—COX-1, COX-2 and COX-3. COX-1 is the constitutive form, present under normal conditions in most tissues and is responsible for housekeeping functions. COX-2 is the inducible form, which is not normally present under basal conditions or is present in very low concentration. However, abundant COX-2 can be rapidly generated in response to a variety of stimuli, including proinflammatory cytokines such as interleukin-1β and tumor necrosis factor-α, growth factors, and tumor promoters, to result in prostaglandin synthesis associated with inflammation and carcinogenesis (FitzGerald 2003). In macrophages, COX-2 expression is regulated through mitogen-activated protein kinase (MAPK) and nuclear factor- κB (NF-κB) signaling pathways (Hwang et al. 1997).

COX-2 is responsible for arachidonic acid (AA)-dependent production of carbon-centered radicals by heme-reconstituted recombinant COX-2. No oxygen radicals or thiyl radicals have been produced by COX2. COX-2 also catalyzes AA-dependent one-electron co-oxidation of ascorbate to ascorbate radicals. These results have been confirmed by two different approaches of COX-2 expression in cells, PCXII cells which express isopropyl-1-thio-beta-D-galactopyranoside inducible COX-2, and PC12 cells transfected with COX-2. AA causes a significant and selective oxidation of one of the major phospholipids; COX-2 does not cause direct oxidation of phosphatidylserine (PS), but induces PS oxidation in the presence of AA. COX-2 inhibitors, niflumic acid, nimesulide, or NS-398 inhibit the radical generation and PS oxidation (Jiang et al. 2004). Post-ischemia treatment with the COX-2 inhibitor, rofecoxib significantly reduces oxidative damage (glutathione depletion and lipid peroxidation), indicating that the late increase in COX-2 activity is involved in the delayed occurrence of oxidative damage in the hippocampus after global ischemia. Selective inhibition of COX-2 or COX-1 significantly increases the number of healthy neurons, suggesting that both COX isoforms are involved in the progression of neuronal damage following global cerebral ischemia (Candelario-Jalil et al. 2003).

1.6.3 Myeloperoxidase (MPO)

Myeloperoxidase is a haem protein secreted from activated neutrophils, monocytes

and some populations of macrophages. Recent work indicates that MPO can generate several reactive species, including hypochlorous acid (HOCl), chloramines, tyrosyl radicals and nitrogen dioxide and is thought to be a major enzymatic catalyst for initiation of lipid peroxidation at sites of inflammation (Zhang et al. 2002). The production of F(2)-isoprostanes, a marker of oxidant stress in vivo, is reduced by 85% in MPO(-/-) mice. Similarly, formation of some important lipid peroxidation products are significantly reduced (by at least 50%) in MPO(-/-) mice during inflammation. Therefore, MPO may play an important role in atherosclerosis (see section ROS and atherosclerosis).

1.7 ROS and atherosclerosis

Research during the last decade has shown that inflammation plays a key role in the development of atherosclerosis (reviewed by (Hansson 2005) and is associated with release of ROS. This increased ROS level additionally results in oxidative modification of LDL, a key player in the process of macrophage foam cell formation. The increase in ROS production reported in atherosclerotic lesions, is associated with the activation of ROS generating enzymes, NADPH oxidase, endothelial NOS (eNOS) and myeloperoxidase (MPO). A number of stimuli initiate ROS generation by phagocytes including: OxLDL, tumor necrosis factor alpha (TNFα) and angiotensin II (Dimmeler and Zeiher 2000).

eNOS generates $O_2^{\cdot-}$ in environments lacking the NO synthase co-factor BH_4 (Wever et al. 1997; Raman et al. 1998; Vasquez-Vivar et al. 1998) and has been proposed to be one of the ROS generation sources in atherosclerosis. Experiments using apolipoprotein E knockout and eNOS overexpressing mice, have demonstrated that eNOS overexpression accelerates the formation of the atherosclerotic lesion (Ozaki et al. 2002). In this mouse model, reduced production of NO and increased generation of $O_2^{\cdot-}$ in the endothelium were observed, which is associated with reduction in vascular BH_4 content. It was therefore suggested that oxidative stress depletes BH_4, resulting in more generation of $O_2^{\cdot-}$ by NOS (Yokoyama 2004). This is supported by Laursen's group who demonstrated that $OONO^-$ uncouples the NOS enzyme through oxidizing intracellular BH_4, more interestingly inhibiting BH_4 binding to eNOS.

NADPH oxidase, as a major source of ROS (Griendling, Sorescu, and Ushio-Fukai 2000; Irani 2000), has an important role in atherosclerosis. p22 *phox*, one of the membrane NADPH components (see fig1) is highly expressed in all cell types of atherosclerotic coronary arteries, whereas gp91 *phox* is most abundant in macrophages (Azumi et al. 1999; Sorescu et al. 2002; Guzik et al. 2000; Rueckschloss et al. 2001). These observations suggest that up-regulated NADPH oxidase components may result in enhanced ROS production.

Lipoxygenase (LOX) plays an important role in atherosclerosis by causing the oxidation of LDL (see section Lipid oxidation). In experiments using 12/15-LOX

knockout mice backcrossed with Apo E or LDL receptor-deficient strains, the lack of 12/15-LOX decreased lipid peroxidation and plaque formation (Cyrus et al. 1999; George et al. 2001). Moreover, the extent of lipid oxidation in vivo in LOX−/−Apo E −/− compared with LOX+/+Apo E−/− mice is significantly reduced, as measured by plasma isoprostane concentrations (Cyrus et al. 2001). Similarly, in Apo E−/− mice, atherogenesis is promoted by overexpression of 15-LOX in vascular endothelium, although unexpectedly, selective macrophage overexpression of 15-LOX in rabbits is protective (Shen et al. 1996; Harats et al. 2000).

ROS play multiple roles in the development of atherosclerosis. First of all, ROS can reduce bioavailable NO by reacting with NO, forming $ONOO^-$. Secondly, ROS regulates cells growth and death in a complex way; in SMC, ROS produced in response of platelet-derived growth factor (PDGF) or Angiotensin II (Ang II), induce proliferation and survival (Sundaresan et al. 1995; Ushio-Fukai et al. 1998; Zafari et al. 1998). However, ROS generated from overexpression of the tumor suppressor gene p53 leads to growth inhibition, and/or apoptosis of SMCs (Johnson et al. 1996). Compared with SMC, ROS mainly induces apoptotic death of ECs in response to stimuli from oxidized LDL, lipoprotein (a), high glucose and insulin, and Ang II (Dimmeler et al. 1997; Li et al. 1999).

Moreover, ROS or oxidized cellular lipids initiate the oxidation of LDL. In the early stage of atherosclerosis, there is little monocyte or macrophage recruitment under the

endothelium to produce high concentrations of ROS, therefore, LDL is only minimally modified (MM). This MM-LDL, which is one of the key players in atherosclerosis (Ross 1986), stimulates endothelial cells to secrete monocyte chemoattractant (Berliner et al. 1986). In particular, monocyte chemotactic protein-1 (MCP-1) and interleukin-8 are induced in human endothelial cells and smooth muscle cells (Cushing et al. 1990). This effect can be mimicked by pro-inflammatory cytokines, such as IL-1 and TNF (Sica et al. 1990a; Sica et al. 1990b; Wang et al. 1991; Strieter et al. 1989; Valente et al. 1988). Engagement of chemokines with reciprocal receptors on monocytes subsequently results in expression of integrins, such as CD11b, on monocytes (Baggiolini, Dewald, and Moser 1994) and subsequently causes monocyte adhesion and transendothelial migration (Navab et al. 1991). Monocytes under the endothelium then differentiate to macrophages, both monocytes and macrophages take up OxLDL through scavenger receptors, forming foam cells. The internalization of OxLDL stimulates macrophages to release more ROS and chemokines (Wang et al. 1996) (Fig 1.5).

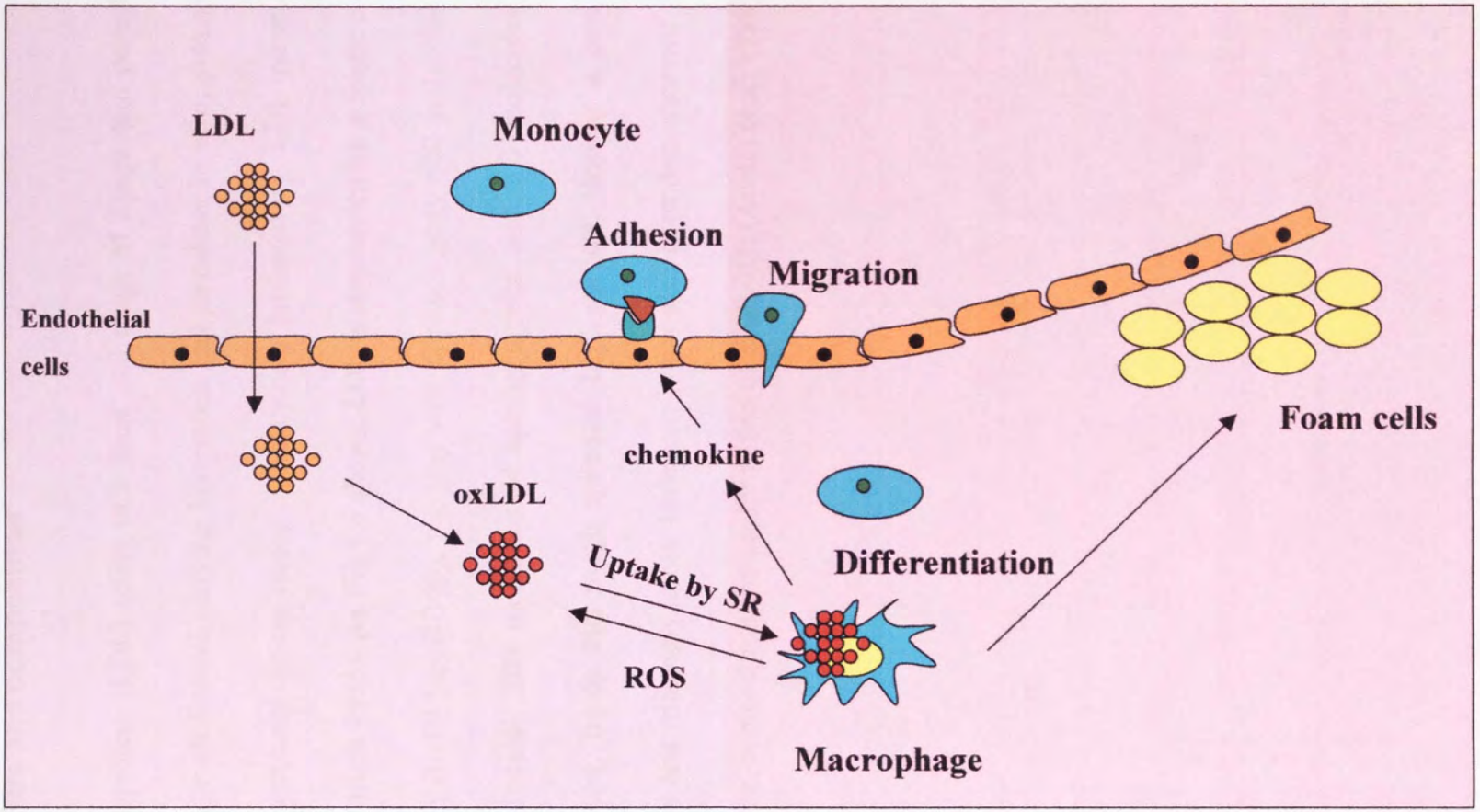

Fig 1.5 Early events in atherosclerosis

1.8 LDL structure and composition

Low-density lipoprotein (LDL) refers to a class and range of lipoprotein particles, which is the major cholesterol carrying lipoprotein and circulates in *vivo*, providing cholesterol to peripheral tissue through endocytosis mediated by LDL receptors (Brown and Goldstein 1986). As Fig 1.6 shows, LDL is surrounded by a single copy of apolipoprotein B-100 (apoB-100), together with approximately 400 molecules of unesterified cholesterol, 200 molecules of sphingomyelin and 500 molecules of phosphatidylcholine. Inside this rough spherical LDL particle, there is a core of cholesteryl esters and triacylglycerols. However, it has also been demonstrated that LDL differs in size, composition and conformation of apoB-100 (Austin et al. 1988).

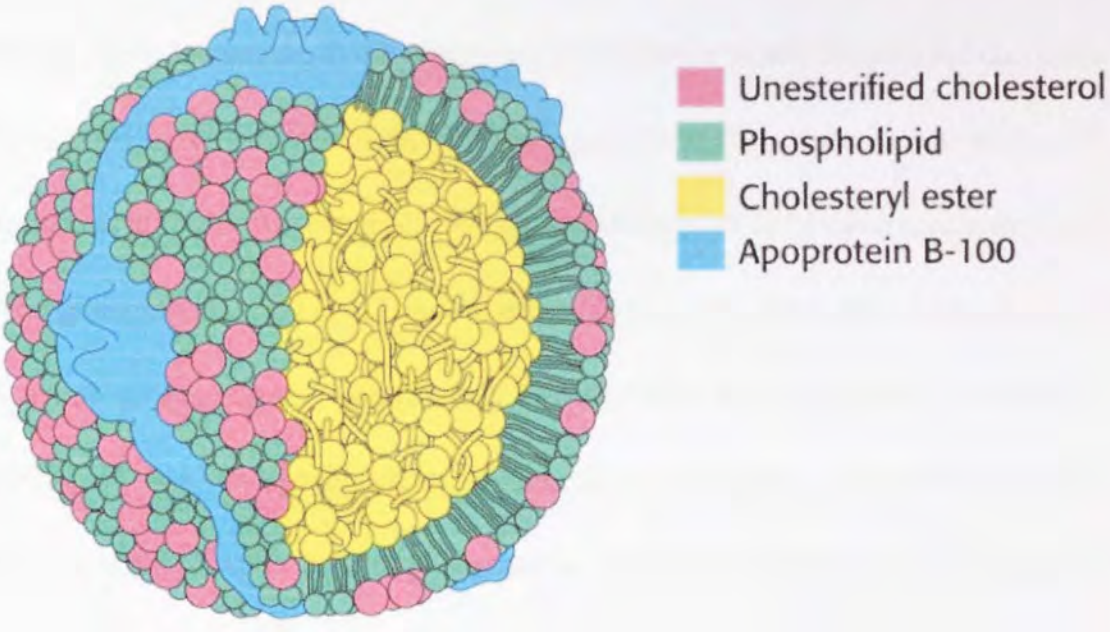

http://oregonstate.edu/instruction/bb451/winter2005/stryer/ch26/Slide41.jpg

Fig 1.6 The structure of LDL.

LDL particle composition has been suggested to be associated with atherogenicity (Lada and Rudel 2004). Moreover, the sphingolipids (SLs) on the spherical LDL surface play important roles in atherosclerosis (as reviewed in (Kinnunen and Holopainen 2002; Levade et al. 2001). Sphingolipids refer to a family of molecules, which are products of the sphingolipid metabolic pathway. Originally, de novo biosynthesis of ceramide occurs in the endoplasmic reticulum (ER), which includes four steps: 1) serine + Palmitoyl-CoA react to form 3-Ketosphinganine catalysed by

serine palmitoyl-transferase; 2) 3-Ketosphinganine is reduced to dihydrosphingosine (sphinganine); 3) sphinganine is subsequently acylated with an unbranched acyl chain, forming dihydroceramide; 4) dihydroceramide desaturase readly induces the C_{4-5} trans double bond on dihydroceramide, yielding ceramide at the cytosolic face of the ER (Mandon et al. 1992; Michel et al. 1997). Ceramide serves as basal structure for most of the sphingolipids. As Fig 1.7 shows, ceramide loses the fatty acid carbon chain on the amino group, forming sphingosine. N-deacylation of sphingosine followed by addition of one phosphate yields sphingosine-1-phosphate. Ceramide can also associate with phosphocholine, phosphate or carbohydrates on its the 1-hydroxyl position, forming sphingomyelin, ceramide -1-phosphate and glucosylceramide respectively. All these ceramide metabolic reactions are catalysed by reciprocal enzymes and are reversible (Table 1.1).

Fig 1.7 The structure of ceramide and the sphingolipid metabolic pathway.

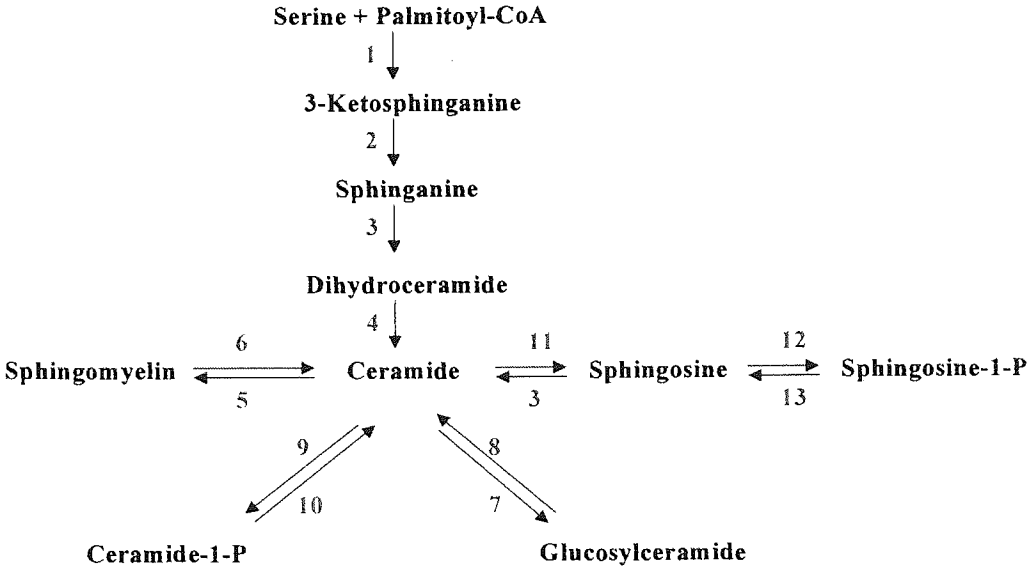

Reaction number	Enzyme name
1	Serine palmitoyl-transferase
2	3-Ketosphinganine-reductase
3	Ceramide synthase
4	Dihydroceramide desaturase
5	SM synthase
6	SMase
7	GlcCer synthase
8	Glucosylceramidase
9	Ceramide kinase
10	Ceramide-1-phosphate phosphatase
11	Ceramidase
12	Sphingosine kinase
13	S1P phosphatase

Table 1.1 Sphingolipid-metabolizing enzymes.
SM represents sphingomyelin, GlcCer represents glucosylceramide, S1P represents sphingosine-1-1phosphate.

Fig 7.1 The structure of ceramide and the sphingolipid metabolic pathway.

The enzymes described are listed in Table 1.1 according to the indicated reaction

numbers.

1.9 Ceramide in atherosclerosis

Sphingolipids have been reported to be associated with atherosclerosis development. In particular, ceramide is 10-50 fold enriched in aggregated lesional LDL than in plasma LDL (Schissel et al. 1996). Ceramide has also been reported to contribute to LDL aggregation (Auge et al. 1996; Kinscherf et al. 1997), which is an essential process in atherosclerosis (Ross 1993), due to its pronounced tendency for self-aggregation (Kinnunen and Holopainen 2002). In this process, it is proposed that LDL itself may induce ceramide production by increasing sphingomyelinase (SMase) activity, an enzyme that catalyses ceramide production (Holopainen, Angelova, and Kinnunen 2000). Moreover, Tabas and colleagues have reported that vascular endothelial cells secrete SMase to both the plasma and subendothelial space tissue during process in chronic inflammation, which is recognized as an important inducer of atherosclerosis (Marathe et al. 1998). These data indicate that ceramide production is promoted during atherosclerosis. Moreover, ceramide has been indicated to activate eNOS and subsequently NO production in endothelial cells. This effect of ceramide was first discovered after the cells were challenged with TNF-α. TNF-α elevates eNOS, neutral sphingomyelinase (N-SMase) and acid sphingomyelinase activity, and the activation of eNOS is inhibited by inhibitor of neutral sphingomyelinase but not acid sphingomyelinase (Barsacchi et al. 2003). More recent work by Mogami and colleague shows that endogenous neutral sphingomyelinase (N-SMase) has the same

effect on inducing eNOS activity, and short chain ceramide mimic the responses of N-SMase (Mogami, Kishi, and Kobayashi 2005).

Ceramide has also been proposed as an important second messenger and may play several key roles in the process of atherosclerosis development including: causing E-selectin dependent lymphocyte adhesion to endothelial cells (EC); promotion or inhibition smooth muscle cell (SMC) proliferation; inducing apoptosis in EC, cardiomyocytes and T-lymphocytes (as reviewed in(Levade et al. 2001). In addition, the apoptotic effect of ceramide has been widely studied; a number of stimuli including TNF, ionising radiation, OxLDL and Fas/FasL trigger ceramide generation and induce apoptosis (Haimovitz-Friedman et al. 1994; Haimovitz-Friedman et al. 1997; De Maria et al. 1996; Harada-Shiba et al. 1998; Deigner et al. 2001). In contrast, sphingosine-1- phosphate (S1P), one of the metabolic products of ceramide mediates cellular proliferation and survival and protection against ceramide-induced apoptosis (Cuvillier et al. 1996; Olivera and Spiegel 1993). Thus the balance between ceramide and S1P has been suggested to be an important factor regulating mammalian cell death or survival (Olivera and Spiegel 1993).

1.10 Scavenger receptors in atherosclerosis

In the transformation of monocyte-derived macrophages to foam cells in atherosclerotic lesions, the key step is the rapid, unregulated uptake of modified LDL.

Modified LDL, in contrast to native LDL that is taken up by the LDL receptor, is recognized and taken up by scavenger receptors (SRs). The LDL receptor contains a sterol regulatory element in the 5' region of the gene and is down-regulated by high intracellular cholesterol levels (Dawson et al. 1988). Therefore, it is unlikely that the LDL receptor is involved in foam cell development. Scavenger receptors, on the other hand, have no sterol regulatory elements and excessive amounts of oxidised LDL are taken up without scavenger receptors being down regulated.

SRs are cell-surface proteins that can bind to a number of ligands including: senescent cells and modified molecules such as lipoproteins. SRs include the class A type-I and type-II receptors (SR-A) (Nakata et al. 1999), the CD36 (Schissel et al. 1996; Auge et al. 1996) receptor, SR-B1/CLA-1 receptor, SR-CI receptor, Fcγ receptor, LOX-1 and SREC receptors (Table 1.2).

Classification	Ligand features
Class A SR: SR-AI/II	anionic proteins, carbohydrates, lipids and polynucleotides
Class B SR: CD36 SR-BI/CLA-1	modified lipoproteins, fatty acids, anionic phospholipids, collagens type I/IV, thrombospondin-1, advanced glycation end products and erythrocytes parasitized with *plasmodium falciparum* Native or modified lipoproteins
Other: SR-CI Fcγ receptor LOX-1 SREC	Polyanions IgG Polyanions, oxidized LDL Acetyl LDL, oxidized LDL

Table 1.2 Classification of scavenger receptors

As reviewed in (Dhaliwal and Steinbrecher 1999).

1.10.1 SR-AI/II

The SR-AI/II was the first SR to be described (Krieger and Herz 1994), and is expressed on macrophages, Kupffer cells, endothelial cells and some other cells. There are a number of ligands that can bind to SR-AI/II including: anionic proteins, carbohydrates, lipids and polynucleotides (Brown, Ho, and Goldstein 1980). The

collagen-like domain on the receptor is thought to mediate ligand binding (Doi et al. 1993), and the binding is possibly dependent on a particular array of charge interactions (Pearson, Rich, and Krieger 1993).

1.10.2 CD36

CD36 is an 88-KDa plasma membrane glycoprotein that is expressed on monocytes, endothelial cells, platelets, retinal pigment epithelium and murine adipocytes (Greenwalt et al. 1992; Abumrad et al. 1993; Han et al. 1997a). CD36 can bind to a diverse array of ligands, including modified lipoproteins, fatty acids, anionic phospholipids, collagens type I/IV, thrombospondin-1, advanced glycation end products and erythrocytes parasitized with *plasmodium falciparum* (Armesilla, Calvo, and Vega 1996; Calvo et al. 1998). CD36 recognizes lipid moieties of OxLDL, which is different from SR-A that recognizes the oxidized protein of the lipoprotein particle (Parthasarathy 1987; Parthasarathy et al. 1987). It has been shown that delipidated OxLDL failed to bind to CD36 transfected cells, but can bind to SR-A (Nicholson et al. 1995). Rigotti and colleagues observed that anionic phospholipid vesicles inhibit the binding of OxLDL to CD36. Subsequently, it was reported that oxidized phospholipids that bind to CD36 are associated with both the lipid and protein moieties of the lipoprotein (Rigotti, Acton, and Krieger 1995). The more detailed analysis of the phospholipids with CD36 binding activity was done by Hazen and colleagues (Podrez et al. 2002); from oxidized 1-palmitoyl-2-linoleoyl-PC, four structural analoges were identified with the characteristics of an sn 2-acyl group that

incorporates a terminalγ-hydroxy (or oxo)-α,β-unsaturated carbonyl, which they suggest are involved in CD36 recognition of OxLDL.

1.10.3 Other scavenger receptors

A number of other receptors, including SR-BI/CLA-1, SR-CI, Fcγ, LOX-1 and SREC receptors, also bind to OxLDL.

Since there are so many different SR that account for the uptake of OxLDL, it becomes important to identify the percentage of OxLDL clearance for each receptor. SR-AI/II is reported to account for more than 80% acetylated LDL, but only 30% extensively oxidized LDL clearance in mouse models (Lougheed et al. 1997). The clearance rate of OxLDL in SR-AI/II knockout mice was equivalent to the wild type mice, suggesting that SR-AI/II is not required for clearance of OxLDL from plasma (Ling et al. 1997). All these results indicate that other receptors rather than SR-AI/II are the major SR for OxLDL.

1.11 CD36 is the major SR of OxLDL

Monocyte-derived macrophages isolated from patients with a genetic-deficiency in the expression of CD36 bind 40% less OxLDL and accumulate 40% less cholesteryl ester (CE) than control cells derived form normal patients (Nozaki et al. 1995). In a murine model of atherosclerosis, apo-E null mice that were maintained on a high fat

diet showed entensive aortic lesions. However, CD36 knockout resulted in 70% reduction of aortic lesions (Febbraio et al. 2000). Moreover, overexpression of this receptor can result in the generation of lipid-laden plaques (Nakata et al. 1999; Munteanu et al. 2005). An immunoreactivity study in lipid-laden macrophages of human atherosclerotic lesions demonstrated that CD36 is expressed at much higher level than SR-A on these cells (Nakata et al. 1999). Taken together, these results support the hypothesis that CD36 is a major receptor for uptake of pro-atherogenic lipids.

1.12 Other functions of CD36

Recent research by Hoebe and colleages discovered a novel function of CD36, the sensor of diacylglycerides serving as an adapter for Toll-like receptor 2 (TLR2) (Hoebe et al. 2005). TLR 2 accounts for the recognization of a number of molecular components of bacteria (Lien et al. 1999; Means et al. 1999; Takeuchi et al. 1999; Takeuchi et al. 2001), fungi (Brown et al. 2003; Gantner et al. 2003), and protozoa (Campos et al. 2001). They demonstrated that macrophages from CD36 immunodeficient mice are insensitive to lipoteichoic acid and the R-enantiomer of MALP-2 (a diacylated bacterial lipopeptide), but are sensitive to a number of other bacterial lipopeptide, such as S-MALP-2, PAM_2CSK_4. These CD36 null mice are hypersusceptible to *Staphylococcus aureus* infection. Therefore, CD36 was identified as a selective sensor of microbial diacylglycerides that signal via TLR2.

Moreover, CD36 is involved in diabetes and insulin resistance, causing defective fatty acid and glucose metabolism in hypertensive rats (Aitman et al. 1999). Monocytes from type 2 diabetes patients have a relatively high level of CD36 expression comparing with control patients. Endogenous glucose induces CD36 mRNA and protein expression (Sampson et al. 2003). However, a recent study by Liang and colleagues demonstrated that CD36 expression did not correlate with plasma glucose level; defective insulin signalling rather than elevated glucose causes up-regulation of CD36 expression (Liang et al. 2004).

1.13 What regulates CD36 expression?

1.13.1 PPAR-γ

A number of stimuli up-regulate CD36 expression including OxLDL, phorbol 12-Myristate 13-Acetate (PMA), macrophage colony stimulating factor (M-CSF) and IL-4 (Han et al. 1997b; Huh et al. 1996b; Yesner et al. 1996). OxLDL increases CD36 mRNA expression that results in an increase in CD36 protein (Han et al. 1997b). The induction of CD36 by OxLDL is through activating the transcription factor, peroxisome proliferator activated receptor-γ (PPAR-γ) (Tontonoz et al. 1998; Nagy et al. 1998). PPAR-γ, a nuclear hormone receptor, has been demonstrated to be critically involved in adipogenesis and lipid metabolism (Tontonoz, Hu, and Spiegelman 1995). The specific ligands in OxLDL that activate PPAR-γare 9-hydroxyoctadecadienoic acid (9-HODE) and 13- hydroxyoctadecadienoic acid (13- HODE), two oxidized

products of linoleic acid (Nagy et al. 1998). Therefore, there is possibly a positive feedback loop between OxLDL uptake and CD36 expression. Briefly, oxidative stress modifies LDL that results in recognition and uptake by CD36. The internalized OxLDL subsequently activates PPAR-γ that up-regulates CD36 expression. The induction of CD36 expression can then uptake more OxLDL.

Other stimuli that induce CD36 expression, such as PMA, M-CSF, IL-4, have also been reported to activate PPAR-γ(Yesner et al. 1996). In the process of differentiation from monocyte to macrophage that can be caused by PMA or M-CSF, CD36 expression dramatically increases. Other ligands of PPAR-γ including the thiazolidinedione (TZDs) class of antidiabetic drugs (rosiglitazone, troglitazone and pioglitazone) and 15-deoxy-12,14-prostaglandin J2 (15d-PGJ2) also stimulate CD36 expression (Tontonoz et al. 1998; Nagy et al. 1998). Interestingly, activation of PPAR-γ by TZDs significantly inhibits atherosclerotic lesion formation in apo-E knock-out mice despite dramatic induction of CD36 expression (Li et al. 2000; Chen et al. 2001; Collins et al. 2001). There are several possible explanations to the inhibition of atherosclerosis by TZDs. One is that TZDs and other PPAR-γ ligands down-regulate proinflammatory transcription factors including: AP-1, NF-κB, STAT (Ricote et al. 1998), which may inhibit inflammation, the critical factor in the development of atherosclerosis. A second explanation is that TZDs inhibit atherosclerosis by activating the expression of ABCA1, a transporter involved in apoAI-mediated cholesterol efflux from macrophages. The induction of ABCA1 is possibly because

TZDs induces expression of liver-x-receptor alpha (LXRα), the nuclear receptor that activates ABCA1 transcription. This effect of TZDs was reported to be functional as PPAR-γ activators induce apoAI-mediated cholesterol efflux from normal macrophages. Therefore, TZDs have dual roles in regulating the cellular cholesterol level by inducing OxLDL uptake through activating PPAR-γ and CD36 expression and enhancing ABCA1-mediated cholesterol efflux through activating LXRα (Chinetti et al. 2001).

Down-regulation of CD36 is thought a potential therapeutic target for atherosclerosis. A number of groups have reported the reduction of CD36 by LPS, dexamethasone, interferon-γ, transforming growth factor-β (TGF-β), statins and HDL (Yesner et al. 1996; Nakagawa et al. 1998; Han et al. 2000; Han et al. 2004). TGR-β, statins and HDL all exert their effects through PPAR-γ. MAP kinase is demonstrated to be able to phosphorylate Ser82 on PPAR-γand result in inhibition of PPAR-γ dependent transcription (Camp and Tafuri 1997). Statins induce PPAR-γ phosphorylation through activating P44/42 MAP kinase activity (Han et al. 2004). Phosphorylation of PPAR-γ markedly reduces both ligand-dependent and ligand-independent transcriptional activation by PPAR-γ (Adams et al. 1997). TGF-βis also reported to induce the phosphorylation PPAR-γ through activating MAP kinase, therefore inhibit PPAR-γ transcriptional activity, subsequently decreasing CD36 expression (Han et al. 2000). HDL again enhances MAP kinase activity and PPAR-γ phosphorylation. Although HDL induces PPAR-γ mRNA and protein expression and translocation

from the cytoplasm to the nucleus, PPAR-γ transcriptional activity is inhibited by phosphorylation caused by HDL (Fig 1.8)(Han et al. 2002). This effect adds an additional protective role of cardiovascular disease to HDL, where previously, HDL is thought to have two beneficial effects to cardiovascular disease through its role in cellular cholesterol efflux and reverse cholesterol transport and through protecting LDL from oxidation (Durrington, Mackness, and Mackness 2001).

1.13.2 Nrf2

Recent work by Ishii and colleague identified NF-E2-related factor-2 (Nrf2) as a second transcription factor that regulates the expression of CD36. One of the lipid peroxidation products, 4-HNE on OxLDL, strongly activates Nrf2. Experiments with Nrf-2-deficient macrophages demonstrate that Nrf2 partially regulates CD36 expression in response to OxLDL and HNE (Ishii et al. 2004).

1.13.3 Vitamin E

Vitamin E, in particular α-tocopherol has been shown to play a protective role in atherosclerosis by down-regulating CD36 expression. Ricciarelli and colleague observed that in cultured human SMCs, α-Tocopherol inhibits OxLDL uptake by a mechanism involving downregulation of CD36 mRNA and protein expression (Ricciarelli, Zingg, and Azzi 2000). α-Tocopherol decreases both CD36 and SR-A

expression and cholesteryl ester accumulation in human primary monocyte-derived macrophages (Devaraj, Hugou, and Jialal 2001). In ritonavir-induced CD36 expression, the induction of CD36 expression is normalized by α-tocopherol, possibly through restoring proteasome activity that is inhibited by ritonavir (Munteanu et al. 2005).

PAGE 62 MISSING

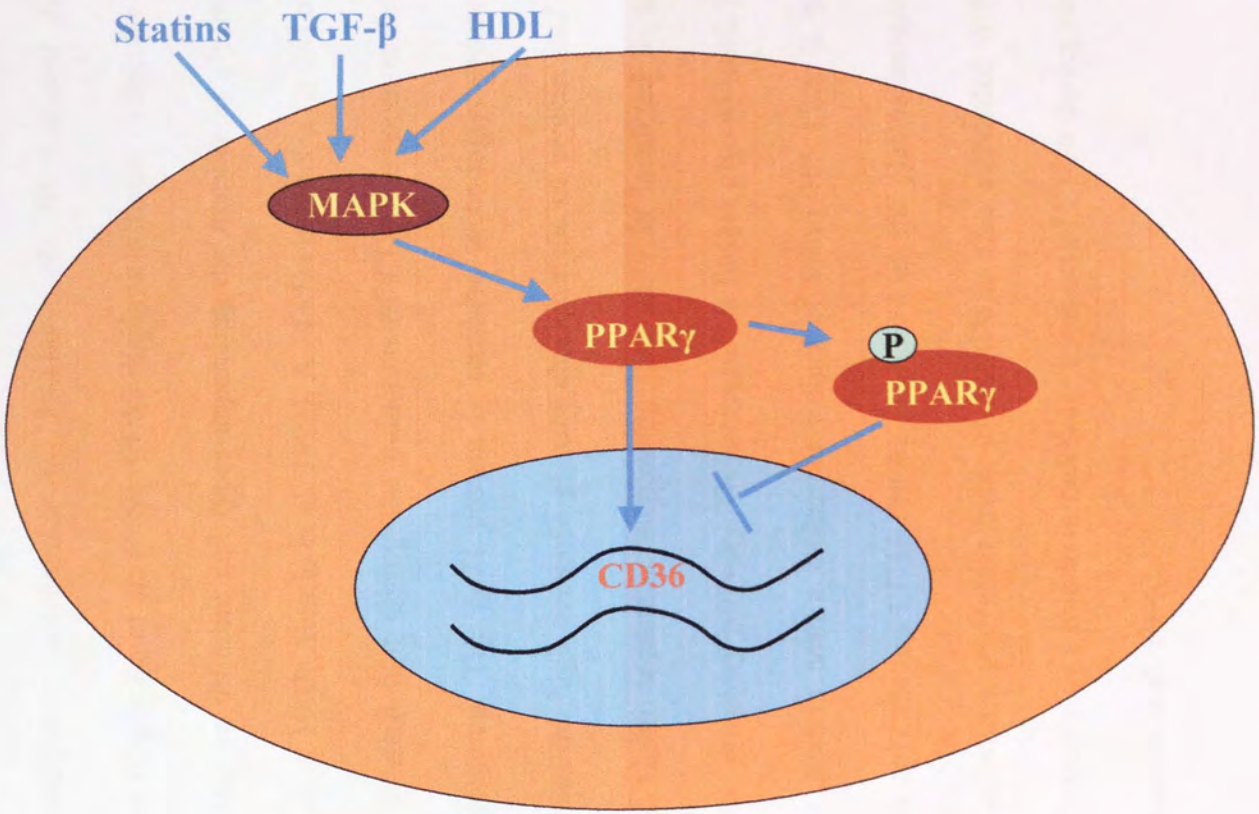

Fig 1.8 Statins, TGF-βand HDL inhibit PPAR-γthrough activating MAPK pathway, which phospharylates PPAR-γ.

1.14 CD36 structure, synthesis, transport, degradation and shedding

CD36 is a highly glycosylated membrane protein with 471 amino acid residues. The CD36 cDNA predicts a polypeptide of 53-kDa with 10 potential N-linked glycosylation sites (Oquendo et al. 1989). CD36 displays different molecular masses (78,88 and 94 kDa) on different cell types depending the number of glycosylation sites (Greenwalt et al. 1992; Alessio et al. 1991). A 74 kDa precursor (gp74) of CD36 is identified by western blot during the induction of CD36 expression following monocyte differentiation. The gp74 protein is sensitive to endoglycosidase H, an enzyme that cleaves the high mannose glycans characteristic of protein that did not reach the medial Golgi apparatus, suggesting that gp74 is localized in an early compartment of the secretory pathway. The precursor is further glycosylated, forming the mature CD36 protein with a molecular weight of 90 to 105 kDa. It has been demonstrated that only mature CD36 can be expressed on the plasma membrane. A small glycoprotein with a molecular mass of 33 kDa is also associated with gp74. This small protein may play a role in intracellular transport of CD36 during monocyte differentiation (Alessio et al. 1996).

CD36 has two hydrophobic domains: one is located at the N-terminus; the other is located in the C-terminus. The C-terminus hydrophobic domain may act as a stop-transfer sequence. Near the C terminus, a transmembrane domain has been

identified from residues 439 to 465, forming a short cytoplasmic tail (residues 466-471). The N terminus hydrophobic domain may associate with the outer cell membrane (residues 184-204). The amino-terminal region (residues 1-438) may be entirely extracellular or may have a second potential transmembrane region near the amino terminal end; the precise topology of this molecule remains unclear (Pearce, Wu, and Silverstein 1994; Tao, Wagner, and Lublin 1996). Two binding domains in CD36 involved in binding to OxLDL are indicated as 155-183 and 5-143 residues (Pearce et al. 1998; Puente et al. 1996).

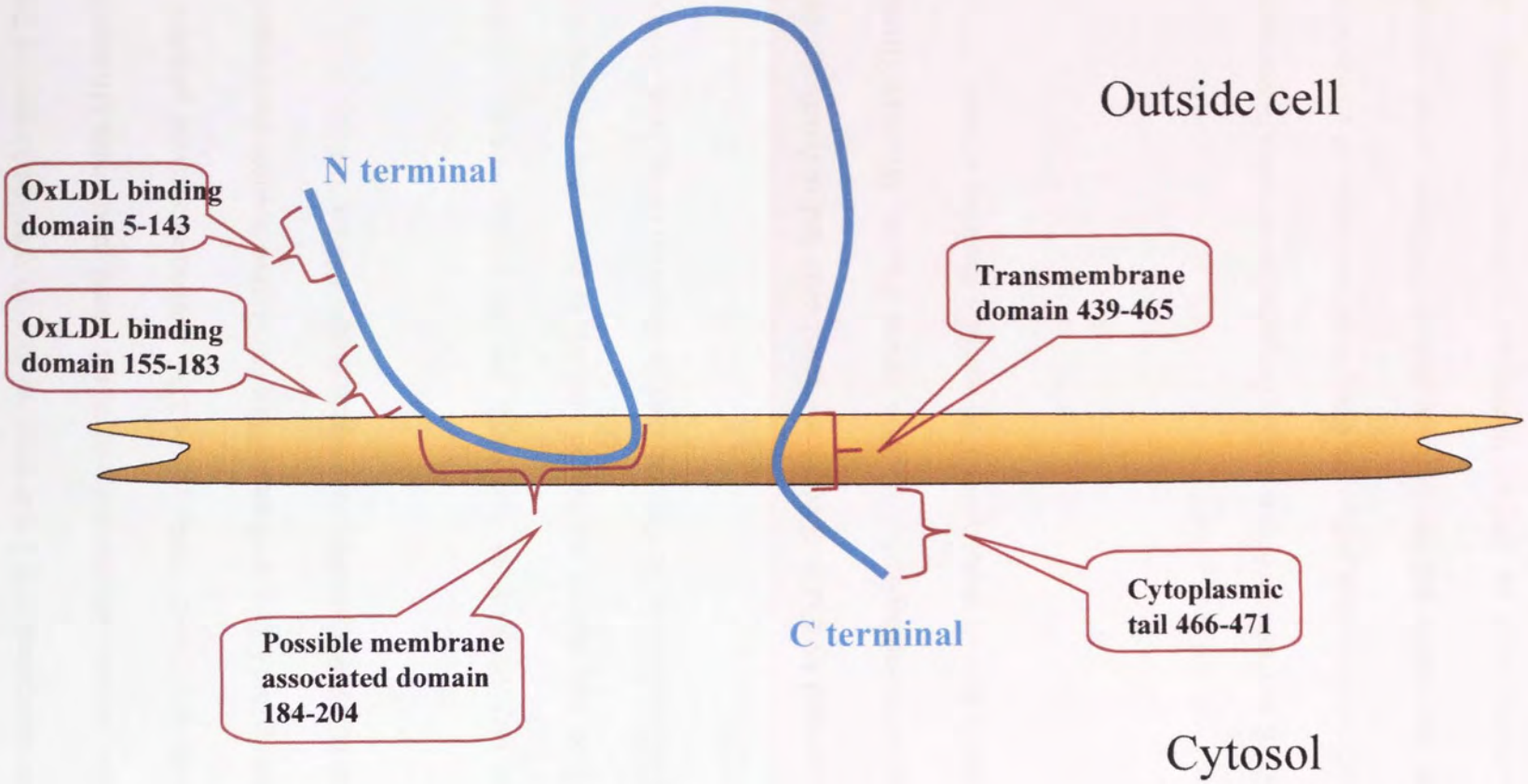

Fig 1.9 Schematic representation of the structure of the scavenger receptor, CD36.

CD36 may play a role in cellular signalling. The intracellular domain(s) have been demonstrated to be associated with 3 non-receptor protein tyrosine kinases of the src family: *fyn*, *lyn* and *yes* on platelets and peripheral blood monocytes (Huang et al. 1991; Bull, Brickell, and Dowd 1994). Anti-CD36 antibodies activate platelets and monocytes, suggesting that CD36 mediates cellular activation in some trans-signalling pathways (Aiken et al. 1990; Ockenhouse, Magowan, and Chulay 1989).

CD36 degradation may progress in two ways: via the proteasome or lysosomes. Endocytosis of CD36 may deliver the bound OxLDL to lysosomes or phagosomes, where both the CD36 protein and the OxLDL may be degraded (Zeng et al. 2003).

Soluble CD36 is secreted by CD36 cDNA transfected cells and is functional as it is capable of binding to thrombospondin, a CD36 ligand (Pearce, Wu, and Silverstein 1994), however, little is known about how CD36 receptor shedding occurs.

1.15 Lipid rafts

Lipid rafts are known as cholesterol and glycosphingolipids enriched microdomains. The original identification of lipid rafts was from their two principal characteristics, non-ionic detergent insolubility and low buoyant density. Different names were given to these microdomains, such as DRMs (detergent resistant membrane), GEMs (glycosphingolipid enriched membranes), and DIGs (detergent-insoluble,

glycosphingolipid-enriched membranes).

The first isolated lipid raft domains were defined as caveolae, small plasma membrane invaginations with a diameter of approximate 25-150nm, stabilized by the protein caveolin-1 (Thorn et al. 2003; Fra et al. 1995; Le et al. 2002). The method yielding caveolae was by extracting cells with 1% Triton X-100, and then floating the lysate on a 5 and 30 % non-continuous sucrose gradient; the detergent insoluble proteins are found in the light buoyant density fractions in the upper phase of the sucrose gradient (Brown and Rose 1992). A number of proteins involved in cell signaling were found associated with these separated domains (Foster, De Hoog, and Mann 2003; von Haller et al. 2001), thus leading the hypothesis that these domains are important in signal transduction. Later studies proved this hypothesis and indicates that lipid rafts are also involved in endocytosis and cholesterol trafficking (Nabi and Le 2003; Parton and Richards 2003; Ikonen and Parton 2000).

Sphingolipids are important components in lipid rafts and play key roles in the structure and properties of lipid rafts. Sphingolipids are a family of numerous metabolic products of the sphingosine pathway (Fig 1.7). Sphingolipids have typical alkyl chains that can be organized and condensed by sterols to form the liquid-ordered phase of lipid rafts. Saturated acyl chains of sphingolipids are essential for the stability of lipid rafts; the same structure with unsaturated acyl chains can not

partition into rafts (Panasiewicz et al. 2003). Unlike cholesterol that equally distributes across the lipid bilayer, sphingolipids predominantly localize in exofacial leaflet of the membrane, at a ratio of 6:1 of exofacial leaflet versus the inner leaflet sphingolipid of the membrane (Edidin 2003).

1.16 CD36 is localized in lipid rafts

CD36 has been reported to localize in the caveolin-rich membrane domains, defined as caveolae. This is based on the method of isolating caveolae by extracting cells with 1% Triton X-100 and then floating the lysate on a 5-30 % non-continuous sucrose gradient (Lisanti et al. 1994). However, this method is now questioned for its selective depletion of lipids and disturbance of the physiological properties of caveolae. In fact, the fractions isolated from this method do not only contain caveolae, but a series of detergent-resistant membrane (DRMs), named lipid rafts. The concept of lipid rafts is still not clear to date, but rafts can be further separated to submicrodomains. The localization of CD36 was studied by Youchun and colleagues by immunoprecipitating the lipid raft with anti-caveolin antibody and localizing CD36 and caveolin by immunofluorescence. In their experiments, the lipid rafts were first isolated using the traditional method of detergent sucrose gradient ultracentrifugation. In the lipid raft fractions, the majority proteins of both CD36 and caveolin were observed. However, the immunoprecipitation of the whole cell lysate or lipid raft fractions with anti-caveolin totally depletes CD36. Direct visualization indicates that CD36 is

homogeneously distributed on the cell membrane, whereas caveolin-1 displayes a punctate surface distribution using both antibody staining images and living cells that express green fluorescent protein attached CD36. Consistently, dual staining with CD36 and caveolin-1 shows no overlap (Zeng et al. 2003). Taken together this data indicates that CD36 does not localize in caveolae, although it may exist in the other lipid raft submicrodomains. However, the localization of CD36 still need to be further elucidated using non-detergent raft identification methods and direct visualization.

Caveolin-1 deficient cells show normal internalization of CD36 induced by OxLDL, suggesting that caveolin is not required for the endocytosis of OxLDL bound to CD36. This was also observed to be the case to SR-BI, a member of the same scavenger receptor subfamily as CD36. These data may suggest that lipid raft or caveolae do not play a significant role in the function of the scavenger receptor B subfamily.

1.17 Ceramide in lipid rafts

Ceramide, as one of the sphingolipids, plays an important role in lipid rafts. Biophysical studies have shown that ceramide increases the order of the acyl chains in the bilayer and has a tendency to self-aggregate presumably driven by intermolecular hydrogen bonding. These characteristics promote ceramide segregation into lipid rafts as a tightly packed domain with other sphingolipids and cholesterol (Dobrowsky 2000;

Holopainen, Subramanian, and Kinnunen 1998; Kolesnick, Goni, and Alonso 2000; Massey 2001; Mayor and Maxfield 1995; Roper, Corbeil, and Huttner 2000; Venkataraman and Futerman 2000). Experiments using model membranes indicate that a small amount of ceramide (3mol%) dramatically increases raft formation and stability (Xu et al. 2001).

Ceramide selectively displaces cholesterol from rafts but not other raft lipids. This effect is related to the tight lipid packing. The similarity in structure beween ceramide and cholesterol with small polar headgroups may force them to compete with each other for the limited capability to accommodate small headgroup lipids in a manner that prevents unfavorable contact between the hydrocarbon groups in the headgroup and the surrounding aqueous environment (Megha and London 2004).

Synthetic short chain ceramides with shorter carbon chains compared with the natural long chain ceramide may have different effects in some situations. Arun and colleagues have shown that short chain ceramides including C_2 and C_6 decrease plasma membrane lipid order and reduce fluorescence resonance energy transfer between lipid raft associated molecules on intact cells. This effect is unique to short chain ceramides, as both long chain ceramide and C_2 dihydroceramide do not give the same effect (Gidwani et al. 2003). The possible mechanism for the different effects of C_2 ceramide and dihydroceramide has been suggested by Simon and Gear to be due to the allylic double bond in C_2 ceramide and not dihydroceramide which can form

hydrogen bond and two rigid planes of H-bonded atoms resulting in a more-rigid head group (Fig 1.10) (Simon CG Jr, Gear AR. 1998). This structure makes C_2 ceramide form a cone-shaped lipid that could disrupt the packing of saturated phospholipids and cholesterol in a liquid-ordered bilayer, whereas, long-chain ceramides with two long carbon chains are more cylindrical in shape, therefore could pack well into a liquid-ordered bilayer (Fig 1.10).

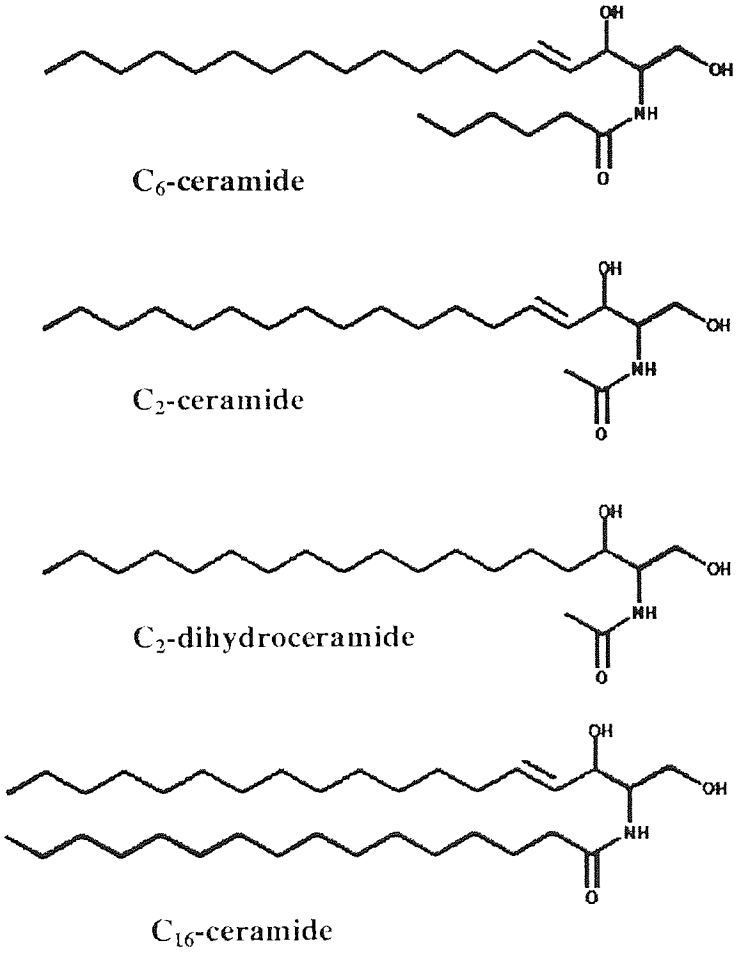

Fig 1.10 Structure of short chain ceramide (C_2 and C_6), long-chain ceramide (C_{16}) and C_2 dihydroceramide.

1.18 Ceramide as a regulator of endocytosis

Studies using a biomembrane model show that ceramide formation results in formation of vesicles (Holopainen, Angelova, and Kinnunen 2000). This effect is also observed in cells, exogenously added SMase to ATP-depleted macrophages and fibroblasts results in the budding of numberous vesicles from the plasma membrane into cytoplasm within 10 minutes (Zha et al. 1998). Short chain ceramides have similar effect to SMase catalyzed long chain ceramide (Li, Blanchette-Mackie, and Ladisch 1999). The endocytotic vesicles induced by ceramide are enriched in ceramide, suggesting that the endocytosis is most likely to occur in SL enriched lipid rafts. It is therefore, reasonable to suggest that proteins clustered in rafts can be endocytosed into the vesicles induced by ceramide and result in less protein surface expression.

1.19 NADPH oxidase in lipid rafts

NADPH oxidase, one of the major reactive oxygen species sources, has two components, gp91 *phox* and p22 *phox,* on the plasma membrane and several components in the cytosol, p40, p47, p67 *phox* and *rac* (See section 1.2.1). Recent works indicate that NADPH oxidase localizes in the lipid rafts of neutrophils (Shao, Segal, and Dekker 2003; Vilhardt and van Deurs 2004; David, Fridlich, and Aviram 2005). The identification of NADPH oxidase in lipid rafts was demonstrated using

detergent sucrose gradient ultracentrifugation and confocal microscopy. The activation of NADPH oxidase results in accumulation of membrane components and cytosolic components in detergent resistant membrane. Depletion of lipid rafts is associated with a lower membrane component concentration and less cytosolic component association with membrane components. However, the existence of NADPH oxidase within rafts in other cell types is still to be elucidated.

1.20 Hypothesis, Aims and Objectives

Previous work from this lab has shown that short chain ceramide can induce an increase in mitochondrial ROS (Phillips, Allen, and Griffiths 2002). This effect is associated with growth arrest. On the other hand, ceramide reduces the whole intracellular peroxide(Phillips and Griffiths 2003). The two major peroxide sources in cells are from mitochondria and NADPH oxidase activity. However, whilst ceramide induces mitochondrial peroxide production, it appears to decrease intracellular peroxide through inhibition of NADPH oxidase. Others have shown that endogenous ceramide enhances lipid raft formation and alters their composition (Xu et al. 2001). As NADPH oxidase membrane subunits cytochrome b558 including gp91 strongly associate with lipid rafts (Vilhardt and van Deurs 2004), this presents the hypothesis that short chain ceramides inhibit NADPH oxidase by disrupting the membrane component of NADPH oxidase.

Synthetic ceramide induced loss of cytosolic peroxide is also associated with reduced cell surface expression of CD11b (integrin) on monocytes (Phillips DC PhD thesis, 2003). Oxidative stress has been demonstrated to up-regulate CD36 expression and OxLDL uptake through inducing lipid peroxidation (Fuhrman, Volkova, and Aviram 2002). Therefore, this presents the hypothesis that ceramide reduces the expression of the CD36 scavenger receptor and cellular OxLDL uptake through protecting lipids from oxidation via reducing cytoplasmic peroxide. These are summarised in Fig 1.11.

Theory of oxidative stress induce CD36 expression and OxLDL uptake

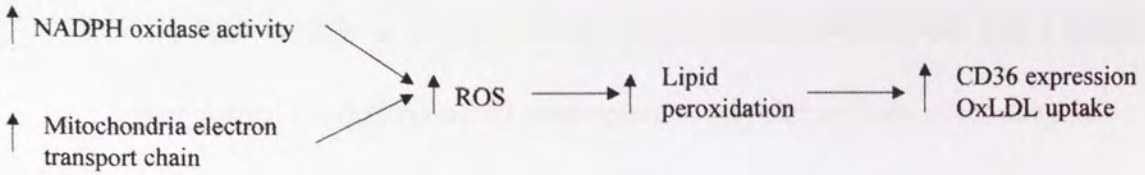

Expanded figure

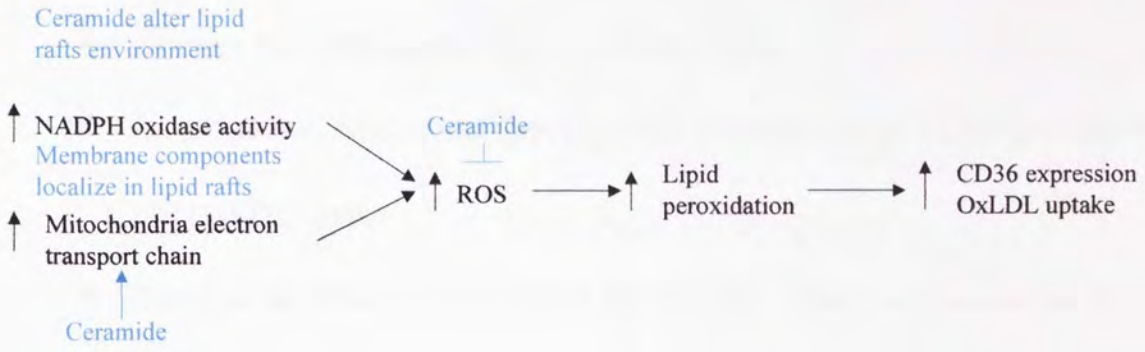

Hypothesis figure

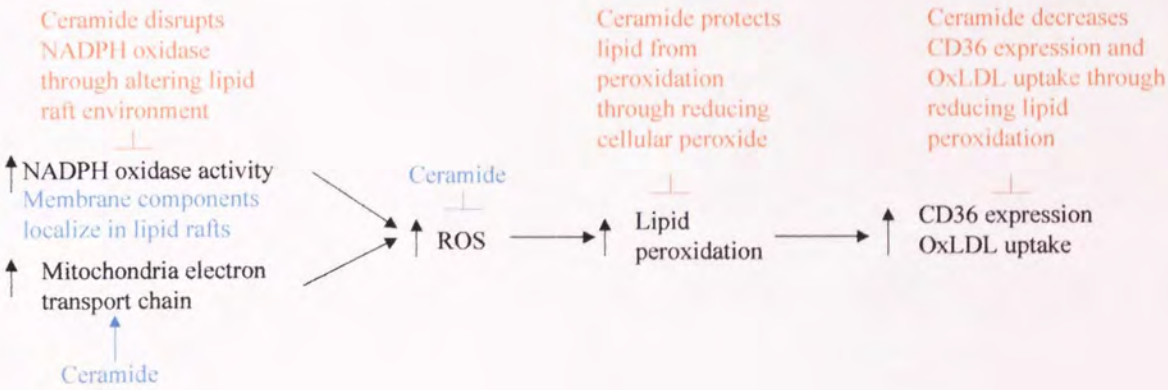

Fig 1.11 Proposed hypothesis that ceramide reduces cellular peroxide, CD36 expression and OxLDL uptake.

Specific aims and objectives are to:

- Establish models to investigate the proposed hypothesis using U937 human monocytes, the differentiated macrophage and primary human monocytes
- Examine the effect of ceramide on CD36 cell surface expression
- Examine the effect of ceramide on CD36 gene expression
- Examine the effect of ceramide on OxLDL uptake
- Investigate the mechanism through which ceramide affects CD36 expression and OxLDL uptake
- Examine the effect of ceramide on the NADPH oxidase components in lipid rafts and any role for intracellular peroxides in inhibition of CD36 expression

Chapter 2 Materials and methods

2.1 Materials

All reagents were obtained from Sigma Chemical (Sigma, Poole, UK) and solvents from Fisher (Loughborough, UK) unless otherwise stated. RPMI 1640, fetal bovine serum, and penicillin (100 U/ml)/streptomycin (100μg/ml) were purchased from Gibco-BRL (Paisley, UK). C_2-ceramide (*N*-acetylsphingosine), C_2 dihydroceramide (N-acetylsphinganine, D-erythro), sphingomyelinase (SMase) and C_{16}-ceramide (*N*-hexanoylsphingosine) were from Biomol Research Laboratories (Plymouth Meeting, PA, USA). Mouse anti-human CD11b, CD36 IgM, CD14, IgM Isotype control, IgG PE Isotype control and IgG PE & FITC Dual Isotype control antibody were from Serotec (UK), anti-CD206 (Mannose receptor) antibody and anti-CD36 IgG antibody was from Immunotech (Marseille, France).

C_2-/C_{16}-ceramide was dissolved in anhydrous dimethyl sulfoxide (DMSO) to stock solutions of 20 mM and 9mM respectively. Subsequent dilutions were made in FBS free RPMI 1640. 2', 7'-Dichlorodihydrofluorescein diacetate (DCFH-DA) was dissolved at 75mM in DMSO. PMA was dissolved at 1mg/ml in DMSO.

All water used is from MILLIPORE water purification system.

2.2 Methods

2.2.1 Cell culture

2.2.1.1 Human monocytic cell line

Fetal Bovine serum (FBS): 50ml aliquots were heat-inactivated in 65°C water bath for 15minutes.

The human monocytic cell line U937 was maintained in RPMI 1640 media, supplemented with 10% heat-inactivated FBS, 100 units/ml penicillin and 100 μg/ml streptomycin. Cells were grown at 37°C in a humidified 5% CO_2 /95% air incubator and passaged every 3 or 4 days with a subcultural density of 2 x 10^4 cells/ml. The number of viable cells was determined by trypan blue exclusion using an improved Nuebauer haemocytometer (Weber Scientific International, Teddington, UK).

2.2.1.2 U937 monocyte differentiation

Phorbol 12-Myristate 13-Acetate (PMA): 1.62mM, 1mg/ml in DMSO.

Since PMA is a very unstable chemical, it was made up as a very high concentration, and kept in -80°C freezer. Every three months, a new vial was ordered.

U937 cells were suspended at 2.5 x 10^5 /ml in RPMI 1640 media, supplemented with 10% FBS and 1% penicillin/streptomycin. Cells were differentiated following 1 or 2 or 3 days incubation with 100 μM PMA (Pietsch, A., Erl, W., and Lorenz, R. L, 1996) in 12 well plates with 2ml cells in each well. This treatment was performed at 37°C in a humidified 5% CO_2 /95% air incubator.

2.2.2 Ceramide treatments

C_2 ceramide: 20mM in DMSO.

2.2 2.1 For monocytic cells

Cells were suspended to 10^6 cells/ml in serum free RPMI for 4hours prior to the treatment with different doses of C_2 ceramide in 12 well plate with 2ml in each well, cells were then incubated for 15, 30 minutes, 1, 4, 16 hours at 37°C in a humidified 5% CO_2 /95% air incubator, prior to determination of cell surface antigen expression, intracellular peroxides and CD36 mRNA levels.

U937 cells were suspended to 10^6 cells/ml in serum free RPMI for 4hours prior to the treatment with 0.5 U SMase in 24 well plate with 1ml in each well, cells were then incubated for 1 or 16 hours at 37°C in a humidified 5% CO_2 /95% air incubator, prior to determination of cell surface antigen expression.

2.2 2.2 For macrophage cells

Cells were suspended to 2.5 x 10^5 /ml in 12 well plate with 2ml in each well, 100nM PMA was added to cells, ceramide was then added at the same time and incubated together with PMA for 1,2 or 3 days. Alternatively, ceramide was added after 8 hours PMA incubation and incubated with PMA for further 16 hours. All incubations were at 37°C in a humidified 5% CO_2 /95% air incubator.

2.2.3 Flow cytometry measurement

Buffers:

Optilyse C solution: Solution contains 1.5% formaldehyde and is suitable for fixing cells for direct immunofluorescence staining by flow cytometric analysis.

BSA solution: different percentages of BSA were dissolved in phosphate buffered saline (PBS) on a weight (g) per volume (100ml) basis.

Saponin solution: 5% saponin was dissolved in 2.5%BSA/PBS.

2.2.3.1 For cell surface antigen detection

The CD36 antigen recognized by anti-CD36 IgM antibody is sensitive to the fixation solution Optilyse C (Immunotech, Marseille, France) (see Fig 2.1). Therefore, living cells were used for antibody staining for flow cytometry. Previous studies in this lab show that optilyse C does not affect the detection of CD11b antigen.

Anti-CD36 IgM antibody was chosen in the beginning of this thesis, and this antibody has been used for most of the flow cytometry. For studying total intracellular and surface expression of CD36, an IgG antibody was ordered because IgM is difficult to get into cells.

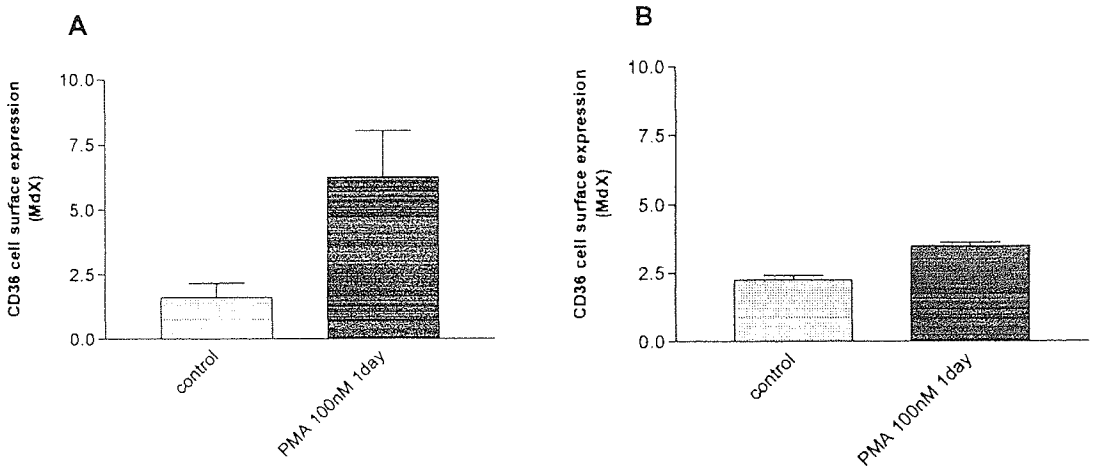

Fig 2.1 Optilyse pretreatment reduces binding to CD36 antigen by monoclonal anti-CD36 IgM antibody.
U937 cells were incubated with 100nM PMA for 1day in a humidified 5% CO_2, 95% air atmosphere at 37°C, CD36 cell surface expression was measured by flow cytometry with or without Optilyse fixation. A: Cells were not treated with optilyse ; B: Cells were treated with optilyse.

Following treatment, U937 cells were harvested by pipette if they were in suspension or by scraping if adherent. Cells were then centrifuged at 280xg for 5minutes at 22-25 °C in Sigma Biofuge Primo centrifuge. The supernatant was removed, prior to washing twice in ice-cold PBS (1%BSA), and suspended in 100µL ice-cold PBS (1%BSA).

Subsequently, cells were incubated on ice for 30 minutes in the dark with appropriate dilutions of either mouse anti-human CD11b (PE) or CD36 (FITC) IgM or anti-CD206 (PE) or IgG PE or IgM FITC Isotype control antibody. After this staining was finished, cells were diluted in 0.5ml ice-cold isoton, vortexed and analysed by

flow cytometry. For each experiment, 5000 events were counted and receptor expression was determined as the median fluorescence intensity.

2.2.3.2 For human primary monocyte surface antigen detection

To test primary monocyte antigen level in the whole leukocyte population, CD14 was used as monocyte marker.

The same method described in 2.2.5.1 was adopted but included additional stain with anti-CD14 (R-PE-Cy5) antibody and anti-CD11b and anti-CD36 antibody. CD14 positive cells were chosen for detection of CD11b and CD36 antigen level.

2.2.3.3 Cell surface antigen and whole cell protein detection by flow cytometry

Following treatment, U937 cells were harvested by pipette. Cells were then centrifuged at 280 xg for 5minutes at 22-25 °C in a Sigma Biofuge Primo centrifuge. The supernatant was removed, prior to washing twice in ice-cold PBS (1%BSA). Cells were fixed in 0.2 ml Optilyse C for 15 minutes at room temperature (RT). 20µl saponin solution was added to each sample with an incubation of 30 minutes at RT to make the cell membrane permeable for antibody. Subsequently, cells were incubated for 30 minutes in the dark with appropriate dilutions of either mouse anti-human CD11b (PE) or CD36 (FITC) IgG or IgG PE & FITC Dual Isotype control antibody. After this staining was finished, cells were diluted in 0.2ml isoton, vortexed and

analysed by flow cytometry. For each experiment, 5000 events were counted and receptor expression was determined as the median fluorescence intensity.

2.2.4 Lipid raft isolation

Buffers

Lysis buffer (MNE Triton X-100): MNE buffer contains150mM NaCl, 2mM EDTA and 25 mM MES. 1% Triton X-100 was added to MNE buffer to make the lysis buffer.

Sucrose solution: 85%, 30%, 5% sucrose was added to MNE buffer. 85% sucrose solution needs to be heated in a water bath to dissolve.

100% TCA: 100g TCA was dissolved in 20ml water. When the solid TCA dissolved, water was added to make the volume to 100ml.

Laemmli buffer: Solution contains 4% SDS, 20% glycerol, 10% 2-mercaptoethanol, 0.004% bromphenol blue and 0.125 M Tris-HCl, pH 6.8 (Sigma).

Sample dissolving buffer: 1X laemmli buffer, 4M Urea, 0.2% ABF-14, 20% DMSO.

2.2.4.1 Preparation of cell lysates for density gradient ultracentrifugation

Cells were harvested and washed twice in ice-cold PBS. Cells were then lysed in 1ml ice-cold MNE buffer (150mM NaCl, 2mM EDTA, 25mM MES, pH6.5) containing 1% Triton X-100 on ice for 30 minutes. Cell lysates were sheared by passing them 5 times through a 25G needle, and then centrifuged at 1200xg for 5minutes to remove nuclei.

2.2.4.2 Sucrose gradient ultracentrifugation

The clear supernatant was mixed 1:1 with 85% sucrose solution, and was layered in the bottom of the tube followed by 6mls of 30% and 3.5mls of 5% sucrose solution layered on the top to make a non-continuous gradient. Different percentage of sucrose solution were layered very slowly and gently to create a discrete interface. The tube was then centrifuged at 200,000xg for 16 hours at 4°C in a SW41i Rotor (Beckman Instruments, Palo.Alto.CA). Nine fractions were collected from the top to the bottom of the tube.

2.2.4.3 Protein precipitation and sample preparation for SDS PAGE and Western blotting

One tenth fraction volume of 100% TCA was added to each fraction tube. As TCA is more dense than the sample, it needs to be thoroughly mixed with the sample. Samples were then incubated in 10% TCA on ice for 15 minutes. Samples were centrifuged at 14,000xg for 5 minutes at 4 °C. Excess TCA was washed off twice in ice-cold Acetone. Precipitated protein was centrifuged at 14,000xg for 5 minutes at 4 °C.

Proteins were then dissolved in 135µl sample dissolving buffer, and boiled at 95°C for 10 minutes. Protein was detected by using western blot (2.2.5), using 30µL/lane.

2.2.5 SDS-PAGE and Western Blotting

2.2.5.1 Gel

2.2.5.1.1 SDS PAGE

Solutions:

Resolving gel buffer: Tris-HCl (36.3g) was dissolved in 150ml water. SDS (0.8g) was added and dissolved. pH was adjusted to 8.8 and the solution was made up to 200ml.

Stacking gel buffer: Tris-HCl (6.06g) was dissolved in 80ml water. 0.4g SDS was added and dissolved. pH was adjusted to 6.8 and solution was made up to 100ml.

10% Ammonium persulphate (APS): 0.1% APS solution was aliquoted to 200µl and frozen at -20°C.

TGS Buffer (10X concentration): Tris-HCl (30.3g) and glycine (144g) were dissolved in 900ml water. SDS (10g) was added and dissolved. pH was adjusted to 8.3 and the solution was made up to 1liter.

CAPS: CAPS (22.13g) in 1L distilled water, pH11.

Transfer Buffer: 1L distilled water, 125ml CAPS, 125ml Methanol.

TBS Buffer (10X concentration): 120g NaCl and 60g Tris-HCl were dissolved in 900ml water. pH was adjusted to 7.5 and the solution was made up to 1liter.

TTBS Buffer: 0.5% Tween 20 in TBS.

Acrylamide-bisacrylamide stock solution: Protogel contains acrylamide (30%w/v)-bisacrylamide (0.8% w/v) stock solution (37:5:1). (Geneflow)

TEMED (1,2-Bis(dimethylamino)ethane): TEMED contains tertiary amine base used to catalyze the formation of free radicals which will cause acrylamide to polymerize to form a gel matrix.

The resolving gel was mixed as Table 2.1 and set in plates using a BioRad Mini-Protean II cell. After the gel had set set, the stacking gel was mixed as described in Table 2.1 and was poured over the resolving gel with a 10 well comb inserted (method provide by manufacturer based on that of Laemlli-1970).

Solution	Resolving gel (12.5%)	Stacking gel
Resolving gel buffer	2.5ml	-
Stacking gel buffer	-	1.5ml
Water	3ml	6ml
Acrylamide	4ml	2ml
APS	100μL	50μL
TEMED	20μL	15μL

Table 2.1 Resolving and stacking gel

2.2.5.1.2 Ready Gel

4-20% gradient Tris-HCl gel was bought from Bio-rad. Gels were electrophoresedin a Mini-Protean III Ready Gel Cell.

2.2.5.2 Electrophoresis and Western blotting

Samples and markers were electrophoresedthrough Tris-HCl gel in TGS buffer at 300mA, 150V for 1 hour. Proteins were then transferred to PVDF in transfer buffer with an ice-pack at 170mA, 150V for 2 hours. The membrane was blocked in 5% milk

TTBS or 1% BSA TTBS for 1 hour or overnight.

Two different markers were used. Dual marker (Amersham, UK) shows colour and X-ray bands from 15 to 150 kDa. Kaleidoscope prestained Markers (Bio-Rad, UK) shows colour bands from 203 to 7.1kDa. 5 μL Dual marker or 10 μL Kaleidoscope prestained Markers was loaded in each well. Dual marker membranes were cut off after blocking in 5% milk TTBS or 1% BSA TTBS for 1hour or overnight. The membrane was stained with 1:20000 diluted HRP-conjugated S-protein (Amersham) in TTBS at room temperature for 30 minutes and was visualized and developed together with the sample membrane.

2.2.5.3 Detection of transferred proteins with antibodies

The membrane was stained with primary antibodies rabbit anti-CD36 (Santa Cruz, USA) (1:500 diluted in 1% BSA TTBS) at room temperature overnight, mouse anti-flotillin-1 (1:1000 in 5% milk TTBS) (BD Biosciences) at room temperature for 1 hour, rabbit anti-gp91 (1:250 in 3% milk TTBS) (Upstate Biotechnology) at 4°C overnight, mouse anti-p47 *Phox* (1:500 in 3% milk TTBS) (Upstate Biotechnology) at room temperature for 2.5 hours. Membranes were washed in TTBS prior to incubation

with secondary antibodies: anti-rabbit IgG (1:1000 in 5% milk TTBS) or anti-mouse IgG (1:1000 in 5% milk TTBS) both HRP conjugated at room temperature for 1 hour.

2.2.5.4 ECL Plus and visualization of immobilised antibodies

ECL plus (Amersham Biosciences, UK) was used to visualize the blots using chemiluminescence (as described by the manufacturer).

The blot was then exposed to X-ray film (Amersham) for 15 seconds to 5minutes for the best image in the darkroom and developed and fixed using developer (Photochem Econotol 2) and fixer (Photochem Econofix 2) solution (Jessop, Birmingham)

2.2.6 Cytotoxicity

Ceramide is widely generated during cellular stress and apoptosis via sphingomyelinase (Hannun and Luberto 2000; Levade and Jaffrezou 1999; Bose et al. 1995; Perry 2000). Synthetic ceramides like C_2 ceramide have been reported to be able to cause apoptosis in Jurkat T cell, however, do not have an apoptotic effect on the human monocytic cell line U937 (Phillips DC, 2002). In this study, the effect of C_2 ceramide on cell viability was monitored by flow cytometric analysis and the MTT assay.

2.2.6.1 Flow cytometric analysis of monocyte cell viability.

Cells undergoing death (apoptosis or necrosis) lose plasma membrane integrity, which allows uptake of dye (Cohen 1993). By incubating cells with a fluorescent dye such as propidium iodide (PI), cell viability can be detected utilizing flow cytometry, cells that are healthy (PI negative) and dead (PI positive). Cell size can be simultaneously determined by the amount of forward light scatter. Forward light scatter (FS) is amount of light deflected as the cell passes through the laser beam and is proportional to the size of the cell. Cells that have undergone apoptosis are characterised by shrinking of the cell causing the cytoplasm to compact. Cells undergoing necrosis which causes swelling of the cells can also be detected. Therefore, a dual parameter histogram of FS and Log FL3 (PI) can be used to separate the cells to a viable or dead population (Mangan et al. 1991).

Cells (10^6 cells per sample) were harvested and washed in PBS (centrifugation were processed at 1000xg for 5minutes by Eppendorf centrifuge 5414D, Hamburg Germany). The cell pellet was resuspended in 1ml PI (25µg) in PBS/0.1% BSA with an incubation of 15minutes in dark at room temperature. Cells were immediately analysed by flow cytometry. An ungated dual parameter histogram of FS versus Log FL3 (PI, red fluorescence, 560-590nm) was used to distinguish the viable and dead population. The percentage of viable and dead cells was given to each single sample as showed in Fig2.3 and Fig2.4.

To test this flow cytometry cell viability protocol, viable and dead cell control were examined through the flow cytometer. As Fig 2.2 shows, viable cells showed low PI uptake which appeared in left hand-side area; dead cells on the contrast showed high PI uptake and followed to the right hand-side area.

2.2.6.2 MTT assay to determine viability of PMA differentiated macrophages.

The 3-(4,5-dimethylthiazol-2-yl)-2,5-diphenyltetrazolium (MTT) assay is a standard colorimetric viability assay. The MTT can be taken up into cells and reduced by mitochondrial succinate dehydrogenase which generates a formazan product (Mossman, 1983). This product cannot pass through the plasma membrane. Therefore by lysing the cells, the formazan product can be released and can be read and quantified by a simple colorimetric method. The ability of cells to reduce MTT can indicate mitochondrial integrity and activity which may be interpreted as a measure of viability and/or cell number. By measuring the ability of MTT reduction of cells after target chemical treatment, compared with control, it is possible to test the toxicity or toxic effect of test chemical.

This assay was used to measure PMA differentiated cell viability. Cells (2 x 10^5 cells per ml, 100µl per well) were seeded into 96 well flat-bottomed microtitre

plates. Control wells consisted of complete medium (no cells) and exposed to the same conditions/additions as the cell containing wells, or untreated cells. Two hours prior to completion of the experiment, MTT solution (25µl of 5mg/ml in 0.01M PBS) was added to all wells including blanks. Plates were then incubated for a further 2 hours at 37°C, 5% CO_2. Lysis buffer (100µl of 20% w/v SDS, in DMF (50%), dH_2O (50%), pH 4.7 adjusted with 2.5% of 80% glacial acetic acid) was then added to each well and the plates incubated for a further 16 hours at 37°C in a humidified 5% CO_2 /95% air incubator. The absorbance of the each well was then read at 570nm in a 96 well plate reader.

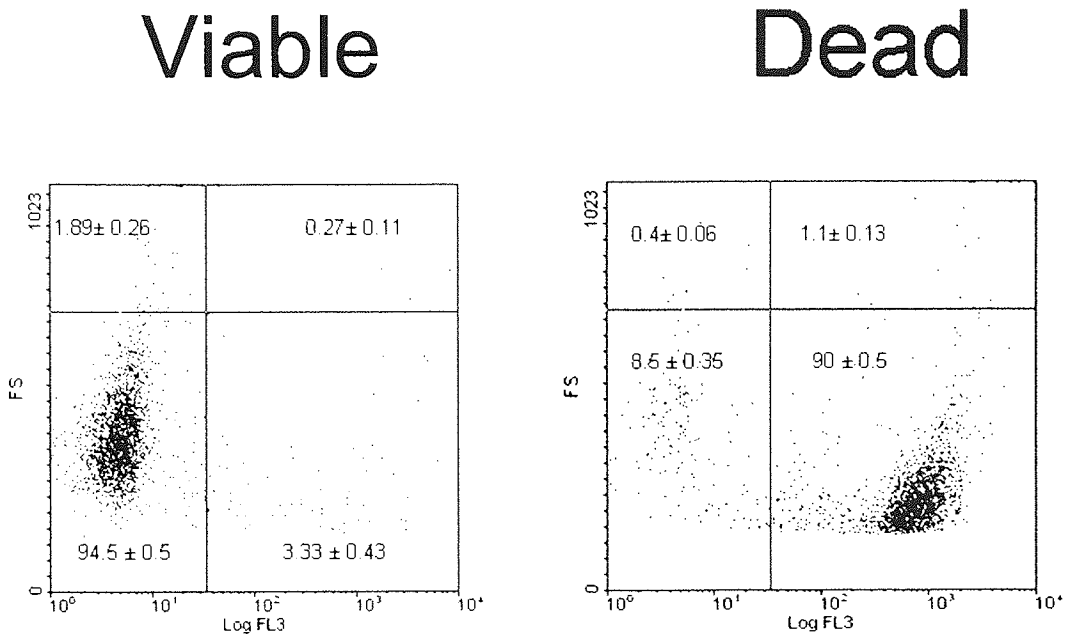

Fig 2.2 Healthy and dead cells from flow cytometric analysis of cell viability.
U937 resting cells were used as control living cells and cells which were starved in FBS free medium for 3 days as dead cell control. Cells (10^6 cells per sample) were harvested and washed in PBS. The cell pellet was resuspended in 1ml PI (25μg) in PBS/0.1% BSA with an incubation of 15minutes in dark at room temperature. Cells were immediately analysed by flow cytometry. A ungated dual parameter histogram of FS versus Log FL3 (PI, red fluorescence, 560-590nm) was used to distinguish the cells to healthy and dead population. Data are expressed as the percentage of cells in each quadrant as the Mean ± s.d.

2.2.7 Preparation of Human primary monocytes

Lymphoprep: a ready to use solution for the isolation of pure lymphocyte suspensions, which contains Sodium Diatrizoate 9.1% (w/v), Polysaccharide 5.7%

(w/v). (AXIS-SHIELD, Norway)

Sigmacote: A special silicone solution in heptane that readily forms a covalent, microscopically thin film on glass (Sigma).

All tubes were treated with sigmacote, and allowed to dry before use. This step is to protect cells from activated by plastic.

2.2.7.1 Isolation of leukocytes from blood

50ml fresh blood was taken from healthy volunteers. Blood was mixed with sodium citrate at 9:1 (blood: sodium citrate). Blood was diluted 1:1 in PBS/0.1%BSA. 15ml of lymphprep was put in each 50ml tube. 25ml diluted blood was very gently and slowly layered on top of lymphprep. The gradient was centrifuged at 160xg for 15minutes at 20°C. 15ml of plasma was taken from the top of the gradient. The gradient was centrifuged at 350xg for 20minutes at 20°C. Red cells were all centrifuged to the very bottom of the tube. A thin layer of cotton like cells appeared on the interface of lymphprep and plasma. Plasma was taken from the top until 0.5cm plasma/PBS remained on top of the lymphprep. About 3-4mls of cells were harvested from the interface using a squeezing plastic pipette.

2.2.7.2 Treatment of leukocytes

Isolated cells were diluted 1:9 in PBS/0.1%BSA and centrifuged in 15ml tubes at 350

xg for 10minutes at 20°C. Cells were suspended in 10% FBS medium. Cell number was adjusted to $2x10^6$/ml/well. C_2 ceramide (10, 20 and 50μM) or C_2 dihydroceramide (20μM) was added to the cells with an incubation time of 16 hours at 37°C in a humidified 5% CO_2 /95% air incubator. Cells were then analyzed by flow cytometry. (See section 2.2.5.2)

2.2.8 Adherent cell determination

After differentiation with PMA, the monocytes adhere to the well bottom. To determine the effect of ceramide on the process of differentiation, the adherent cell number was counted for each sample. Briefly, the old medium was removed and wells were washed in PBS. Adherent cells were harvested by scraping. Subsequently, cells were counted using the haemocytometer.

2.2.9 Immunofluorescence

Buffers:

Hoechst 33342: 1mg/ml in distilled water.

Saponin solution: 0.5% saponin was dissolved in 1%BSA/PBS.

2.2.9.1 Cell fixation.

Following treatment, cells were harvested and washed twice in V-bottomed tubes with cold PBS (0.1%BSA) by centrifugation (400 x g for 5 minutes). Finally, cells were resuspended to 1-5 x 10^6cells/ml in PBS (0.1% BSA). 30μL of the cell suspension were centrifuged onto the Superfrost plus slide (Fisher) using a cytospin centrifuge. Ice-cold acetone or 4% formaldehyde (50 μL) were added to each field to fix the cells. Slides were incubated for 20 minutes at 4°C, and then washed three times with PBS (0.1%BSA) to remove free fixer. 5% milk was added to block unbound surface area on the slide, by incubating for 10 minutes at 37°C.

2.2.9.2 Cell staining.

If whole cell antigen was detected, cells were incubated in 0.5% saponin solution for 20 minutes at room temperature; all washes were processed using saponin solution to maintain cell membrane permeability to antibody.

20μl Hoechst 33342 solution (1mg/ml in DMSO) was added to each slide, then incubated at room temperature for 30 minutes. Cells were washed three times with PBS (1%BSA) or saponin solution, and again 2% fetal bovine serum in PBS (25 μl) was added to block the unbound surface area of the slide, cells were then stained with 20 μl 10 μg/ml polyclonal rabbit anti-CD36 primary antibody (Santa Cruz) for 30 minutes at room temperature, and washed three times with PBS (1% BSA).

Subsequently, cells were stained with 20 µl 1:70 diluted monoclonal anti-rabbit FITC conjugated antibody (Sigma) for 20 minutes at room temperature, and washed three times with PBS (1% BSA). A drop of mounting medium was added to each slide and then cells were covered with cover slip, and wrapped in foil. Using Zeiss Axioskop microscope the nucleus and proteins were visualised and recorded using Zeiss Axiocam HRc digital camera.

2.2.10 Oxidized Low density lipoprotein (LDL) uptake

Solutions:

NaCl: 0.15M NaCl in distilled water, pH 7.4.

EDTA: 0.05M EDTA in distilled water, pH8.0.

Barbital buffer: 50mM Barbital in distilled water, pH 8.6.

Lysis buffer: 5% Triton in PBS.

2.2.10.1 LDL Isolation

Fresh blood was taken from informed consenting volunteers by venepuncture. 10mls blood was taken into a 30ml universal containing 1ml sodium citrate. Blood was centrifuged at 280 xg for 20 minutes at room temperature on Kendro labafuge 400R centrifuge (Kendro, Germany). 5ml plasma was separated and mixed with 1.6g KBr (mixture A). After the KBr dissolved, 5ml mixture A was taken to a new universal.

KBr was added to the mixture A until the mass of solution was 6.5g. 1ml of this solution was put into each 3.9ml quick-seal ultracentrifuge tube (Beckman, Palo Alto, CA, America). 0.15M NaCl was carefully layered on top of the plasma until the whole tube was filled. The tube was sealed with a hot-sealer (method from manufacturer) and centrifuged at 280,000 xg (90,000rpm) at 16°C for 90 minutes in TLN100 Rotor utilizing a TL-100 ultracentrifuge (Beckman, Palo Alto, CA, America). After centrifugation, two yellow rings appeared in the middle of the tube. The first ring is LDL and the second ring is HDL (Fig 2.3). This method is based on that of Chung (1986) (Chung et al. 1986).

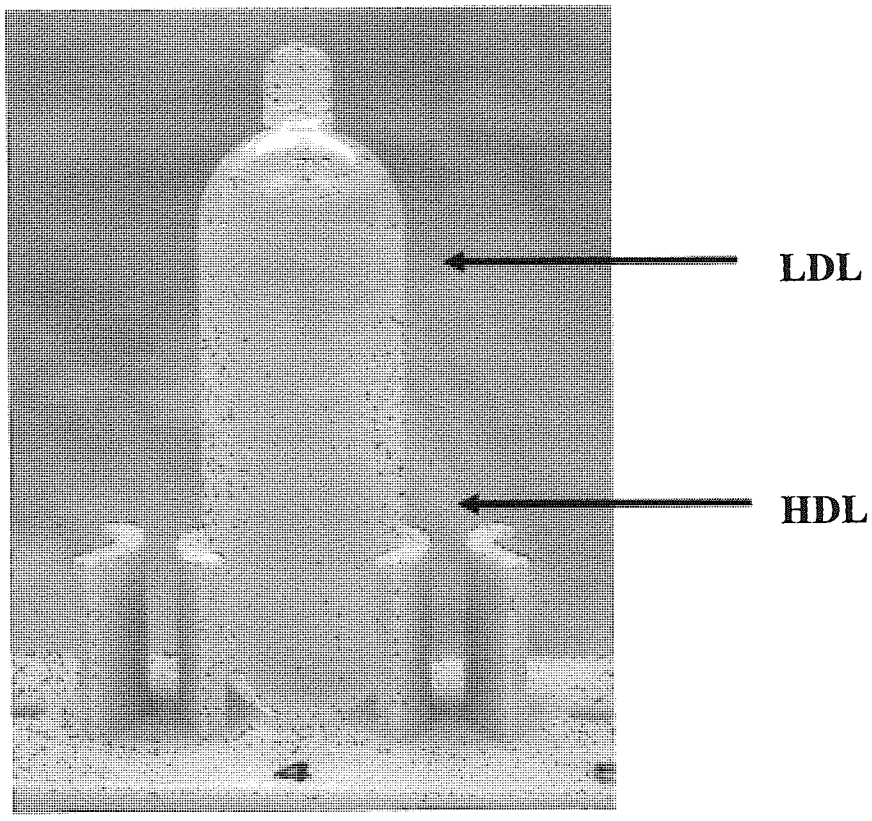

Fig 2.3 LDL is isolated using ultracentrifugation.

2.2.10.2 Preparation of oxidised DiI-labelled LDL

2.2.10.2.1 LDL oxidation

LDL (purchased from Calbiochem, UK or self-prepared) was desalted by using a PD 10 column (see section 2.2.12.2). Briefly, 0.4ml of LDL (5mg/ml) was added to a 0.15M NaCl solution pre-washed column. 2.6mls of NaCl solution was added. NaCl (1.5 x volume of LDL) was added to the column. The eluant was collected to

4-labelled eppendorf tubes. The protein concentration in each eppendorf was measured by using the BCA assay (see section 2.2.12.4). Aliquots of appropriate protein concentration were mixed together. LDL was then oxidized in 10μM $CuSO_4$ / (200μg/ml LDL) at 37°C for 1hour. 50mM EDTA was added to oxidized LDL to stop the reaction.

Several batches of LDL were prepaired and LDL oxidation was tested for each batch as stated below.

2.2.10.2.2 Agarose gel electrophoresis

In the process of LDL oxidation, lysine residues in LDL are modified by lipid peroxidation product, eg: Malondialdehyde (MDA) and 4-hydroxynonenal (HNE) (Requena et al. 1997). Oxidized LDL, therefore loses its positive charge, which belong to unmodified lysine residues. This can be measured by running LDL and OxLDL on an agarose gel.

10μg OxLDL, 10μg LDL and 1μL plasma were diluted to 40μL and mixed with bromphenol blue (0.04% in distilled water containing 10% glycerol). Samples were electrophoresedthrough a 1% agarose gel at 70V for 1 and half hours in barbital buffer (50mM Barbital in distilled water, pH 8.6).

2.2.10.2.3 Coomassie blue staining of agarose gels

Coomassie blue staining solution: 1% v/v Coomassie Blue R-250 in destain solution.

Destain solution: 40% methanol, 10% acetic acid, 50% distilled water v/v.

Agarose gel was stained with 100ml Coomassie blue staining solution for 45 minutes. Background was removed with 100ml destain solution for 30 minutes. Destain solution was discarded and 100ml fresh destain solution was added.

2.2.10.3 Oxidized LDL (OxLDL) labeling with DiI

3,3'-dioctadecylindocarbocyanine (DiI): DiI was bought from Molecular Probes and 300 μg was used to label 1mg LDL.

OxLDL was labeled with 300mg DiI /mg OxLDL at 37°C overnight in the dark. Extra dye was removed through a PD10 column (see section 2.2.12.2).

2.2.10.4 Oxidized LDL uptake by monocytes and macrophages

U937 cells were suspended in FBS 10% medium at $2.5x10^5$/ml and seeded at 4ml per well in 6 well plate. Cells were treated with 100nM PMA for 4 hours. Then different doses of C_2 ceramide were added with an incubation of 4 hours prior to adding 50μg DiI OxLDL to each well followed by 16 hours incubation at 37°C in a humidified 5% CO_2 /95% air incubator.

2.2.10.5 Cell lysis and DiI determination

After treatment, cells were harvested and washed twice in PBS (800 xg for 5minutes). The cell pellet was lysed in 400 μL lysis buffer. 100μL lysate was added to each well of 96 well plate. Fluorescence was read utilizing a XS02573 microplate fluorometer at the wavelength of excitation 520nm and emission of 590nm. (Molecular Devices, Sunnyvale, CA, USA).

2.2.10.6 DiI OxLDL standard curve

A DiI OxLDL fluorescence standard curve was made by diluting 0, 0.5, 1, 1.5, 2 μg DiI OxLDL in lysis buffer. Sample DiI OxLDL was calculated using this standard curve. A standard curve was made for each separate experiment.

2.2.10.7 Measuring protein concentration and calculation of LDL uptake

The protein concentration of each sample was measured using BCA assay (See section 2.2.12.4). OxLDL uptake was calculated as below:

$$\frac{\text{Amount of DiI OxLDL (}\mu\text{g)}}{\text{Protein concentration (mg)}}$$

2.2.11 RT-PCR

Solutions:

DYNAL mRNA DIRECT KIT (DYNAL, Norway):

Lysis buffer: contains 100nM Tris-HCl, pH7.5; 500mM LiCl; 10mM EDTA, pH8.0; 1% LiDs (SDS); 5mM dithiothreitol (DTT).

Washing buffer A: contains 10nM Tris-HCl, pH7.5; 0.15M LiCl; 1mM EDTA; 0.1% LiDS.

Washing buffer B: contains 10nM Tris-HCl, pH7.5; 0.15M LiCl; 1mM EDTA.

RNasin: Natural and Recombinant RNasin Ribonuclease Inhibitors which have broad spectrum RNase inhibitory properties (Promega).

dNTP: Mixture of ATP, TTP, CTP, GTP, DEPC water at 1:1:1:1:1.

Expand reverse transcriptase (RT): A RNA directed DNA polymerase (Roche).

Expand buffer: contains 250mM Tris-HCl, 200mM KCl, 25mM $MgCl_2$, 2.5

Tween20, pH8.3 (Roche).

RQ1 RNase free DNase: used to remove template DNA in RNA preparation (Promega).

PCR buffer: contains100mM Tris-HCl, 15mM MgCl2, 500mM KCl, pH 8.3.

All processes below were done in sterile and RNase free conditions, wearing double gloves. The eppendorfs and PCR tubes (Fisher Scientific UK) were all sterile and RNase free. Pipettes were always used with RNase /DNase free filter tips. Water was treated by 0.1% diethyl pyrocarbonate (DEPC), which inactivates RNase, thus protecting RNA against degradation.

Ribosomal RNA is the most abundant RNA species in eukaryotic cells, being approximately 80-90% of total cellular RNA. mRNA represents only 1-5% of total cellular RNA and ranges in size from 0.5kb to over 10kb. mRNA transcripts are polyadenylated at the 3'-end. The tail of adenylate residues extends between 50-200 bases. This mRNA poly (A) tail allows extraction of total mRNA using oligo-dT-linked Dynabeads® (Dynal), which possess a complementary poly (T) tail.

2.2.11.1 Dynal bead preparation

For each sample (2.5 x 10^5 cells), 30µL of Dynabeads were used. Using the Dynal magnet a working stock of Dynabeads was prepared. The beads were magnetised, the supernatant was removed and the beads were resuspended in lysate buffer.

2.2.11.2 Cell preparation for mRNA extraction

Cells were removed from the well plate and resuspended in PBS in an eppendorf. Cells were then centrifuged 13000xg for 0.5 min at room temperature. Supernatant was removed and cells were washed in 1ml PBS. Finally, supernatant was removed and the pellet was resuspended in 200µL Dynal lysate buffer. Genomic DNA was sheared by five passages each through 21 gauge and then 25 gauge needles. To reduce foaming, samples were centrifuged for 30 seconds at 10 000*g*. 200µl of the lysate was taken for mRNA extraction using 30µl of oligo-dT-linked Dynabeads® (Dynal) and washed in washing buffer A and washing buffer B as described by the manufacter. mRNA–linked Dynabeads were resuspended in 30µl DEPC water.

2.2.11.3 Reverse transcription

Dynabead-linked mRNA was used as a template for reverse transcription at 37°C for 1 hour, with Expand reverse transcriptase (RT) (Roche), 20 units RNasin® (Promega) 10mM DEPC-treated dNTPs (ABgene) and 10µM dithiothreitol (Roche), expand buffer(Roche), RQ1 RNase free DNase (Promega, 1unit/µl) The negative control (-RT) comprised the same components without reverse transcriptase. DNase was heat-inactivated at 70°C for 10 minutes

2.2.11.4 PCR

PCR was performed using primers specific for Glyceraldehyde-3-phosphate dehydrogenase (*GAPDH*) and *CD36* forward primer GAGAACTGTTATGGGGCTAT and reverse primer TTCAACTGGAGAGGCAAAGG (Vallve et al. 2002) using a Progene Thermocycler. CD36 primers were synthesised by Invitrogen (Paisley, Scotland). 1µl cDNA-linked dynabeads® from all samples was added to PCR buffer (45mM Tris pH8.8; 11mM $(NH_4)SO_4$; 4.5mM $MgCl_2$;), 200µM dNTPs (ABgene), 10pmol forward and reverse primers and 1 Unit Taq polymerse (Roche). Table 2.2 and 2.3 below describe GAPDH PCR and CD36 PCR cycles:

GAPDH

Conditions	Time	Cycles
98°C	3minutes	1
46°C	2minutes	
72°C	2minutes	
98°C	30 s	28
46°C	30 s	
72°C	30 s	
98°C	30 s	1
46°C	30 s	
72°C	4minutes	

Table 2.2 PCR cycles for GADPH

CD36

Conditions	Time	Cycles
98°C	3minutes	1
55°C	2minutes	
72°C	2minutes	
98°C	30 s	30
55°C	30 s	
72°C	30 s	
98°C	30 s	1
55°C	30 s	
72°C	4minutes	

Table 2.3 PCR cycles for CD36

2.2.11.5 Agarose Gel Electrophoresis

Buffer:

TBE (10X): 40ml of EDTA 0.5M was made at pH8.0. 108g Tris-HCl, 55g Boric Acid was dissolved in 960ml distilled water and was mixed with EDTA.

1.5% agarose gel was made in TBE buffer. 10µl of PCR products + 2.5µl 0.4%bromphenol blue/well were electrophoresed through the gel at 150mV for 1 hour. The Agarose gel was immersed in 10µl of 10µg/µl ethidium bromide (10mg/ml, Gibco-BRL) in 100mls dH_2O and allowed to develop in the dark for 20 minutes. The gel was visualised on a UVP transilluminator. The image was catched utilizing a SynGene digital camera through software GeneSnap 4.01.00 (SynGene, Cambridge, UK). Bands were analyzed and quantified using GeneTool 3.00.22 (SynGene).

2.2.11.6 Optimizing PCR cycle

To see the obvious band density change, PCR cycle number was optimized. Fig 2.4 shows the results of cycle sampling for CD36. At 27 cycles the band is too light to be measured, from 31 to 35 the band is too bright to show the change given by treatment. The optimal number of cycles for CD36 primers is therefore 30.

The specific RT-PCR products were obtained for CD36 mRNA at 389 bp (Vallve et al. 2002), and if there were contamination with genomic DNA, a second band would be obtained at 540 bp. According to the 123bp ladder we know that the bands are between 369 bp and 492 bp, therefore the PCR products are specific for CD36 without genomic DNA contamination.

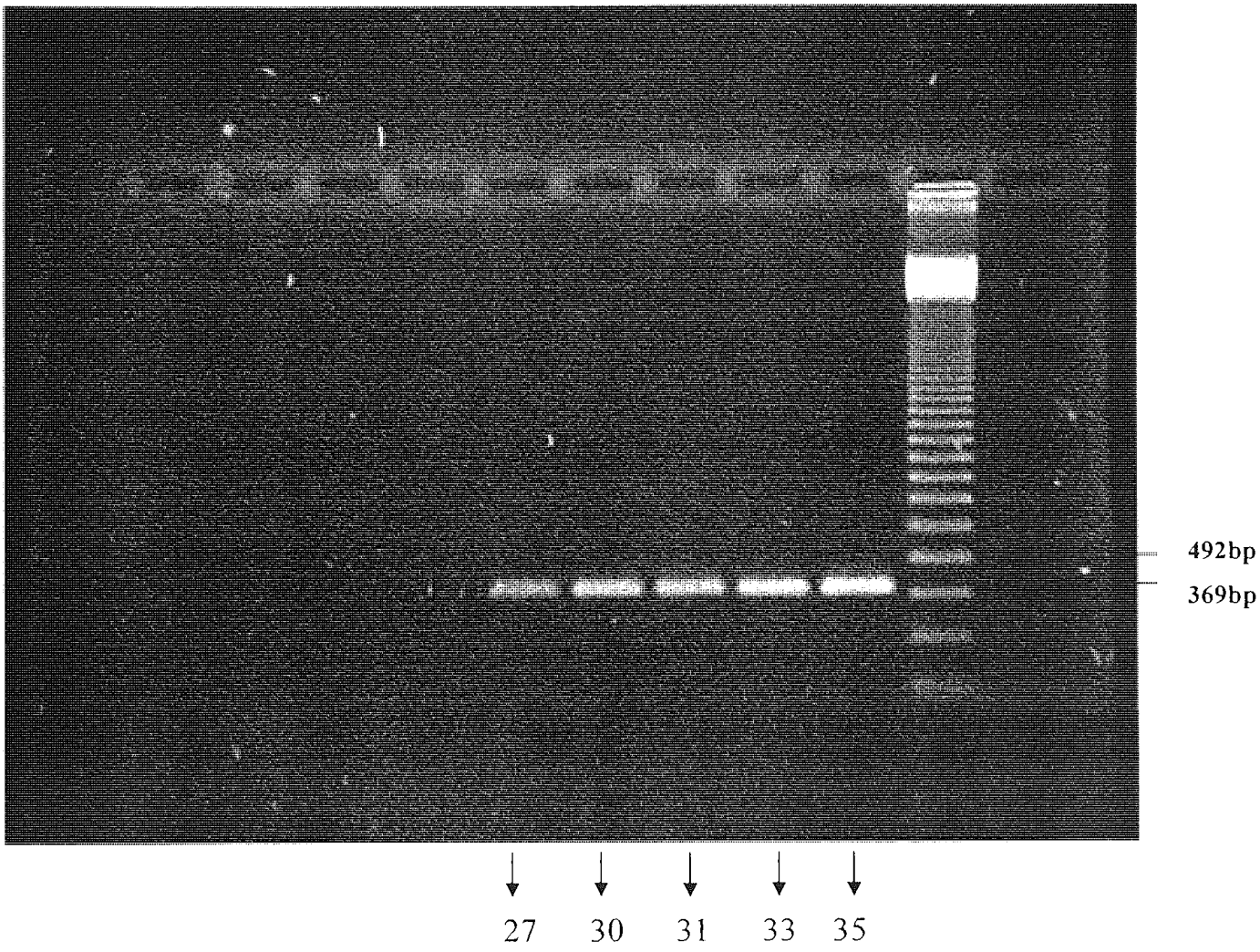

Fig 2.4 Gel electrophoresis for cDNA using CD36 primers in a PCR reaction to optimise the PCR thermocycler.

RT samples used for this optimisation procedure were randomly selected from stocks of mRNA extractions. PCR product was removed from the thermocycler after 27, 30, 31, 33, 35cycles (table 2.1). To each lane of the 1.5% Agarose gel, 10µl of PCR product was added. PCR products were electrophoresed through the gel at 150mV for 1 hour. The Agarose gel was immersed in 10µl of 10µg/µl ethidium bromide in 100mls dH_2O and allowed to develop in the dark for 20 minutes.

2.2.12 Tissue culture supernatant analysis for CD36

2.2.12.1 Cell treatment and supernatant collection

Monocytes were treated in FBS free medium as described previously (see section 2.2.4.1). Cells were then harvested and centrifuged at 800 xg for 5 minutes. Cell culture supernatant was collected and frozen at -80°C until analyzed. Cells were used for flow cytometry surface protein detection (see section 2.2.5.1).

2.2.12.2 Desalting the supernatant

Tris-HCl: 0.4mM Tris-HCl, pH 7.0.

Cell culture supernatant was desalted and concentrated. Briefly, 3mls of medium of each treatment was desalted through 0.4mM Tris-HCl pre-washed PD 10 column (Bio-Rad, USA). 4ml of 0.4mM Tris-HCl was then added to the column. Drops were collected and mixed properly with 10µl protease cocktail inhibitor.

2.2.12.3 Concentrating the supernatant

These desalted supernatants were concentrated at 30°C to $1/10^{th}$ volume using vacuum centrifuge concentrator 5301 (Eppendorf-Netheler-Hinz GmbH, Germany). The volumes of supernatants were measured carefully and adjusted to 200µl.

2.2.12.4 BCA assay for determination of protein concentration

Bicinchoninic acid (BCA) reagent solution: contains bicinchoninic acid, sodium carbonate, sodium tartrate and sodium bicarbonate in sodium hydroxide (0.1M, pH 11.25) (Sigma).

Copper (II) sulphate pentahydrate solution: 4% (w/v) solution (Sigma).

Protein standard: BSA (1.0mg/ml in sodium chloride (0.15M) and sodium azide (0.05%) (Sigma).

200µl Copper sulphate solution was added to 10mls of BCA solution. This mixture was prepared freshly each time. A standard curve (2µg-10µg) was made using BSA as protein standard. 10µl sample or standard was added to each well in 96 well plate. Both standard curve and samples were done in triplicate. 200µl Copper/BCA mixture was added to each well with 30 min incubation at 37°C. The absorbance was read at 570nm.

2.2.12.5 Sample preparation for SDS-PAGE

An equal volume of 2X Laemmli buffer was added to each sample and was boiled at 95°C for 10minutes. Protein was detected by using western blot (6µg/lane) following SDS-PAGE.

2.2.13 PPARγassay

2.2.13.1 Preparation of nuclear extract (Kit from Active Motif)

Solution:

(For 100mm plate or 8.8 x 10^6 cells)

PBS/Phosphatase Inhibitors: contains 0.8ml 10X PBS, 6.8ml distilled water and 0.4ml phosphatase inhibitors. This solution was prepared freshly.

1X Hypotonic Buffer: contains 50µl 10X hypotonic buffer and 450µl distilled water. This solution can be stored at 4°C for 1 week.

Complete Lysis Buffer: contains 5µl 10mM DTT, 44.5µl lysis buffer AM1 and 0.5µl protease inhibitor cocktail. This solution was prepared freshly.

Detergent: provided with the kit.

Buffers and tubes were placed on ice before beginning the assay. 8.8 x 10^6 cells for each sample were harvested and washed twice with 5ml ice-cold PBS/phosphatase inhibitors. Cells were centrifuged at 160 xg for 5 minutes in a centrifuge pre-cooled to 4°C. The pellet was gently resuspended in 500µl 1X hypotonic buffer and transferred to a pre-chilled microcentrifuge tube followed by 15 minutes incubation on ice. 25µl detergent was added to each cell preparation and the samples were vortexed for 10 seconds at the highest setting. The suspension was centrifuged for 30 seconds at 14,000 xg in a microcentrifuge pre-cooled at 4°C. The supernatant was then discarded. The nuclear pellet was resuspended in 50µl complete lysis buffer and the samples were vortexed for 10 seconds at the highest setting. The suspension was incubated for

30 minutes on ice on a rocking platform set at 150 xg, and the samples were vortexed for 30 seconds at the highest setting followed by 10 minutes centrifugation at 14,000 xg in a microcentrifuge pre-cooled to 4°C. The nuclear exact was then aliquoted and stored at -80°C until use.

2.2.13.2 Protein concentration measurement

Protein concentration was measured using BCA assay (see section 2.2.12.4). Diluted nuclear extract (1:10) can be measured within the standard curve using the BCA assay. 1.1µl complete lysis buffer was added to each standard curve well to control for any effect of detergent in cell lysates.

2.2.13.3 PPARγDNA-binding assay (Kit from Active Motif)

Solution:

For 1 strip (8 wells)

Complete lysis buffer: DTT 0.1µl + protease inhibitor cocktail 0.9µl + lysis buffer AM1 89µl. This solution was prepared freshly.

Complete binding buffer: herring sperm DNA 3.6µl + binding buffer AM6 356µl. This solution was prepared freshly.

1X washing buffer: 10X washing buffer AM2 1.8ml + distilled water 16.2ml and can be stored at 4°C for one week.

1X antibody binding buffer: 10X antibody binding buffer AM2 180µl + distilled water 1.62ml.

Develop solution and stop solution: Ready prepared solutions were provided with the kit.

PPAR γ wild-type and mutated consensus oligonucleotides: the wild-type consensus oligonucleotide, the competitor for PPARγ binding is provided to monitor the specificity of the assay. The mutated consensus oligonucleotide should not bind PPARγ.

One 96 well ELISA plate was provided with the kit. 40μl complete binding buffer was added to each testing well. 40μl complete binding buffer containing 40pmol (2μl) of the wild-type or mutated consensus oligonucleotide was added to each competitor well. 10μl complete lysis buffer containing 10μg nuclear extract was added to each sample well. 10μl complete lysis buffer containing 5μg provided THP-1 nuclear extract was added to each positive control well. 10μl complete lysis buffer was added to each blank well. The plate was then sealed and incubated for 1 hour at room temperature with mild agitation (100xg on a rocking platform). After incubation, the plate was washed 3 times with 200μl washing buffer. 100μl diluted anti-PPARγ antibody (1:1000 dilution in 1X antibody binding buffer) was added to all wells being used followed by 1 hour incubation at room temperature without agitation. Wells were then washed 3 times with 200μl 1X washing buffer. 100μl diluted anti-goat HRP-conjugated antibody (1:1000 dilution in 1X antibody binding buffer) was added to all wells followed by 1 hour incubation at room temperature without agitation. During this incubation, the developing solution was placed at room temperature.

Wells were then washed 4 times with 200µl 1X washing buffer. 100µl Developing solution was added to all wells followed by approximately 10 minutes incubation at room temperature protected from direct light. The blue color development was monitored in the sample and positive wells until it turns medium to dark blue. 100µl stop solution was added to each well. The absorbance was read within 5 minutes at 450nm with a reference wavelength of 750nm utilizing an A-5022 spectrophotometer (Anthos Labtec Instruments, USA).

The sample and positive well absorbance was represented as:

(sample or positive well reading) – (blank well reading).

2.2.14 Peroxides

DCFDA: 75mM in DMSO.

The intracellular peroxide level was monitored following exposure of cells to a fluorescent probe utilising flow cytometry. 2', 7', -dichlorofluorescein diacetate (DCFH-DA) is a non-polar, non-fluorescent compound, which freely diffuses across selectively permeable membranes. Intracellular DCFH-DA is activated by intracellular esterases to hydrolyse the acetate groups forming the non-fluorescent 2',

7', -dichlorofluorescein (DCFH), effectively trapping the compound within the cell. In the presence of cytosolic peroxide ($[peroxide]_{cyt}$) R-OOH, DCFH acts as a substrate which is rapidly oxidised to the highly fluorescent 2',7',-dichlorofluorescein (DCF) (see Fig 2.5). DCF is excited at 488nm, emits fluorescence within the range 505-545nm, and hence can be measured by flow cytometry.

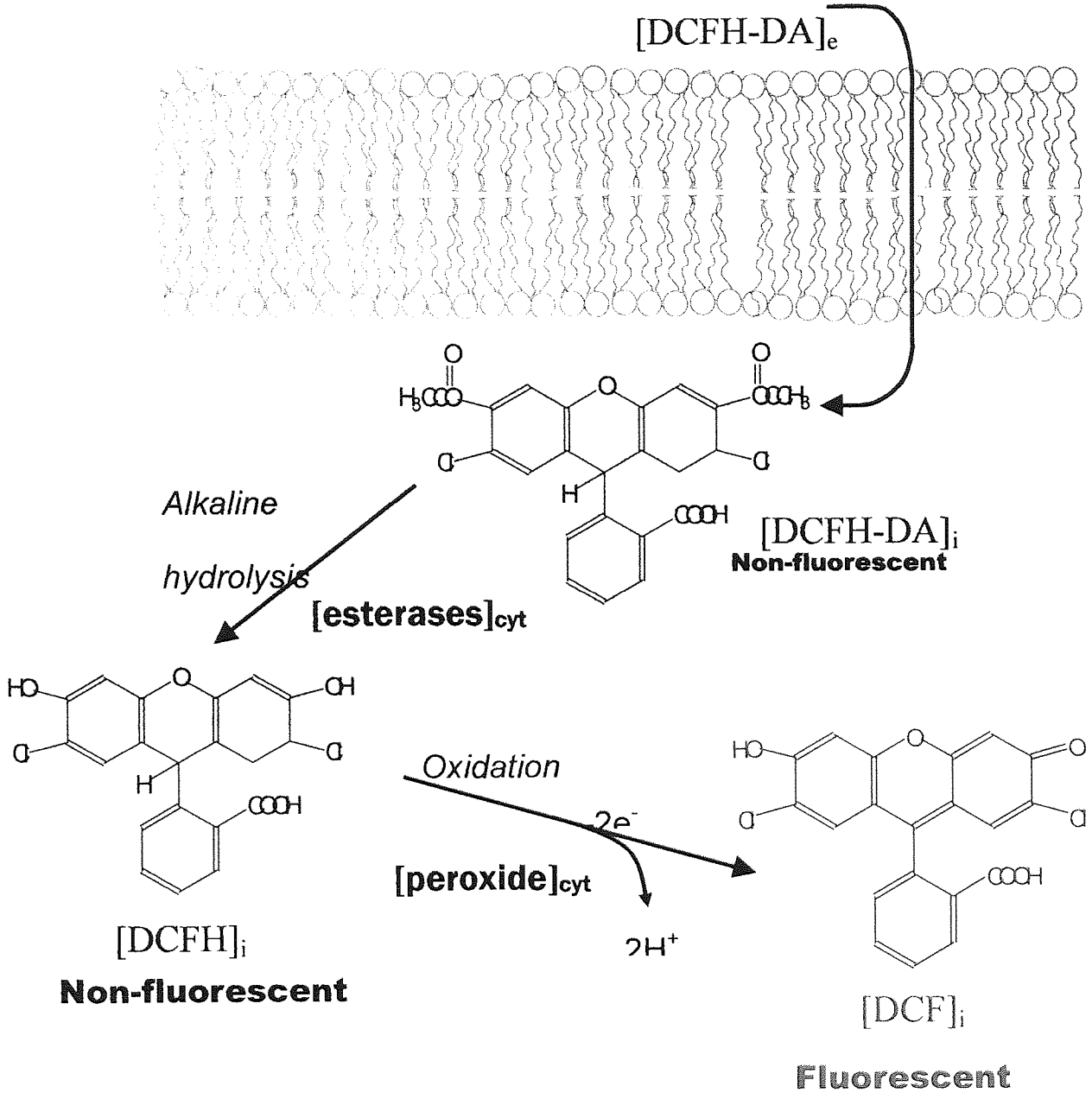

Fig 2.5 Mechanism of action of the peroxide sensitive probe 2',7',-dichlorofluorescein diacetate (DCFH-DA).

Cells were suspended to 10^6/ml /well in 12well plate, 10µl of DCFH-DA (7.5mM) was added to each well with 3-minute intervals. Plates with DCFH-DA were all packaged in catering foil (Appleton woods), and incubated for 30 minutes for each sample, prior to analysis by flow cytometry. Measurements of forward scatter, side scatter and log FL1 fluorescence (green light, band width 505-545nm.) were recorded. Cells were gated to exclude debris, clumped cells or machine noise. 10,000 cells were examined from each sample on a histogram of count versus log FL1.

Chapter 3 Ceramide decreases CD36 expression and inhibits monocyte differentiation

Previously this laboratory has demonstrated that synthetic short chain ceramides decrease intracellular peroxides (Phillips and Griffiths 2003). This was associated with the loss of integrin (CD11b) cell surface expression (Phillips DC PhD Thesis, 2003). The scavenger receptor, CD36, which is strongly expressed on monocytes/macrophages has been reported to be modulated by oxidative stress, in particular by the oxidation product, oxidized LDL (Fuhrman, Volkova, and Aviram 2002; Yoshida et al. 1998). To investigate whether ceramide can reduce CD36 expression, CD36 cell surface expression was measured by antibody staining using flow cytometry and fluorescence microscopy.

3.1 Introduction

Accumulation of foam cells under the endothelium of the vascular wall forming lipid laden plaques is the hallmark of atherosclerosis (Lusis 2000; Lusis 2000; Libby 2002). One of the early events in this process is the increasing recruitment of leukocytes principally monocytes, from the blood through attachment to vascular endothelium. This process is stimulated by many factors including: endothelial injury, shear stress, oxidized-low density lipoprotein (OxLDL) induced adhesion molecule expression and chemotactic gradients. This effect can be mimicked by pro-inflammatory cytokines, such as IL-1 and TNFα (Sica et al. 1990a; Sica et al. 1990b; Wang et al. 1991; Strieter et al. 1989; Valente et al. 1988). Engagement of chemokines with reciprocal receptors

on monocytes results in expression of integrins, such as CD11b (Baggiolini, Dewald, and Moser 1994) (Oppenheim JJ et al., 1996) and subsequently causes monocyte adhesion and transendothelial migration (Navab et al. 1991). Following activation, the monocytes migrate into the subendothelial space and differentiate to macrophages where they ingest OxLDL leading to foam cell formation.

Receptors involved in the binding and internalising of OxLDL, called "scavenger receptors", are thought to play an important role in foam cell formation (Steinberg et al. 1989; Steinberg 1987; Gown, Tsukada, and Ross 1986; Fogelman et al. 1988). The scavenger receptors include the class A type-I and type-II receptors (SR-A) (Kodama et al. 1990), the class B I receptors and CD36 (Endemann et al. 1993; Huh et al. 1996a) receptors. Recent evidence has implicated CD36 as a major macrophage scavenger receptor for oxidized LDL. Previous studies showed that monocyte-derived macrophages, which were isolated from patients with genetic-deficiency in the expression of CD36, bind 40% less OxLDL and accumulate 40% less cholesteryl ester (CE) than control cells derived from normal patients (Nozaki et al. 1995). In the murine model of atherosclerosis, apo-E null mice that were maintained on a high fat diet showed a 70% reduction of aortic lesions after CD36 knockout (Febbraio et al. 2000). Moreover, overexpression of this receptor can result in the generation of lipid-laden plaques (Nakata et al. 1999). Taken together, these results support the concept that CD36 is a major receptor for pro-atherogenic lipids. However, there is no published report on the effects of ceramide on CD36 expression. This study, therefore,

aims to evaluate the impact of ceramide on the expression of CD36 in U937 monocytes, macrophages and human primary monocytes.

3.2 Results

3.2.1 Ceramide reduces CD36 and CD11b protein expression on monocytes

3.2.1.1 C_2 ceramide reduces CD36 and CD11b expression after 16 hours incubation

The U937 human monocytic cell line was used to investigate ceramide effects on CD36 expression. Previous work in this lab showed that C_2 ceramide reduces CD11b expression in U937 cells after an incubation of 16 hours. Therefore, CD11b expression was monitored to confirm previously reported ceramide effects and 16 hours was chosen as the optimal time for incubation in the beginning of this study. U937 cells were starved in serum free RPMI 1640 for 4 hours prior treatment with 10μM or 20μM C_2 ceramide with an incubation time of 16 hours. Cell viability was examined by propidium iodide exclusion using flow cytometry. 10μM and 20μM C_2 ceramide exhibits no cytoxicity over 16 hours (see appendix).

CD36 cell surface expression was first examined by monoclonal antibody staining utilizing flow cytometry. 10μM and 20μM C_2 ceramide significantly reduced CD36

cell surface expression after 16 hours treatment P<0.001 (Fig3.1). This effect exhibited dose dependency. CD11b expression was examined together with CD36. Consistent with previous work, 10μM and 20μM C_2 ceramide significantly reduced CD11b cell surface expression after 16 hours treatment P<0.001 (Fig3.2), and again this effect was dose dependent. In contrast, C_2 dihydroceramide (20μM; 16 hours) did not alter either CD36 or CD11b cell surface expression (Fig 3.1 and 3.2).

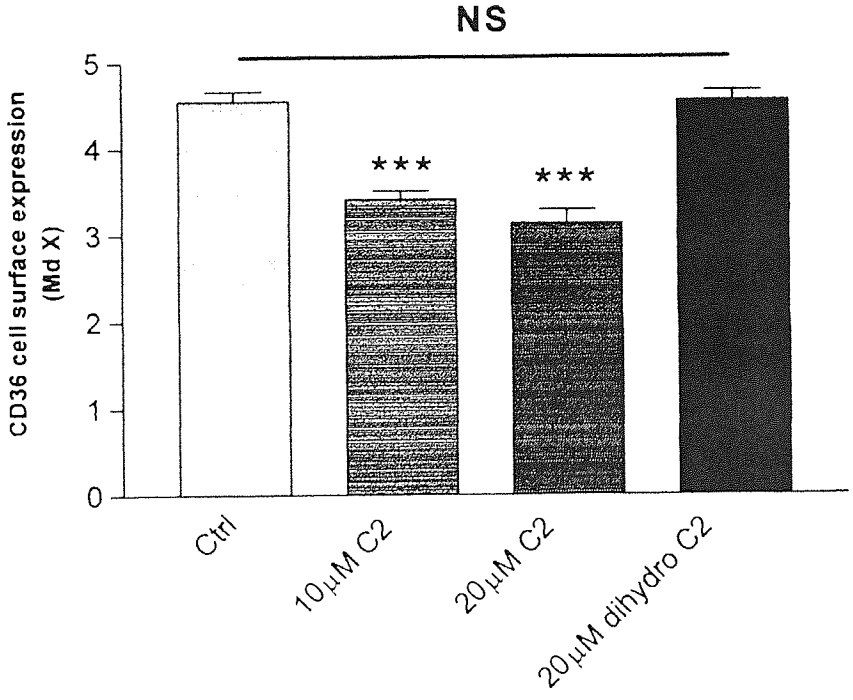

Fig 3.1 The effect of C_2 ceramide (C_2) and C_2 dihydroceramide (dihydro C_2) on the expression of CD36 on U937 monocytes.
U937 monocytes were starved in serum free medium for 4 hours, and then different doses of C_2 ceramide or 20μM C_2 dihydroceramide were added for 16 hours incubation in a humidified 5% CO_2, 95% air atmosphere at 37°C, CD36 cell surface expression was measured by flow cytometry. The data are presented as the arithmetic mean ± SEM. n=9, *** represents P<0.001 for 10μM and 20μM C_2 and NS represents no significance for 20μM dihydro C_2 compared to resting U937 monocytes by one-way ANOVA statistical analysis followed by Tukey's multiple comparison test.

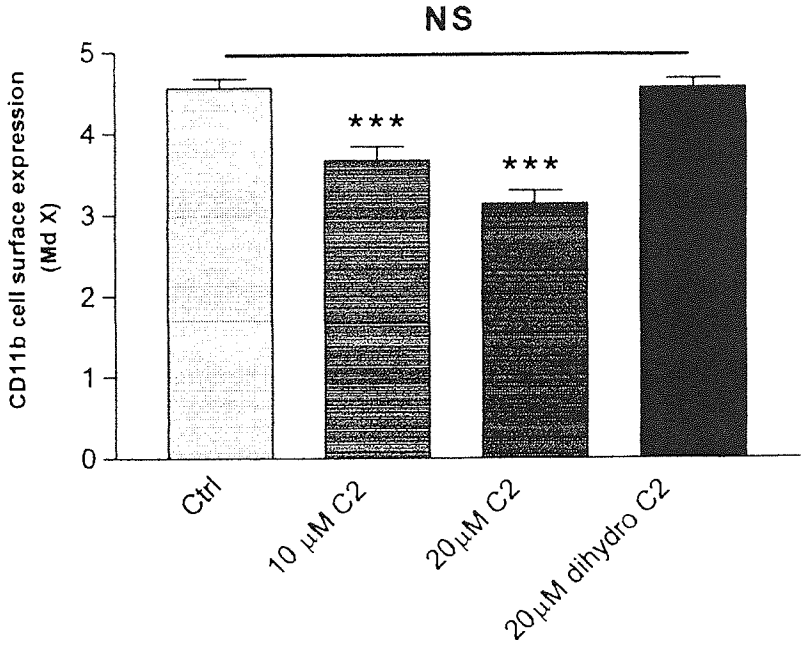

Fig 3.2 The effect of C_2 ceramide (C_2) and C_2 dihydroceramide (dihydro C_2) on the expression of CD11b on U937 monocytes.

U937 monocytes were starved in serum free medium for 4 hours, and then different doses of C_2 ceramide or 20μM C_2 dihydroceramide were added for 16 hours incubation in a humidified 5% CO_2, 95% air atmosphere at 37°C. CD11b cell surface expression was measured by flow cytometry. The data are presented as the arithmetic mean ± SEM. n=6, *** represents $P<0.001$ for 10μM and 20μM C_2 and NS represents no significance for 20μM dihydro C_2 compared to resting U937 monocytes by one-way ANOVA statistical analysis followed by Tukey's multiple comparison test.

3.2.1.2 Evaluation of time course of the effect of C_2 ceramide on CD36 and CD11b expression

3.2.1.2.1 Effect of ceramide on CD36 and CD11b surface expression determined by flow cytometry

The reduction of CD36 and CD11b expression by C_2 ceramide was further investigated by varying the incubation time. 10μM and 20μM C_2 ceramide exhibited no cytoxicity from 15 minutes to 16 hours incubation, whereas 50μM C_2 ceramide appears to be toxic to cells after 4 hours incubation. For all experiments, only viable cells were studied as determined by gating on the flow cytometer (see Fig 1). Fig3.3 shows that C_2 ceramide inhibits CD36 expression in a dose dependent manner between 15 minutes and 16 hours. 10μM and 20μM C_2 ceramide give the greatest reduction ($P<0.001$) after 16 hours incubation with cells. The effect of ceramide on CD11b over time is similar to CD36; after 16 hours incubation, ceramide most efficiently reduces CD11b cell surface expression (Fig3.4).

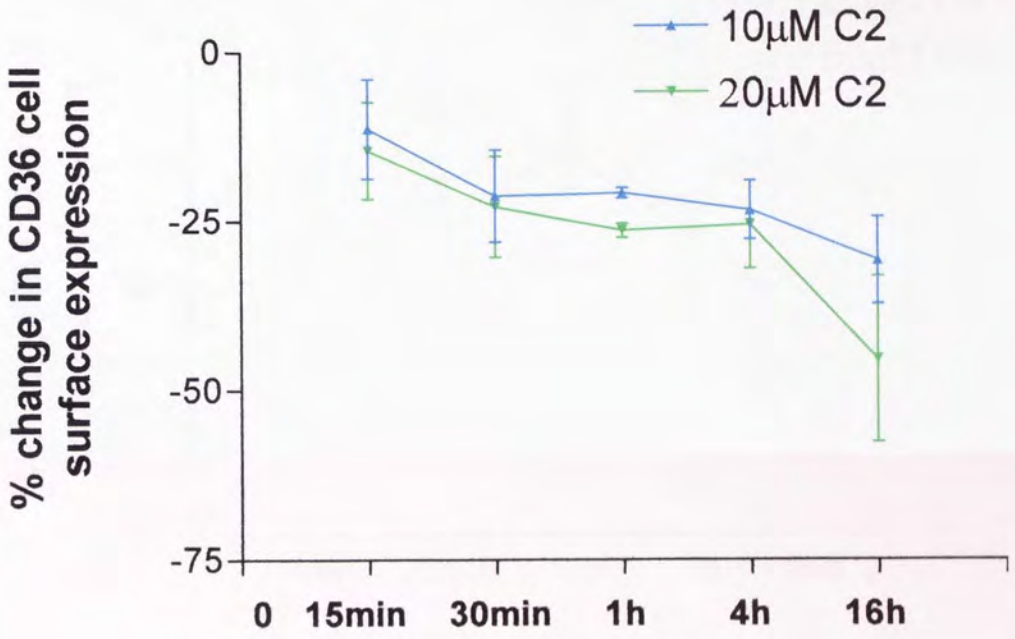

Fig 3.3 The effect of C_2 ceramide on the expression of CD36 on U937 monocytes. U937 monocytes were starved in serum free medium for 4 hours, and then different doses of C_2 ceramide were added over an incubation time of 15 minutes to 16 hours in a humidified 5% CO_2, 95% air atmosphere at 37°C. CD36 cell surface expression was measured by flow cytometry. The data are presented as mean percentage change of the MdX CD36 level ± SEM. n=9.

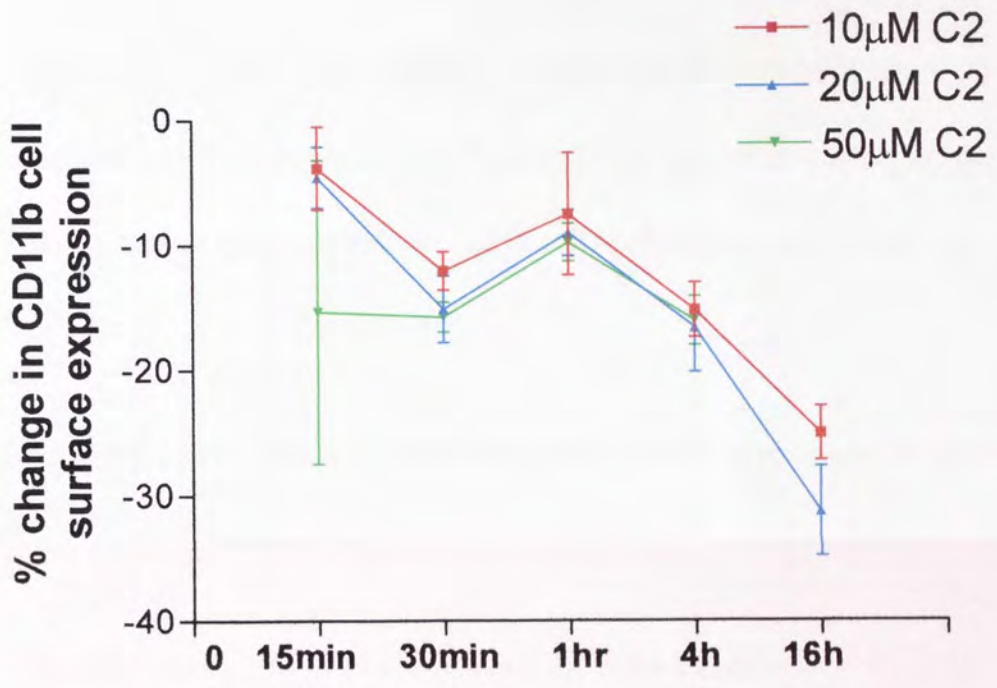

Fig 3.4 The effect of C_2 ceramide on the expression of CD11b on U937 monocytes. U937 monocytes were starved in serum free medium for 4 hours, and then different doses of C_2 ceramide were added over an incubation time of 15 minutes to 16 hours in a humidified 5% CO_2, 95% air atmosphere at 37°C. CD11b cell surface expression was measured by flow cytometry. The data are presented as mean percentage change of the MdX CD11b level ± SEM. n=9.

3.2.1.2.1 Effect of ceramide on CD36 surface expression determined by immunofluorescence

Immunofluorescence was also used to examine CD36 cell surface expression. U937 cells were treated with 20 μM C_2 ceramide for 30 minutes. Cells were stained with anti-human CD36 antibody and Hoechst 33342 was used to stain the nucleus. Fig 3.5 shows that C_2 ceramide reduces CD36 cell surface expression compared with control.

3.2.1.3 C_2 ceramide reduces CD36 and CD11b expression on human primary monocytes

Primary monocytes were also examined for ceramide effects on CD11b expression. Following 16 hours incubation with different dose of C_2 ceramide, a significant reduction in CD36 and CD11b expression on the CD14 positive cell population was observed (Fig3.6 and 3.7). Again this effect exhibited dose dependency.

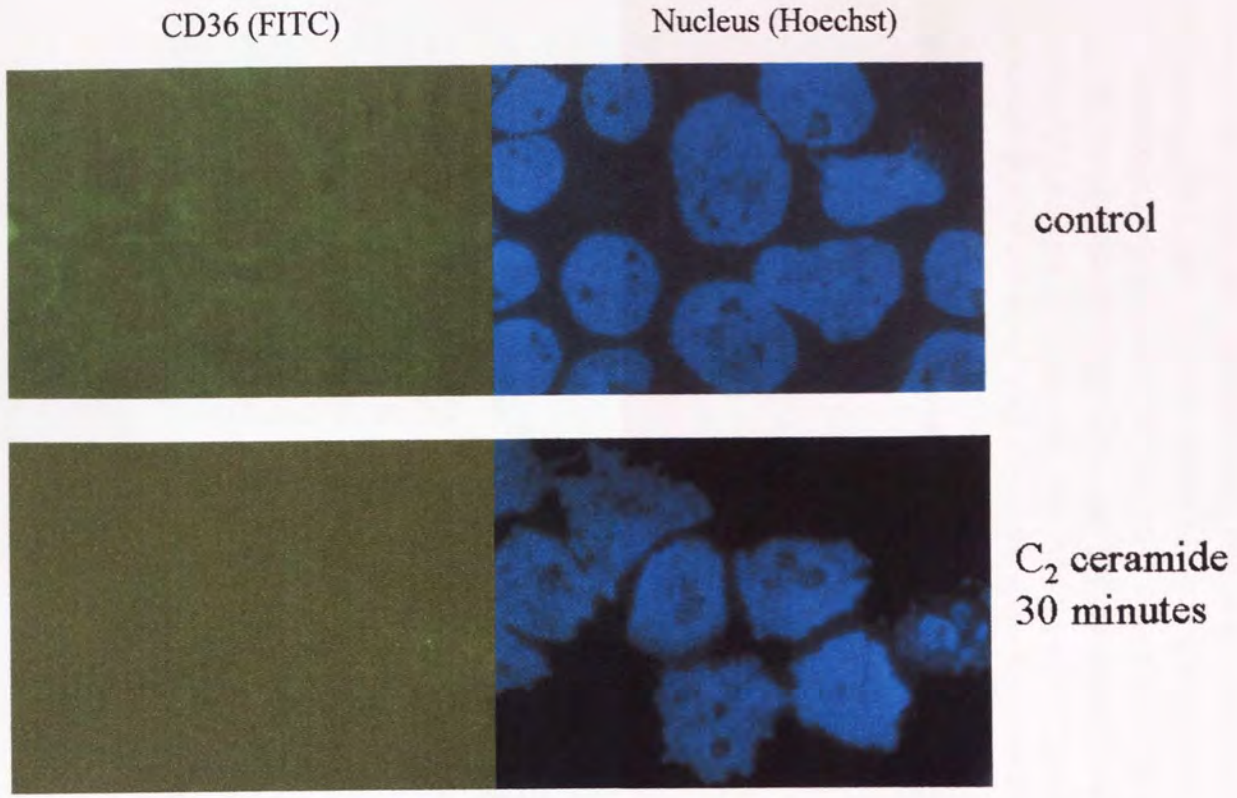

Fig 3.5 The effect of C_2 ceramide on CD36 cell surface expression on U937 monocytes by immunofluorescence staining.
U937 monocytes were starved in serum free medium for 4 hours. 20 μM C_2 ceramide was added for an incubation of 30 minutes in a humidified 5% CO_2, 95% air atmosphere at 37°C. Cells were fixed in 4% formaldehyde and then stained with 20 μl of 1mg/ml Hoechst 33342, 20 μl of 10 μg/ml rabbit anti-human CD36 IgG primary antibody and subsequently with 1:70 diluted FITC conjugated secondary antibody. A drop of mounting medium was added to each slide and then cells were covered with cover slip, and wrapped in foil. Using a Zeiss Axioskop microscope, the nuclear and CD36 (FITC) fluorescence were visualised and recorded using a Zeiss Axiocam HRc digital camera.

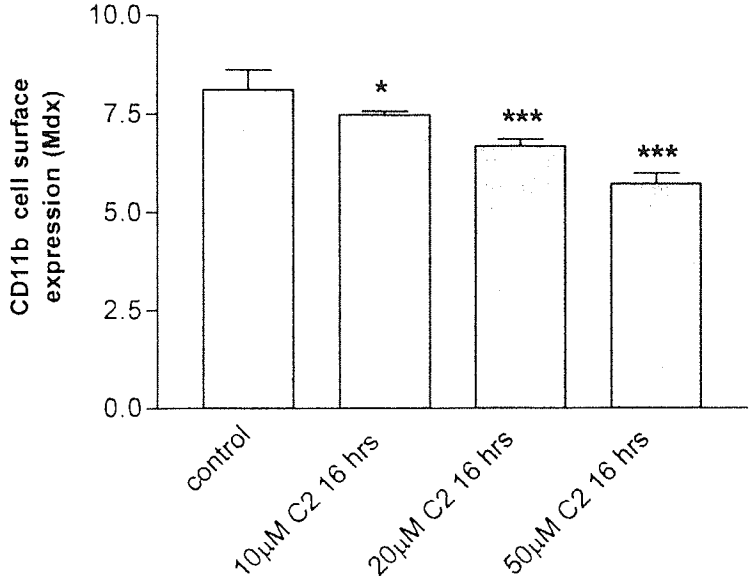

Fig 3.6 The effect of C_2 ceramide on the expression of CD11b on human primary monocytes.

Human primary mononuclear cells were separated from fresh blood and cultured in 10% serum containing medium for 4 hours, and then different doses of C_2 ceramide were added for 16 hours in a humidified 5% CO_2, 95% air atmosphere at 37°C, CD11b surface expression on CD14+ve cells was measured by flow cytometry. The data are presented as the arithmetic mean ± SEM. n=6, "*" represents $P<0.05$ and *** represents $P<0.001$ compared to resting human primary monocytes by one-way ANOVA statistical analysis followed by Tukey's multiple comparison test.

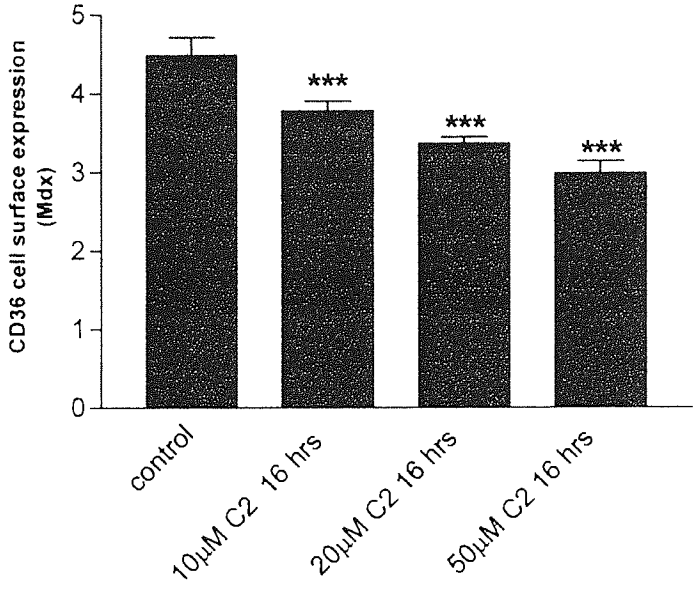

Fig 3.7 The effect of C_2 ceramide on the expression of CD36 on human primary monocytes.

Human primary mononuclear cells were separated from fresh blood and cultured in 10% serum containing medium for 4 hours. Different doses of C_2 ceramide were added for 16 hours in a humidified 5% CO_2, 95% air atmosphere at 37°C. CD36 cell surface expression on CD14+ve cells was measured by flow cytometry. The data are presented as the arithmetic mean ± SEM. n=6, *** represents $P<0.001$ compared to resting human primary monocytes by one-way ANOVA statistical analysis followed by Tukey's multiple comparison test.

3.2.1.4 Sphingomyelinase reduces CD36 expression on U937 monocytes

To determine whether this reduction in CD36 and CD11b expression is a specific property of synthetic short chain ceramides like C_2 ceramide or a common effect of ceramides, sphingomyelinase (SMase) was used to generate physiological long chain ceramides. SMase also caused a significant reduction effect in CD36 expression after 1 hour treatment. This effect is equivalent to 20μM C_2 ceramide treatment (Fig3.8). However, SMase failed to reduce CD36 expression after 16 hours treatment, where C_2 ceramide elicited the most significant reduction in CD36 expression reduction (Fig3.9).

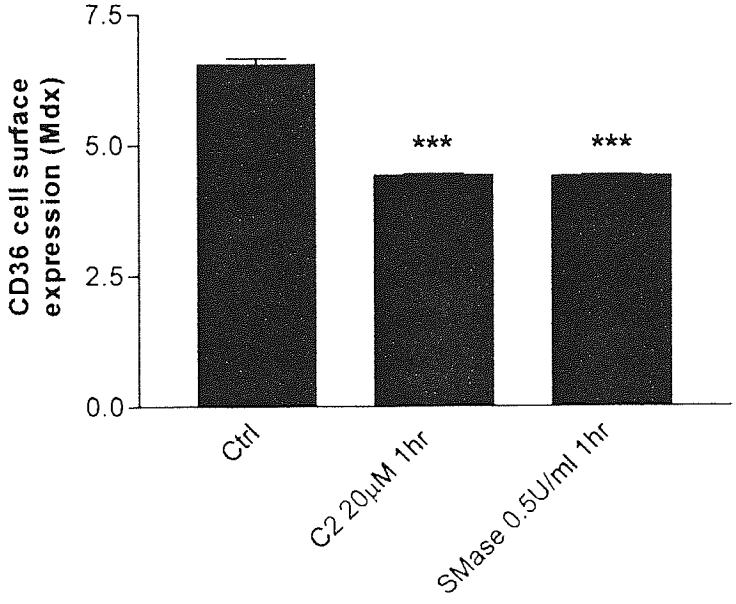

Fig 3.8 The effect of Sphingomyelinase of 1 hour incubation on the expression of CD36 on U937 monocytes.

U937 monocytes were starved in serum free medium for 4 hours, and then 20µM C_2 ceramide (C_2) or 0.5U/ml SMase were added for 1 hour incubation in a humidified 5% CO_2, 95% air atmosphere at 37°C, CD36 cell surface expression was measured by flow cytometry. The data are presented as the arithmetic mean ± SEM of MdX CD36 level. n=9, ***P<0.001 for C_2 ceramide and SMase treated monocytes compared to resting U937 monocytes by one-way ANOVA statistical analysis followed by Tukey's multiple comparison test.

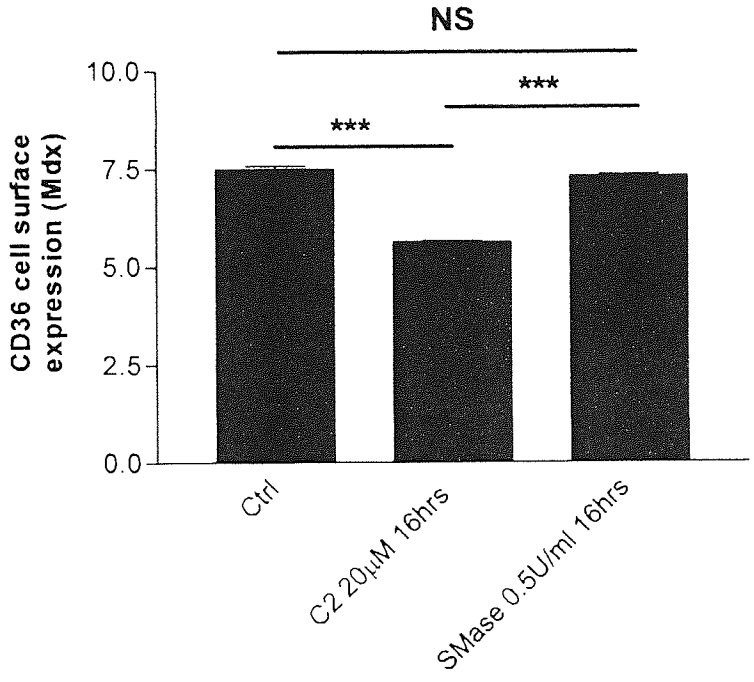

Fig 3.9 The effect of Sphingomyelinase (SMase) of 16 hours incubation on the expression of CD36 on U937 monocytes.

U937 monocytes were starved in serum free medium for 4 hours, and then 20μM C_2 ceramide (C_2) or 0.5U/ml SMase were added for 16 hours incubation in a humidified 5% CO_2, 95% air atmosphere at 37°C. CD36 cell surface expression was measured by flow cytometry. The data are presented as the arithmetic mean ± SEM of MdX CD36 level. n=9, *** represents $P<0.001$, NS represents no significance and the solid bars indicate the statistical tests by one-way ANOVA statistical analysis followed by Tukey's multiple comparison test.

3.2.2 Ceramide reduces CD36 protein expression on PMA- differentiated macrophages

3.2.2.1 CD36 and CD11b expression increase during the process of monocyte differentiation

Since CD36 protein expression increases during the monocyte differentiation process (Vallve et al. 2002), the effect of C_2 ceramide on macrophage CD36 levels was examined by flow cytometry. During differentiation, CD36 expression peaked after 24 hours incubation with 100nM PMA, and then returned to the baseline level by 48-72 hours (Fig3.10).

CD11b expression on PMA differentiated cell was monitored together with CD36. During differentiation, CD11b expression increased continuously and exhibited the highest level after 72 hours differentiation (Fig3.11).

Differentiation of monocytes was monitored by measuring the differentiation marker, mannose receptor (MR) level before and after differentiation. Fig 3.12 shows that MR level remarkably increased after differentiation, $P<0.001$.

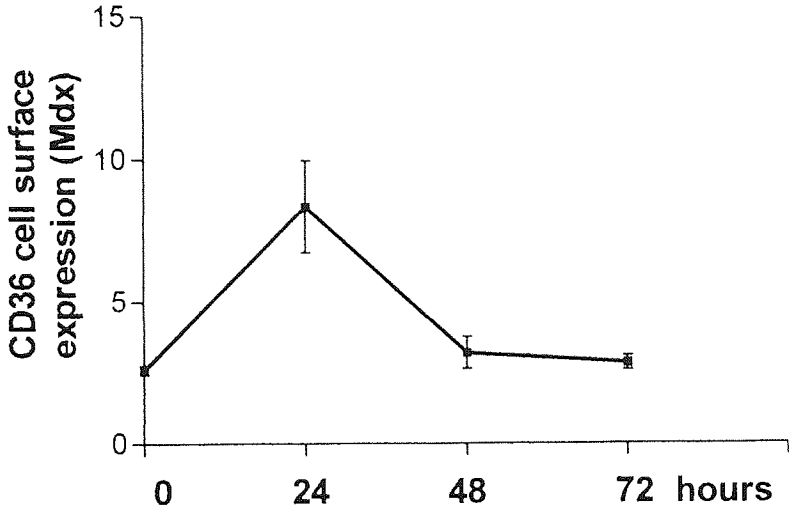

Fig 3.10 The expression of CD36 during monocyte differentiation.
U937 monocytes ($2x10^5$/ml) were incubated with 100nM PMA for 1, 2 or 3 days in a humidified 5% CO_2, 95% air atmosphere at 37°C, then CD36 cell surface expression was measured by flow cytometry.

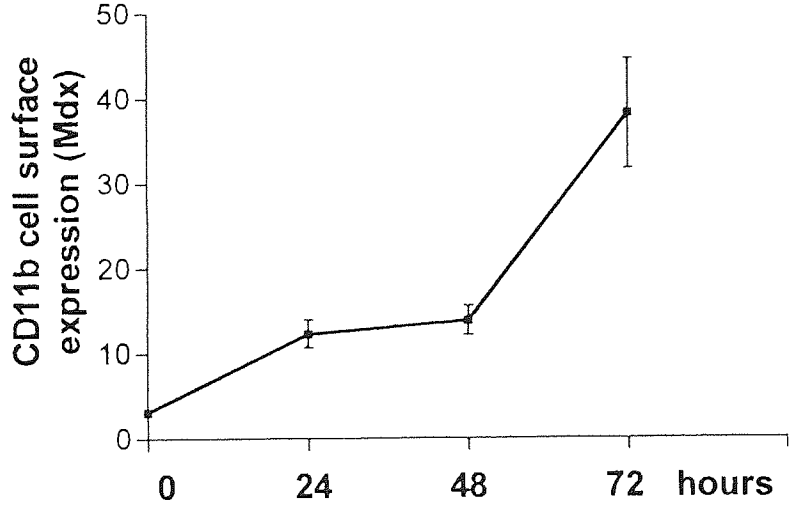

Fig 3.11 The expression of CD11b during monocyte differentiation.
U937 monocytes ($2x10^5$/ml) were incubated with 100nM PMA for 1, 2 or 3 days in a humidified 5% CO_2, 95% air atmosphere at 37°C, then CD11b cell surface expression was measured by flow cytometry.

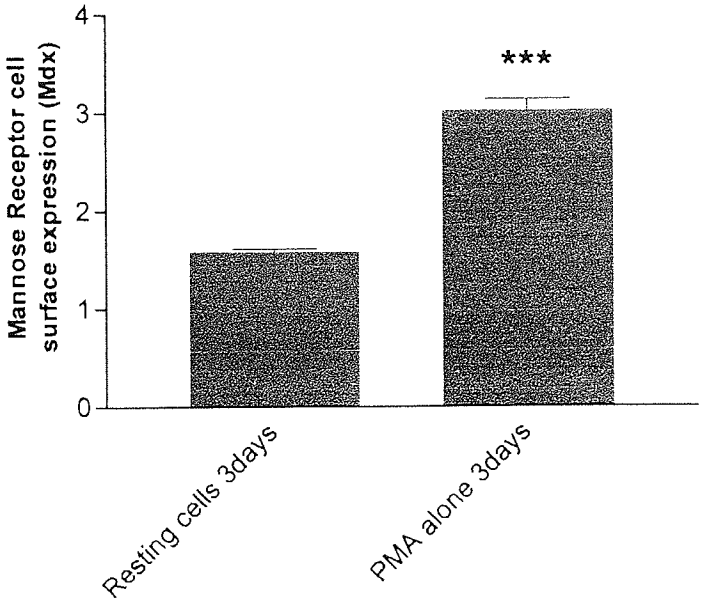

Fig 3.12 Mannose receptor cell surface expression is altered by PMA treatment of U937 cells.

U937 (2×10^5) monocytes were incubated with 100nM PMA 3 days in a humidified 5% CO_2, 95% air atmosphere at 37°C, then mannose receptor (MR) cell surface expression was measured by flow cytometry. The data are presented as the arithmetic mean ± SEM of three different experiments, n=9. *** represents $P<0.001$ and the solid bars indicate the statistical tests by one-way ANOVA statistical analysis followed by Tukey's multiple comparison test.

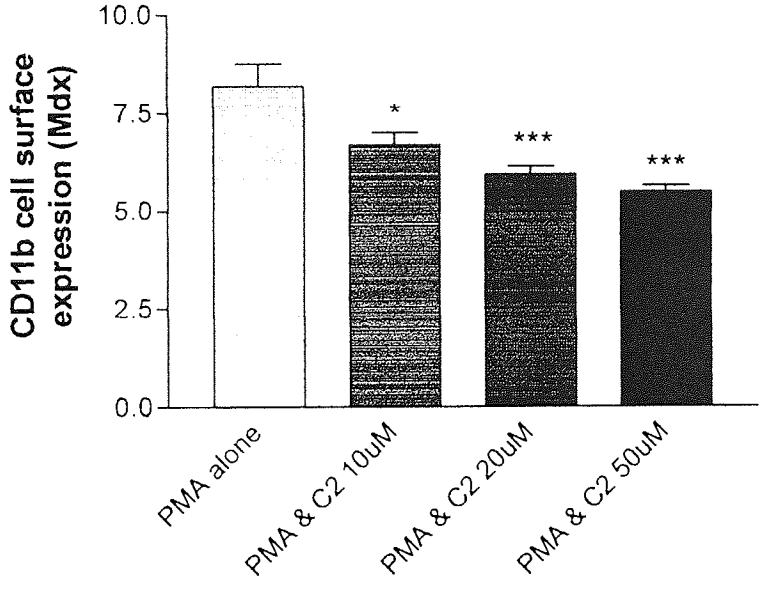

Fig 3.13 The effect of C_2 ceramide on the expression of CD11b on PMA differentiated U937 cells.

U937 cells were incubated with 100nM PMA for 8 hours, then with both PMA and C_2 ceramide for 16 hours in a humidified 5% CO_2, 95% air atmosphere at 37°C, CD11b cell surface expression was measured by flow cytometry. The data are presented as the arithmetic mean ± SEM of three individual experiments. n=6, * represents $P<0.05$ and *** represents $P<0.001$ compared to PMA treated cells by one-way ANOVA statistical analysis followed by Tukey's multiple comparison test.

3.2.2.2 Ceramide reduces CD36 expression on early PMA-differentiated U937 macrophages

During differentiation, CD36 expression peaked after 24 hours incubation with PMA and then returned to the baseline level by 48-72 hours (Fig3.10). Therefore, 24 hours was chosen as an optimal time for induction of CD36 and thus for evaluating the effects of ceramide. U937 cells were treated with 100nM PMA for 8 hours, then with both PMA and C_2 ceramide for 16 hours in a humidified 5% CO_2, 95% air atmosphere at 37°C. CD36 cell surface expression was measured using flow cytometry. C_2 ceramide significantly reduced CD36 expression in a dose dependent manner, attaining significance for both 20 μM ($P<0.05$) and 50 μM ($P<0.01$) doses, but not for the 10 μM dose (Fig3.14).

Under the optimal condition for examination of C_2 ceramide on CD36 expression, the effect of ceramide on CD11b expression was also tested. Similar to CD36, C_2 ceramide reduced CD11b expression in PMA differentiated macrophages in a dose dependent manner, attaining significance for 10 μM ($P<0.05$), 20 μM ($P<0.001$) and 50 μM ($P<0.001$) doses (Fig3.13).

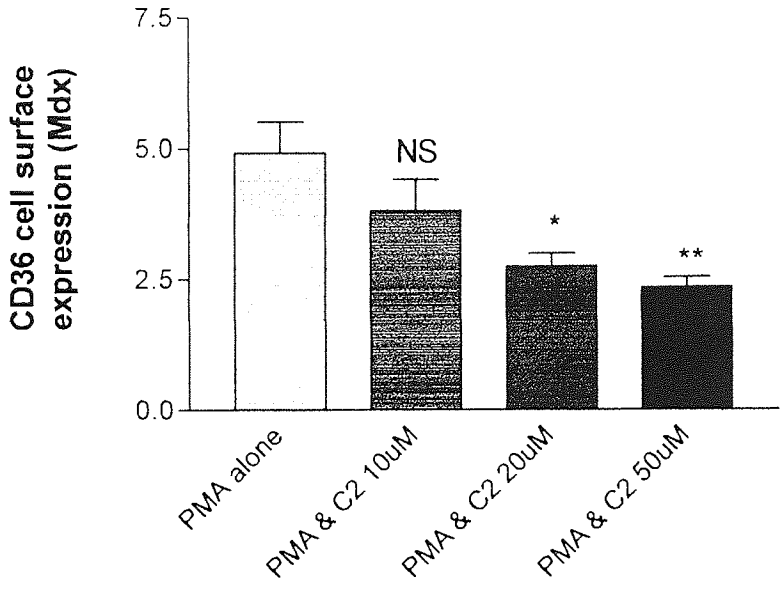

Fig 3.14 The effect of C_2 ceramide on the expression of CD36 on PMA differentiated U937 cells.

U937 cells were incubated with 100nM PMA for 8 hours, then with both PMA and C_2 ceramide for 16 hours in a humidified 5% CO_2, 95% air atmosphere at 37°C, CD36 cell surface expression was measured by flow cytometry. The data are presented as the arithmetic mean ± SEM of three individual experiments. n=6, NS represents no significant difference, * represents $P<0.05$ and *** represents $P<0.001$ compared to PMA treated cells by one-way ANOVA statistical analysis followed by Tukey's multiple comparison test .

3.2.3 Ceramide inhibits monocyte differentiation

3.2.3.1 Ceramide inhibits monocyte differentiation examined by flowcytometry

Ceramide was previously reported to play roles in differentiation (Sprott et al. 2002; Pietzsch et al. 1997). To investigate the effects of ceramide on U937 in their differentiation, mannose receptor (CD206) was used as a macrophage marker (Noorman et al. 1997). U937 monocytes were incubated with 100nM PMA and different doses of C_2 ceramide for 3days, and then mannose receptor (MR) cell surface expression was measured by flow cytometry.

Fig3.15 shows that MR expression was induced by PMA ($P<0.001$), and this change was inhibited by C_2 ceramide in a dose dependent manner, attaining significance for both 10 μM ($P<0.05$), 20 μM ($P<0.001$) doses.

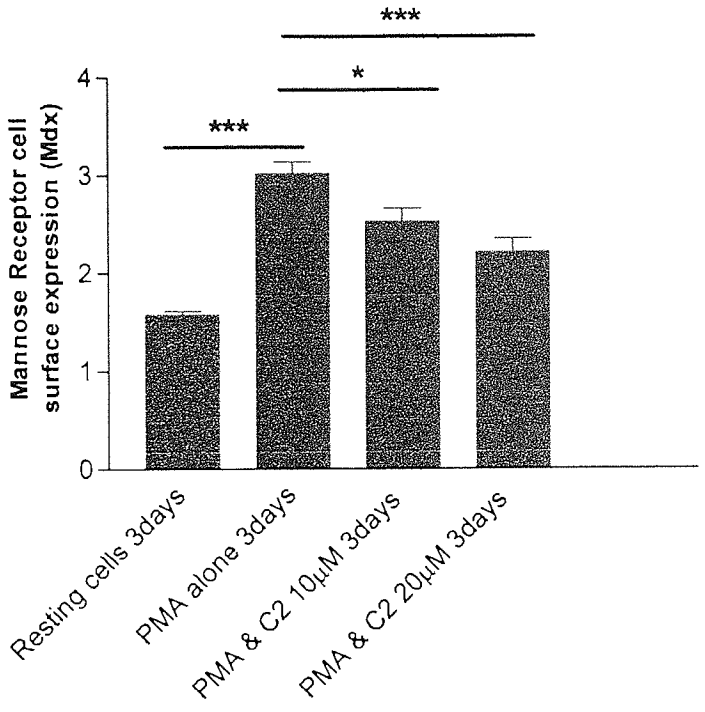

Fig 3.15 Mannose receptor cell surface expression is altered by PMA and C_2 ceramide treatment of U937 cells.

U937 (2 x 10^5) monocytes were incubated with 100nM PMA and different doses of C_2 ceramide for 3 days in a humidified 5% CO_2, 95% air atmosphere at 37°C, then mannose receptor (MR) cell surface expression was measured by flow cytometry. The data are presented as the arithmetic mean ± SEM mannose receptor levels from of three different experiments, n=9. * represents $P<0.05$ or *** represents $P<0.001$ and the solid bars indicate the statistical tests by one-way ANOVA statistical analysis followed by Tukey's multiple comparison test.

3.2.3.2 Adherent cell counts

During the differentiation of monocytes to macrophages, cells aggregate together and adhere on the bottom of the well. This effect was also inhibited by ceramide. To quantitate this effect, the adherent cell number was determined as described in section 2.2.3. As Table 3.1 shows, C_2 ceramide inhibits the adhesion of cells in a dose dependent manner.

	3days incubation
PMA alone	$0.63 \pm 0.04 \times 10^6$
PMA & 10μMC_2 ceramide	$0.55 \pm 0.04 \times 10^6$
PMA & 20μMC_2 ceramide	$0.22 \pm 0.02 \times 10^6$

Table 3.1 C_2 ceramide inhibits the adhesion of differentiated cells.
U937 monocytes were incubated with 100nM PMA and different doses of C_2 ceramide for 3days. Briefly, the old medium was removed and wells were washed in PBS. Adherent cells were harvested by scraping. Subsequently, cells were counted using the haemocytometer after 3 days treatment. The data are presented as the arithmetic mean ± SEM of three different experiments, n=9.

3.3 Discussion

Ceramide has previously been suggested to contribute to atherosclerosis by causing LDL aggregation in plaques (Auge et al. 1996; Kinscherf et al. 1997), lymphocyte adhesion to the endothelium, and EC and T-lymphocyte apoptosis (Levade et al. 2001). Under pro-atherogenic conditions, endothelial cells secrete more SMase into the lumen, which in turn triggers more ceramide generation (Marathe et al. 1998). Other pro-atherogenic factors including TNF and OxLDL, promote ceramide production (Haimovitz-Friedman et al. 1994; Harada-Shiba et al. 1998; Deigner et al. 2001). Ceramide may therefore, play an important role in atherosclerosis.

In the present study, however, it has been demonstrated that synthetic short chain ceramide (C_2) decreases surface expression of CD36, the major OxLDL scavenger receptor (SR), on the human monocytic cell line U937. Surface expression of CD36 was measured using flow cytometry. C_2 ceramide decreases CD36 surface expression from 15 minutes to 16 hours incubation. The effect of ceramide on CD36 expression was also detected by immunofluorescence microscopy. The immunofluorescence experiment shows that CD36 expression is low on resting U937 monocytes. This is consistent with the flow cytometry data. When cells were treated with ceramide, the expression of CD36 was further decreased. Under the microscope, the anti-CD36 FITC antibody stain showed no evidence of CD36 expression following C_2 ceramide treatment (Fig3.5). This is probably because the

expression of CD36 is too low, therefore is under the antibody detection limit under microscope.

Other stimuli including LPS, dexamethasone, interferon-γ, transforming growth factor-β (TGF-β), statins and HDL have also been demonstrated to down-regulate expression of CD36 (Yesner et al. 1996; Nakagawa et al. 1998; Han et al. 2000; Han et al. 2004). TGR-β, statins and HDL all exert their effects through inhibiting the transcription factor PPAR-γ. Others have suggested that CD36 loss may be due to increased degradation (Munteanu, Ricciarelli, and Zingg 2004).

C_2 ceramide has been used in the early experiments because it is easily soluble in aqueous media and can easily cross the plasma membrane. However, physiological ceramides have a longer carbon chain than C_2 ceramide and have been reported to play different roles from short chain ceramides in cell biology through altering membrane structure (Sot, Goni, and Alonso 2005; Sot et al. 2005). Moreover, C_2 ceramide plays a different role from long chain ceramides in lipid rafts. C_2 or other synthetic short chain ceramides have been reported to disrupt the order of lipid rafts (Gidwani et al. 2003; Zeng et al. 2003), whereas long chain ceramides enhance raft formation. CD36 has been demonstrated in rafts but not in caveolae (Zeng et al. 2003), thus may be affected by raft modulators like ceramides. Therefore, C_2 ceramide and SMase catalyzed long chain ceramide may affect CD36 surface expression differentially. For these reasons, the effect of ceramides on CD36

expression was further investigated by using SMase to catalyse the production of physiological long chain ceramide. SMase reduced CD36 expression on U937 monocytes after 1-hour incubation, but no effect after16 hours incubation, the time when C_2 ceramide most efficiently reduces CD36 expression. The reason for this difference is not clear yet. However, there are some possible reasons that may explain this phenomenon. SMase may have used all the available sphingomyelin substrate in a short period of time, for example 1 hour, thus cannot sustain the increase in ceramide over 16 hours. Alternatively, the SMase catalyzed ceramide may be metabolized before 16 hours. Therefore, after 16 hours incubation, SMase has no effect on CD36 expression.

As receptor expression is less stable in cell lines than in primary cells, the effect of ceramide on CD36 expression was also investigated on primary human monocytes. Experiments using human primary monocytes confirmed the observation in U937 cells and indicate that the effect of ceramide on CD36 and CD11b expression is not due to instability of U937 cells.

The mechanism by which ceramide reduces CD36 expression is still not clear. However, there are several targets that ceramide affects. Firstly, studies utilizing a biomembrane model show that ceramide formation results in formation of vesicles (Holopainen, Angelova, and Kinnunen 2000). This effect was also observed in cells, where exogenously added SMase to ATP-depleted macrophages and fibroblasts results in the budding of numerous vesicles from the plasma membrane into

cytoplasm within 10 minutes (Zha et al. 1998). Short chain ceramides have similar effects to SMase catalyzed long chain ceramide (Li, Blanchette-Mackie, and Ladisch 1999). The endocytosis induced by ceramide is most likely to happen in sphingolipid enriched lipid rafts. It is therefore, reasonable to suggest that proteins clustered in rafts can be endocytosed into vesicles induced by ceramide and result in less protein surface expression. The rapid speed of this endocytosis is consistent with current results on CD36 expression reduction induced by ceramide. Enhanced endocytosis may result in more protein degradation. Recent work has indicated that CD36 surface expression can be down-regulated by promoting proteasome activity (Munteanu, Ricciarelli, and Zingg 2004). Secondly, ceramide was observed to slow the transport of endocytosed protein from endosomes to lysosomes (Chen, Rosenwald, and Pagano 1995). Therefore, ceramide may cause protein jamming inside the cells and down-regulate protein surface expression. Thirdly, ceramide has been demonstrated to be involved in membrane protein shedding. L-selectin shedding was inducible by treatment of cells with bacterial sphingomyelinase, and also through exogenous application of a cell-permeable ceramide (Walev et al. 2000). In contrast, the amount of soluble form of CD54 (sCD54) in the culture supernatants of HUVECs was reduced by C_2 ceramide (Kawakami et al. 2002). A soluble CD36 form has been discovered (Pearce, Wu, and Silverstein 1994) and ceramide may regulate CD36 surface expression by altering the rate of shedding of CD36. Fourthly, CD36 expression is regulated by PPARγ. Stimulation of PPARγ by OxLDL or PPARγ agonists result in overexpression of CD36 (Tontonoz et al. 1998; Nagy et al.

1998). Tumor necrosis factor alpha (TNFalpha) signalling, which is mediated through ceramide, decreases the expression of peroxisome proliferator-activated receptor gamma (PPARgamma). Endogenous, C_6- and C_2- ceramide are reported to reduce the expression of PPARgamma mRNA and protein in a time and concentration dependent manner (Kajita et al. 2004; Sprott et al. 2002). Thus, ceramide may also decrease CD36 expression through inhibiting PPARγ transcriptional activity. Finally, ceramide may work through the original hypothesis , that ceramide downregulates CD36 expression through decreasing cellular peroxide.

Ceramide inhibits monocyte differentiation, which was demonstrated by reduced expression of the differentiation marker, mannose receptor, and fewer adherent cells in this study. It has been reported that ceramide plays different role on differentiation depending on cell type. Ceramide inhibits 3T3-L1 preadipocyte differentiation in part by enhancing dephosphorylation and premature nuclear export of CCAAT-enhancer-binding proteins β at a time when its maximal transcriptional activity is required to drive adipogenesis (Sprott et al. 2002). On the other hand, ceramide induces cell differentiation on human primary monocytes through stimulating differentiation-dependent cDNA (DIF-2) (Pietzsch et al. 1997). The effect of ceramide on differentiation is still not clear and needs to be investigated further.

In summary, these results show that ceramides reduce CD36 cell surface expression, but the functional importance of this remains to be determined.

Chapter 4 Ceramide decreases OxLDL uptake

Previous work from chapter 3 has demonstrated that ceramide induces a loss of expression of the major OxLDL scavenger receptor, CD36. To examine whether the reduction of the expression of CD36 initiated by ceramide is functional, the effect of ceramide on OxLDL uptake was studied using U937 monocytes and macrophages.

4.1 Introduction

Oxidized low-density lipoproteins (OxLDL) play roles in a number of biological process, including promotion of the production of adhesion molecules, chemotactic proteins, growth factors and cytokines, and inhibition of the production of nitric oxide in endothelial cells (Ross 1999; Lusis 2000; Berliner and Heinecke 1996). OxLDL are therefore believed to play a key role in atherosclerosis.

Early events in the development of atherosclerosis involve increasing recruitment of leukocytes, principally monocytes, from the blood through attachment to vascular endothelium. The monocytes migrate into the subendothelial space tissue and differentiate to macrophages where they ingest OxLDL leading to foam cell formation.

It was reported that OxLDL induces the activation of sphingomyelinase (SMase) and a resultant increase in ceramide, leading to proliferation or apoptosis in vascular

smooth muscle cells and human umbilical endothelial cells (Harada-Shiba et al. 1998; Escargueil-Blanc et al. 1998; Auge et al. 1996; Auge et al. 1998). There is also supporting evidence for the involvement of ceramide in atherosclerosis through studies on the behaviour of SMase treated LDL and from atherosclerotic plaques, which has been presented in Chapter 1 (section1.9)

In addition, it has been demonstrated that SMase enhances LDL-receptor mediated endocytosis of LDL, which leads to an increase of LDL degradation and CE accumulation in the J774 murine macrophage cell line. This effect was determined to be cell type specific (Xu and Tabas 1991). However, there are no reports on the effects of short chain ceramides on OxLDL uptake. The uptake of OxLDL is mediated by scavenger receptors including the class A type-I and type-II receptors (SR-A) (Kodama et al. 1990), the CD36 receptor (Endemann et al. 1993; Endemann et al. 1993; Acton et al. 1994), SR-B1/CLA-1 receptor, SR-CI receptor, Fcγ receptor, LOX-1 and SREC receptors. Among these different receptors, CD36 has been identified as the major receptor responding to OxLDL uptake (Nozaki et al. 1995; Febbraio et al. 2000; Nakata et al. 1999). Ceramide has been indicated to reduce the cell surface expression of CD36 on monocytes and macrophages (Chapter 3). It is, therefore, reasonable to hypothesize that ceramide may down-regulate the OxLDL uptake by monocytes and macrophages.

4.2 Results

4.2.1 LDL oxidation measurement

LDL was slightly oxidized using $CuSO_4$ and labeled with DiI. This was measured by electrophoresing LDL and OxLDL in an agarose gel. As Fig 4.1 shows OxLDL, which has fewer positively charged free lysine residues, migrated further than LDL. Migration length from wells is 2.7cm for LDL and 3.0cm for OxLDL. This confirmed that the oxidation of LDL had occurred.

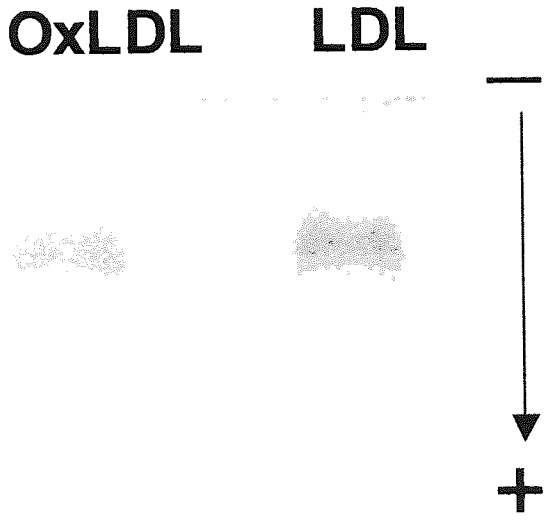

Fig 4.1 Agarose gel electrophoresis of OxLDL and LDL.
10μg OxLDL and 10μg LDL were mixed with bromophenol blue and electrophoresedthrough a 1% agarose Gel at 70V for 1 and half hours in barbital buffer (50mM barbital in distilled water, pH 8.6). Gel was stained with Coomassie blue.

4.2.2 OxLDL recovery rate from desalting column

LDL (the preparation is described in the methods section) was desalted prior to oxidation using PD 10 column. LDL was then oxidized by $CuSO_4$ and then was labeled with DiI. Excess free dye was removed through a PD10 column. The protein concentration was measured before and after desalted through the column. The recovery rate was calculated as below:

$$\frac{\text{Protein concentration before running through column}}{\text{Protein concentration after running through column}} \times 100\%$$

As Table 4.1 shows, the recovery rate from the LDL preparation following its first running through the column is 68.8 ± 1.72 %; following the second elution from a PD10 column it is 74 ± 13.9 %.

4.2.3 OxLDL fluorescence is directly proportional to protein concentration

To demonstrate that the quantity of DiI labeled OxLDL can be determined by measuring DiI fluorescence, a DiI OxLDL fluorescence standard curve was made for each separate experiment. Increasing OxLDL amount affords a linear increase in DiI fluorescence between 0-2 μg OxLDL (Fig 4.2).

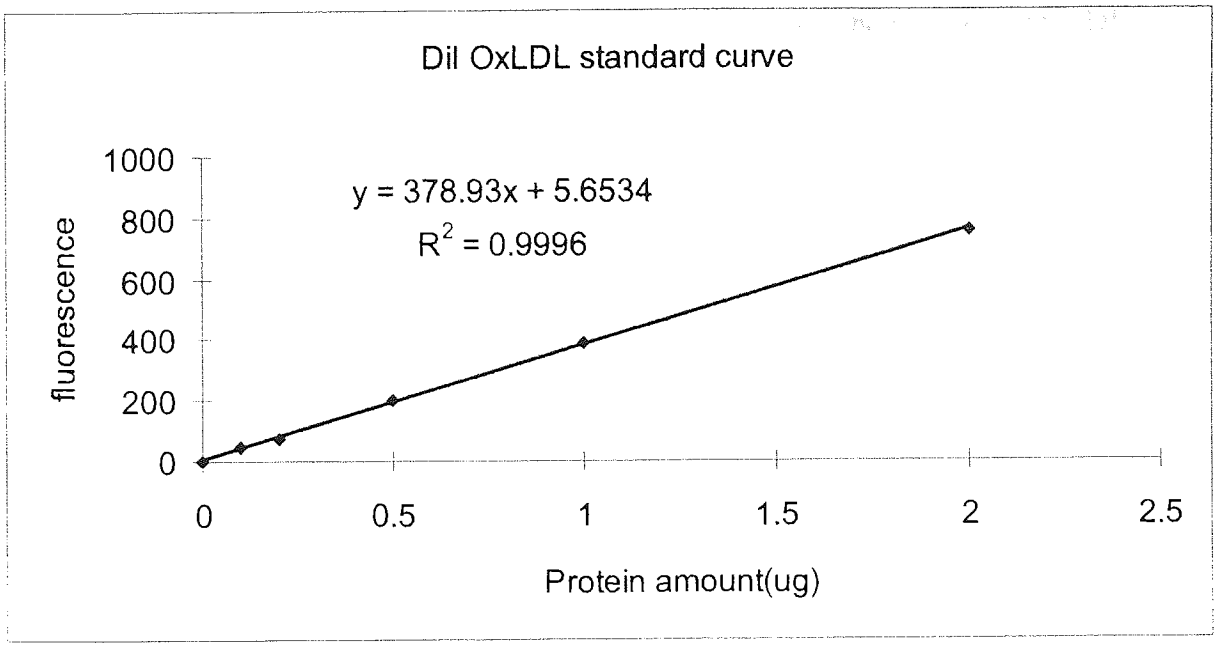

Fig 4.2 Labeled OxLDL standard curve

A DiI OxLDL fluorescence standard curve was made by diluting 0, 0.5, 1, 1.5, 2 μg DiI OxLDL in lysis buffer. Fluorescence was read at the wavelength of excitation 520nm and emission of 590nm utilizing a microplate fluorometer. R^2 is the correlation coefficient.

4.2.4 OxLDL uptake is mediated by receptors

To demonstrate that OxLDL uptake is mediated by receptors, excess (3 times) unlabeled OxLDL was added to compete with labeled OxLDL for uptake by U937 macrophages. As Fig 4.3 shows, unlabeled OxLDL significantly competes with labeled OxLDL, and the uptake of labeled OxLDL was reduced by approximately two thirds.

As CD36 has been suggested to be the major OxLDL receptor, the uptake of OxLDL mediated by receptors was further investigated by adding anti-CD36 antibody. However, anti-CD36 antibody failed to reduce DiI-OxLDL uptake, whereas anti-CD36 antibody further reduced DiI OxLDL uptake in the presence of excess OxLDL, $P<0.01$ (Fig 4.3).

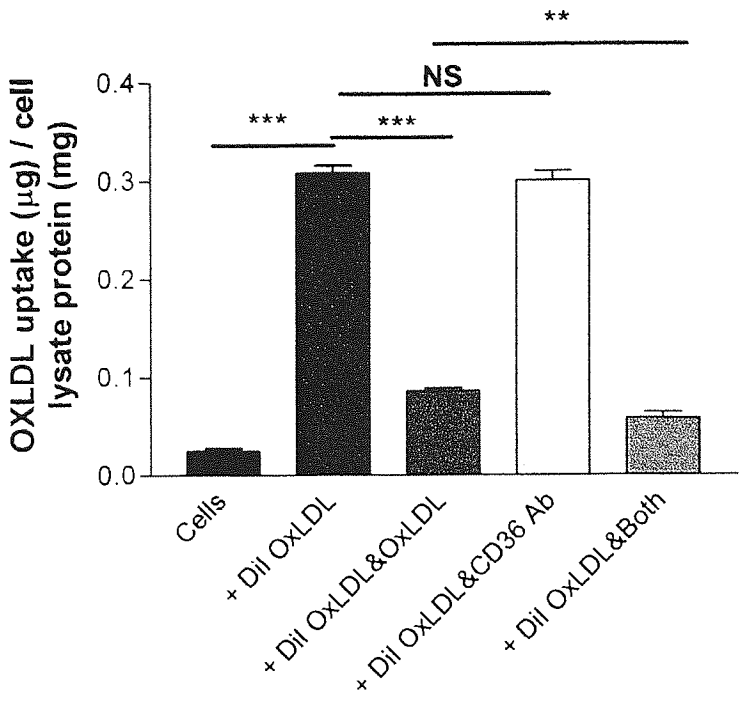

Fig 4.3 OxLDL uptake is mediated by receptors.
U937 cells were differentiated for 24 hours in 100nM PMA in 10% FBS medium in a humidified 5% CO_2, 95% air atmosphere at 37°C. 8ug (8ul) anti-CD36 antibody was added for 30 minutes. 50μg DiIOxLDL in the presence or absence of 150 μg OxLDL were then added for 5 hours. Cells were lysed in 5% Triton X-100 PBS and DiI fluorescence was measured by fluorescence spectrometry at the wavelength of excitation 520nm and emission of 590nm. *** represents P<0.001 for +DiI OxLDL 5 hour compared to cells; *** represents P<0.001 for +DiI OxLDL 5 hours compared to +DiI OxLDL & OxLDL 5 hours; NS represents no significance for +DiI OxLDL 5 hours compared to + DiIOxLDL & CD36; ** represents P<0.01 for +DiI OxLDL & OxLDL 5 hours compared to DiIOxLDL & OxLDL & CD36 by one-way ANOVA statistical analysis followed by Tukey's multiple comparison test.

4.2.5 The effect of ceramide on OxLDL uptake by monocytes

The effect of ceramide on OxLDL uptake was first examined using the U937 monocytic cell line. As ceramide reduces CD36 and CD11b expression after incubation of 15 minutes to 16 hours, 5 and 16 hours were chosen to investigate the effect of ceramide on OxLDL uptake. Fig 4.5 shows that monocytes treated with 20

μM C_2 ceramide for 16 hours took up 20% less OxLDL than control cells, $P<0.01$. However, treatment with C_2 ceramide for 5 hours did not achieve a significant decrease of OxLDL uptake (Fig 4.4).

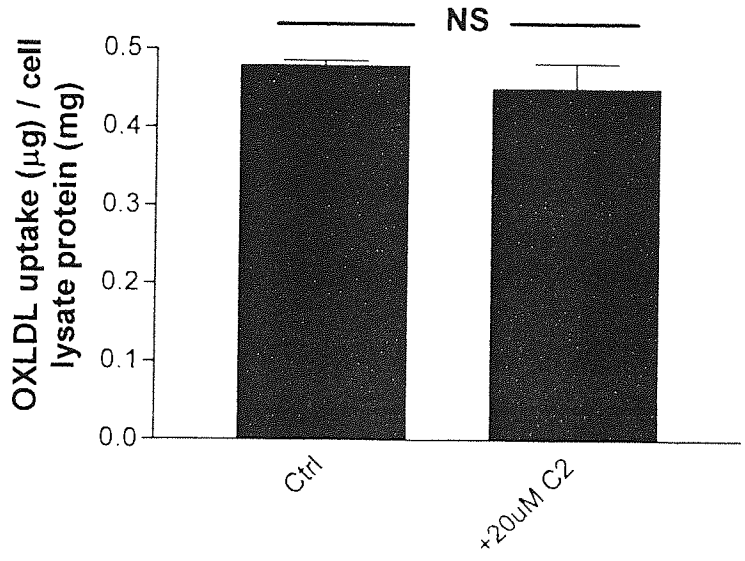

Fig 4.4 C_2 ceramide did not decrease OxLDL uptake by U937 monocyte over 5 hours.

U937 cells were incubated with C_2 ceramide for 5 hours in 10% FBS medium in a humidified 5% CO_2, 95% air atmosphere at 37°C. 50μg DiIOxLDL were added and following incubation of 5 hours, cells were lysed in 5% Triton X-100 PBS. DiI fluorescence was measured by fluorescence spectrometry at the wavelength of excitation 520nm and emission of 590nm. The data are presented as the arithmetic mean ± SEM of triplicate analysis of one individual experiment. NS represents no significance for + 20μM C_2 ceramide compared to control cells by t test statistical analysis

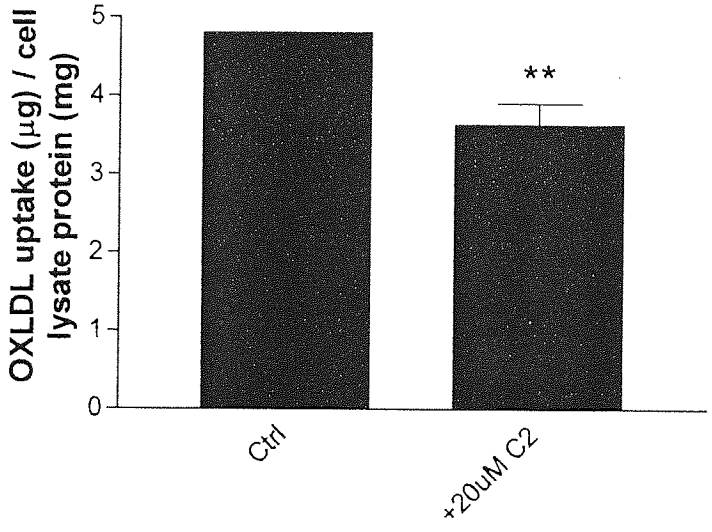

Fig 4.5 C_2 ceramide decreased OxLDL uptake by U937 monocytes over 16 hours.

U937 cells were incubated with 20 μM C_2 ceramide for 4 hours, then with C_2 ceramide and 50μg DiIOxLDL for 16 hours in 10% FBS medium in a humidified 5% CO_2, 95% air atmosphere at 37°C. Cells were lysed in 5% Triton X-100 PBS. Fluorescence was measured by fluorescence spectrometry at the wavelength of excitation 520nm and emission of 590nm. The data are presented as the arithmetic mean ± SEM of one individual experiment. ** represents $P<0.01$ for + 20μM C_2 ceramide compared to control cells by t test statistical analysis

4.2.6 The effect of ceramide on OxLDL uptake by macrophages

The effect of ceramide on OxLDL uptake by macrophages was similar to the effect on monocytes. U937 monocytes were differentiated with 100nM PMA for 8 hours, then incubated with or without C_2 ceramide for 16 hours in presence of PMA; 50μg

DiIOxLDL was added for a final 5 hours of incubation in presence of PMA and ceramide. Alternatively, U937 monocytes were differentiated with 100nM PMA for 4 hours, then with both PMA and C_2 ceramide for 4 hours, 50μg DiIOxLDL were added for a further 16 hours of incubation in presence of PMA and ceramide. The uptake of OxLDL by macrophages after 5 hours incubation was significantly decreased by 20μM C_2 ceramide, $P<0.05$ (Fig 4.6), but levels of uptake were in the order of ten fold less than following 16 hours co-incubation during the differentiation process. After 16 hours treatment, C_2 ceramide (10-50μM) showed an inhibitory effect on OxLDL uptake where 50μM C_2 ceramide significantly reduced OxLDL uptake, $P<0.01$ (Fig 4.7).

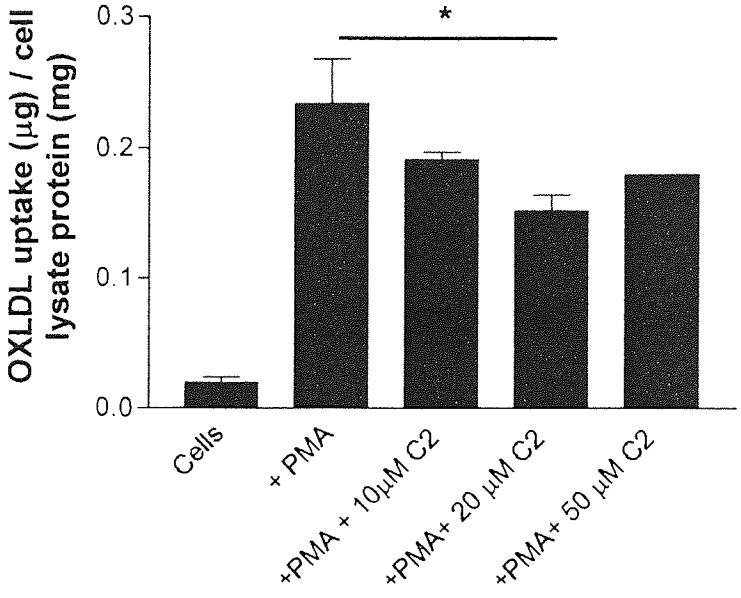

Fig 4.6 C_2 ceramide decreased OxLDL uptake by U937 macrophages.
U937 cells were incubated with 100nM PMA for 8 hours, then with or without C_2 ceramide for 16 hours, 50μg DiIOxLDL was added for a final 5 hours of incubation in 10% FBS medium in a humidified 5% CO_2, 95% air atmosphere at 37°C and cells were then lysed in 5% Triton X-100 PBS. Fluorescence was measured by fluorescence spectrometry at the wavelength of excitation 520nm and emission of 590nm. The data are presented as the arithmetic mean ± SEM of two individual experiments performed in triplicate. * represents $P<0.05$ for +PMA & 20μM C_2 ceramide compared to +PMA by repeated ANOVA statistical analysis followed by Tukey's multiple comparison test .

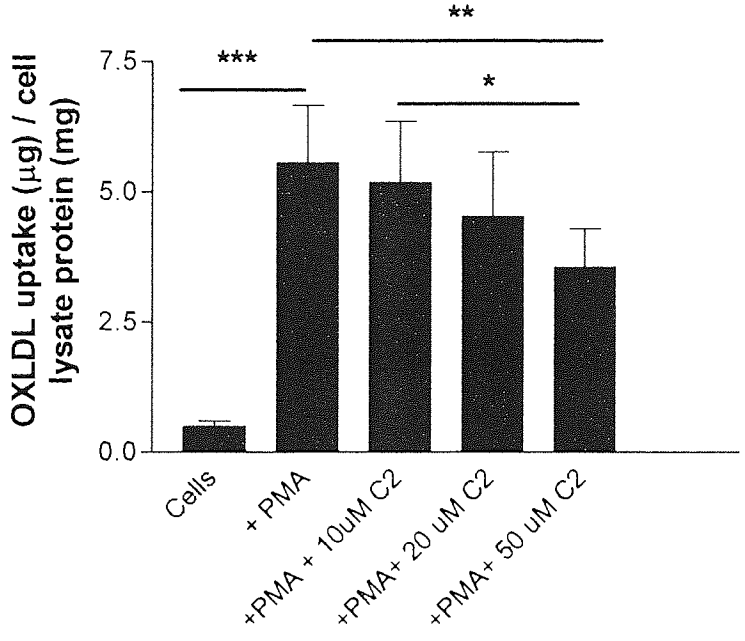

Fig 4.7 C_2 ceramide decreased OxLDL uptake by U937 macrophages.
U937 cells were incubated with 100nM PMA for 4 hours, then with both PMA and C_2 ceramide for 4 hours, 50μg DilOxLDL were added for a further 16 hours of incubation in 10% FBS medium in a humidified 5% CO_2, 95% air atmosphere at 37°C. Cells were lysed in 5% Triton X-100 PBS. Fluorescence was measured by fluorescence spectrometry at the wavelength of excitation 520nm and emission of 590nm. The data are presented as the arithmetic mean ± SEM of two individual experiments performed in triplicate. *** represents $P<0.001$ for +PMA compared to control cells; ** represents $P<0.01$ for +PMA & 50μM C_2 ceramide compared to +PMA; * represents $P<0.05$ for +PMA & 50μM C_2 compared to +PMA & 10μM C_2 by repeated ANOVA statistical analysis followed by Tukey's multiple comparison test.

4.3 Discussion

Ceramide has previously been suggested to play a variety of roles in atherosclerosis. In this chapter, the effect of ceramide on oxidized LDL uptake was studied. In contrast to LDL which is taken up by the LDL receptor, OxLDL uptake is mediated by scavenger receptors (Brown and Goldstein 1986). Mildly oxidized apolipoprotein on LDL is recognized by SR A and other receptors, whereas the oxidized lipid moiety is recognized by CD36 (Nicholson et al. 1995; Rigotti, Acton, and Krieger 1995; Rigotti, Acton, and Krieger 1995; Podrez et al. 2002). However, high levels of oxidation of LDL can denature the recognizable part for receptors, therefore, it cannot be recognized by any receptors. Thus, it was necessary to mildly modify LDL only. It was reported that during LDL oxidation, lysine residues in LDL are modified by lipid peroxidation products, eg: Malondialdehyde (MDA) and 4-hydroxynonenal (HNE) (Requena et al. 1997). Oxidized LDL, therefore loses its positive charge associated with unmodified lysine residues. This is confirmed in this thesis by electrophoresis of LDL and OxLDL.

To measure the amount of OxLDL uptake by monocytes and macrophages after treatment with ceramide, OxLDL was labelled with DiI. Excess DiI was excluded using a PD10 column. This step was to avoid the uptake of free dye by cells. The amount of OxLDL uptake was then quantified by measuring fluorescence and this work shows that the amount of OxLDL is directly proportional to the fluorescence.

To demonstrate that the DiI taken up by cells is still associated with OxLDL rather than transferring from OxLDL to the cells, it is necessary to show that the uptake of DiI is competed out by excess unlabelled OxLDL. The number of receptors on the cell is limited by expression level, therefore, within a fixed period of time, the amount of OxLDL that can be taken up through receptors is defined and should be subject to competition. The role of receptors in OxLDL uptake was thus investigated by adding excess-unlabeled OxLDL to compete with the uptake of labeled OxLDL. These experiments showed that 3 fold addition of unlabelled OxLDL significantly competed the uptake of labeled OxLDL, suggesting that OxLDL uptake in these experiments was mediated by receptors. As CD36 has been reported to be the major OxLDL receptor, engagement of CD36 was expected to reduce the uptake of OxLDL. However, addition of anti-CD36 antibody failed to inhibit the uptake of OxLDL. This is not likely to be due to insufficient antibody, since 8μg amount of anti-CD36 IgG antibody was shown to block the uptake of OxLDL significantly (Lougheed and Steinbrecher 1996). However, these authors studied lower amounts of OxLDL uptake, which may have enabled successful competition with antibody. This is supported by the observation that anti-CD36 antibody was able to significantly enhance the blockade of OxLDL uptake in the presence of excess unlabelled OxLDL. Moreover, ceramide may reduce the levels of other receptors which scavenge OxLDL, thus blockade of CD36 alone would not significantly inhibit the uptake of OxLDL, therefore OxLDL may block scavenger receptors other than CD36.

Ceramide reduces OxLDL uptake by both monocytes and macrophages. OxLDL was added for different times, thus reduced OxLDL uptake induced by ceramide was shown not to be due to the extent of differentiation or ceramide incubation time between 5 and 16 hours. However, uptake of OxLDL by monocytes after 5 hours incubation was not reduced by ceramide, although 5 hours treatment with ceramide significantly reduced the uptake of OxLDL by macrophages. Chapter 3 showed that macrophages were more sensitive to the effects of ceramide as evidenced by greater loss of surface CD36 and this may explain the different effects on uptake.

The uptake of OxLDL after 5 hours incubation with OxLDL was 10 times less than at 16 hours. This maybe because scavenger receptor recycling from the cytosol to the plasma membrane is incomplete over 5 hours and transport of OxLDL is not complete, therefore, the longer the OxLDL was incubated with cells, the more chance cells can take up OxLDL.

As chapter 3 showed a significant reduction of CD36 within 15 minutes, there is the possibility that even after a short time incubation with ceramide, the uptake of OxLDL by cells may still be down-regulated by ceramide. These results are consistent with previous work done by Chen et al (Chen, Rosenwald, and Pagano 1995). In their study, ceramide was shown to reduce both fluid phase and receptor mediated (LDL) endocytosis in Chinese hamster fibroblasts. Ceramide was

pre-incubated with cells in both this study and in their study. However, others have shown that when sphingomyelinase was added to LDL and cells at the same time, LDL uptake was upregulated by SMase (Xu and Tabas 1991). These results suggest that ceramide pre-incubation with cells alone prior to LDL addition is crucial to its effect on LDL or OxLDL uptake. It is possibly because pre-incubation of ceramide with cells results in reduction of receptor expression, so that results in less LDL or OxLDL uptake. When SMase was added to LDL and cells at the same time, it may tend to associate with LDL, and promote LDL aggregation by increasing ceramide content in LDL. Interestingly, aggregated LDL was observed to enhance CD36 expression (Chen, Rosenwald, and Pagano 1995). Further study is needed to investigate the effect of ceramide on OxLDL or LDL uptake. The reduction of OxLDL uptake by macrophages reduces the risk of foam cell formation, however, this raises the question of how OxLDL is cleared from plasma. In vivo, an alternative mechanism instead of macrophage uptake of OxLDL clearance is indicated by using SR knockout mice. These mice lack SR and a were fed a high-fat diet. The OxLDL uptake and atherogenic lipid laden lesions were successfully reduced compared with SR +/+ mice. On the other hand, the OxLDL level in plasma was still normal. This result suggests that there is an alternative non-atherogenic way of OxLDL clearance from the circulation (Suzuki et al. 1997).

Chapter 5 The mechanism of the down-regulation of CD36 by ceramide

Previous work described in Chapters 3 and 4 has demonstrated that ceramide down-regulates the expression of the OxLDL scavenger receptor CD36 and OxLDL uptake by monocytes and macrophages. This chapter describes an investigation of the mechanism through which ceramide exerts its effects by examining whether ceramide reduces surface CD36 through decreasing cellular peroxide, reducing the CD36 mRNA expression, preventing intracellular CD36 transport, promoting shedding of soluble CD36, and disrupting CD36 in lipid rafts.

5.1 Introduction

Oxidative stress has been demonstrated to up-regulate CD36 expression and OxLDL uptake through inducing lipid peroxidation. Inhibition or stimulation of cellular oxidative stress resulted in inhibition or increase of OxLDL uptake by macrophage and cellular CD36 mRNA expression, respectively (Fuhrman, Volkova, and Aviram 2002). Ceramide has been previously reported to reduce the cytosolic peroxide (Phillips and Griffiths 2003). Therefore, ceramide may decrease CD36 expression through down-regulating cellular peroxide.

There are also some other mechanisms by which ceramide may reduce CD36. Firstly, ceramide may transcriptionally reduce the expression of CD36. CD36 expression is regulated by PPARγ. Stimulation of PPARγ by OxLDL or PPARγ agonists result in overexpression of CD36 (Tontonoz et al. 1998; Nagy et al. 1998). Tumor necrosis

factor alpha (TNFalpha) signalling, which is mediated through ceramide, decreases the expression of peroxisome proliferator-activated receptor gamma (PPARgamma). Endogenous, C_6- and C_2- ceramide are reported to reduce the expression of PPARgamma mRNA and protein in a time and concentration dependent manner (Kajita et al. 2004; Sprott et al. 2002). Thus, ceramide may decrease CD36 expression through inhibiting PPARγ transcriptional activity.

Secondly, ceramide may reduce CD36 expression by increasing the degradation of the protein. Studies utilizing a biomembrane model show that ceramide results in formation of vesicles (Holopainen, Angelova, and Kinnunen 2000). The experiments using cells resulted in a similar effect, where adding SMase exogenously to ATP-depleted macrophages and fibroblasts results in the budding of numerous vesicles from the plasma membrane into cytoplasm (Zha et al. 1998). Short chain ceramides have similar effects to SMase catalyzed long chain ceramides (Li, Blanchette-Mackie, and Ladisch 1999). Enhanced endocytosis may result in more protein degradation. It was reported that CD36 surface expression can be down-regulated by promoting proteasome activity (Munteanu, Ricciarelli, and Zingg 2004). Therefore, ceramide may induce the degradation of CD36 protein.

Ceramide has also been observed to slow the transport of endocytosed protein from endosomes to lysosomes (Chen, Rosenwald, and Pagano 1995). Therefore, ceramide may cause protein "jamming" inside the cells and down-regulate protein surface

expression.

In other studies, ceramide has been demonstrated to be involved in membrane protein shedding. L-selectin shedding was inducible by treatment of cells with bacterial sphingomyelinase, and also through exogenous application of a cell-permeable ceramide (Walev et al. 2000). In contrast, the amount of soluble form of CD54 (sCD54) in the culture supernatants of HUVECs was reduced by C_2 ceramide (Kawakami et al. 2002). A soluble CD36 form has also been discovered (Pearce, Wu, and Silverstein 1994), suggesting that ceramide may regulate CD36 surface expression by altering the rate of shedding of CD36.

5.2 Results

5.2.1 C_2 ceramide induces a loss of intracellular peroxide.

Total cellular peroxide level was measured by adding the redox sensitive fluorescent dye DCFHDA and measuring ROS induced fluorescence by flow cytometry. Figure 5.1 shows that C_2 ceramide induced a loss of monocytic intracellular peroxide with both 10μM and 20μM doses ($P<0.01$).

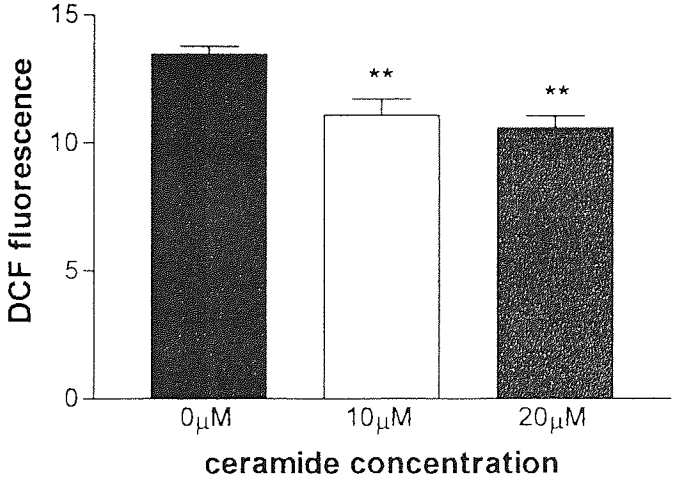

Fig 5.1 C_2 ceramide reduces the intracellular ROS level in U937 monocytes.
U937 monocytes were starved in serum free medium for 4 hours, and then different doses of C_2 ceramide were added with 16 hours incubation in a humidified 5% CO_2, 95% air atmosphere at 37°C. The DCFHDA assay was used to measure intracellular peroxide level and DCF fluorescence was measured by flow cytometry. The data are presented as the arithmetic mean ± SEM. n=6, **represents $P<0.01$ for 10μM and 20μM C_2 ceramide 16 hours compared to resting U937 monocytes by one-way ANOVA statistical analysis followed by Tukey's multiple comparison test.

5.2.2 C_2 ceramide reduces CD36 independent of the NADPH oxidase activity

Ceramide reduces the cellular peroxide level probably through inhibiting NADPH oxidase activity(Phillips and Griffiths 2003). To investigate whether C_2 ceramide reduces CD36 cell surface expression through down-regulating cellular peroxide level, the NADPH oxidase inhibitor, diphenyleneiodonium sulfate (DPI) was used to down regulate ROS production. Fig 5.2 shows that 1μM DPI 16 hours did not decrease the expression of CD36, whereas C_2 ceramide significantly reduces CD36 cell surface expression ($P<0.001$). Co-treatment with DPI and C_2 ceramide did not significantly change CD36 expression compared with C_2 ceramide alone. These results suggest that C_2 ceramide reduced cell surface expression of CD36 independently of inhibiting NADPH oxidase.

As a positive control, 100nM PMA 16 hours treatment, significantly increased CD36 expression ($P<0.001$).

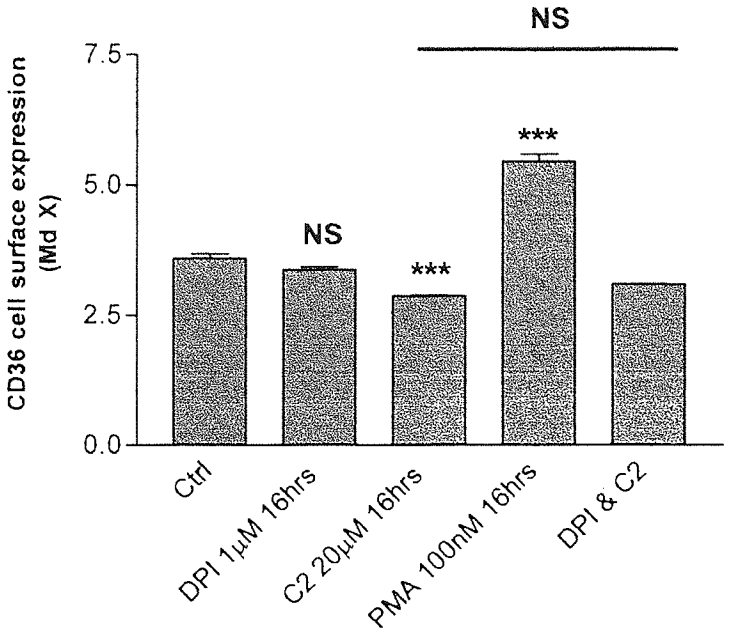

Fig 5.2 C_2 ceramide reduces CD36 cell surface expression independent of the NADPH oxidase activity.

U937 monocytes were starved in serum free medium for 4 hours prior to incubation with 20μM C_2 ceramide, 1μM DPI or both, or 100nM PMA for 16 hours in a humidified 5% CO_2, 95% air atmosphere at 37°C. Cell surface CD36 expression was measured by flow cytometry. NS represents no significance for 1μM DPI compared to control cells; *** represents $P<0.001$ reduction for 20μM C_2 ceramide compared to control cells; *** represents $P<0.001$ induction for 100nM PMA compared to control cells; NS represents no significance for DPI & C_2 ceramide compared to 20μM C_2 ceramide. The data are presented as the arithmetic mean ± SEM. n=9, one-way ANOVA statistical analysis was used followed by Tukey's multiple comparison test.

5.2.3 C_2 ceramide does not reduce CD36 total cellular protein level

5.2.3.1 C_2 ceramide does not reduce CD36 total cellular protein level examined by flow cytometry

To assess whether ceramide reduces the total cellular protein level of CD36 and CD11b, a detergent, saponin was used to make the cell membrane permeable for antibodies. Total cellular CD36 and CD11b level was measured by flow cytometry. 10μM C_2 ceramide reduced surface but not total cellular CD36 and CD11b. 20 μM C_2 ceramide significantly decreased whole cellular CD36 protein, $P<0.05$ (Fig 5.3). The loss of whole cellular CD36 induced by 20 μM C_2 ceramide (approximately 20% of control) was not as much as the reduced cell surface level (approximately 10% of control).

Similarly, 10 and 20 μM C_2 ceramide did not significantly reduce the whole cellular CD11b protein (Fig 5.3), but significantly reduced cell surface expression of CD11b.

A

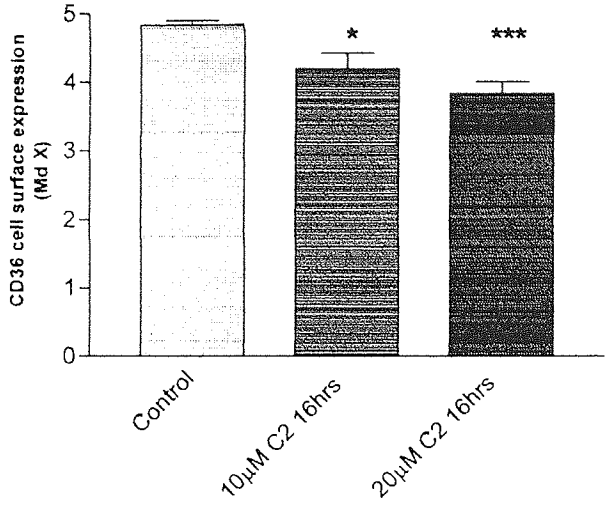

B

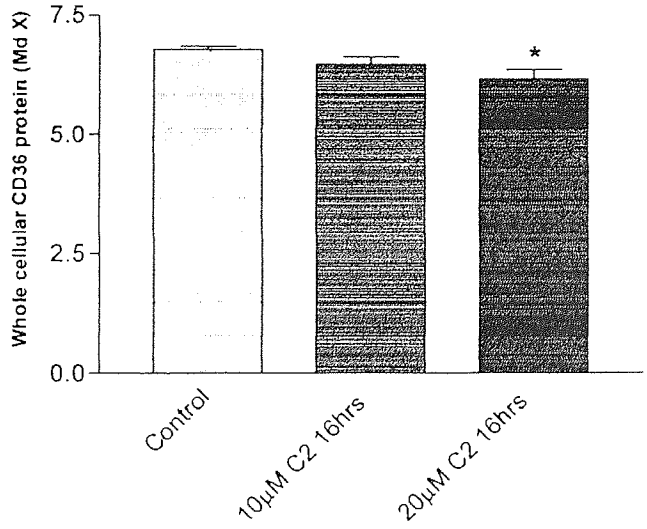

Fig 5.3 C_2 ceramide reduces CD36 cell surface expression to a greater extent than total cellular protein.

U937 monocytes were starved in serum free medium for 4 hours prior to incubation with 10 and 20μM C_2 ceramide for 16 hours in a humidified 5% CO_2, 95% air atmosphere at 37°C. A: Cell surface CD36 expression was measured by flow cytometry. * represents $P<0.05$ for 10μM C_2 ceramide compared to control cells; *** represents $P<0.001$ for 20μM C_2 ceramide compared to control cells; B: Total cellular CD36 protein was measured by flow cytometry. * represents $P<0.05$ for 20μM C_2 ceramide compared to control cells. The data are presented as the arithmetic mean of MdX ± SEM. n=9, one-way ANOVA statistical analysis was used followed by Tukey's multiple comparison test.

A

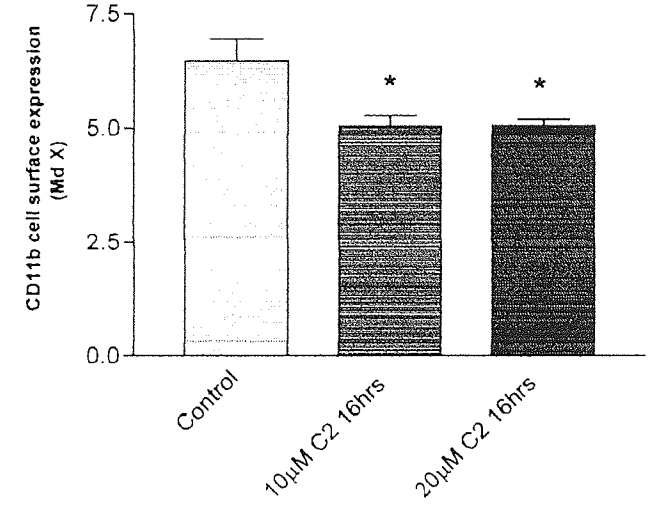

B

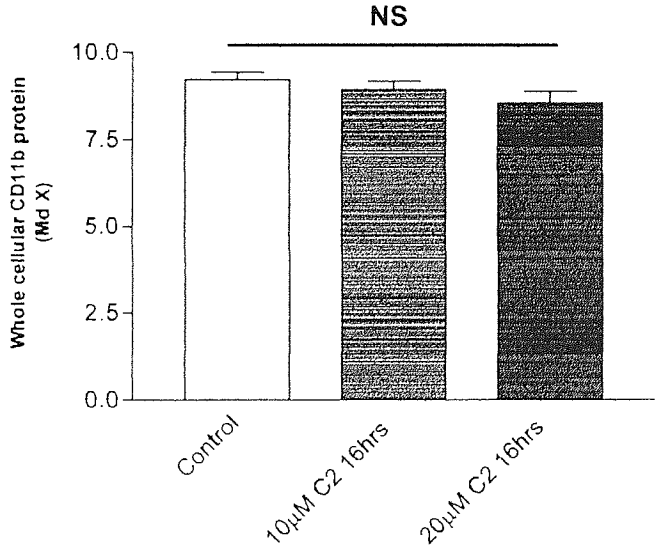

Fig 5.4 C_2 ceramide reduces CD11b cell surface expression, but not total cellular protein.

U937 monocytes were starved in serum free medium for 4 hours prior to incubation with 10 and 20μM C_2 ceramidefor 16 hours in a humidified 5% CO_2, 95% air atmosphere at 37°C. A: Cell surface CD11b expression was measured by flow cytometry. * represents $P<0.05$ for 10 and 20 μM C_2 ceramide compared to control cells; B: Total cellular CD11b protein was measured by flow cytometry. NS represents no significance for 10 and 20 μM C_2 ceramide compared to control cells. The data are presented as the arithmetic mean of MdX ± SEM. n=9, one-way ANOVA statistical analysis was used followed by Tukey's multiple comparison test.

5.2.3.2 C_2 ceramide induces CD36 total cellular protein level examined by western blot

The total cellular CD36 protein was also determined using western blot. In contrast to the flow cytometry data, Fig 5.5 shows that 20μM C_2 ceramide 16 hours treatment upregulated total cellular CD36 level. Both mature protein and the precursor of CD36 were upregulated.

A

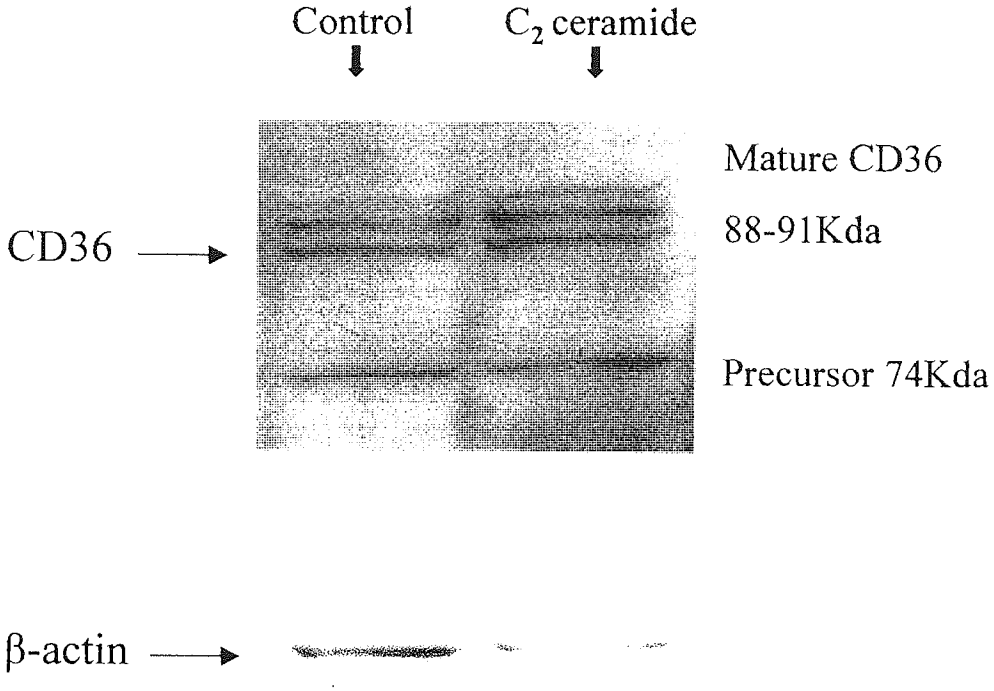

B

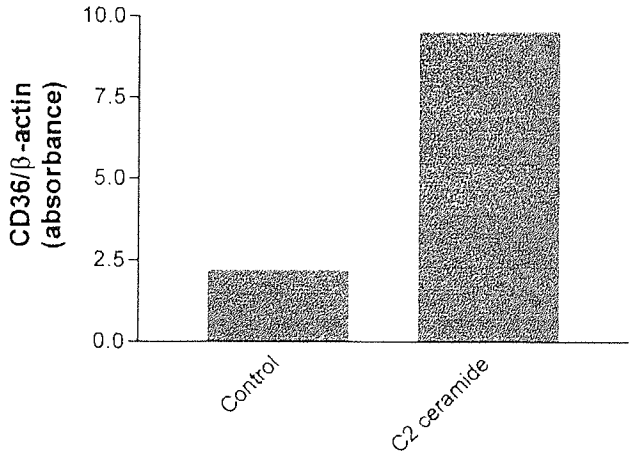

Fig 5.5 C_2 ceramide induces total cellular CD36.
U937 monocytes were starved in serum free medium for 4 hours prior to incubation with 20μM C_2 ceramide for 16 hours in a humidified 5% CO_2, 95% air atmosphere at 37°C. A: CD36 and β-actin (internal control) in cell lysate were detected by western blot; B: Densitometric analysis of bands from A. These experiments were repeated individually 3 times.

5.2.4 Ceramide promotes CD36 mRNA expression in macrophages

To determine whether CD36 expression was reduced at the transcriptional level by C_2 ceramide, CD36 mRNA expression was determined by RT-PCR after ceramide treatment. Ceramide did not reduce CD36 mRNA expression after 24 hours. In contrast, C_2 ceramide induced the mRNA expression of CD36 in PMA differentiated U937 macrophages. As Fig 5.6 shows, 20 and 50μM C_2 ceramide treatment for 16 hours incubation significantly induced CD36 mRNA expression in early differentiated U937 macrophages ($P<0.05$).

A

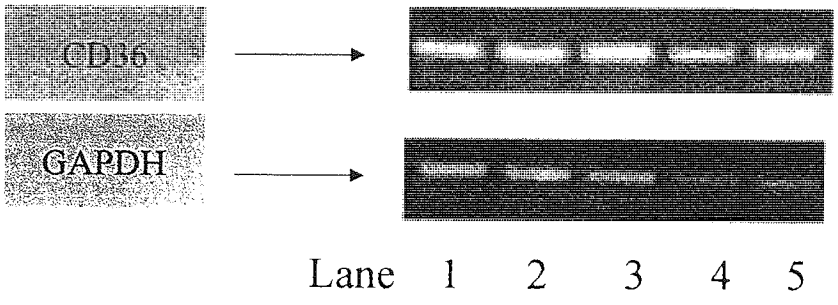

B

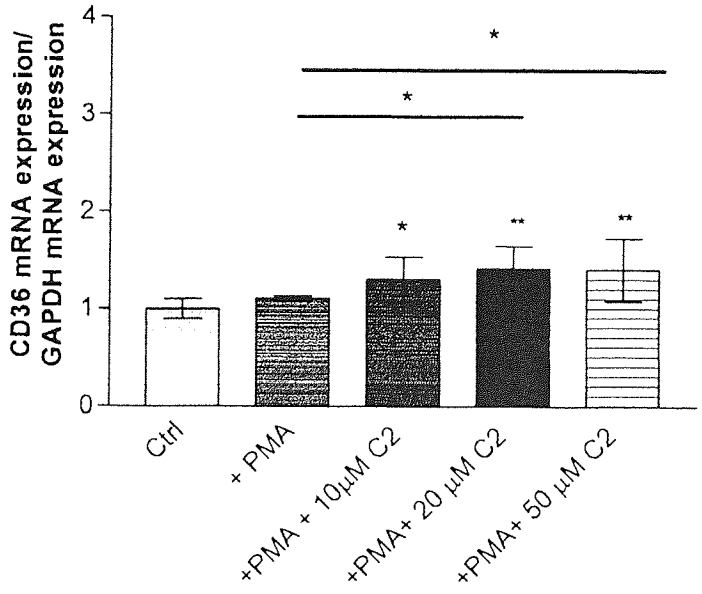

Fig 5.6 C_2 ceramide increases CD36 mRNA expression.
U937 cells were incubated with 100nM PMA for 8 hours, then with both PMA and C_2 ceramide for 16 hours in a humidified 5% CO_2, 95% air atmosphere at 37°C, CD36 mRNA expression was measured by RT-PCR. **A:** Bands on agarose gel. Lane 1: Control; 2: PMA 24hrs; 3: PMA 24hrs& 10μM C2 16hrs; 4: PMA 24hrs& 20μM C2 16hrs; 5: PMA 24hrs& 50μM C2 16hrs. B: Bands were analysed. The data are presented as the arithmetic mean ± SEM of three individual experiments. n=6, * represents $P<0.05$ for PMA + 20μM C_2 ceramide and PMA + 50μM C_2 ceramide compared to PMA treated cells; * represents $P<0.05$ for PMA + 10μM C_2 ceramide compared to control cells; ** represents $P<0.01$ for PMA + 20μM C_2 ceramide and PMA + 50μM C_2 ceramide compared to control cells by repeated ANOVA statistical analysis followed by Tukey's multiple comparison test .

5.2.5 Effect of ceramide on PPARγ

As Fig 5.6 shows, C_2 ceramide treatment induces CD36 mRNA expression in early differentiated U937 macrophages, and PPARγ has been demonstrated to be an important transcription factor in the expression of CD36, therefore the effect of ceramide on PPARγ was investigated.

Two PPARγ agonists, troglitazone (Tro) and rosiglitazone (Rosi) were used to activate PPARγactivity and their ability to enhance CD36 expression was studied. However, a variety of doses of Tro and Rosi over 24 hours incubation did not stimulate CD36 expression on U937 monocytes. In contrast, 100nM PMA 24 hours treatment significantly induced surface expression of CD36 (Fig 5.7A). Different dose of Tro over 48 hours also did not successfully induce CD36 expression (Fig 5.7B).

A

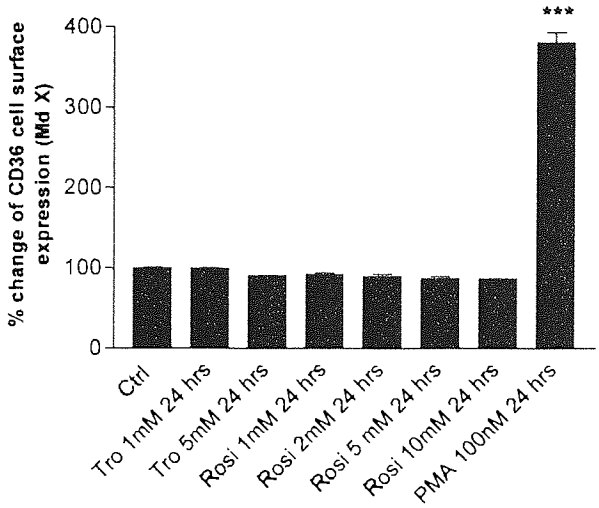

B

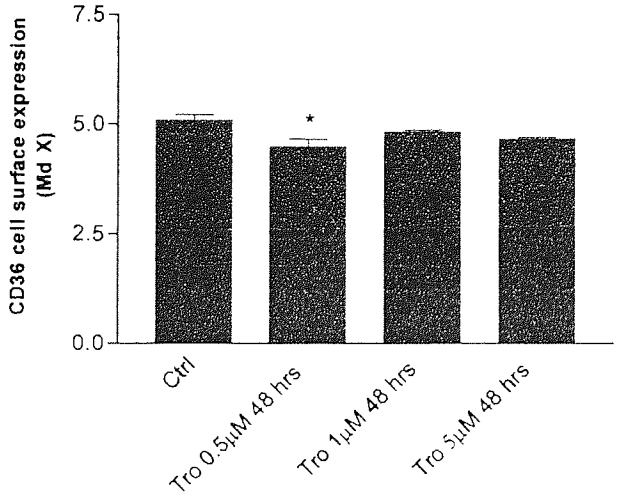

Fig 5.7 PPARγagonists do not activate CD36 cell surface expression on U937 monocytes.

U937 monocytes were starved in serum free medium for 4 hours prior to incubation with 100nM PMA for 24 hours or with different doses of troglitazone (Tro) and rosiglitazone (Rosi) for 24 or 48 hours in a humidified 5% CO_2, 95% air atmosphere at 37°C. Cell surface CD36 expression was measured by flow cytometry. **A**: *** represents $P<0.001$ for 100nM PMA 24 hours compared to control cells; Treatment with 1 and 5μM troglitazone and 1, 2, 5, 10μM rosiglitazone 24 hours incubation had no significant effect compared to control cells. **B**: 1 or 5 μM troglitazone 48 hours incubation shared no significant effect compared to control cells; * represents $P<0.05$ for 0.5 μM troglitazone 48 hours incubation compared to control cells. The data are presented as the arithmetic mean ± SEM from 3 individual experiments, n=9, one-way ANOVA statistical analysis was used followed by Tukey's multiple comparison test.

The effect of ceramide on PPARγ was further investigated using a PPARγ DNA-binding assay kit from Active Motif. As Fig 5.8 shows the positive control nuclear extract (PMA stimulated THP-1 cells) caused significant induction of PPARγ DNA binding activity compared to control cells ($P<0.001$). Both positive and negative competitors (mutate oligo and wild type oligo, respectively) failed to compete with the positive control nuclear extract (THP-1 + ve ctrl). Treatment of U937 monocytes with the PPARγantagonist bisphenol A diglycidyl ether (BADGE; 10 and 100μM) over 4 hours incubation causes a significant reduction in DNA-binding activity of nuclear extract compared to control cells ($P<0.05$). 10μM Tro for 4 hours, 1μM Tro 24 for hours, 20μM C_2 ceramide treatment of U937 cells for 15 minutes and 16 hours, 100nM PMA 24 hours and co-incubation of 100nM PMA 24 hours and 20μM C_2 ceramide 16 hours did not significantly change DNA-binding activity of extracted proteins compared to proteins extracted from corresponding control cells.

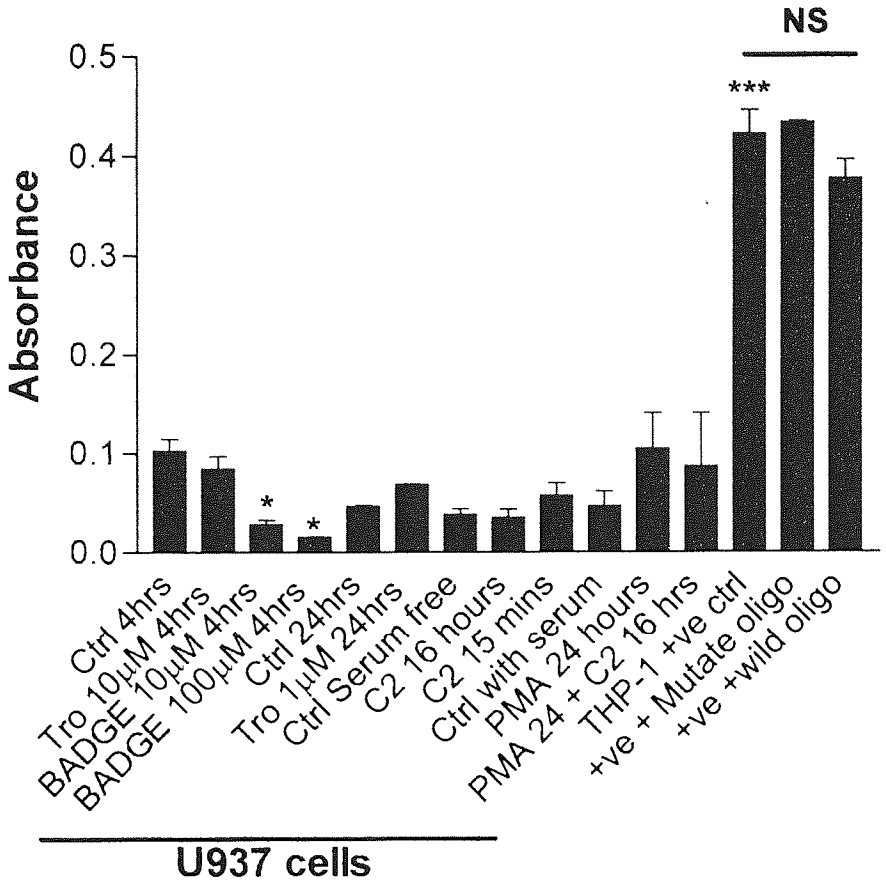

Fig 5.8 The effect of ceramide on PPARγ DNA binding activity.

U937 monocytes were starved in serum free medium for 4 hours prior to incubation with 10μM troglitazone, 10 and 100μM BADGE for 4 hours, or with 1μM troglitazone for 24 hours, or 20μM C_2 ceramide for 15 minutes or 16 hours in a humidified 5% CO_2, 95% air atmosphere at 37°C. For the study of early differentiated U937 macrophages, cells were incubated with 100nM PMA for 8 hours, then with or without 20μM C_2 ceramide for 16 hours in a humidified 5% CO_2, 95% air atmosphere at 37°C. Nuclear proteins were extracted from cells and PPARγ DNA-binding was measured using TransAM PPARγ assay kit following the protocol offered by manufacturer. *** represents $P<0.001$ for positive control nuclear extract (PMA stimulated THP-1 cells) compared to control cells; NS represents no significance for stimulated THP-1 cells + mutated oligo and stimulated THP-1 cells + wild oligo competitor compared to stimulated THP-1 cells; * represents $P<0.05$ for 10 and 100μM BADGE 4 hours incubation compared to control cells. The remaining treatment treatments were not significantly different compared to corresponding control cells. The data are presented as the arithmetic mean ± SEM from one experiment, n=3, one-way ANOVA statistical analysis was used followed by Tukey's multiple comparison test.

5.2.6 Ceramide reduces the shedding of CD36

The effect of ceramide on soluble CD36 level was measured by collecting the supernatant of cell cultures after treatment with C_2 ceramide and measuring soluble CD36 using western blot. Fig 5.9 shows that 20μM C_2 ceramide 16 hours treatment strongly reduced the shedding of CD36 to one quarter of the control level.

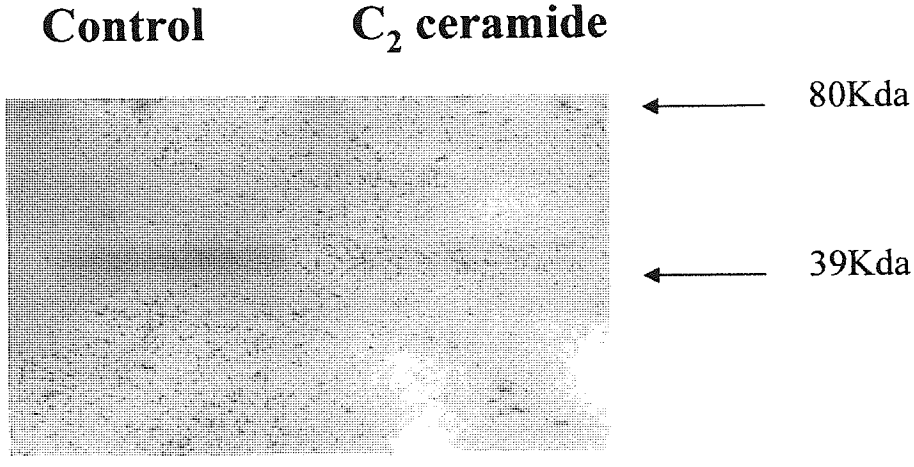

Treatment	Control	20 μM C_2 ceramide 16 hours
Band intensity	12876	2883

Fig 5.9 Ceramide reduces the shedding of CD36.
U937 monocytes were starved in serum free medium for 4 hours prior to incubation with 20μM C_2 ceramide for 16 hours in a humidified 5% CO_2, 95% air atmosphere at 37°C. The supernatant was then collected and concentrated in a vacuum centrifuge. The supernatant protein (6μg) was then separated by SDS-PAGE, and analyzed by western blot for soluble CD36. These experiments were repeated individually 3 times. Bands density was analysed and quantified using GeneTool software. 20μM C_2 ceramide reduced the soluble CD36 to approximately one quarter of the control level.

5.2.7 Effect of ceramide on CD36 in lipid rafts

To determine whether ceramide reduces CD36 cell surface expression through affecting lipid raft formation, detergent insoluble low-density domains (rafts) were separated by detergent sucrose gradient ultracentrifugation. Flotillin-1 was chosen as the marker of rafts. As Fig 5.10 shows, rafts were separated at the interface of 5 and 30 % sucrose (Fraction 3, 4 and 5). Staining with anti-CD36 antibody indicates that the majority of CD36 protein was found in non-raft fractions and ceramide treatment did not change the CD36 distribution in rafts.

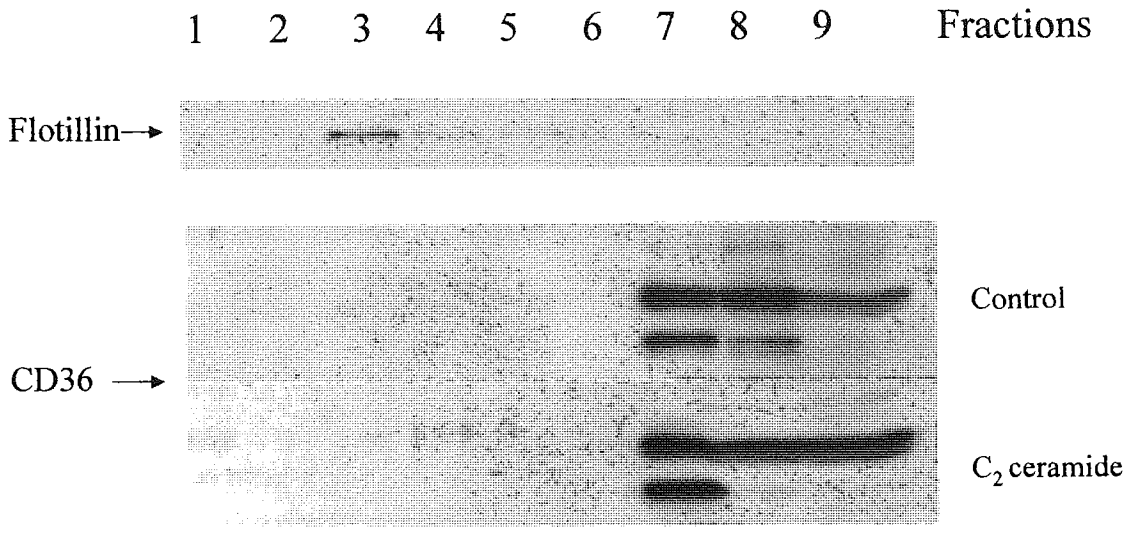

Fig 5.10 Ceramide did not alter CD36 distribution of CD36 in lipid rafts

U937 cells were incubated at 37°C with or without 20μM ceramide for 16 hours. Lipid rafts were then isolated by sucrose gradient ultracentrifugation of the cold Triton X-100 cell lysate. Nine fractions were collected from the top to the bottom of the tube. Fractions were then electrophoresed on SDS-PAGE. Western blotting was used to measure raft marker, flotillin-1 and CD36.

5.2.8 Effects on intracellular transport and proteasome inhibition on CD36 expression

A recent study suggested that CD36 expression is modulated by the ubiquitin-proteasome system (Munteanu, Ricciarelli, and Zingg 2004). To assess whether ceramide reduces surface CD36 by affecting proteasome activity, lactacystin (lacta) known as an inhibitor of 20S proteasome, was used, and the CD36 cell surface expression was measured by flow cytometry. CD11b expression was monitored under the same treatment. Lacta (50μM; 18 hours treatment) did not significantly increase surface CD36 and CD11b expression. Co-treatment with lacta and ceramide achieved a similar reduction as ceramide alone (Fig 5.11 and 5.12).

Brefeldin A (BFA) is known to inhibit protein secretion and expression on the plasma membrane (Misumi et al. 1986) through blocking protein transport from the endoplasmic reticulum (ER) to the Golgi complex (Zuber et al. 1991). To investigate whether ceramide mimicks BFA in reducing CD36 and CD11b expression through blocking receptor exportation to the plasma membrane, BFA was used to treat the cells. CD36 and CD11b surface expression was measured by flow cytometry. Fig 5.11 and 5.12 show that 10μg/ml BFA successfully decreased CD36 and CD11b cell surface expression compared to control cells, $P<0.001$ and $P<0.01$ respectively.

Co-treatment with ceramide and BFA further reduced CD36 expression compared to ceramide alone, $P<0.01$ (Fig 5.11). Co-treatment with ceramide and BFA reduces CD11b expression, $P<0.001$ to a greater extent than ceramide alone, $P<0.05$ (Fig 5.12), but there was no significant difference between the effect of C_2 ceramide and the effect of C_2 ceramide with BFA on CD11b expression.

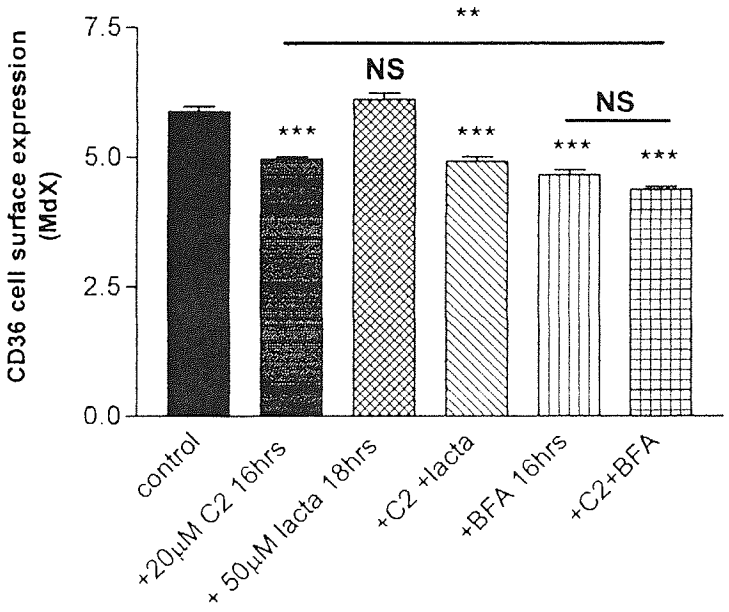

Fig 5.11 Ceramide may not reduce CD36 cell surface expression through activating proteasome but possibly though blocking protein transport from the ER to the Golgi.

U937 monocytes were starved in serum free medium for 4 hours prior to incubation with C_2 ceramide or BFA or both for 16 hours in a humidified 5% CO_2, 95% air atmosphere at 37°C. Cells were pre-incubated with lactacystin for 2 hours before ceramide was added. Cell surface CD36 expression was measured by flow cytometry. *** represents $P<0.001$ for C_2 ceramide (20μM 16 hours), lacta (50μM; 18 hours) + C_2 ceramide (20μM 16 hours), BFA (10μg/ml; 16 hours) and BFA + C_2 ceramide (16 hours) compared to control; NS represents no significance for lacta (50μM; 18 hours) compared to control and for BFA + C_2 ceramide (16 hours) compared to BFA (10μg/ml; 16 hours); ** represents $P<0.01$ for BFA + C_2 ceramide (16 hours) compared to C_2 ceramide (20μM 16 hours). The data are presented as the arithmetic mean ± SEM. n=9, one-way ANOVA statistical analysis was used followed by Tukey's multiple comparison test.

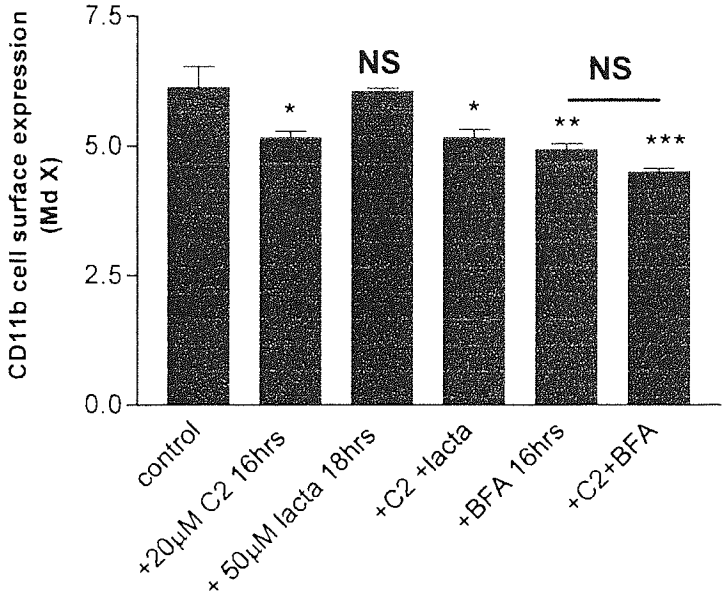

Fig 5.12 Ceramide may not reduce CD11b cell surface expression through activating proteasome but possibly through blocking protein transport from the ER to the Golgi.

U937 monocytes were starved in serum free medium for 4 hours prior to incubation with C_2 ceramide or BFA or both for 16 hours in a humidified 5% CO_2, 95% air atmosphere at 37°C. Cells were pre-incubated with lactacystin for 2 hours before ceramide was added. Cell surface CD11b expression was measured by flow cytometry. * represents $P<0.05$ for C_2 ceramide (20μM 16 hours) and lacta (50μM; 18 hours) + C_2 ceramide (20μM 16 hours) compared to control; ** represents $P<0.01$ for BFA (10μg/ml; 16 hours) compared to control; *** represents $P<0.001$ for BFA + C_2 ceramide (16 hours) compared to control; NS represents no significance for lacta (50μM; 18 hours) compared to control and for BFA + C_2 ceramide (16 hours) compared to BFA (10μg/ml;16 hours). The data are presented as the arithmetic mean ± SEM. n=9, one-way ANOVA statistical analysis was used followed by Tukey's multiple comparison test.

5.3 Discussion

Ceramide has been shown to reduce CD36 cell surface expression and OxLDL uptake as demonstrated in chapter 3 and 4. The mechanism through which ceramide reduce CD36 expression was investigated further in this chapter. The original hypothesis that ceramide reduces CD36 expression through down-regulating cellular peroxide, was first tested by examining the effect of peroxide on the expression of CD36. The NADPH oxidase inhibitor, diphenyleneiodonium sulfate (DPI) was therefore used to inhibit the production of ROS in this study. 1μM DPI (16 hours) incubation significantly reduced the intracellular peroxide, whereas this treatment did not reduce the expression of CD36 and CD11b. Co- incubation with DPI and ceramide did not result in significant change on the expression of CD36 and CD11b. These results suggest that ceramide reduces CD36 and CD11b surface expression independent of inhibiting NADPH oxidase. The effects of ceramide on the expression of CD36 and CD11b and NADPH oxidase appear to be parallel.

Fuhrman and his colleague have shown that oxidative stress increases the expression of CD36 and OxLDL, however, their experiments were done using a mouse model and 6 weeks of dietary antioxidant treatment (Fuhrman, Volkova, and Aviram 2002). These may suggest that long incubation is needed for oxidative stress to activate CD36 expression.

The total cellular CD36 and CD11b protein content was also monitored after ceramide treatment by permeabilising the cell membrane with saponin followed by antibody staining and flow cytometry. Ceramide reduced the surface expression of CD36 more than total cellular protein and did not significantly reduce the total cellular CD11b, suggesting that ceramide may prevent CD36 and CD11b export from inside cells. However, the total cellular CD36 level examined by western blotting shows that the level of mature protein and precursor of CD36 were all strongly upregulated after ceramide treatment. The reason why the total cellular CD36 protein from flow cytometry data is lower than western blot data is not clear. However, ceramide may block CD36 inside the ER, where the receptor may be de-glycosylated and may not be recognized by the antibody for flow cytometry. However, if the receptor is denatured to its primary structure as in SDS-PAGE, the antibody used in flow cytometry should still be able to recognize the receptor, since the antibody can recognize CD36 in immunoblotting under both non-reducing and reducing conditions (Information provided by manufacturer) (Zeng et al. 2003).

Brefeldin A (BFA) is known to inhibit protein secretion and expression on the plasma membrane (Misumi et al. 1986) by blocking protein transport from the ER to the Golgi (Zuber et al. 1991). In the present study, BFA was used to investigate whether ceramide reduces CD36 and CD11b exportation to the cell surface in a similar manner. The data observed here suggest that C_2 ceramide may reduce cell surface CD36

expression partly through blocking the receptor transportation from the ER to the Golgi because addition of ceramide had little effect on the BFA mediated reduction in CD36. This effect of ceramide can be further examined using antibody staining and confocal microscopy to localize subcellular compartmentalisation action.

CD36 expression has also been demonstrated to be modulated by ubiquitin-proteasome system (Munteanu et al. 2005). Lactacystin (lacta), an inhibitor of 20S proteasome inhibitor, was used to investigate whether CD36 expression by U937 cells is affected by proteasomal activity and to determine whether inhibition of the proteasome decreases the effect of ceramide on surface CD36 expression. Lacta did not significantly increase CD36 and CD11b expression. Co-treatment with lacta and ceramide did not protect the reduction of receptors induced by ceramide, suggesting that ceramide did not activate proteasome activity. The possibility that Lacta did not effectively inhibit proteasome cannot be excluded, since Lacta treatment did not induce surface CD36 expression. The effect of ceramide and Lacta on proteasome can be further examined by extracting the whole cell protein and measuring the proteasome activity using the assay kit from Chemicon (Munteanu et al. 2005).

The degradation of CD36 by proteasomes is suggested because inhibition of proteasomes by the HIV drug ritonavir and proteasome inhibitor ALLN is associated with an increase in CD36 surface expression. However, the inhibition of proteasome

does not result in direct promotion of CD36 ubiquitination despite of a general increase in ubiquitinated proteins (Munteanu et al. 2005). As membrane proteins are not usually degraded by the proteasome, there are two possible pathways by which CD36 may be degraded by proteasome. One is that an undefined protein, which regulates CD36 endocytosis and subsequently degradation, is modulated by the proteasome. This possibility has been demonstrated to be the case for SR-BI, a scavenger receptor closely related to CD36. Another possibility is that CD36 may have a particular proteasome-targeting domain, or that OxLDL bound to CD36 can be recognized by proteasome. The proteasome selectively recognizes and degrades mildly oxidized proteins in cytosol, endoplasmic reticulum and nucleus. The 20S proteasome complex is reported to be sensitive to the oxidized protein, whereas the 26S is not very effective (Davies 2001; Grune et al. 2003). The 20S proteasome mainly recognizes the hydrophobic surface patches on oxidized proteins and degrades the recognized protein in an ATP- and ubiquitin-independent manner (Shringarpure, Grune, and Davies 2001). Therefore, the proteasome may recognize the hydrophobic ligand-binding site of CD36 or its oxidized load (OxLDL), or the possible oxidized domain of CD36 that may modified by the oxidative burst occurring after binding to OxLDL (Maxeiner et al. 1998).

Kroesen and his group have reported that long chain ceramide is involved in B-cell receptor-induced apoptosis and activation of proteasome (Kroesen et al. 2003). Molecular interactions exist between oxidative stress and ceramide pathways

concerning the control of epidermal growth factor receptor (EGFR) desensitization by ubiquitylation; hydrogen peroxide-mediated oxidative stress induces apoptosis in lung epithelium through modulating ceramide levels. Glutathione decrease in lung epithelial cells results in ceramide accumulation, suggesting that ceramide production, related to oxidative stress, initiates apoptosis. However, oxidants may also activate growth factor receptors and promote cell proliferation. Oxidative stress inhibits the phosphorylation of EGFR at tyrosine 1,045, the docking site for the ubiquitin ligase c-Cbl, so that EGFR is unable to recruit c-Cbl and be ubiquitinylated and degraded. It is therefore possible that there are some interactions between oxidative stress, the ceramide pathway, protein ubiquitinylation and degradation (Goldkorn, Ravid, and Khan 2005). However, the effect of short chain ceramide on proteasomal funtion has not been reported. Both short chain ceramide and long chain ceramide reduce CD36 cell surface expression (Fig 3.8), the possibility that they may work though different pathways cannot be excluded.

Lipid rafts were separated by lysing cells in detergent followed by cold sucrose gradient ultracentrifugation. Fig 5.10 shows that very small amounts of CD36 are localized in lipid rafts fractions, and ceramide treatment did not change CD36 distribution in rafts. This result differs from previous work by Zeng, where most CD36 was in raft fractions. In their experiment, they used 0.5% Triton X-100, whereas in this study 1% Triton X-100 was used to solublize the non-rafts proteins (Zeng et al. 2003). Therefore, high detergent concentration may exclude more protein

from rafts fractions, which may explain why CD36 localizes in non-lipid raft fractions in the present study.

As ceramide has been reported to be involved in receptor shedding events, the effect of ceramide on soluble CD36 level was examined. Supernant analysis using Western blot shows that ceramide reduces shedding of CD36 (Fig 5.9). The size of soluble CD36 is smaller that mature cell membrane CD36 (88Kda). However, in this experiment, it is difficult to address the amount of protein loaded in each gel line because of the lack of a shedding marker. Preliminary experiments using a TNF-alpha converting enzyme (TACE) inhibitor, TAPI, show that inhibition of TACE does not reverse the reduction of CD36 induced by ceramide, suggesting that ceramide decreases CD36 cell surface expression independently of this enzyme. These data suggest that ceramide reduces surface CD36 expression independent of shedding of the receptor. Ceramide has been demonstrated to have opposing effects on L-selectin and CD54 membrane protein shedding (Kawakami et al. 2002; Walev et al. 2000). 1-Phenyl-2-decanoylamino-3-morpholino-1-propanol (PDMP), a synthetic inhibitor of glucosyl transferase diminishes the amount of soluble form of CD54 (sCD54) in the culture supernatants of human umbilical vein endothelial cells (HUVECs). This effect of PDMP is mimicked by metalloproteinase inhibitor, KB-R8301, suggesting that PDMP may suppress the activity of metalloproteinase-like enzyme, which is responsible for the decrement of sCD54. Treatment with PDMP induces accumulation of ceramide, and endogenous C_2 ceramide mimicks the effect of

PDMP on reducing sCD54. It is therefore suggested that ceramide functions as a second messenger during PDMP treatment with HUVECs and inhibits metalloproteinase-like protease, which is responsible for the shedding of CD54 (Kawakami et al. 2002). In contrast, ceramide was reported to cause L-selectin shedding on granulocytes. Pore-forming bacterial toxin streptolysin O (SLO) induces rapid and massive shedding of L-selectin, which is accompanied by a 1.5-fold increase in the activity of neutral sphingomyelinase, subsequently induction of ceramide formation. Endogenous bacterial sphingomyelinase or a cell-permeable ceramide analog induce L-selectin cleavage (Walev et al. 2000). These reports indicate that the effect of ceramide on membrane protein shedding is complex and may be protein and cell type specific. The exact role of ceramide on protein cleavage is still largely unknown and need to be further elucidated.

The effect of ceramide on expression of CD36 was investigated at transcript level by measuring CD36 mRNA expression after ceramide treatment. C_2 ceramide induced CD36 mRNA expression on U937 macrophages in a dose dependent manner. 100nM PMA 24 hours incubation did not significantly activate CD36 mRNA expression. Yesner and colleagues reported that PMA stimulates CD36 mRNA expression, however, their experiments were on human primary monocytes, and PMA was only incubated for 2 to 12 hours with the cells. A number of stimuli up-regulate CD36 expression including OxLDL, macrophage colony stimulating factor (M-CSF) and IL-4 (Han et al. 1997b; Huh et al. 1996b; Yesner et al. 1996). The induction of CD36

by OxLDL was further reported to be through activating the transcription factor peroxisome proliferator activated receptor-γ (PPAR-γ) (Tontonoz et al. 1998; Nagy et al. 1998). The specific ligands in OxLDL that activate PPAR- γ are 9-hydroxyoctadecadienoic acid (9-HODE) and 13- hydroxyoctadecadienoic acid (13-HODE), two oxidized products of linoleic acid (Nagy et al. 1998). Other stimuli that induce CD36 expression, such as M-CSF, IL-4, have also been reported to activate PPAR-γ(Yesner et al. 1996). Therefore, the effect of ceramide on PPAR-γ was studied by using a ELISA based PPAR-γDNA-binding assay kit. However, the competitor supplied with the kit did not successfully inhibit binding of ligand to substrate, suggesting that the binding is not specific for PPAR-γ. Therefore, no conclusion can be drawn from this assay. The effect of ceramide on PPAR-γ could be further examined using reporter gene construct and electrophoretic mobility shift assay. PPAR-γagonists, troglitazone and rosiglitazone, were used to activate the expression of CD36, however, none of them induced the expression of CD36. It is likely that U937 monocytes must be differentiated to macrophage before any challenge by PPAR-γagonists can activate the expression of CD36.

Recent work by Ishii and colleague identified NF-E2-related factor-2 (Nrf2) as a second transcription factor that regulates the expression of CD36. 4-HNE, one of lipid peroxidation products on OxLDL, strongly activates Nrf2. Experiments with Nrf-2-deficient macrophages demonstrate that Nrf2 partially regulates CD36 expression in response to OxLDL and HNE (Ishii T., 2004). Studies on H4IIE cells, a

rat hepatocyte-derived cell line, indicates that ceramide suppress the nuclear Nrf2. Decreases in nuclear Nrf2 by C_2 ceramide was reversed by treatment of cells with N-benzoyloxycarbonyl (Z)-Leu-Leu-leucinal (MG132), a proteasome inhibitor (Park, Cho, and Kim 2004). These reports suggest that ceramide may play a role in regulating Nrf2, therefore may modulate CD36 expression.

In conclusion, ceramide reduces the cell surface expression of CD36, the shedding of CD36 but intracellular CD36 protein level increased probably due to blocking of the receptor inside cells. The induced mRNA expression of CD36 by ceramide is not fully understood and needs to be further investigated.

Chapter 6 Ceramide reduces NADPH oxidase activity through altering the lipid raft environment

Previous work in this lab has shown that short chain ceramides can induce a loss of intracellular peroxide (Phillips, Allen, and Griffiths 2002). The two major peroxide sources in cells are from mitochondria and NADPH oxidase activity. Whilst ceramide induces mitochondrial peroxide production, it appears to, however, decrease intracellular peroxide partially through reduceing NADPH oxidase activity(Phillips and Griffiths 2003). NADPH oxidase membrane subunits cytochrome b558 including gp91 strongly associate with lipid rafts (Vilhardt and van Deurs 2004). Others have shown that endogenous ceramide enhances lipid raft formation and alters their composition (Xu et al. 2001). Therefore, this chapter will investigate whether short chain ceramide reduces NADPH activity oxidase through altering the lipid raft environment.

6.1 Introduction

Ceramide and reactive oxygen species (ROS) have been reported to be important second messengers in cell signal transduction (Levade and Jaffrezou 1999; Levade et al. 2001). Previous work in this lab has shown that ceramides play a role in modulating cellular peroxide level. Cell permeable, synthetic short chain C_2-/C_6-ceramide induce growth arrest in U937 monocytes and apoptosis in Jurkat T-cells due to a rise in mitochondrial peroxide production. The apoptosis of Jurkat T-cells is associated with a large time- and dose-dependent loss of cellular glutathione. However, glutathione loss is transient in U937 monocytes (Phillips, Allen, and Griffiths 2002). On the other hand, ceramide reduces total cellular peroxide level in U937 monocytes (Phillips and Griffiths 2003). As described in Chapter 1, the two major sources of cellular ROS are NADPH oxidase activity and mitochondrial electron transport chain. Therefore, the loss of total cellular ROS in U937 cells induced by ceramide maybe due to reducing NADPH oxidase activity.

NADPH oxidase includes two major components. One major component, which is situated in the plasma membrane, is referred to as a flavo-cytochrome, named as cytochrome b558. The cytochrome b558 is known to be a heterodimer, containing a small α-subunit, named p22 *phox* and a large β- subunit, gp91 *phox*. Other major components are found in the cytosol when the enzyme is non-activated, and bind to the membrane components when activated. These cytosolic components include p47

phox, p67 *phox*, p40 *phox* and $p21^{Rac}$ (Griendling, Sorescu, and Ushio-Fukai 2000) (see Fig1.1). Recent works indicate that NADPH oxidase localizes in the lipid rafts of neutrophils (Shao, Segal, and Dekker 2003; Vilhardt and van Deurs 2004; David, Fridlich, and Aviram 2005). The identification of NADPH oxidase in lipid rafts was demonstrated using detergent sucrose gradient ultracentrifugation and confocal microscopy. Accumulation of membrane components and cytosolic components in rafts contributes to the activation of NADPH oxidase. Depletion of lipid rafts is associated with a lower NADPH oxidase membrane component concentration, less cytosolic component association with membrane components, and subsequently less ROS production. However, the existence of NADPH oxidase within rafts in other cell types is still to be elucidated.

Ceramide, as one of the sphingolipids, plays an important role in lipid rafts. Biophysical studies have shown that ceramide increases the order of the acyl chains in the bilayer and has a tendency to self-aggregate presumably driven by intermolecular hydrogen bonding (Kinnunen and Holopainen 2002). These characteristics promote ceramide segregation into lipid rafts as a tightly packed domain with other sphingolipids and cholesterol (Dobrowsky 2000; Holopainen, Subramanian, and Kinnunen 1998; Kolesnick, Goni, and Alonso 2000; Massey 2001; Mayor and Maxfield 1995; Roper, Corbeil, and Huttner 2000; Venkataraman and Futerman 2000). Experiments using model membranes indicate that a small amount of ceramide (3mol%) dramatically increases raft formation and stability (Xu et al. 2001).

In this study, the existence of NADPH oxidase in lipid rafts in U937 cells was examined. The effect of ceramide on peroxide production and NADPH oxidase components in raft environments was also examined.

6.2 Results

6.2.1 C_2 ceramide alters the lipid raft environment

Lipid rafts were separated using detergent sucrose gradient ultracentrifugation. After ultracentrifugation, the detergent insoluble proteins are found in the light buoyant density fractions in the upper phase of the sucrose gradient. Flotillin-1 was used as a lipid raft marker; Fig 6.1 shows that lipid rafts were separated to the interface of 5% and 30% sucrose (fraction 3, 4, 5), whereas 20μM C_2 ceramide changes the raft formation with flotillin present into two different parts: fraction 3 and fractions 6 and 7. Fraction 3 represents the position more hydrophobic and detergent insoluble membrane components than fractions 6 and 7.

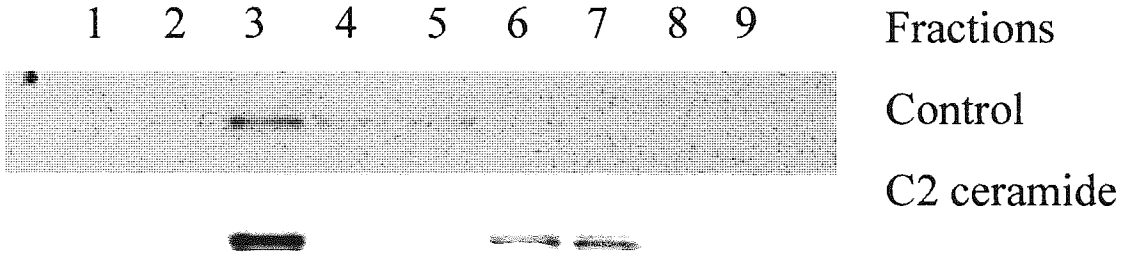

Fig 6.1 C_2 ceramide disrupts the membrane localization of the lipid raft marker flotillin-1.

U937 cells were incubated at 37°C with or without 20μM ceramide for 16 hours. Cells were lysed with 1% Triton X-100 and lipid rafts were then isolated by sucrose gradient ultracentrifugation. Nine fractions were collected from the top to the bottom of the tube. Fractions were then separated on SDS-PAGE. Western blotting was used to measure the lipid raft marker flotillin-1. These experiments were repeated individually 3 times.

6.2.2 C_2 ceramide reduces NADPH oxidase membrane component gp91 *phox* in lipid rafts.

The presence of the membrane component gp91 was also examined in the detergent insoluble fractions. Fig 6.2 shows that the majority of gp91 *phox* is localized in raft fractions (fraction 3, 4). C_2 ceramide 20μM reduced the amount of gp91 *phox* in lipid raft fractions. The addition of the raft disrupting agent, methyl-β-cyclodextrin demonstrated that raft disruption dramatically reduced gp91 association with detergent insoluble raft fractions (Fig 6.2).

Gp91 *phox* band density in lipid rafts was further analysed using Genetool software. 20μM C_2 ceramide reduced both the amount of gp91 *phox* in raft fractions 3 and 4 to about 80% of control raft fractions 3 and 4 and the percentage of gp91 *phox* in raft fractions 3 and 4 / all fractions from the cell lysate approximately from 45% to 35 % (Fig 6.3).

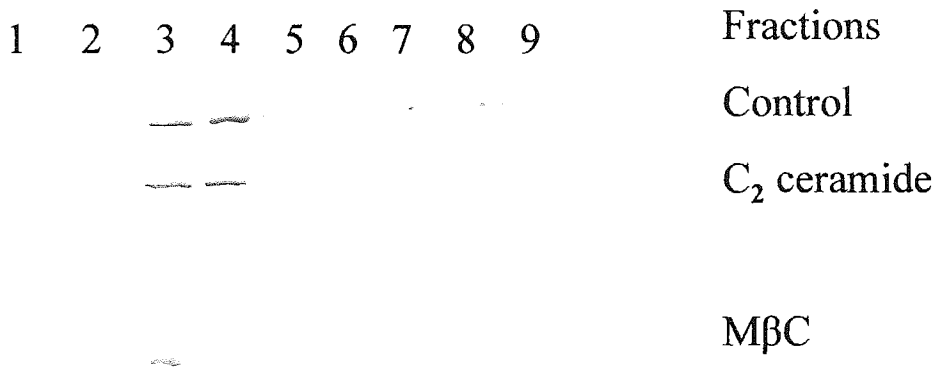

Fig 6.2 C_2 ceramide disrupts the NADPH oxidase membrane component gp91 *phox* in U937 monocytes.

U937 cells were incubated at 37°C with 20μM ceramide for 16 hours or with 2% methyl –β-cyclodextrin for 60 minutes. Cells were lysed with 1% Triton X-100 and lipid rafts were then isolated by sucrose gradient ultracentrifugation. Nine fractions were collected from the top to the bottom of the tube. Fractions were then separated on SDS-PAGE. Western blotting was used to identify the membrane component gp91 *phox*. These experiments were repeated individually 3 times.

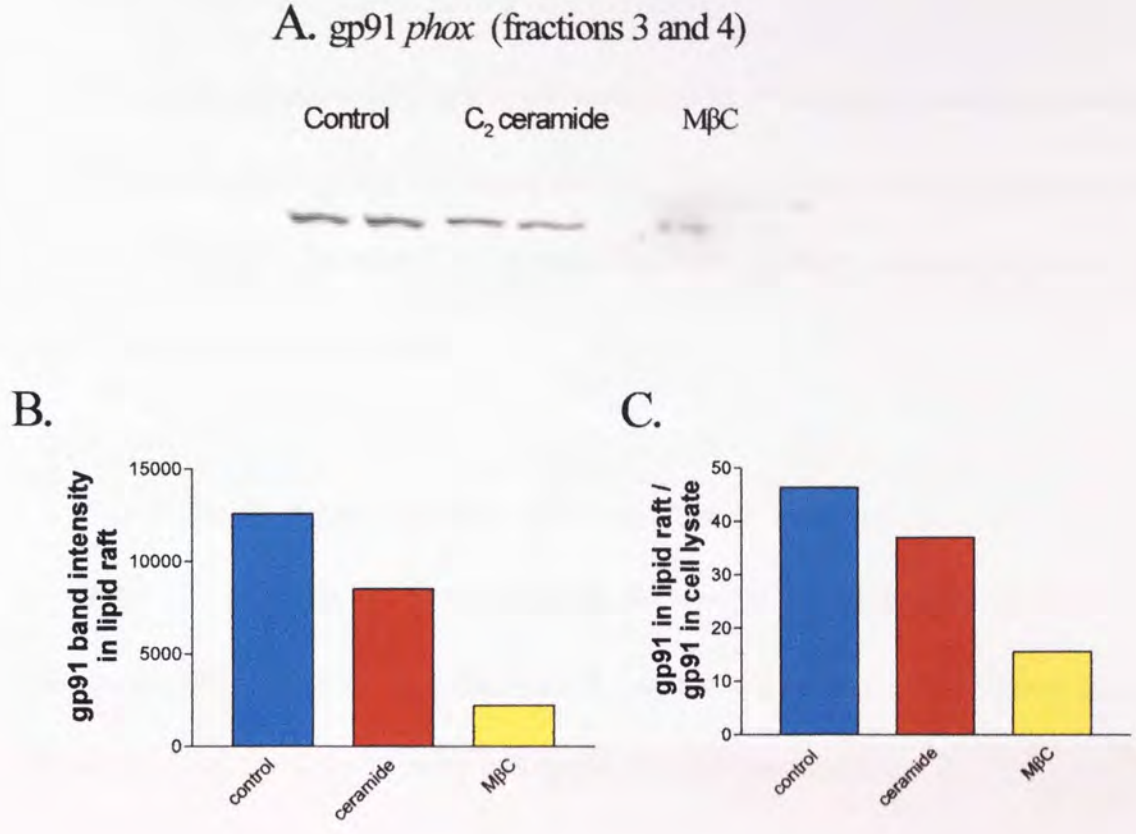

Fig 6.3 C_2 ceramide disrupts NADPH oxidase membrane component gp91 *phox* in lipid rafts and reduces the percentage of gp91 *phox* in lipid rafts.
A: U937 cells were incubated at 37°C with 20μM ceramide for 16 hours or with 2% methyl –β-cyclodextrin for 60 minutes. Cells were lysed with 1% Triton X-100 and lipid rafts were then isolated by sucrose gradient ultracentrifugation. Nine fractions were collected from the top to the bottom of the tube. Fractions were then separated on SDS-PAGE. Western blotting was used to identify the membrane component gp91. B, C: quantification of bands. Bands were analyzed using Gene-tool (Syngene, Cambridge, UK), as B the whole amount of gp91 in lipid raft fraction 4 and C the percentage of gp91 in lipid raft fraction 4 out of all fractions from the cell lysate.

6.2.3 C_2 ceramide reduces NADPH oxidase cytosolic component p47 *phox* in lipid rafts.

The cytosolic component p47 *phox* was measured in the detergent insoluble fractions using western blotting. Fig 6.4 shows that p47 *phox* is localized in raft fractions 4 in resting U937 cells (fraction 4). C_2 ceramide 20μM strongly reduced the amount of p47 *phox* in lipid raft fraction 4.

P47 *phox* bands density in lipid rafts was further analysed using the software Genetool. C_2 ceramide 20μM reduced both the amount of p47 *phox* in raft fraction 4 to about 25% of control raft fractions 4 and the percentage of p47 *phox* in raft fractions 4 / all fractions from the cell lysate to trance amount (Fig 6.5).

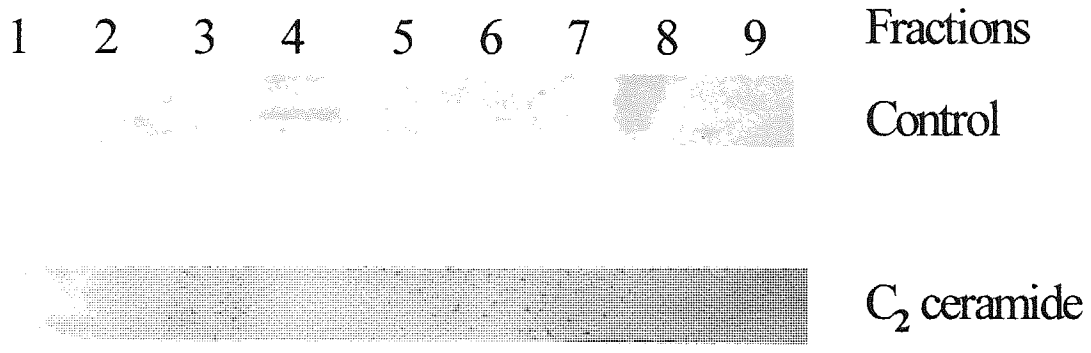

Fig 6.4 C2 ceramide disrupts the membrane localization of the NADPH oxidase membrane component p47 *Phox* in U937 monocytes.
U937 cells were incubated at 37°C with or without 20μM ceramide for 16 hours. Cells were lysed with 1% Triton X-100 and lipid rafts were then isolated by sucrose gradient ultracentrifugation. Nine fractions were collected from the top to the bottom of the tube. Fractions were then separated on SDS-PAGE. Western blotting was used to measure the membrane component p47 *Phox*. These experiments were repeated individually 3 times.

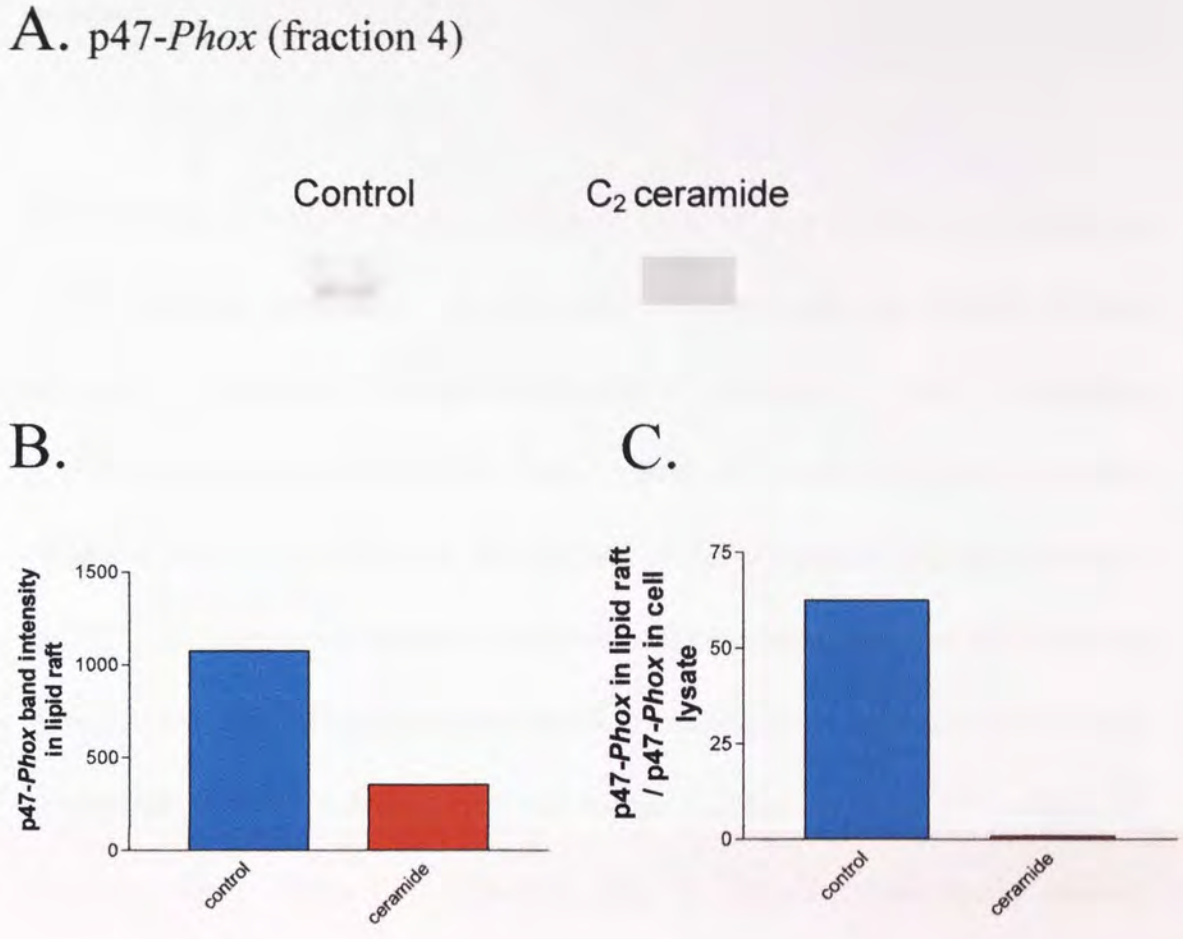

Fig 6.5 C_2 ceramide disrupts the membrane localization of the NADPH oxidase membrane component p47-*Phox* in lipid rafts and reduces the percentage of p47-*Phox* in lipid rafts.

A: U937 cells were incubated at 37°C with or without 20μM ceramide for 16 hours.

Cells were lysed with 1% Triton X-100 and lipid rafts were then isolated by sucrose gradient ultracentrifugation. Nine fractions were collected from the top to the bottom of the tube. Fractions were then separated on SDS-PAGE. Western blotting was used to identify the component p47-*Phox*. B, C: quantification of bands. Bands were analyzed using the Gene-tool (Syngene, Cambridge, UK), as B the whole amount of p47-*Phox* in lipid raft faction 4 and C the percentage of p47-Phox in lipid raft fraction 4 out of all fractions from the cell lysate.

6.2.4 C_2 ceramide reduces cellular peroxide through reducing NADPH oxidase activity

The reduction of NADPH oxidase activity by ceramide was confirmed by measuring cellular peroxide using flow cytometry after treatment with the NADPH oxidase activator, phorbol-12-myristate-13-acetate (PMA), and inhibitor, diphenyleneiodonium sulfate (DPI). PMA (3.3nM) for 1 hour significantly induced cellular peroxide, $P<0.001$ and DPI (1μM; 16 hours) reduces cellular peroxide, $P<0.05$. 16 hours pre-incubation of cells with C_2 ceramide diminished PMA induced peroxides $P<0.001$. Ceramide treatment alone (20 μM; 16 hours) caused a reduction of peroxide and this reduction was not further knocked down by DPI. Lipid raft disrupting agent, methy-β-cyclodextrin (2%; 60 minutes) dramatically reduced intracellular peroxide, $P<0.001$(Fig 6.6).

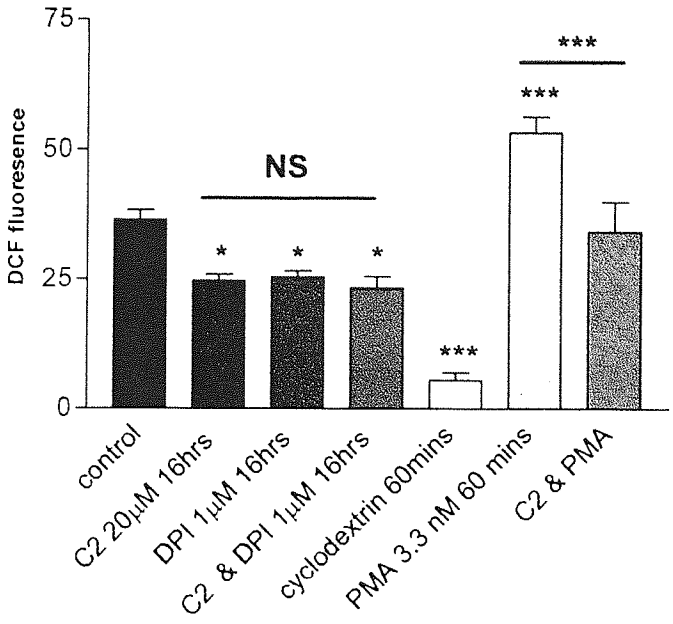

Fig 6.6 C_2 ceramide reduces the intracellular peroxide level through disturbing NADPH oxidase in U937 monocytes.

U937 monocytes were starved in serum free medium for 4 hours, and then 20 μM C_2 ceramide or 1 μM DPI or both were added for 16 hours incubation in an humidified 5% CO2, 95% air atmosphere at 37°C. 3.3nM PMA or 2% cyclodextrin was added for 60 minutes incubation in a humidified 5% CO_2, 95% air atmosphere at 37°C. The DCFHDA assay was used to measure intracellular peroxide level and DCF fluorescence was measured by flow cytometry. * represents $P<0.05$ for 20 μM C_2 ceramide, 1μM DPI and 20 μM C_2 + 1μM DPI compared to control cells; NS represents no significance for 20 μM C_2 + DPI 1 μM and DPI 1 μM compared to 20 μM C_2; *** represents $P<0.001$ reduction and induction for cyclodextrin and PMA respectively compared to control; *** represents $P<0.001$ for PMA + C_2 ceramide compared with PMA. The data are presented as the arithmetic mean ± SEM of three individual experiments, n=9. Results were analyzed by one-way ANOVA statistical analysis followed by Tukey's multiple comparison test.

6.3 Discussion

Monocytes produce reactive oxygen species against microbial pathogens or in response to proinflammatory factors for host defenses (El Benna et al. 2005). However, recent works have demonstrated that resting monocytes also produce low amount of ROS (Wikman et al. 2003), which are suggested to function as messenger for signaling (Droge 2002; Finkel 2003; Nathan 2003).

Ceramide has been previously shown to down-regulate cellular peroxide, and up-regulate mitochondrial peroxide production (Phillips and Griffiths 2003; Phillips, Allen, and Griffiths 2002). As the two major sources of cellular peroxide are from NADPH oxidase activity and mitochondrial electron transport chain, it is likely that ceramide decreases cellular peroxide through down-regulating NADPH oxidase activity.

The loss of cellular ROS induced by C_2 ceramide (10 and 20 μM; 16 hours) in U937 cells is consistent with previous reports (Phillips and Griffiths 2003). The fluorogenic compound DCFHDA has been used widely to monitor oxidative stress, and is suggested to reflect the overall oxidative status of the cell (Wang and Joseph 1999). However, this assay has been questioned for specificity by a number of groups (Myhre et al. 2003). DCFHDA was initially used for the measurement of H_2O_2 in the

presence of peroxidase (Fig 2.5) (KESTON and BRANDT 1965). DCFH can also be oxidized to fluoresent probe DCF by HRP alone, and to a larger extent in combination with H_2O_2 (LeBel, Ischiropoulos, and Bondy 1992). DCF fluorescence can be due to $^{\cdot}NO$ related species as well as H_2O_2 in cells or in cell-free systems (Rao et al. 1992; Vowells et al. 1995; Gunasekar et al. 1995; Gabriel et al. 1997); DCFH shows rather low sensitivity towards oxidation by NO, $O_2^{\cdot-}$, or H_2O_2, but displays a much greater sensitivity for $ONOO^-$ (Gabriel et al. 1997; Kooy, Royall, and Ischiropoulos 1997; Possel et al. 1997). Therefore, the possibility that ceramide reduces $ONOO^-$ in present study cannot be excluded. However, increased DCF formation is also suggested to implicate $O_2^{\cdot-}$, H_2O_2, and $OH^{\cdot}$ (Scott et al. 1988; Zhu et al. 1994). Moreover, there are conflicting findings regarding the inhibition of DCF formation by superoxide dismutase (Scott et al. 1988; Atlante et al. 1997; Takeuchi, Nakajima, and Morimoto 1996; Yang et al. 1997). For the above reasons, previous researchers in this lab have substantiated the findings with DCF using cytochrome *c* reduction assay, a widely used and accepted specific measurement of oxidant formation (Phillips and Griffiths 2003).

NADPH oxidase localizes in the lipid rafts of neutrophils (Shao, Segal, and Dekker 2003; Vilhardt and van Deurs 2004; David, Fridlich, and Aviram 2005). However, the existence of NADPH oxidase within rafts in other cell types is still to be elucidated. Ceramide is an important component of rafts; the change of ceramide content dramatically alters raft formation (Xu et al. 2001). Therefore, the effect of ceramide

on NADPH oxidase in rafts was tested. Lipid rafts were separated by the detergent sucrose gradient ultracentrifugation method and tested by western blot. The raft marker, flotillin-1 floated up to the interface of 5% and 30% sucrose, indicating that the detergent insoluble domain (rafts) were separated from detergent soluble proteins. These experiments showed that the distribution of flotillin into raft fractions was affected by ceramide. As ceramide has a tendency of self-aggregation presumably driven by intermolecular hydrogen bonding, these results suggest that C_2 ceramide may form a raft subdomain, which contains higher amounts of ceramide than other rafts and may have a different density from other rafts. In fact, the detergent insoluble domains can be further separated to different subdomains was demonstrated by a number of groups (Pike 2004) Therefore, the two different types of rafts may appear to separate to different density in the sucrose gradient.

This work has demonstrated that NADPH oxidase membrane component gp91 *phox* localizes in rafts in U937 cells. This is the first discovery of NADPH oxidase presence in lipid rafts in monocytes. C_2 ceramide (20 μM; 16 hours) reduced both the amount of gp91 *phox* in lipid rafts and the percentage of gp91 in rafts / total cell lysate. The reduction in level of gp91 *phox* maybe because the new-formed raft environment following ceramide treatment is unfavorable to gp91 *phox*. As previously described in Chapter 1, C_2 ceramide has been indicated to deplete cholesterol in rafts probably due to the tight lipid packing and this may contribute to the loss of gp91 *phox* from the rafts. Cholesterol depletion using methyl-β-cyclodextrin also resulted

in a reduction of gp91 *phox*, suggesting that C_2 ceramide may reduce gp91 *phox* in rafts through depleting cholesterol. Moreover, ceramide has been demonstrated to cause endocytosis (as reviewed in (Kinnunen and Holopainen 2002). The endocytotic vesicles induced by ceramide are enriched in ceramide (Holopainen, Angelova, and Kinnunen 2000), suggesting that the endocytosis is most likely to occur in SL enriched lipid rafts. Therefore, proteins that are clustered within rafts may be endocytosed together with ceramide. This may cause the reduction of gp91 *phox* in the detergent insoluble fractions.

The NADPH oxidase cytosolic component p47 *phox* was also detected in raft fractions and reduced by C_2 ceramide (20 μM; 16 hours). The reduction of p47 *phox* in the raft fractions suggests that less p47 *phox* is associated with cytochrome b558, which subsequently may result in less ROS production by NADPH oxidase. This maybe due to the reduction of gp91 *phox* in rafts available for association with p47 *phox*. However, the extent of p47 *phox* reduction in expression by ceramide appears greater than the reduction of expressed gp91 *phox*. A possible mechanism is that ceramide reduces p47 *phox* association with rafts and the new environment formed altered by ceramide may be more hydrophobic, whereas, p47 *phox* favours a hydrophilic environment as it localizes in cytosol when not activated. Therefore, the ceramide-enriched raft environment may be unfavorable to p47 *phox* and is more difficult for it to associate with cytochrome b558 (including gp91 and p22 *phox*).

The effect of C_2 ceramide on NADPH oxidase was also confirmed using the NADPH oxidase activator, PMA and inhibitor, DPI. PMA activates protein kinase C (PKC) and subsequently results in phosphorylation of NADPH oxidase cytosolic components and association of cytosolic components with membrane components (El Benna et al. 2005). PMA induced cellular peroxide was diminished by ceramide. DPI diminishes NADPH oxidase activity by inhibiting electron transport by gp91 *phox* (El Benna et al. 2005). The reduction of peroxide caused by ceramide was not further decreased by DPI (Fig 6.5). These results suggest that C_2 ceramide may reduce cellular peroxide through reducing NADPH oxidase activity. Cholesterol depleting agent, methy-β -cyclodextrin reduced the ROS production, $P<0.001$, suggesting that cholesterol depletion results in down-regulation of ROS production. C_2 ceramide may mildly deplete cholesterol (Megha and London 2004) and gp91 *phox* in raft fractions, which may count for the reduction of ROS caused by ceramide.

Other groups have also reported that the disruption of lipid raft reduces NADPH oxidase activity and ROS production. Vilhardt and van Deurs reported that cholesterol depletion severely diminishes superoxide production in intact cells or in a cell-free reconstituted system, associating with a reduction in translocation of cytosolic phox subunits to the membrane (Vilhardt and van Deurs 2004). Guichard and colleagues have demonstrated that IL-8 potentiates the oxidative burst induced by stimuli such as formyl-methionyl-leucyl-phenylalanine (fMLP) via a priming mechanism. This effect of IL-8 involves the recruitment of the NADPH oxidase components in the lipid rafts

of neutrophils. These authors showed that methyl-beta-cyclodextrin, which disrupts lipid rafts, reduced IL-8-induced priming in response to fMLP (Guichard et al. 2005). Treatment of neutrophils with methyl-beta-cyclodextrin reduced raft associated p22phox and significantly reduced PMA-induced activity of the NADPH oxidase (David, Fridlich, and Aviram 2005).

In conclusion, C_2 ceramide reduces the production of ROS in U937 cells partly through altering lipid raft environment and subsequently preventing the formation of active NADPH oxidase. The mechanism of ceramide reducing NADPH oxidase activity could be further investigated using confocal microscopy and fluorescence-labelled ceramide to test whether ceramide causes endocytosis of gp91 *phox* and to visualise the sites where ceramide induces *phox* component trafficking. The effect of ceramide on lipid raft environments may enable ceramide to be capable of modulating the membrane expression of any raft-associated protein.

Studies on lipid raft isolation involve many different methods. Interestingly, different methods yield different lipid rafts. These observations raise the question; what is a lipid raft? Before considering this question it is important to consider how rafts are studied. There are two main methods used to isolate lipid rafts, detergent based and non-detergent based.

Detergent-based methods use TritonX-100 sucrose gradient ultracentrifugation. In this raft preparation, cholesterol is found to be enriched 3-5 fold in raft fractions compared with total membranes; lipids of raft fractions represent half or one third of total membrane lipid. Raft fractions are also enriched in sphingomyelin and glycosphingolipids, such as cerebrosides and gangliosides (Brown and Rose 1992; Pike et al. 2002; Prinetti et al. 2000), whereas, lipids of the inner-leaflet including phosphatidylethanolamine and anionic phospholipids are particularly depleted (Pike 2003).

In addition to Triton X-100, a number of other detergents have been used in different concentrations, such as Lubrol WX, Lubrol PX, Brij 58, Brij 96, Brij 98, Nonidet P40, CHAPS and octylglucoside to isolate lipid rafts (Drevot et al. 2002; Ilangumaran et al. 1999; Madore et al. 1999; Roper, Corbeil, and Huttner 2000; Slimane et al. 2003). Raft preparations from these different detergents yield different protein compositions from the standard TritonX-100 resistant domains (Schuck et al. 2003). Tween 20, Brij5 and Lubrol WX yield low density membranes that have little enrichment in cholesterol and sphingolipids, the hallmark of Triton X-100 resistant domains (Schuck et al. 2003). Brij 96 and Brij 98 yield rafts that have more cholesterol and sphingolipids than Tween 20 resistant domains but less than Triton X-100 resistant domains. Therefore, different detergents were thought to have different lipid selectivity, hence yield different raft preparation (Schuck et al. 2003).

However, the detergent extraction methods have been questioned for disturbance of physiological structure of the lipid raft. Some studies indicate that detergent extraction causes fusion of rafts and exchange of lipid between membranes, for example, GPI-anchored proteins, which are shown by immunofluorescence to be diffusely distributed at the cell surface becomes incorporated into detergent-insoluble low-density complexes together with caveolae, which occupy only a small fraction of the cell surface (< 4%) (Edidin 2003; Mayor and Maxfield 1995; Roper, Corbeil, and Huttner 2000; Shogomori and Brown 2003). Microscopy studies also showed that TritonX-100 extraction results in large sheets of raft, instead of small individual domains and causes GPI-anchored protein aggregation compared to non-detergent treated cells (Mayor and Maxfield 1995; Friedrichson and Kurzchalia 1998). Therefore, non-detergent methods were also investigated to isolate lipid rafts.

Non-detergent methods used sonication of membrane to release lipid rafts in small membrane pieces, followed by isolation of the light membrane fraction by density gradient centrifugation (Smart et al. 1995). Lipid rafts yielded by this method have a similar composition as TritonX-100 resistant domains with enrichment in cholesterol and sphingomyelin (Pike et al. 2002). However, in contrast to TritonX-100 resistant domains, the non-detergent isolated lipid rafts were not depleted of glycerophospholipids. The non-detergent method excluded the problem of membrane mixing and the selective extraction of lipid caused by detergent extraction. However,

non-detergent isolation of rafts may result in non-efficient depletion of non-raft lipids and proteins since rafts were only isolated on the basis of their low density.

Different models of raft structure and behavior have been proposed that are consistent with the observed experimental results (as reviewed by (Pike 2004). As Fig 6.7 shows, in model I, lipid rafts consist of well-organized cholesterol and sphingolipids, which distribute in a decreasing lipid order from the center to the edge. In model II, rafts contain homogeneous constituents which are not as well ordered as model I and have different affinities to rafts. Detergents selectively extract these components. In model III, different rafts with distinct lipid compositions co-exist in the membrane. Rafts with higher level of cholesterol and sphingolipids are highly structured and are resistant to strong detergents like TritonX-100, whereas rafts with lower level of cholesterol and sphingolipids but higher level of glycerophospholipids are more soluble in TritonX-100.

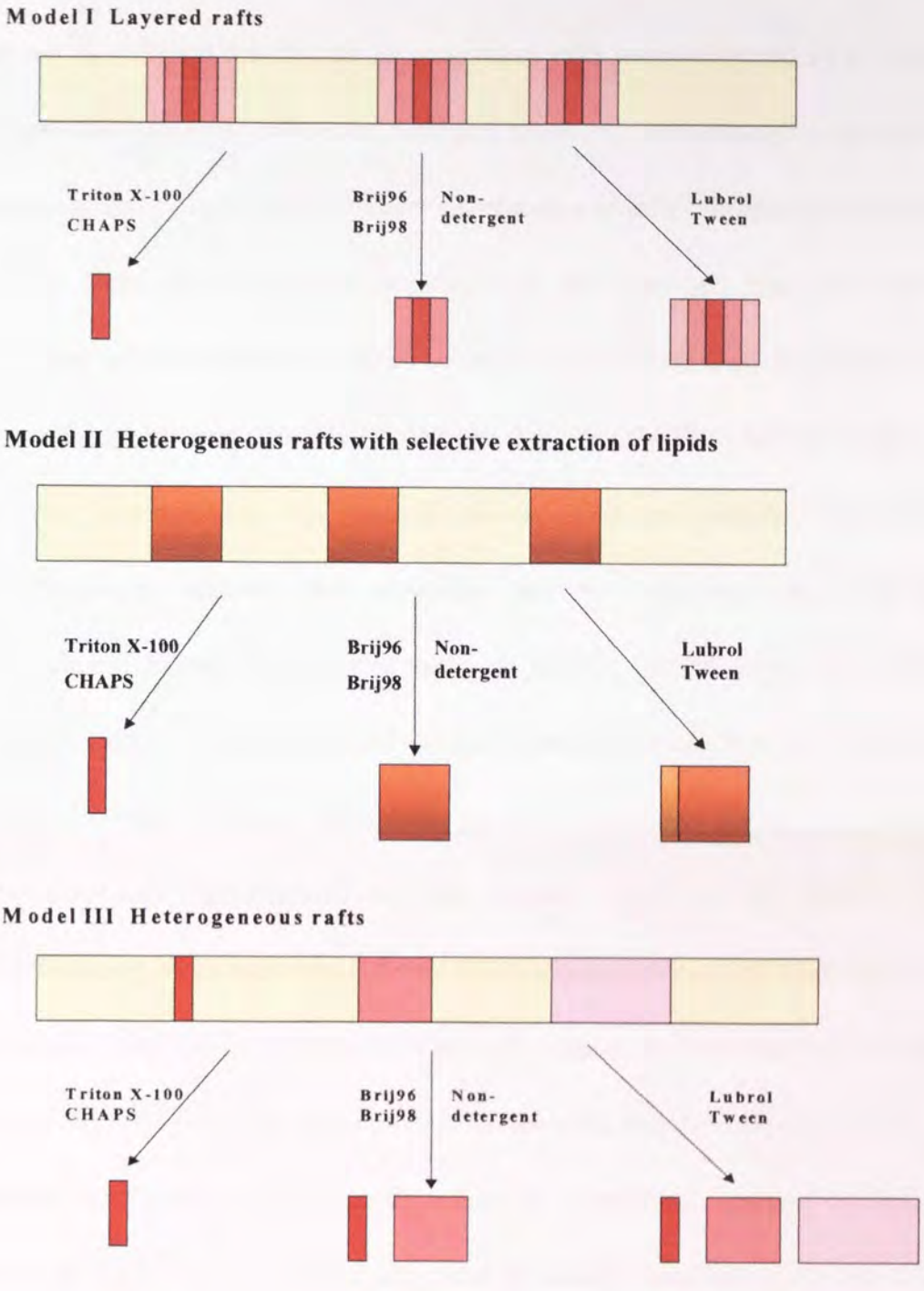

Fig 6.7 The schematic rafts models.

Model I represents lipid rafts that are consist of well-organized cholesterol and sphingolipids, which distribute in a decreasing lipid order from the center to the edge. Model II represents rafts contain homogeneous constituents which are not as well ordered as model I and have different affinities to rafts and can be selectively extracted by detergents. Model III represents different raft subdomains with distinct lipid compositions co-exist in the membrane. Rafts with higher level of cholesterol and sphingolipids are highly structured and are resistant to strong detergents like TritonX-100, whereas rafts with lower level of cholesterol and sphingolipids but higher level of glycerophospholipids are more soluble in TritonX-100.

Among the different models, the heterogeneous rafts were supported by a variety of experiments including: differential detergent sensitivity, immunological separation of subpopulations of lipid rafts and direct visualization of rafts. The detergent sensitivity of three different GPI-anchored proteins from the same cell type was tested by separating raft factions using different detergents. The results show that three proteins have different detergent sensitivity although they are all GPI-linked and in the same cell type. Immunological separation of caveolae using anti-caveolin immunoaffinity chromatography showed that caveolae can be separated physically from GPI-anchored proteins that exist in the same TritonX-100 raft preparation (Oh and Schnitzer 1999). Caveolae separated using this method are largely depleted of several typical detergent resistant membrane proteins including: eNOS, heterotrimeric G-proteins and non-receptor tyrosine kinases (Stan et al. 1997). Using immunoaffinity-based methods, different GPI-anchored proteins are found in different raft subsets. Taken together, these data strongly support the heterogenous rafts model that not all rafts share the same protein components, but different small rafts with different compositions co-exist in the whole raft population separated by detergent extraction. This theory is further supported by direct visualization of rafts. Recent work by Youchun and colleagues (2003) shows that CD36 homogeneously distributes on the cell membrane, whereas caveolin-1 display punctate surface distribution in both antibody staining images and living cells that express green fluorescent protein attached CD36. Consistently, dual staining with CD36 and caveolin-1 shows no overlap (Zeng et al. 2003). A similar effect is seen on two different GPI-anchored

proteins, GPI-anchored folate receptors and Thy-1 (Mayor, Rothberg, and Maxfield 1994). Stronger proof for the existence of rafts subdomains is that different raft markers are found to localize in different domains in living cells. Ganglioside GM3 and the GPI-anchored protein, urokinase plasminogen activator receptor, mainly distribute to the leading edge of the polarized T-cells, whereas ganglioside GM1 and CD44, a transmembrane protein in lipid rafts, are localized at the trailing edge of the cells. In biochemically isolated detergent resistant low density domains, all these four proteins are found and all disappear after cholesterol depletion by methyl-β -cyclodextrin. However, direct visualization shows that they are in different lipid raft subdomains (Gomez-Mouton et al. 2001). The presence of different lipid raft subdomains may support the current discovery that ceramide alters the distribution of the raft marker, flotillin from one part to two discrete densities.

There are some studies that question the existence of lipid rafts. Anne and colleagues undertook experiments to test the dynamics of raft and non-raft proteins by measuring the lone-range protein mobility at the cell surface. Their results showed that different raft proteins showed a variety of diffusion abilities after photobleaching. Well-known perturbations to lipid rafts, such as cholesterol depletion, decreased temperature and cholesterol loading have similar effects on diffusional mobility of raft and non-raft proteins. They, therefore, question the theory that lipid rafts have dominant effect on long-range protein mobility (Kenworthy et al. 2004). However, the different

subdomains with different characteristics that share the same detergent resistant low-density qualities may also explain these results.

Study of the micro-structure of lipid rafts shows that lipid rafts are possibly folded membrane and ruffles on membrane instead of packed rafts (Glebov and Nichols 2004; van Rheenen and Jalink 2002). The concept and structure of lipid rafts are still not clear to date; further studies are needed to discover the structure and function of these microdomains and the role of sphinglolipid metabolism in raft structure.

Chapter 7 Discussion, conclusion and further work

7.1 Discussion

Research during the last decade has shown that inflammation plays a key role in the development of atherosclerosis (as reviewed by (Hansson 2005). During inflammation, reactive oxygen species (ROS) released by phagocytes additionally result in oxidative modification of LDL, which is central to the process of macrophage foam cell formation. ROS have been indicated to play important roles as intracellular signaling molecules in physiological and pathophysiological processes including the development of atherosclerosis (Poli et al. 2004; Touyz, Tabet, and Schiffrin 2003; Loscalzo 2003; Moran, Gutteridge, and Quinlan 2001; Bauer 2000; Sundaresan et al. 1995; Ushio-Fukai et al. 1998; Zafari et al. 1998). Consistent with the increase of ROS production, enzymes that generate ROS are reported to be activated in atherosclerotic lesions, including NADPH oxidase, endothelial NOS (eNOS) and myeloperoxidase (MPO). A number of stimuli initiate ROS generation by phagocytes including: OxLDL, tumor necrosis factor alpha (TNF α) and angiotensin II (Dimmeler and Zeiher 2000).

7.1.1 Ceramide and ROS

Previous work from this lab has shown that ceramide reduces the intracellular peroxides (Phillips and Griffiths 2003), most likely through inhibition of NADPH

oxidase. NADPH oxidase membrane subunits cytochrome b558 including gp91 strongly associate with lipid rafts (Vilhardt and van Deurs 2004). It has been reported that endogenous ceramide enhances lipid raft formation and alters their composition (Xu et al. 2001). These present one of the hypotheses investigated in this thesis, that short chain ceramides reduce NADPH oxidase activity by disrupting the components of NADPH oxidase in lipid rafts.

The previous report that ceramide reduces cellular ROS was first confirmed using the DCFHDA assay by flow cytometry. C_2 ceramide (10 and 20 μM; 16 hours) significantly reduced cellular ROS in U937 cells. This result is consistent with previous reports (Phillips and Griffiths 2003).

Lipid rafts were separated after C_2 ceramide (20μM; 16 hours) treatment. C_2 ceramide altered the lipid rafts marker, flotillin distribution in the gradient from one part to two parts in the sucrose gradient and reduced both the amount of NADPH oxidase membrane component gp91 *phox* and cytosolic component p47 *phox* in lipid rafts and the percentage of gp91 and p47 *phox* in rafts / total cell lysate. The change in flotillin distribution suggests that ceramide treatment altered the raft environment. A previous report indicates that ceramide strongly enhances raft formation (Xu et al. 2001) and these rafts contain more ceramide. As different subdomains may co-exist in rafts (Pike 2004), the ceramide-enriched domains could possibly separated as

subdomains from other raft. These ceramide-enriched rafts may exclude some of the proteins like flotillin and have different detergent resistant ability and density, thus was separated to two different parts in sucrose gradient.

The reduction of NADPH oxidase components in lipid rafts was accompanied by the decrease of NADPH oxidase activity and subsequent ROS production as demonstrated using the NADPH oxidase activator, PMA and inhibitor, DPI. The cholesterol depleting agent, methyl-β-cyclodextrin reduced the ROS production, suggesting that disruption of lipid rafts results in down-regulation of ROS production.

These observation support the hypothesis that C_2 ceramide reduces NADPH oxidase activity through disrupting the components of this enzyme in lipid rafts (Fig 7.1).

There are a number of reports which indicate that the disruption of lipid raft reduces NADPH oxidase activity and ROS production in cell free systems and neutrophils (Vilhardt and van Deurs 2004; Guichard et al. 2005; David, Fridlich, and Aviram 2005). The present study demonstrated for the first time that NADPH oxidase is present in lipid rafts on monocytes and that C_2 ceramide reduces NADPH oxidase activity, probably through altering the raft environment.

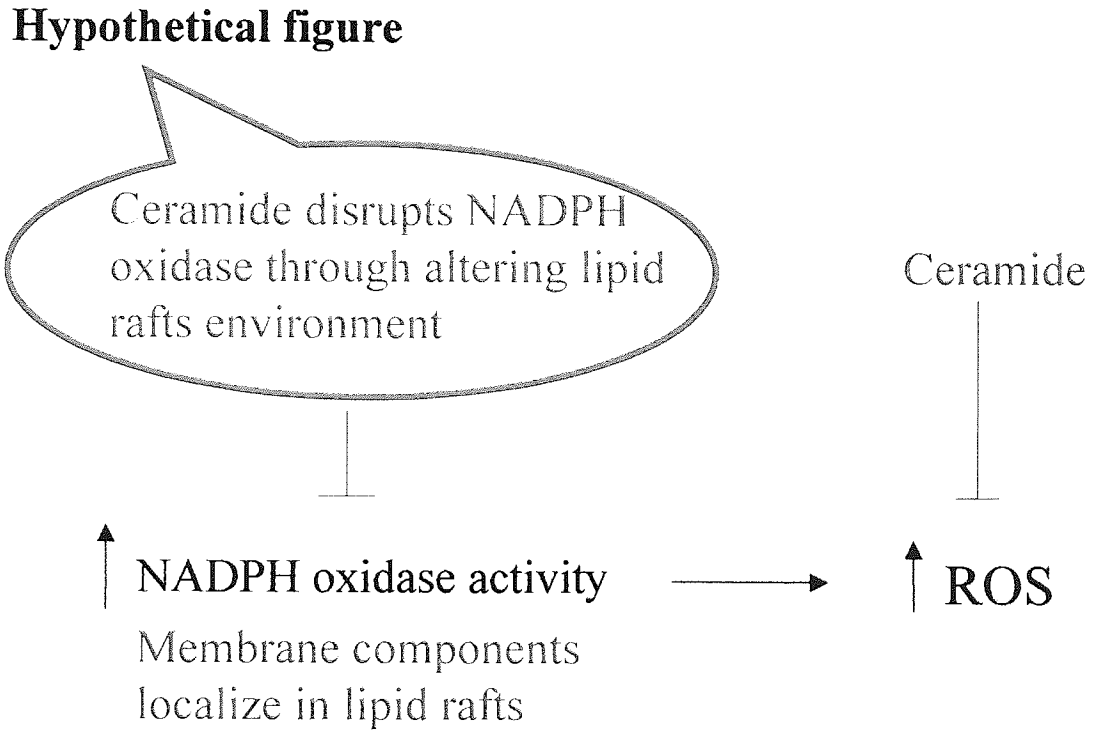

Fig 7.1 Support of original hypothesis that C_2 ceramide reduces NADPH oxidase activity through disrupting the components of this enzyme in lipid rafts.

7.1.2 Ceramide and CD36

The integrin, CD11b, which is expressed on leukocytes and is involved in adhesion to endothelial cells, is upregulated by ROS (Kormoczi et al. 2001). Moreover, synthetic ceramide-induced loss of cytosolic peroxide is also associated with reduced cell surface expression of CD11b (integrin) on monocytes (Phillips DC PhD thesis, 2003). Oxidative stress also has been demonstrated to up-regulate CD36 expression and OxLDL uptake through inducing lipid peroxidation (Fuhrman, Volkova, and Aviram 2002). Therefore, this presents another hypothesis that ceramide reduces the expression of the CD36 scavenger receptor and OxLDL uptake through reducing cytoplasmic peroxide.

Results in Chapter 3 have demonstrated that synthetic short chain ceramide (C_2) decreases surface expression of CD36 on the human monocytic cell line U937 using both flow cytometry and immunofluorescence microscopy. Sphingomyelinase catalyzed long chain ceramide has similar effect on reducing CD36 cell surface expression, suggesting the reduction of CD36 is not specific to synthetic short chain ceramide but the common quality of ceramide. Since physiological ceramides have been reported to have different effects from short chain ceramides in cell biology, through altering membrane structure (Sot, Goni, and Alonso 2005; Sot et al. 2005),

the reduction of CD36 caused by ceramides may be independent of the change in membrane structure induced by ceramides. The result was also confirmed using primary monocytes and PMA differentiated U937 cells, suggesting that the effect is not due to the special receptor expression by the U937 cell line. The mechanism though which ceramide causes the reduction of CD36 cell surface expression was studied in Chapter 5. The original hypothesis that ceramide reduces CD36 expression through down-regulating cellular peroxide was not confirmed. The effects of ceramide on cellular peroxide and on CD36 expression appear to be independent of each other.

Since the original hypothesis was not fulfilled, the mechanism by which ceramide reduces the expression of CD36 was further investigated by monitoring the total cellular level, the degradation and the shedding of CD36 as well as the presence of CD36 in lipid rafts. Results showed that ceramide reduces shedding of CD36 and intracellular CD36 accumulates probably due to inhibition of the receptor transport inside cells (Fig 7.2). Also, ceramide induces the transcriptional expression of CD36.

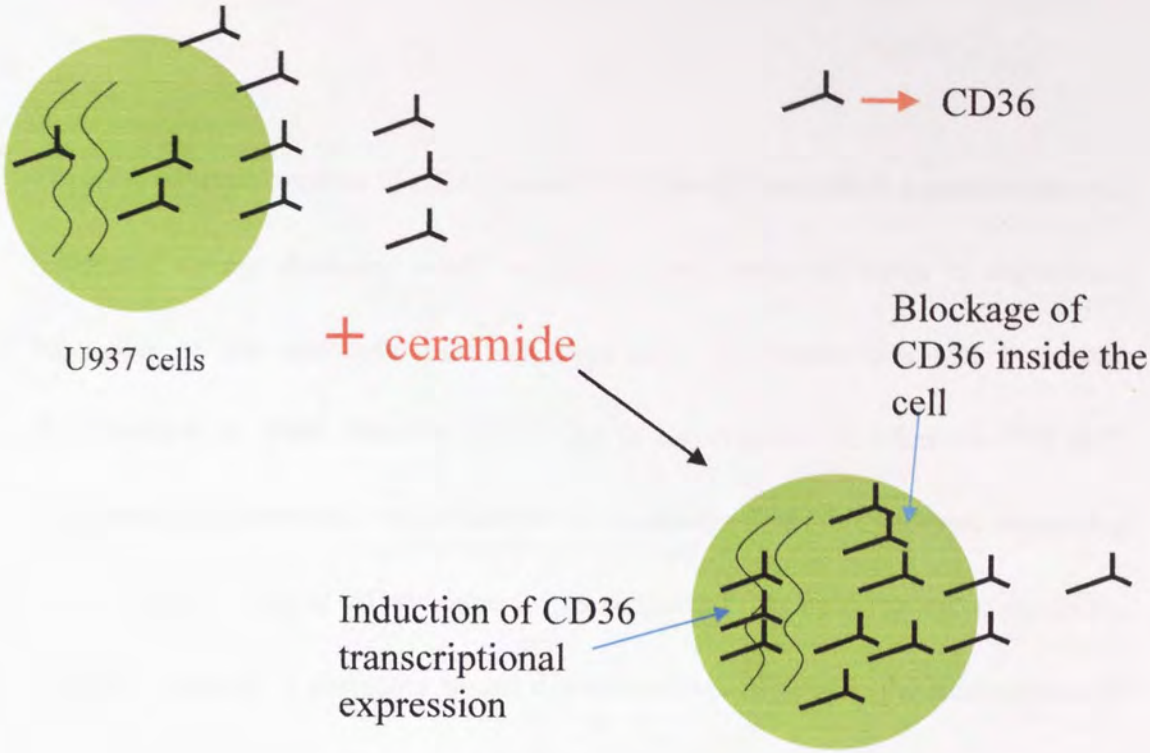

Fig 7.2 Ceramide reduces the cell surface expression and shedding of CD36 and leads to intracellular CD36 level accumulation.

The mechanism that ceramide blocks CD36 inside cells is not totally clear yet. Experiments with brefeldin (BFA), an inhibitor of protein secretion and expression on the plasma membrane (Misumi et al. 1986), shows similar effects to ceramide and suggests that ceramide may block the export of CD36 to plasma membrane.

The intracellular retention of CD36 caused by ceramide may share a mechanism with lysosomal storage diseases, which result in accumulation of lipids in degradative organelles of the endocytic pathway, especially late endosomes and lysosomes (Kobayashi et al. 1999; Neufeld 1991). One of the examples is Niemann-Pick (NP) syndrome. Sphingomyelin or cholesterol is accumulated in this syndrome depending on the different type of NP syndrome. It is suggested that lipid raft recycling in the endocytic pathway is disrupted in this disease and contributes to the mistargeting of lipids as reviewed by (Simons and Gruenberg 2000). Proteins that normally are associated with rafts in the peripheral plasma membrane or early endosomal circuit may be accumulated in the late endosomes and lysosomes, which has been proved to be true for anexin II (Simons and Gruenberg 2000). Raft accumulation within the endosomes and lysosomes also alters the properties of these compartments and results in late endosomes/lysosomes containing lipid lamellae. This transformation interferes with the normal sorting/trafficking capacity of these compartments, for example, mannose 6-phosphate receptor distribution is switched from the Golgi to the late endosomes in NP type C fibroblasts (Kobayashi et al., 1999). In the research reported in this thesis, ceramide was shown to alter the raft marker, flotillin distribution in the sucrose gradient. The lower part containing flotillin in the gradient may localize in peripheral plasma membrane or in the compartments of endocytotic pathway, which may suggest lipid accumulation as in lipid storage diseases. The

present study shows that CD36 may not be in the lipid rafts. However, as discussed in Fig 6.7, the exclusion of CD36 from Triton X-100 resistant domains maybe because CD36 exists in the low sphingolipid and cholesterol containing subdomains, thus is less resistant to detergents like Triton X-100. In fact, 0.5% Triton X-100 extracted rafts exclude the majority of CD36 (Zeng et al. 2003). Therefore, accumulation of rafts that may be caused by ceramide could possibly result in CD36 storage. Alternatively, the endosomal and lysosomal alteration induced by lipid accumulation may redistribute CD36. These mechanisms could possibly explain the extent of downregulated cell surface proteins by ceramide (Phillips DC PhD thesis, 2003).

The mechanism by which CD36 is shed from the cell membrane is not clear to date. The reduction of soluble CD36 caused by ceramide is maybe due to less surface expression and the tendency of cells to retain a minimum level of receptors on the plasma membrane.

In addition, the present work demonstrated that C_2 ceramide (10 and 20 μM) inhibits U937 monocyte differentiation, which was seen by reduced expression of the differentiation marker, mannose receptor, and fewer adherent cells in this study. Ceramide has been reported to play different roles in differentiation depending on the cell type. C_2 ceramide (20 μM) inhibit 3T3-L1 preadipocyte differentiation in part by enhancing dephosphorylation and premature nuclear export of CCAAT-enhancer-binding proteins β at a time when its maximal transcriptional

activity is required to drive adipogenesis (Sprott et al. 2002). On the other hand, C_2 ceramide (8 μM) induces cell differentiation on human primary monocytes through stimulating differentiation-dependent cDNA (DIF-2) (Pietzsch et al. 1997). The effect of ceramide on differentiation is still not clear and needs to be investigated further.

7.1.3 Ceramide and OxLDL

As CD36 is the major scavenger receptor for uptake of OxLDL (as described in section 1.11), the effect of ceramide on OxLDL uptake was investigated (chapter 4). Ceramide reduces OxLDL uptake by both monocytes and macrophages. Anti-CD36 antibody alone did not successfully inhibit the uptake of OxLDL, however, significant reduction was obtained in the presence of excess unlabelled OxLDL. When receptors of OxLDL were partly blocked by excess unlabelled OxLDL, anti-CD36 antibody then significantly blocked further CD36 and reduced OxLDL uptake. However, the possibility that ceramide reduces the other receptors of OxLDL like scavenger receptor A cannot be excluded.

The downstream effects of OxLDL on intracellular ceramide signalling pathways also needs further investigation following the recent findings that SMase activity is promoted in vascular smooth muscle cells by OxLDL (Loidl et al. 2004).

Ceramide has been reported to be associated with atherosclerosis development. Production of ceramide is highly promoted during atherosclerosis (Marathe et al. 1998). Ceramide has also been proposed as an important second messenger and may contribute to the development of atherosclerosis by causing E-selectin dependent lymphocyte adhesion to endothelial cells (EC); promoting or inhibiting smooth muscle cell (SMC) proliferation; inducing apoptosis in EC, cardiomyocytes and T-lymphocytes as reviewed in (Levade et al. 2001). Ceramide has also been reported to contribute to LDL aggregation (Auge et al. 1996; Kinscherf et al. 1997), which is an essential process in atherosclerosis (Ross 1993). This could be due to its pronounced tendency for self-aggregation (Kinnunen and Holopainen 2002). However, the present studies indicated protective roles of ceramide in atherosclerosis development including: reducing CD36 cell surface expression and OxLDL uptake; inhibiting U937 monocyte differentiation; and down-regulating cellular ROS level. Previous work in this lab has shown that ceramide inhibits the adhesion of monocytes to endothelial cells, an essential step in atherosclerosis. Moreover, ceramide has been indicated to activate eNOS, NO production in endothelial cells, and subsequently endothelium-dependent vasorelaxation (Barsacchi et al. 2003; Mogami, Kishi, and Kobayashi 2005). These data shed new light on the role of ceramide in atherosclerosis. The promotion of ceramide content may be a self-protective response of cells to stress.

7.2 Conclusion

In conclusion, C_2 ceramide reduces the production of ROS in U937 cells partly through altering lipid raft environment and subsequently preventing the formation of active NADPH oxidase. Ceramide reduces the cell surface expression of CD36, reduces shedding of CD36, activates transcriptional expression of CD36 and induces intracellular CD36 level most likely through retaining the receptor inside cells.

7.3 further work

- The mechanism by which ceramide reduces NADPH oxidase activity could be investigated further using confocal microscopy and fluorescence-labelled ceramide to examine whether ceramide causes endocytosis of gp91 *phox* and to visualise the sites where ceramide induces *phox* component trafficking. The effect of ceramide on lipid raft environments may enable ceramide to be capable of modulating the membrane expression of any raft-associated protein.

- Ceramide may reduce the CD36 and CD11b cell surface expression by inhibiting its transportation from the ER to the Golgi. This effect of ceramide could be further examined using antibody staining and confocal microscopy.

- Ceramide induced endocytosis may contribute to the reduction of CD36 and OxLDL uptake. This can be further investigated using fluorescence labelled ceramide and confocal microscopy.

Chapter 8 References

References

1. Abate, C. et al., "Redox regulation of fos and jun DNA-binding activity in vitro," *Science* 249 (4973): 1157-1161 (1990).

2. Abumrad, N. A. et al., "Cloning of a rat adipocyte membrane protein implicated in binding or transport of long-chain fatty acids that is induced during preadipocyte differentiation. Homology with human CD36," *J.Biol.Chem.* 268 (24): 17665-17668 (1993).

3. Acton, S. L. et al., "Expression cloning of SR-BI, a CD36-related class B scavenger receptor," *J.Biol.Chem.* 269 (33): 21003-21009 (1994).

4. Adams, M. et al., "Transcriptional activation by peroxisome proliferator-activated receptor gamma is inhibited by phosphorylation at a consensus mitogen-activated protein kinase site," *J.Biol.Chem.* 272 (8): 5128-5132 (1997).

5. Aiken, M. L. et al., "Effects of OKM5, a monoclonal antibody to glycoprotein IV, on platelet aggregation and thrombospondin surface expression," *Blood* 76 (12): 2501-2509 (1990).

6. Aitman, T. J. et al., "Identification of Cd36 (Fat) as an insulin-resistance gene causing defective fatty acid and glucose metabolism in hypertensive rats," *Nat.Genet.* 21 (1): 76-83 (1999).

7. Akerboom, T. P. and H. Sies, "Assay of glutathione, glutathione disulfide, and glutathione mixed disulfides in biological samples," *Methods Enzymol.* 77:

373-382 (1981).

8. Alessio, M. et al., "Synthesis, processing, and intracellular transport of CD36 during monocytic differentiation," *J.Biol.Chem.* 271 (3): 1770-1775 (1996).

9. Alessio, M. et al., "Analysis of the human CD36 leucocyte differentiation antigen by means of the monoclonal antibody NL07," *Cell Immunol.* 137 (2): 487-500 (1991).

10. Andrieu-Abadie, N. et al., "Ceramide in apoptosis signaling: relationship with oxidative stress," *Free Radic.Biol.Med.* 31 (6): 717-728 (2001).

11. Armesilla, A. L., D. Calvo, and M. A. Vega, "Structural and functional characterization of the human CD36 gene promoter: identification of a proximal PEBP2/CBF site," *J.Biol.Chem.* 271 (13): 7781-7787 (1996).

12. Atlante, A. et al., "Glutamate neurotoxicity in rat cerebellar granule cells: a major role for xanthine oxidase in oxygen radical formation," *J.Neurochem.* 68 (5): 2038-2045 (1997).

13. Auge, N. et al., "The sphingomyelin-ceramide signaling pathway is involved in oxidized low density lipoprotein-induced cell proliferation," *J.Biol.Chem.* 271 (32): 19251-19255 (1996).

14. Auge, N. et al., "Potential role for ceramide in mitogen-activated protein kinase activation and proliferation of vascular smooth muscle cells induced by oxidized low density lipoprotein," *J.Biol.Chem.* 273 (21): 12893-12900 (1998).

15. Austin, M. A. et al., "Low-density lipoprotein subclass patterns and risk of myocardial infarction," *JAMA* 260 (13): 1917-1921 (1988).

16. Azumi, H. et al., "Expression of NADH/NADPH oxidase p22phox in human coronary arteries," *Circulation* 100 (14): 1494-1498 (1999).

17. Baggiolini, M., B. Dewald, and B. Moser, "Interleukin-8 and related chemotactic cytokines--CXC and CC chemokines," *Adv.Immunol.* 55: 97-179 (1994).

18. Barsacchi, R. et al., "Activation of endothelial nitric-oxide synthase by tumor necrosis factor-alpha: a novel pathway involving sequential activation of neutral sphingomyelinase, phosphatidylinositol-3' kinase, and Akt," *Mol.Pharmacol.* 63 (4): 886-895 (2003).

19. Bauer, G., "Reactive oxygen and nitrogen species: efficient, selective, and interactive signals during intercellular induction of apoptosis," *Anticancer Res.* 20 (6B): 4115-4139 (2000).

20. Belkner, J., H. Stender, and H. Kuhn, "The rabbit 15-lipoxygenase preferentially oxygenates LDL cholesterol esters, and this reaction does not require vitamin E," *J.Biol.Chem.* 273 (36): 23225-23232 (1998).

21. Berliner, J. A. and J. W. Heinecke, "The role of oxidized lipoproteins in atherogenesis," *Free Radic.Biol.Med.* 20 (5): 707-727 (1996).

22. Berliner, J. A. et al., "Monocyte chemotactic factor produced by large vessel endothelial cells in vitro," *Arteriosclerosis* 6 (3): 254-258 (1986).

23. Beyer, R. E., "An analysis of the role of coenzyme Q in free radical generation and as an antioxidant," *Biochem.Cell Biol.* 70 (6): 390-403 (1992).

24. Bocan, T. M. et al., "A specific 15-lipoxygenase inhibitor limits the progression and monocyte-macrophage enrichment of hypercholesterolemia-induced

atherosclerosis in the rabbit," *Atherosclerosis* 136 (2): 203-216 (1998).

25. Bokoch, G. M., "Chemoattractant signaling and leukocyte activation," *Blood* 86 (5): 1649-1660 (1995).

26. Bose, R. et al., "Ceramide synthase mediates daunorubicin-induced apoptosis: an alternative mechanism for generating death signals," *Cell* 82 (3): 405-414 (1995).

27. Boveris, A., "Mitochondrial production of superoxide radical and hydrogen peroxide," *Adv.Exp.Med.Biol.* 78: 67-82 (1977).

28. Bowie, A. G., P. N. Moynagh, and L. A. O'Neill, "Lipid peroxidation is involved in the activation of NF-kappaB by tumor necrosis factor but not interleukin-1 in the human endothelial cell line ECV304. Lack of involvement of H2O2 in NF-kappaB activation by either cytokine in both primary and transformed endothelial cells," *J.Biol.Chem.* 272 (41): 25941-25950 (1997).

29. Bradshaw, R. A., L. Kanarek, and R. L. Hill, "The preparation, properties, and reactivation of the mixed disulfide derivative of egg white lysozyme and L-cystine," *J.Biol.Chem.* 242 (17): 3789-3798 (1967).

30. Brandes, R. P. and J. Kreuzer, "Vascular NADPH oxidases: molecular mechanisms of activation," *Cardiovasc.Res.* 65 (1): 16-27 (2005).

31. Brash, A. R., "Lipoxygenases: occurrence, functions, catalysis, and acquisition of substrate," *J.Biol.Chem.* 274 (34): 23679-23682 (1999).

32. Brennan, P. and L. A. O'Neill, "Effects of oxidants and antioxidants on nuclear factor kappa B activation in three different cell lines: evidence against a

universal hypothesis involving oxygen radicals," *Biochim.Biophys.Acta* 1260 (2): 167-175 (1995).

33. Brown, D. A. and J. K. Rose, "Sorting of GPI-anchored proteins to glycolipid-enriched membrane subdomains during transport to the apical cell surface," *Cell* 68 (3): 533-544 (1992).

34. Brown, G. D. et al., "Dectin-1 mediates the biological effects of beta-glucans," *J.Exp.Med.* 197 (9): 1119-1124 (2003).

35. Brown, M. S. and J. L. Goldstein, "A receptor-mediated pathway for cholesterol homeostasis," *Science* 232 (4746): 34-47 (1986).

36. Brown, M. S., Y. K. Ho, and J. L. Goldstein, "The cholesteryl ester cycle in macrophage foam cells. Continual hydrolysis and re-esterification of cytoplasmic cholesteryl esters," *J.Biol.Chem.* 255 (19): 9344-9352 (1980).

37. Bull, H. A., P. M. Brickell, and P. M. Dowd, "Src-related protein tyrosine kinases are physically associated with the surface antigen CD36 in human dermal microvascular endothelial cells," *FEBS Lett.* 351 (1): 41-44 (1994).

38. Bump, E. A. and D. J. Reed, "A unique property of fetal bovine serum: high levels of protein-glutathione mixed disulfides," *In Vitro* 13 (2): 115-118 (1977).

39. Calvo, D. et al., "Human CD36 is a high affinity receptor for the native lipoproteins HDL, LDL, and VLDL," *J.Lipid Res.* 39 (4): 777-788 (1998).

40. Camp, H. S. and S. R. Tafuri, "Regulation of peroxisome proliferator-activated receptor gamma activity by mitogen-activated protein kinase," *J.Biol.Chem.* 272 (16): 10811-10816 (1997).

41. Campos, M. A. et al., "Activation of Toll-like receptor-2 by glycosylphosphatidylinositol anchors from a protozoan parasite," *J.Immunol.* 167 (1): 416-423 (2001).

42. Candelario-Jalil, E. et al., "Assessment of the relative contribution of COX-1 and COX-2 isoforms to ischemia-induced oxidative damage and neurodegeneration following transient global cerebral ischemia," *J.Neurochem.* 86 (3): 545-555 (2003).

43. Cathcart, M. K., A. K. McNally, and G. M. Chisolm, "Lipoxygenase-mediated transformation of human low density lipoprotein to an oxidized and cytotoxic complex," *J.Lipid Res.* 32 (1): 63-70 (1991).

44. Chen, C. S., A. G. Rosenwald, and R. E. Pagano, "Ceramide as a modulator of endocytosis," *J.Biol.Chem.* 270 (22): 13291-13297 (1995).

45. Chen, Z. et al., "Troglitazone inhibits atherosclerosis in apolipoprotein E-knockout mice: pleiotropic effects on CD36 expression and HDL," *Arterioscler.Thromb.Vasc.Biol.* 21 (3): 372-377 (2001).

46. Cheng, G. et al., "Homologs of gp91phox: cloning and tissue expression of Nox3, Nox4, and Nox5," *Gene* 269 (1-2): 131-140 (2001).

47. Chinetti, G. et al., "PPAR-alpha and PPAR-gamma activators induce cholesterol removal from human macrophage foam cells through stimulation of the ABCA1 pathway," *Nat.Med.* 7 (1): 53-58 (2001).

48. Cho, S. et al., "Glutathione downregulates the phosphorylation of I kappa B: autoloop regulation of the NF-kappa B-mediated expression of NF-kappa B

subunits by TNF-alpha in mouse vascular endothelial cells," *Biochem.Biophys.Res.Commun.* 253 (1): 104-108 (1998).

49. Chung, B. H. et al., "Single vertical spin density gradient ultracentrifugation," *Methods Enzymol.* 128: 181-209 (1986).

50. Claiborne, A. et al., "Protein-sulfenic acids: diverse roles for an unlikely player in enzyme catalysis and redox regulation," *Biochemistry* 38 (47): 15407-15416 (1999).

51. Cobb, M. H., "MAP kinase pathways," *Prog.Biophys.Mol.Biol.* 71 (3-4): 479-500 (1999).

52. Cohen, J. J., "Apoptosis," *Immunol.Today* 14 (3): 126-130 (1993).

53. Collins, A. R. et al., "Troglitazone inhibits formation of early atherosclerotic lesions in diabetic and nondiabetic low density lipoprotein receptor-deficient mice," *Arterioscler.Thromb.Vasc.Biol.* 21 (3): 365-371 (2001).

54. Cushing, S. D. et al., "Minimally modified low density lipoprotein induces monocyte chemotactic protein 1 in human endothelial cells and smooth muscle cells," *Proc.Natl.Acad.Sci.U.S.A* 87 (13): 5134-5138 (1990).

55. Cuvillier, O. et al., "Suppression of ceramide-mediated programmed cell death by sphingosine-1-phosphate," *Nature* 381 (6585): 800-803 (1996).

56. Cyrus, T. et al., "Absence of 12/15-lipoxygenase expression decreases lipid peroxidation and atherogenesis in apolipoprotein e-deficient mice," *Circulation* 103 (18): 2277-2282 (2001).

57. Cyrus, T. et al., "Disruption of the 12/15-lipoxygenase gene diminishes

atherosclerosis in apo E-deficient mice," *J.Clin.Invest* 103 (11): 1597-1604 (1999).

58. David, A., R. Fridlich, and I. Aviram, "The presence of membrane Proteinase 3 in neutrophil lipid rafts and its colocalization with FcgammaRIIIb and cytochrome b558," *Exp.Cell Res.* 308 (1): 156-165 (2005).

59. Davies, K. J., "Degradation of oxidized proteins by the 20S proteasome," *Biochimie* 83 (3-4): 301-310 (2001).

60. Dawson, P. A. et al., "Sterol-dependent repression of low density lipoprotein receptor promoter mediated by 16-base pair sequence adjacent to binding site for transcription factor Sp1," *J.Biol.Chem.* 263 (7): 3372-3379 (1988).

61. De Maria, R. et al., "Functional expression of Fas and Fas ligand on human gut lamina propria T lymphocytes. A potential role for the acidic sphingomyelinase pathway in normal immunoregulation," *J.Clin.Invest* 97 (2): 316-322 (1996).

62. Deigner, H. P. et al., "Ceramide induces aSMase expression: implications for oxLDL-induced apoptosis," *FASEB J.* 15 (3): 807-814 (2001).

63. DeLeo, F. R. et al., "Neutrophils exposed to bacterial lipopolysaccharide upregulate NADPH oxidase assembly," *J.Clin.Invest* 101 (2): 455-463 (1998).

64. DeLucia, A. J. et al., "Ozone interaction with rodent lung. III. Oxidation of reduced glutathione and formation of mixed disulfides between protein and nonprotein sulfhydryls," *J.Clin.Invest* 55 (4): 794-802 (1975).

65. Devaraj, S., I. Hugou, and I. Jialal, "Alpha-tocopherol decreases CD36 expression in human monocyte-derived macrophages," *J.Lipid Res.* 42 (4): 521-527

(2001).

66. Dhaliwal, B. S. and U. P. Steinbrecher, "Scavenger receptors and oxidized low density lipoproteins," *Clin.Chim.Acta* 286 (1-2): 191-205 (1999).

67. Dimmeler, S. et al., "Angiotensin II induces apoptosis of human endothelial cells. Protective effect of nitric oxide," *Circ.Res.* 81 (6): 970-976 (1997).

68. Dimmeler, S. and A. M. Zeiher, "Reactive oxygen species and vascular cell apoptosis in response to angiotensin II and pro-atherosclerotic factors," *Regul.Pept.* 90 (1-3): 19-25 (2000).

69. Dobrowsky, R. T., "Sphingolipid signalling domains floating on rafts or buried in caves?," *Cell Signal.* 12 (2): 81-90 (2000).

70. Doi, T. et al., "Charged collagen structure mediates the recognition of negatively charged macromolecules by macrophage scavenger receptors," *J.Biol.Chem.* 268 (3): 2126-2133 (1993).

71. Drevot, P. et al., "TCR signal initiation machinery is pre-assembled and activated in a subset of membrane rafts," *EMBO J.* 21 (8): 1899-1908 (2002).

72. Droge, W., "Free radicals in the physiological control of cell function," *Physiol Rev.* 82 (1): 47-95 (2002).

73. Du, G., A. Mouithys-Mickalad, and F. E. Sluse, "Generation of superoxide anion by mitochondria and impairment of their functions during anoxia and reoxygenation in vitro," *Free Radic.Biol.Med.* 25 (9): 1066-1074 (1998).

74. Dupont, G. P. et al., "Regulation of xanthine dehydrogenase and xanthine oxidase activity and gene expression in cultured rat pulmonary endothelial

cells," *J.Clin.Invest* 89 (1): 197-202 (1992).

75. Durrington, P. N., B. Mackness, and M. I. Mackness, "Paraoxonase and atherosclerosis," *Arterioscler.Thromb.Vasc.Biol.* 21 (4): 473-480 (2001).

76. Edidin, M., "The state of lipid rafts: from model membranes to cells," *Annu.Rev.Biophys.Biomol.Struct.* 32: 257-283 (2003).

77. El Bekay, R. et al., "Oxidative stress is a critical mediator of the angiotensin II signal in human neutrophils: involvement of mitogen-activated protein kinase, calcineurin, and the transcription factor NF-kappaB," *Blood* 102 (2): 662-671 (2003).

78. El Benna, J. et al., "Phagocyte NADPH oxidase: a multicomponent enzyme essential for host defenses," *Arch.Immunol.Ther.Exp.(Warsz.)* 53 (3): 199-206 (2005).

79. Endemann, G. et al., "CD36 is a receptor for oxidized low density lipoprotein," *J.Biol.Chem.* 268 (16): 11811-11816 (1993).

80. Escargueil-Blanc, I. et al., "Apoptosis and activation of the sphingomyelin-ceramide pathway induced by oxidized low density lipoproteins are not causally related in ECV-304 endothelial cells," *J.Biol.Chem.* 273 (42): 27389-27395 (1998).

81. Febbraio, M. et al., "Targeted disruption of the class B scavenger receptor CD36 protects against atherosclerotic lesion development in mice," *J.Clin.Invest* 105 (8): 1049-1056 (2000).

82. Finkel, T., "Oxidant signals and oxidative stress," *Curr.Opin.Cell Biol.*

15 (2): 247-254 (2003).

83. FitzGerald, G. A., "COX-2 and beyond: Approaches to prostaglandin inhibition in human disease," *Nat.Rev.Drug Discov.* 2 (11): 879-890 (2003).

84. Fogelman, A. M. et al., "Macrophage lipoprotein receptors," *J.Cell Sci.Suppl* 9: 135-149 (1988).

85. Folcik, V. A. and M. K. Cathcart, "Assessment of 5-lipoxygenase involvement in human monocyte-mediated LDL oxidation," *J.Lipid Res.* 34 (1): 69-79 (1993).

86. Folcik, V. A. et al., "Lipoxygenase contributes to the oxidation of lipids in human atherosclerotic plaques," *J.Clin.Invest* 96 (1): 504-510 (1995).

87. Foster, L. J., C. L. De Hoog, and M. Mann, "Unbiased quantitative proteomics of lipid rafts reveals high specificity for signaling factors," *Proc.Natl.Acad.Sci.U.S.A* 100 (10): 5813-5818 (2003).

88. Fra, A. M. et al., "De novo formation of caveolae in lymphocytes by expression of VIP21-caveolin," *Proc.Natl.Acad.Sci.U.S.A* 92 (19): 8655-8659 (1995).

89. Friedrichson, T. and T. V. Kurzchalia, "Microdomains of GPI-anchored proteins in living cells revealed by crosslinking," *Nature* 394 (6695): 802-805 (1998).

90. Fuhrman, B., N. Volkova, and M. Aviram, "Oxidative stress increases the expression of the CD36 scavenger receptor and the cellular uptake of oxidized low-density lipoprotein in macrophages from atherosclerotic mice: protective role of

antioxidants and of paraoxonase," *Atherosclerosis* 161 (2): 307-316 (2002).

91. Gabriel, C. et al., "Determination of nitric oxide generation in mammalian neurons using dichlorofluorescin diacetate and flow cytometry," *J.Pharmacol.Toxicol.Methods* 38 (2): 93-98 (1997).

92. Gantner, B. N. et al., "Collaborative induction of inflammatory responses by dectin-1 and Toll-like receptor 2," *J.Exp.Med.* 197 (9): 1107-1117 (2003).

93. George, J. et al., "12/15-Lipoxygenase gene disruption attenuates atherogenesis in LDL receptor-deficient mice," *Circulation* 104 (14): 1646-1650 (2001).

94. Gidwani, A. et al., "Disruption of lipid order by short-chain ceramides correlates with inhibition of phospholipase D and downstream signaling by FcepsilonRI," *J.Cell Sci.* 116 (Pt 15): 3177-3187 (2003).

95. Gilbert, H. F., "Biological disulfides: the third messenger? Modulation of phosphofructokinase activity by thiol/disulfide exchange," *J.Biol.Chem.* 257 (20): 12086-12091 (1982).

96. Ginn-Pease, M. E. and R. L. Whisler, "Optimal NF kappa B mediated transcriptional responses in Jurkat T cells exposed to oxidative stress are dependent on intracellular glutathione and costimulatory signals," *Biochem.Biophys.Res.Commun.* 226 (3): 695-702 (1996).

97. Glebov, O. O. and B. J. Nichols, "Lipid raft proteins have a random distribution during localized activation of the T-cell receptor," *Nat.Cell Biol.* 6 (3):

238-243 (2004).

98. Goldkorn, T., T. Ravid, and E. M. Khan, "Life and death decisions: ceramide generation and EGF receptor trafficking are modulated by oxidative stress," *Antioxid.Redox.Signal.* 7 (1-2): 119-128 (2005).

99. Gomez-Mouton, C. et al., "Segregation of leading-edge and uropod components into specific lipid rafts during T cell polarization," *Proc.Natl.Acad.Sci.U.S.A* 98 (17): 9642-9647 (2001).

100. Gown, A. M., T. Tsukada, and R. Ross, "Human atherosclerosis. II. Immunocytochemical analysis of the cellular composition of human atherosclerotic lesions," *Am.J.Pathol.* 125 (1): 191-207 (1986).

101. Greenwalt, D. E. et al., "Membrane glycoprotein CD36: a review of its roles in adherence, signal transduction, and transfusion medicine," *Blood* 80 (5): 1105-1115 (1992).

102. Griendling, K. K., D. Sorescu, and M. Ushio-Fukai, "NAD(P)H oxidase: role in cardiovascular biology and disease," *Circ.Res.* 86 (5): 494-501 (2000).

103. Gruetter, C. A. et al., "Relaxation of bovine coronary artery and activation of coronary arterial guanylate cyclase by nitric oxide, nitroprusside and a carcinogenic nitrosoamine," *J.Cyclic.Nucleotide.Res.* 5 (3): 211-224 (1979).

104. Grune, T. et al., "Selective degradation of oxidatively modified protein substrates by the proteasome," *Biochem.Biophys.Res.Commun.* 305 (3): 709-718 (2003).

105. Guichard, C. et al., "Interleukin-8-induced Priming of Neutrophil

Oxidative Burst Requires Sequential Recruitment of NADPH Oxidase Components into Lipid Rafts," *J.Biol.Chem.* 280 (44): 37021-37032 (2005).

106. Gunasekar, P. G. et al., "Monitoring intracellular nitric oxide formation by dichlorofluorescin in neuronal cells," *J.Neurosci.Methods* 61 (1-2): 15-21 (1995).

107. Guzik, T. J. et al., "Mechanisms of increased vascular superoxide production in human diabetes mellitus: role of NAD(P)H oxidase and endothelial nitric oxide synthase," *Circulation* 105 (14): 1656-1662 (2002).

108. Guzik, T. J. et al., "Functional effect of the C242T polymorphism in the NAD(P)H oxidase p22phox gene on vascular superoxide production in atherosclerosis," *Circulation* 102 (15): 1744-1747 (2000).

109. Haimovitz-Friedman, A. et al., "Lipopolysaccharide induces disseminated endothelial apoptosis requiring ceramide generation," *J.Exp.Med.* 186 (11): 1831-1841 (1997).

110. Haimovitz-Friedman, A. et al., "Ionizing radiation acts on cellular membranes to generate ceramide and initiate apoptosis," *J.Exp.Med.* 180 (2): 525-535 (1994).

111. Han, J. et al., "Native and modified low density lipoproteins increase the functional expression of the macrophage class B scavenger receptor, CD36," *J.Biol.Chem.* 272 (34): 21654-21659 (1997b).

112. Han, J. et al., "Native and modified low density lipoproteins increase the functional expression of the macrophage class B scavenger receptor, CD36," *J.Biol.Chem.* 272 (34): 21654-21659 (1997a).

113. Han, J. et al., "Transforming growth factor-beta1 (TGF-beta1) and TGF-beta2 decrease expression of CD36, the type B scavenger receptor, through mitogen-activated protein kinase phosphorylation of peroxisome proliferator-activated receptor-gamma," *J.Biol.Chem.* 275 (2): 1241-1246 (2000).

114. Han, J. et al., "Regulation of peroxisome proliferator-activated receptor-gamma-mediated gene expression. A new mechanism of action for high density lipoprotein," *J.Biol.Chem.* 277 (26): 23582-23586 (2002).

115. Han, J. et al., "Pitavastatin downregulates expression of the macrophage type B scavenger receptor, CD36," *Circulation* 109 (6): 790-796 (2004).

116. Hannun, Y. A. and C. Luberto, "Ceramide in the eukaryotic stress response," *Trends Cell Biol.* 10 (2): 73-80 (2000).

117. Hansson, G. K., "Inflammation, atherosclerosis, and coronary artery disease," *N.Engl.J.Med.* 352 (16): 1685-1695 (2005).

118. Harada-Shiba, M. et al., "Oxidized low density lipoprotein induces apoptosis in cultured human umbilical vein endothelial cells by common and unique mechanisms," *J.Biol.Chem.* 273 (16): 9681-9687 (1998).

119. Harats, D. et al., "Overexpression of 15-lipoxygenase in vascular endothelium accelerates early atherosclerosis in LDL receptor-deficient mice," *Arterioscler.Thromb.Vasc.Biol.* 20 (9): 2100-2105 (2000).

120. Hemmens, B. and B. Mayer, "Enzymology of nitric oxide synthases," *Methods Mol.Biol.* 100: 1-32 (1998).

121. Hiltunen, T. et al., "Induction of 15-lipoxygenase mRNA and protein in

early atherosclerotic lesions," *Circulation* 92 (11): 3297-3303 (1995).

122. Hirota, K. et al., "AP-1 transcriptional activity is regulated by a direct association between thioredoxin and Ref-1," *Proc.Natl.Acad.Sci.U.S.A* 94 (8): 3633-3638 (1997).

123. Hoebe, K. et al., "CD36 is a sensor of diacylglycerides," *Nature* 433 (7025): 523-527 (2005).

124. Holopainen, J. M., M. I. Angelova, and P. K. Kinnunen, "Vectorial budding of vesicles by asymmetrical enzymatic formation of ceramide in giant liposomes," *Biophys.J.* 78 (2): 830-838 (2000).

125. Holopainen, J. M., M. Subramanian, and P. K. Kinnunen, "Sphingomyelinase induces lipid microdomain formation in a fluid phosphatidylcholine/sphingomyelin membrane," *Biochemistry* 37 (50): 17562-17570 (1998).

126. Houston, M. et al., "Binding of xanthine oxidase to vascular endothelium. Kinetic characterization and oxidative impairment of nitric oxide-dependent signaling," *J.Biol.Chem.* 274 (8): 4985-4994 (1999).

127. Huang, M. M. et al., "Membrane glycoprotein IV (CD36) is physically associated with the Fyn, Lyn, and Yes protein-tyrosine kinases in human platelets," *Proc.Natl.Acad.Sci.U.S.A* 88 (17): 7844-7848 (1991).

128. Huh, H. Y. et al., "Regulated expression of CD36 during monocyte-to-macrophage differentiation: potential role of CD36 in foam cell formation," *Blood* 87 (5): 2020-2028 (1996a).

129. Huh, H. Y. et al., "Regulated expression of CD36 during monocyte-to-macrophage differentiation: potential role of CD36 in foam cell formation," *Blood* 87 (5): 2020-2028 (1996b).

130. Hwang, D. et al., "Expression of mitogen-inducible cyclooxygenase induced by lipopolysaccharide: mediation through both mitogen-activated protein kinase and NF-kappaB signaling pathways in macrophages," *Biochem.Pharmacol.* 54 (1): 87-96 (1997).

131. Ignarro, L. J. et al., "Pharmacological evidence that endothelium-derived relaxing factor is nitric oxide: use of pyrogallol and superoxide dismutase to study endothelium-dependent and nitric oxide-elicited vascular smooth muscle relaxation," *J.Pharmacol.Exp.Ther.* 244 (1): 181-189 (1988).

132. Ikonen, E. and R. G. Parton, "Caveolins and cellular cholesterol balance," *Traffic.* 1 (3): 212-217 (2000).

133. Ilangumaran, S. et al., "Microdomain-dependent regulation of Lck and Fyn protein-tyrosine kinases in T lymphocyte plasma membranes," *Mol.Biol.Cell* 10 (4): 891-905 (1999).

134. Inoguchi, T. et al., "Protein kinase C-dependent increase in reactive oxygen species (ROS) production in vascular tissues of diabetes: role of vascular NAD(P)H oxidase," *J.Am.Soc.Nephrol.* 14 (8 Suppl 3): S227-S232 (2003).

135. Irani, K., "Oxidant signaling in vascular cell growth, death, and survival : a review of the roles of reactive oxygen species in smooth muscle and endothelial cell mitogenic and apoptotic signaling," *Circ.Res.* 87 (3): 179-183

(2000).

136. Ishii, T. et al., "Role of Nrf2 in the regulation of CD36 and stress protein expression in murine macrophages: activation by oxidatively modified LDL and 4-hydroxynonenal," *Circ.Res.* 94 (5): 609-616 (2004).

137. Janssen-Heininger, Y. M., I. Macara, and B. T. Mossman, "Cooperativity between oxidants and tumor necrosis factor in the activation of nuclear factor (NF)-kappaB: requirement of Ras/mitogen-activated protein kinases in the activation of NF-kappaB by oxidants," *Am.J.Respir.Cell Mol.Biol.* 20 (5): 942-952 (1999).

138. Jessup, W. et al., "5-Lipoxygenase is not essential in macrophage-mediated oxidation of low-density lipoprotein," *Biochem.J.* 278 (Pt 1): 163-169 (1991).

139. Jiang, J. et al., "Arachidonic acid-induced carbon-centered radicals and phospholipid peroxidation in cyclo-oxygenase-2-transfected PC12 cells," *J.Neurochem.* 90 (5): 1036-1049 (2004).

140. Johnson, T. M. et al., "Reactive oxygen species are downstream mediators of p53-dependent apoptosis," *Proc.Natl.Acad.Sci.U.S.A* 93 (21): 11848-11852 (1996).

141. Kajita, K. et al., "TNFalpha reduces the expression of peroxisome proliferator-activated receptor gamma (PPARgamma) via the production of ceramide and activation of atypical PKC," *Diabetes Res.Clin.Pract.* 66 Suppl 1: S79-S83 (2004).

142. Kamata, H. et al., "Hydrogen peroxide activates IkappaB kinases through phosphorylation of serine residues in the activation loops," *FEBS Lett.* 519 (1-3): 231-237 (2002).

143. Kawakami, A. et al., "Modulation of the expression of membrane-bound CD54 (mCD54) and soluble form of CD54 (sCD54) in endothelial cells by glucosyl transferase inhibitor: possible role of ceramide for the shedding of mCD54," *Biochem.Biophys.Res.Commun.* 296 (1): 26-31 (2002).

144. Kempe, S. et al., "NF-kappaB controls the global pro-inflammatory response in endothelial cells: evidence for the regulation of a pro-atherogenic program," *Nucleic Acids Res.* 33 (16): 5308-5319 (2005).

145. Kenworthy, A. K. et al., "Dynamics of putative raft-associated proteins at the cell surface," *J.Cell Biol.* 165 (5): 735-746 (2004).

146. KESTON, A. S. and R. BRANDT, "THE FLUOROMETRIC ANALYSIS OF ULTRAMICRO QUANTITIES OF HYDROGEN PEROXIDE," *Anal.Biochem.* 11: 1-5 (1965).

147. Kinnunen, P. K. and J. M. Holopainen, "Sphingomyelinase activity of LDL: a link between atherosclerosis, ceramide, and apoptosis?," *Trends Cardiovasc.Med.* 12 (1): 37-42 (2002).

148. Kinscherf, R. et al., "Modified low density lipoprotein delivers substrate for ceramide formation and stimulates the sphingomyelin-ceramide pathway in human macrophages," *FEBS Lett.* 405 (1): 55-59 (1997).

149. Klatt, P. et al., "Redox regulation of c-Jun DNA binding by reversible

S-glutathiolation," *FASEB J.* 13 (12): 1481-1490 (1999).

150. Kobayashi, T. et al., "Late endosomal membranes rich in lysobisphosphatidic acid regulate cholesterol transport," *Nat.Cell Biol.* 1 (2): 113-118 (1999).

151. Kodama, T. et al., "Type I macrophage scavenger receptor contains alpha-helical and collagen-like coiled coils," *Nature* 343 (6258): 531-535 (1990).

152. Kolesnick, R. N., F. M. Goni, and A. Alonso, "Compartmentalization of ceramide signaling: physical foundations and biological effects," *J.Cell Physiol* 184 (3): 285-300 (2000).

153. Kooy, N. W., J. A. Royall, and H. Ischiropoulos, "Oxidation of 2',7'-dichlorofluorescin by peroxynitrite," *Free Radic.Res.* 27 (3): 245-254 (1997).

154. Kormoczi, G. F. et al., "Serum proteins modified by neutrophil-derived oxidants as mediators of neutrophil stimulation," *J.Immunol.* 167 (1): 451-460 (2001).

155. Krause, K. H., "Tissue distribution and putative physiological function of NOX family NADPH oxidases," *Jpn.J.Infect.Dis.* 57 (5): S28-S29 (2004).

156. Krieger, M. and J. Herz, "Structures and functions of multiligand lipoprotein receptors: macrophage scavenger receptors and LDL receptor-related protein (LRP)," *Annu.Rev.Biochem.* 63: 601-637 (1994).

157. Kroesen, B. J. et al., "BcR-induced apoptosis involves differential regulation of C16 and C24-ceramide formation and sphingolipid-dependent activation of the proteasome," *J.Biol.Chem.* 278 (17): 14723-14731 (2003).

158. Kuhn, H. et al., "Involvement of 15-lipoxygenase in early stages of atherogenesis," *J.Exp.Med.* 179 (6): 1903-1911 (1994).

159. Kuhn, H. et al., "In vivo action of 15-lipoxygenase in early stages of human atherogenesis," *J.Clin.Invest* 99 (5): 888-893 (1997).

160. Kuhn, H. and B. J. Thiele, "The diversity of the lipoxygenase family. Many sequence data but little information on biological significance," *FEBS Lett.* 449 (1): 7-11 (1999).

161. Kunsch, C. and R. M. Medford, "Oxidative stress as a regulator of gene expression in the vasculature," *Circ.Res.* 85 (8): 753-766 (1999).

162. Kuo, W. N. et al., "Modification of proteins and polynucleotides by peroxynitrite," *Cytobios* 99 (390): 47-55 (1999).

163. Lada, A. T. and L. L. Rudel, "Associations of low density lipoprotein particle composition with atherogenicity," *Curr.Opin.Lipidol.* 15 (1): 19-24 (2004).

164. Le, P. U. et al., "Caveolin-1 is a negative regulator of caveolae-mediated endocytosis to the endoplasmic reticulum," *J.Biol.Chem.* 277 (5): 3371-3379 (2002).

165. LeBel, C. P., H. Ischiropoulos, and S. C. Bondy, "Evaluation of the probe 2',7'-dichlorofluorescin as an indicator of reactive oxygen species formation and oxidative stress," *Chem.Res.Toxicol.* 5 (2): 227-231 (1992).

166. Levade, T. et al., "Sphingolipid mediators in cardiovascular cell biology and pathology," *Circ.Res.* 89 (11): 957-968 (2001).

167. Levade, T. and J. P. Jaffrezou, "Signalling sphingomyelinases: which, where, how and why?," *Biochim.Biophys.Acta* 1438 (1): 1-17 (1999).

168. Li, A. C. et al., "Peroxisome proliferator-activated receptor gamma ligands inhibit development of atherosclerosis in LDL receptor-deficient mice," *J.Clin.Invest* 106 (4): 523-531 (2000).

169. Li, D. et al., "Proapoptotic effects of ANG II in human coronary artery endothelial cells: role of AT1 receptor and PKC activation," *Am.J.Physiol* 276 (3 Pt 2): H786-H792 (1999).

170. Li, R., E. J. Blanchette-Mackie, and S. Ladisch, "Induction of endocytic vesicles by exogenous C(6)-ceramide," *J.Biol.Chem.* 274 (30): 21121-21127 (1999).

171. Li, Y. et al., "Dilated cardiomyopathy and neonatal lethality in mutant mice lacking manganese superoxide dismutase," *Nat.Genet.* 11 (4): 376-381 (1995).

172. Li, Y., H. Zhu, and M. A. Trush, "Detection of mitochondria-derived reactive oxygen species production by the chemilumigenic probes lucigenin and luminol," *Biochim.Biophys.Acta* 1428 (1): 1-12 (1999).

173. Liang, C. P. et al., "Increased CD36 protein as a response to defective insulin signaling in macrophages," *J.Clin.Invest* 113 (5): 764-773 (2004).

174. Libby, P., "Inflammation in atherosclerosis," *Nature* 420 (6917): 868-874 (2002).

175. Lien, E. et al., "Toll-like receptor 2 functions as a pattern recognition receptor for diverse bacterial products," *J.Biol.Chem.* 274 (47): 33419-33425 (1999).

176. Ling, W. et al., "Oxidized or acetylated low density lipoproteins are rapidly cleared by the liver in mice with disruption of the scavenger receptor class A type I/II gene," *J.Clin.Invest* 100 (2): 244-252 (1997).

177. Lisanti, M. P. et al., "Characterization of caveolin-rich membrane domains isolated from an endothelial-rich source: implications for human disease," *J.Cell Biol.* 126 (1): 111-126 (1994).

178. Loidl, A. et al., "Role of ceramide in activation of stress-associated MAP kinases by minimally modified LDL in vascular smooth muscle cells," *Biochim.Biophys.Acta* 1690 (2): 150-158 (2004).

179. Loscalzo, J., "Oxidant stress: a key determinant of atherothrombosis," *Biochem.Soc.Trans.* 31 (Pt 5): 1059-1061 (2003).

180. Lougheed, M. et al., "High affinity saturable uptake of oxidized low density lipoprotein by macrophages from mice lacking the scavenger receptor class A type I/II," *J.Biol.Chem.* 272 (20): 12938-12944 (1997).

181. Lougheed, M. and U. P. Steinbrecher, "Mechanism of uptake of copper-oxidized low density lipoprotein in macrophages is dependent on its extent of oxidation," *J.Biol.Chem.* 271 (20): 11798-11805 (1996).

182. Lusis, A. J., "Atherosclerosis," *Nature* 407 (6801): 233-241 (2000).

183. Lynch, R. E. and I. Fridovich, "Permeation of the erythrocyte stroma by superoxide radical," *J.Biol.Chem.* 253 (13): 4697-4699 (1978).

184. Madore, N. et al., "Functionally different GPI proteins are organized in different domains on the neuronal surface," *EMBO J.* 18 (24): 6917-6926 (1999).

185. Mandon, E. C. et al., "Subcellular localization and membrane topology of serine palmitoyltransferase, 3-dehydrosphinganine reductase, and sphinganine N-acyltransferase in mouse liver," *J.Biol.Chem.* 267 (16): 11144-11148 (1992).

186. Mangan, D. F. et al., "Lethal effects of Actinobacillus actinomycetemcomitans leukotoxin on human T lymphocytes," *Infect.Immun.* 59 (9): 3267-3272 (1991).

187. Marathe, S. et al., "Human vascular endothelial cells are a rich and regulatable source of secretory sphingomyelinase. Implications for early atherogenesis and ceramide-mediated cell signaling," *J.Biol.Chem.* 273 (7): 4081-4088 (1998).

188. Marui, N. et al., "Vascular cell adhesion molecule-1 (VCAM-1) gene transcription and expression are regulated through an antioxidant-sensitive mechanism in human vascular endothelial cells," *J.Clin.Invest* 92 (4): 1866-1874 (1993).

189. Massey, J. B., "Interaction of ceramides with phosphatidylcholine, sphingomyelin and sphingomyelin/cholesterol bilayers," *Biochim.Biophys.Acta* 1510 (1-2): 167-184 (2001).

190. Maxeiner, H. et al., "Complementary roles for scavenger receptor A and CD36 of human monocyte-derived macrophages in adhesion to surfaces coated with oxidized low-density lipoproteins and in secretion of H2O2," *J.Exp.Med.* 188 (12): 2257-2265 (1998).

191. Mayor, S. and F. R. Maxfield, "Insolubility and redistribution of GPI-anchored proteins at the cell surface after detergent treatment," *Mol.Biol.Cell* 6 (7): 929-944 (1995).

192. Mayor, S., K. G. Rothberg, and F. R. Maxfield, "Sequestration of

GPI-anchored proteins in caveolae triggered by cross-linking," *Science* 264 (5167): 1948-1951 (1994).

193. Means, T. K. et al., "Human toll-like receptors mediate cellular activation by Mycobacterium tuberculosis," *J.Immunol.* 163 (7): 3920-3927 (1999).

194. Megha and E. London, "Ceramide selectively displaces cholesterol from ordered lipid domains (rafts): implications for lipid raft structure and function," *J.Biol.Chem.* 279 (11): 9997-10004 (2004).

195. Michel, C. et al., "Characterization of ceramide synthesis. A dihydroceramide desaturase introduces the 4,5-trans-double bond of sphingosine at the level of dihydroceramide," *J.Biol.Chem.* 272 (36): 22432-22437 (1997).

196. Misumi, Y. et al., "Novel blockade by brefeldin A of intracellular transport of secretory proteins in cultured rat hepatocytes," *J.Biol.Chem.* 261 (24): 11398-11403 (1986).

197. Mogami, K., H. Kishi, and S. Kobayashi, "Sphingomyelinase causes endothelium-dependent vasorelaxation through endothelial nitric oxide production without cytosolic Ca(2+) elevation," *FEBS Lett.* 579 (2): 393-397 (2005).

198. Moran, L. K., J. M. Gutteridge, and G. J. Quinlan, "Thiols in cellular redox signalling and control," *Curr.Med.Chem.* 8 (7): 763-772 (2001).

199. Munteanu, A., R. Ricciarelli, and J. M. Zingg, "HIV protease inhibitors-induced atherosclerosis: prevention by alpha-tocopherol," *IUBMB.Life* 56 (10): 629-631 (2004).

200. Munteanu, A. et al., "CD36 overexpression in ritonavir-treated THP-1

cells is reversed by alpha-tocopherol," *Free Radic.Biol.Med.* 38 (8): 1047-1056 (2005).

201. Myhre, O. et al., "Evaluation of the probes 2',7'-dichlorofluorescin diacetate, luminol, and lucigenin as indicators of reactive species formation," *Biochem.Pharmacol.* 65 (10): 1575-1582 (2003).

202. Nabi, I. R. and P. U. Le, "Caveolae/raft-dependent endocytosis," *J.Cell Biol.* 161 (4): 673-677 (2003).

203. Nagy, L. et al., "Oxidized LDL regulates macrophage gene expression through ligand activation of PPARgamma," *Cell* 93 (2): 229-240 (1998).

204. Nakagawa, T. et al., "Oxidized LDL increases and interferon-gamma decreases expression of CD36 in human monocyte-derived macrophages," *Arterioscler.Thromb.Vasc.Biol.* 18 (8): 1350-1357 (1998).

205. Nakata, A. et al., "CD36, a novel receptor for oxidized low-density lipoproteins, is highly expressed on lipid-laden macrophages in human atherosclerotic aorta," *Arterioscler.Thromb.Vasc.Biol.* 19 (5): 1333-1339 (1999).

206. Nakazono, K. et al., "Does superoxide underlie the pathogenesis of hypertension?," *Proc.Natl.Acad.Sci.U.S.A* 88 (22): 10045-10048 (1991).

207. Nathan, C., "Specificity of a third kind: reactive oxygen and nitrogen intermediates in cell signaling," *J.Clin.Invest* 111 (6): 769-778 (2003).

208. Navab, M. et al., "Monocyte transmigration induced by modification of low density lipoprotein in cocultures of human aortic wall cells is due to induction of monocyte chemotactic protein 1 synthesis and is abolished by high density

lipoprotein," *J.Clin.Invest* 88 (6): 2039-2046 (1991).

209. Neufeld, E. F., "Lysosomal storage diseases," *Annu.Rev.Biochem.* 60: 257-280 (1991).

210. Neuzil, J. et al., "Secretory phospholipase A2 and lipoprotein lipase enhance 15-lipoxygenase-induced enzymic and nonenzymic lipid peroxidation in low-density lipoproteins," *Biochemistry* 37 (25): 9203-9210 (1998).

211. Nicholson, A. C. et al., "Oxidized LDL binds to CD36 on human monocyte-derived macrophages and transfected cell lines. Evidence implicating the lipid moiety of the lipoprotein as the binding site," *Arterioscler.Thromb.Vasc.Biol.* 15 (2): 269-275 (1995).

212. Noorman, F. et al., "Monoclonal antibodies against the human mannose receptor as a specific marker in flow cytometry and immunohistochemistry for macrophages," *J.Leukoc.Biol.* 61 (1): 63-72 (1997).

213. Nozaki, S. et al., "Reduced uptake of oxidized low density lipoproteins in monocyte-derived macrophages from CD36-deficient subjects," *J.Clin.Invest* 96 (4): 1859-1865 (1995).

214. Nozik-Grayck, E., H. B. Suliman, and C. A. Piantadosi, "Extracellular superoxide dismutase," *Int.J.Biochem.Cell Biol.* 37 (12): 2466-2471 (2005).

215. Ockenhouse, C. F., C. Magowan, and J. D. Chulay, "Activation of monocytes and platelets by monoclonal antibodies or malaria-infected erythrocytes binding to the CD36 surface receptor in vitro," *J.Clin.Invest* 84 (2): 468-475 (1989).

216. Oh, P. and J. E. Schnitzer, "Immunoisolation of caveolae with high

affinity antibody binding to the oligomeric caveolin cage. Toward understanding the basis of purification," *J.Biol.Chem.* 274 (33): 23144-23154 (1999).

217. Ohara, Y., T. E. Peterson, and D. G. Harrison, "Hypercholesterolemia increases endothelial superoxide anion production," *J.Clin.Invest* 91 (6): 2546-2551 (1993).

218. Ohnishi, T., "Iron-sulfur clusters/semiquinones in complex I," *Biochim.Biophys.Acta* 1364 (2): 186-206 (1998).

219. Okazaki, K. and N. Sagata, "The Mos/MAP kinase pathway stabilizes c-Fos by phosphorylation and augments its transforming activity in NIH 3T3 cells," *EMBO J.* 14 (20): 5048-5059 (1995).

220. Olivera, A. and S. Spiegel, "Sphingosine-1-phosphate as second messenger in cell proliferation induced by PDGF and FCS mitogens," *Nature* 365 (6446): 557-560 (1993).

221. Oquendo, P. et al., "CD36 directly mediates cytoadherence of Plasmodium falciparum parasitized erythrocytes," *Cell* 58 (1): 95-101 (1989).

222. Ozaki, M. et al., "Overexpression of endothelial nitric oxide synthase accelerates atherosclerotic lesion formation in apoE-deficient mice," *J.Clin.Invest* 110 (3): 331-340 (2002).

223. Palmer, R. M., D. S. Ashton, and S. Moncada, "Vascular endothelial cells synthesize nitric oxide from L-arginine," *Nature* 333 (6174): 664-666 (1988).

224. Palmer, R. M., A. G. Ferrige, and S. Moncada, "Nitric oxide release accounts for the biological activity of endothelium-derived relaxing factor," *Nature*

327 (6122): 524-526 (1987).

225. Panasiewicz, M. et al., "Structure of the ceramide moiety of GM1 ganglioside determines its occurrence in different detergent-resistant membrane domains in HL-60 cells," *Biochemistry* 42 (21): 6608-6619 (2003).

226. Park, I. N., I. J. Cho, and S. G. Kim, "Ceramide, an apoptotic rheostat, inhibits CCAAT/enhancer binding protein-beta and NF-E2-related factor-2 activation: the role in glutathione S-transferase A2 gene repression," *Drug Metab Dispos.* 32 (9): 893-897 (2004).

227. Parthasarathy, S., "Oxidation of low-density lipoprotein by thiol compounds leads to its recognition by the acetyl LDL receptor," *Biochim.Biophys.Acta* 917 (2): 337-340 (1987).

228. Parthasarathy, S. et al., "Recognition of solubilized apoproteins from delipidated, oxidized low density lipoprotein (LDL) by the acetyl-LDL receptor," *Proc.Natl.Acad.Sci.U.S.A* 84 (2): 537-540 (1987).

229. Parton, R. G. and A. A. Richards, "Lipid rafts and caveolae as portals for endocytosis: new insights and common mechanisms," *Traffic.* 4 (11): 724-738 (2003).

230. Pearce, S. F. et al., "Recombinant glutathione S-transferase/CD36 fusion proteins define an oxidized low density lipoprotein-binding domain," *J.Biol.Chem.* 273 (52): 34875-34881 (1998).

231. Pearce, S. F., J. Wu, and R. L. Silverstein, "A carboxyl terminal truncation mutant of CD36 is secreted and binds thrombospondin: evidence for a

single transmembrane domain," *Blood* 84 (2): 384-389 (1994).

232. Pearson, A. M., A. Rich, and M. Krieger, "Polynucleotide binding to macrophage scavenger receptors depends on the formation of base-quartet-stabilized four-stranded helices," *J.Biol.Chem.* 268 (5): 3546-3554 (1993).

233. Perry, D. K., "The role of de novo ceramide synthesis in chemotherapy-induced apoptosis," *Ann.N.Y.Acad.Sci.* 905: 91-96 (2000).

234. Phillips, D. C., K. Allen, and H. R. Griffiths, "Synthetic ceramides induce growth arrest or apoptosis by altering cellular redox status," *Arch.Biochem.Biophys.* 407 (1): 15-24 (2002).

235. Phillips, D. C. and H. R. Griffiths, "Ceramide induces a loss in cytosolic peroxide levels in mononuclear cells," *Biochem.J.* 375 (Pt 3): 567-579 (2003).

236. Pietzsch, A. et al., "Identification and characterization of a novel monocyte/macrophage differentiation-dependent gene that is responsive to lipopolysaccharide, ceramide, and lysophosphatidylcholine," *Biochem.Biophys.Res.Commun.* 235 (1): 4-9 (1997).

237. Pike, L. J., "Lipid rafts: bringing order to chaos," *J.Lipid Res.* 44 (4): 655-667 (2003).

238. Pike, L. J., "Lipid rafts: heterogeneity on the high seas," *Biochem.J.* 378 (Pt 2): 281-292 (2004).

239. Pike, L. J. et al., "Lipid rafts are enriched in arachidonic acid and plasmenylethanolamine and their composition is independent of caveolin-1 expression: a quantitative electrospray ionization/mass spectrometric analysis,"

Biochemistry 41 (6): 2075-2088 (2002).

240. Pitkanen, S. et al., "Familial cardiomyopathy with cataracts and lactic acidosis: a defect in complex I (NADH-dehydrogenase) of the mitochondria respiratory chain," *Pediatr.Res.* 39 (3): 513-521 (1996).

241. Pitkanen, S. and B. H. Robinson, "Mitochondrial complex I deficiency leads to increased production of superoxide radicals and induction of superoxide dismutase," *J.Clin.Invest* 98 (2): 345-351 (1996).

242. Podrez, E. A. et al., "Identification of a novel family of oxidized phospholipids that serve as ligands for the macrophage scavenger receptor CD36," *J.Biol.Chem.* 277 (41): 38503-38516 (2002).

243. Poli, G. et al., "Oxidative stress and cell signalling," *Curr.Med.Chem.* 11 (9): 1163-1182 (2004).

244. Possel, H. et al., "2,7-Dihydrodichlorofluorescein diacetate as a fluorescent marker for peroxynitrite formation," *FEBS Lett.* 416 (2): 175-178 (1997).

245. Prinetti, A. et al., "Sphingolipid-enriched membrane domains from rat cerebellar granule cells differentiated in culture. A compositional study," *J.Biol.Chem.* 275 (16): 11658-11665 (2000).

246. Puente, Navazo et al., "Identification on human CD36 of a domain (155-183) implicated in binding oxidized low-density lipoproteins (Ox-LDL)," *Arterioscler.Thromb.Vasc.Biol.* 16 (8): 1033-1039 (1996).

247. Rahman, I. and W. MacNee, "Role of transcription factors in inflammatory lung diseases," *Thorax* 53 (7): 601-612 (1998).

248. Rahman, I. and W. MacNee, "Regulation of redox glutathione levels and gene transcription in lung inflammation: therapeutic approaches," *Free Radic.Biol.Med.* 28 (9): 1405-1420 (2000).

249. Rahman, I., J. Marwick, and P. Kirkham, "Redox modulation of chromatin remodeling: impact on histone acetylation and deacetylation, NF-kappaB and pro-inflammatory gene expression," *Biochem.Pharmacol.* 68 (6): 1255-1267 (2004).

250. Raman, C. S. et al., "Crystal structure of constitutive endothelial nitric oxide synthase: a paradigm for pterin function involving a novel metal center," *Cell* 95 (7): 939-950 (1998).

251. Rao, K. M. et al., "Flow cytometric analysis of nitric oxide production in human neutrophils using dichlorofluorescein diacetate in the presence of a calmodulin inhibitor," *J.Leukoc.Biol.* 51 (5): 496-500 (1992).

252. Requena, J. R. et al., "Quantification of malondialdehyde and 4-hydroxynonenal adducts to lysine residues in native and oxidized human low-density lipoprotein," *Biochem.J.* 322 (Pt 1): 317-325 (1997).

253. Requena, J. R. et al., "Lipoxidation products as biomarkers of oxidative damage to proteins during lipid peroxidation reactions," *Nephrol.Dial.Transplant.* 11 Suppl 5: 48-53 (1996).

254. Rhee, S. G. et al., "A family of novel peroxidases, peroxiredoxins," *Biofactors* 10 (2-3): 207-209 (1999).

255. Ricciarelli, R., J. M. Zingg, and A. Azzi, "Vitamin E reduces the uptake

of oxidized LDL by inhibiting CD36 scavenger receptor expression in cultured aortic smooth muscle cells," *Circulation* 102 (1): 82-87 (2000).

256. Ricote, M. et al., "The peroxisome proliferator-activated receptor-gamma is a negative regulator of macrophage activation," *Nature* 391 (6662): 79-82 (1998).

257. Rigotti, A., S. L. Acton, and M. Krieger, "The class B scavenger receptors SR-BI and CD36 are receptors for anionic phospholipids," *J.Biol.Chem.* 270 (27): 16221-16224 (1995).

258. Roper, K., D. Corbeil, and W. B. Huttner, "Retention of prominin in microvilli reveals distinct cholesterol-based lipid micro-domains in the apical plasma membrane," *Nat.Cell Biol.* 2 (9): 582-592 (2000).

259. Ross, R., "The pathogenesis of atherosclerosis--an update," *N.Engl.J.Med.* 314 (8): 488-500 (1986).

260. Ross, R., "The pathogenesis of atherosclerosis: a perspective for the 1990s," *Nature* 362 (6423): 801-809 (1993).

261. Ross, R., "Atherosclerosis--an inflammatory disease," *N.Engl.J.Med.* 340 (2): 115-126 (1999).

262. Rouquette, M. et al., "Xanthine oxidoreductase is asymmetrically localised on the outer surface of human endothelial and epithelial cells in culture," *FEBS Lett.* 426 (3): 397-401 (1998).

263. Rubbo, H. and V. O'Donnell, "Nitric oxide, peroxynitrite and lipoxygenase in atherogenesis: mechanistic insights," *Toxicology* 208 (2): 305-317

(2005).

264. Rueckschloss, U. et al., "Induction of NAD(P)H oxidase by oxidized low-density lipoprotein in human endothelial cells: antioxidative potential of hydroxymethylglutaryl coenzyme A reductase inhibitor therapy," *Circulation* 104 (15): 1767-1772 (2001).

265. Sampson, M. J. et al., "Increased expression of a scavenger receptor (CD36) in monocytes from subjects with Type 2 diabetes," *Atherosclerosis* 167 (1): 129-134 (2003).

266. Satriano, J. A. et al., "Oxygen radicals as second messengers for expression of the monocyte chemoattractant protein, JE/MCP-1, and the monocyte colony-stimulating factor, CSF-1, in response to tumor necrosis factor-alpha and immunoglobulin G. Evidence for involvement of reduced nicotinamide adenine dinucleotide phosphate (NADPH)-dependent oxidase," *J.Clin.Invest* 92 (3): 1564-1571 (1993).

267. Scheidegger, K. J., S. Butler, and J. L. Witztum, "Angiotensin II increases macrophage-mediated modification of low density lipoprotein via a lipoxygenase-dependent pathway," *J.Biol.Chem.* 272 (34): 21609-21615 (1997).

268. Schenk, H. et al., "Distinct effects of thioredoxin and antioxidants on the activation of transcription factors NF-kappa B and AP-1," *Proc.Natl.Acad.Sci.U.S.A* 91 (5): 1672-1676 (1994).

269. Schissel, S. L. et al., "Rabbit aorta and human atherosclerotic lesions hydrolyze the sphingomyelin of retained low-density lipoprotein. Proposed role for

arterial-wall sphingomyelinase in subendothelial retention and aggregation of atherogenic lipoproteins," *J.Clin.Invest* 98 (6): 1455-1464 (1996).

270. Schuck, S. et al., "Resistance of cell membranes to different detergents," *Proc.Natl.Acad.Sci.U.S.A* 100 (10): 5795-5800 (2003).

271. Scott, J. A. et al., "Quantitation of intracellular oxidation in a renal epithelial cell line," *Free Radic.Biol.Med.* 4 (2): 79-83 (1988).

272. Sendobry, S. M. et al., "Attenuation of diet-induced atherosclerosis in rabbits with a highly selective 15-lipoxygenase inhibitor lacking significant antioxidant properties," *Br.J.Pharmacol.* 120 (7): 1199-1206 (1997).

273. Shao, D., A. W. Segal, and L. V. Dekker, "Lipid rafts determine efficiency of NADPH oxidase activation in neutrophils," *FEBS Lett.* 550 (1-3): 101-106 (2003).

274. Shen, J. et al., "Macrophage-mediated 15-lipoxygenase expression protects against atherosclerosis development," *J.Clin.Invest* 98 (10): 2201-2208 (1996).

275. Shogomori, H. and D. A. Brown, "Use of detergents to study membrane rafts: the good, the bad, and the ugly," *Biol.Chem.* 384 (9): 1259-1263 (2003).

276. Shringarpure, R., T. Grune, and K. J. Davies, "Protein oxidation and 20S proteasome-dependent proteolysis in mammalian cells," *Cell Mol.Life Sci.* 58 (10): 1442-1450 (2001).

277. Sica, A. et al., "IL-1 transcriptionally activates the neutrophil chemotactic factor/IL-8 gene in endothelial cells," *Immunology* 69 (4): 548-553

(1990a).

278. Sica, A. et al., "Monocyte chemotactic and activating factor gene expression induced in endothelial cells by IL-1 and tumor necrosis factor," *J.Immunol.* 144 (8): 3034-3038 (1990b).

279. Sigari, F. et al., "Fibroblasts that overexpress 15-lipoxygenase generate bioactive and minimally modified LDL," *Arterioscler.Thromb.Vasc.Biol.* 17 (12): 3639-3645 (1997).

280. Simons, K. and J. Gruenberg, "Jamming the endosomal system: lipid rafts and lysosomal storage diseases," *Trends Cell Biol.* 10 (11): 459-462 (2000).

281. Slimane, T. A. et al., "Raft-mediated trafficking of apical resident proteins occurs in both direct and transcytotic pathways in polarized hepatic cells: role of distinct lipid microdomains," *Mol.Biol.Cell* 14 (2): 611-624 (2003).

282. Smart, E. J. et al., "A detergent-free method for purifying caveolae membrane from tissue culture cells," *Proc.Natl.Acad.Sci.U.S.A* 92 (22): 10104-10108 (1995).

283. Sorescu, D. et al., "Superoxide production and expression of nox family proteins in human atherosclerosis," *Circulation* 105 (12): 1429-1435 (2002).

284. Sot, J. et al., "Different effects of long- and short-chain ceramides on the gel-fluid and lamellar-hexagonal transitions of phospholipids: a calorimetric, NMR, and x-ray diffraction study," *Biophys.J.* 88 (5): 3368-3380 (2005).

285. Sot, J., F. M. Goni, and A. Alonso, "Molecular associations and surface-active properties of short- and long-N-acyl chain ceramides,"

Biochim.Biophys.Acta 1711 (1): 12-19 (2005).

286. Sparrow, C. P., S. Parthasarathy, and D. Steinberg, "Enzymatic modification of low density lipoprotein by purified lipoxygenase plus phospholipase A2 mimics cell-mediated oxidative modification," *J.Lipid Res.* 29 (6): 745-753 (1988).

287. Sprott, K. M. et al., "Decreased activity and enhanced nuclear export of CCAAT-enhancer-binding protein beta during inhibition of adipogenesis by ceramide," *Biochem.J.* 365 (Pt 1): 181-191 (2002).

288. Stamler, J. S. and A. Hausladen, "Oxidative modifications in nitrosative stress," *Nat.Struct.Biol.* 5 (4): 247-249 (1998).

289. Stan, R. V. et al., "Immunoisolation and partial characterization of endothelial plasmalemmal vesicles (caveolae)," *Mol.Biol.Cell* 8 (4): 595-605 (1997).

290. Steinberg, D., "Lipoproteins and the pathogenesis of atherosclerosis," *Circulation* 76 (3): 508-514 (1987).

291. Steinberg, D. et al., "Beyond cholesterol. Modifications of low-density lipoprotein that increase its atherogenicity," *N.Engl.J.Med.* 320 (14): 915-924 (1989).

292. Strieter, R. M. et al., "Endothelial cell gene expression of a neutrophil chemotactic factor by TNF-alpha, LPS, and IL-1 beta," *Science* 243 (4897): 1467-1469 (1989).

293. Suh, Y. A. et al., "Cell transformation by the superoxide-generating oxidase Mox1," *Nature* 401 (6748): 79-82 (1999).

294. Sundaresan, M. et al., "Requirement for generation of H2O2 for

platelet-derived growth factor signal transduction," *Science* 270 (5234): 296-299 (1995).

295. Suzuki, H. et al., "The multiple roles of macrophage scavenger receptors (MSR) in vivo: resistance to atherosclerosis and susceptibility to infection in MSR knockout mice," *J.Atheroscler.Thromb.* 4 (1): 1-11 (1997).

296. Suzuki, H. et al., "In vivo evidence for microvascular oxidative stress in spontaneously hypertensive rats. Hydroethidine microfluorography," *Hypertension* 25 (5): 1083-1089 (1995).

297. Takeshige, K. and S. Minakami, *Biochem.J.* 180 (1): 129-135 (1979).

298. Takeuchi, O. et al., "Differential roles of TLR2 and TLR4 in recognition of gram-negative and gram-positive bacterial cell wall components," *Immunity.* 11 (4): 443-451 (1999).

299. Takeuchi, O. et al., "Discrimination of bacterial lipoproteins by Toll-like receptor 6," *Int.Immunol.* 13 (7): 933-940 (2001).

300. Takeuchi, T., M. Nakajima, and K. Morimoto, "Relationship between the intracellular reactive oxygen species and the induction of oxidative DNA damage in human neutrophil-like cells," *Carcinogenesis* 17 (8): 1543-1548 (1996).

301. Tao, N., S. J. Wagner, and D. M. Lublin, "CD36 is palmitoylated on both N- and C-terminal cytoplasmic tails," *J.Biol.Chem.* 271 (37): 22315-22320 (1996).

302. Thiele, A. et al., "Regulation of adenosine receptor subtypes during cultivation of human monocytes: role of receptors in preventing

lipopolysaccharide-triggered respiratory burst," *Infect.Immun.* 72 (3): 1349-1357 (2004).

303. Thorn, H. et al., "Cell surface orifices of caveolae and localization of caveolin to the necks of caveolae in adipocytes," *Mol.Biol.Cell* 14 (10): 3967-3976 (2003).

304. Tontonoz, P., E. Hu, and B. M. Spiegelman, "Regulation of adipocyte gene expression and differentiation by peroxisome proliferator activated receptor gamma," *Curr.Opin.Genet.Dev.* 5 (5): 571-576 (1995).

305. Tontonoz, P. et al., "PPARgamma promotes monocyte/macrophage differentiation and uptake of oxidized LDL," *Cell* 93 (2): 241-252 (1998).

306. Touyz, R. M., F. Tabet, and E. L. Schiffrin, "Redox-dependent signalling by angiotensin II and vascular remodelling in hypertension," *Clin.Exp.Pharmacol.Physiol* 30 (11): 860-866 (2003).

307. Trumpower, B. L., "The protonmotive Q cycle. Energy transduction by coupling of proton translocation to electron transfer by the cytochrome bc1 complex," *J.Biol.Chem.* 265 (20): 11409-11412 (1990).

308. Tsutsui, M., "Neuronal nitric oxide synthase as a novel anti-atherogenic factor," *J.Atheroscler.Thromb.* 11 (2): 41-48 (2004).

309. Ushio-Fukai, M. et al., "p38 Mitogen-activated protein kinase is a critical component of the redox-sensitive signaling pathways activated by angiotensin II. Role in vascular smooth muscle cell hypertrophy," *J.Biol.Chem.* 273 (24): 15022-15029 (1998).

310. Valente, A. J. et al., "Purification of a monocyte chemotactic factor secreted by nonhuman primate vascular cells in culture," *Biochemistry* 27 (11): 4162-4168 (1988).

311. Vallve, J. C. et al., "Unsaturated fatty acids and their oxidation products stimulate CD36 gene expression in human macrophages," *Atherosclerosis* 164 (1): 45-56 (2002).

312. van Rheenen, J. and K. Jalink, "Agonist-induced PIP(2) hydrolysis inhibits cortical actin dynamics: regulation at a global but not at a micrometer scale," *Mol.Biol.Cell* 13 (9): 3257-3267 (2002).

313. Vasquez-Vivar, J. et al., "Superoxide generation by endothelial nitric oxide synthase: the influence of cofactors," *Proc.Natl.Acad.Sci.U.S.A* 95 (16): 9220-9225 (1998).

314. Venkataraman, K. and A. H. Futerman, "Ceramide as a second messenger: sticky solutions to sticky problems," *Trends Cell Biol.* 10 (10): 408-412 (2000).

315. Vilhardt, F. and B. van Deurs, "The phagocyte NADPH oxidase depends on cholesterol-enriched membrane microdomains for assembly," *EMBO J.* 23 (4): 739-748 (2004).

316. von Haller, P. D. et al., "Mass spectrometric characterization of proteins extracted from Jurkat T cell detergent-resistant membrane domains," *Proteomics.* 1 (8): 1010-1021 (2001).

317. Vowells, S. J. et al., "Flow cytometric analysis of the granulocyte

respiratory burst: a comparison study of fluorescent probes," *J.Immunol.Methods* 178 (1): 89-97 (1995).

318. Walev, I. et al., "Streptolysin O-permeabilized granulocytes shed L-selectin concomitantly with ceramide generation via neutral sphingomyelinase," *J.Leukoc.Biol.* 68 (6): 865-872 (2000).

319. Wang, H. and J. A. Joseph, "Quantifying cellular oxidative stress by dichlorofluorescein assay using microplate reader," *Free Radic.Biol.Med.* 27 (5-6): 612-616 (1999).

320. Wang, J. M. et al., "Expression of monocyte chemotactic protein and interleukin-8 by cytokine-activated human vascular smooth muscle cells," *Arterioscler.Thromb.* 11 (5): 1166-1174 (1991).

321. Wang, N. et al., "Interleukin 8 is induced by cholesterol loading of macrophages and expressed by macrophage foam cells in human atheroma," *J.Biol.Chem.* 271 (15): 8837-8842 (1996).

322. Weber, C. et al., "Antioxidants inhibit monocyte adhesion by suppressing nuclear factor-kappa B mobilization and induction of vascular cell adhesion molecule-1 in endothelial cells stimulated to generate radicals," *Arterioscler.Thromb.* 14 (10): 1665-1673 (1994).

323. Wever, R. M. et al., "Tetrahydrobiopterin regulates superoxide and nitric oxide generation by recombinant endothelial nitric oxide synthase," *Biochem.Biophys.Res.Commun.* 237 (2): 340-344 (1997).

324. White, C. R. et al., "Circulating plasma xanthine oxidase contributes to

vascular dysfunction in hypercholesterolemic rabbits," *Proc.Natl.Acad.Sci.U.S.A* 93 (16): 8745-8749 (1996).

325. Wikman, A. et al., "Monocyte activation and relationship to anti-proteinase 3 in acute vasculitis," *Nephrol.Dial.Transplant.* 18 (9): 1792-1799 (2003).

326. Wink, D. A. and J. B. Mitchell, "Chemical biology of nitric oxide: Insights into regulatory, cytotoxic, and cytoprotective mechanisms of nitric oxide," *Free Radic.Biol.Med.* 25 (4-5): 434-456 (1998).

327. Wissel, H. et al., "Chlamydophila pneumoniae induces expression of toll-like receptor 4 and release of TNF-alpha and MIP-2 via an NF-kappaB pathway in rat type II pneumocytes," *Respir.Res.* 6 (1): 51 (2005).

328. Wolin, M. S., M. Ahmad, and S. A. Gupte, "Oxidant and redox signaling in vascular oxygen sensing mechanisms: basic concepts, current controversies, and potential importance of cytosolic NADPH," *Am.J.Physiol Lung Cell Mol.Physiol* 289 (2): L159-L173 (2005).

329. Wung, B. S. et al., "Cyclic strain-induced monocyte chemotactic protein-1 gene expression in endothelial cells involves reactive oxygen species activation of activator protein 1," *Circ.Res.* 81 (1): 1-7 (1997).

330. Xanthoudakis, S. and T. Curran, "Identification and characterization of Ref-1, a nuclear protein that facilitates AP-1 DNA-binding activity," *EMBO J.* 11 (2): 653-665 (1992).

331. Xu, W. et al., "LDL receptor-related protein plays an essential role in

12/15-lipoxygenase-mediated LDL oxidation by macrophages," *Adv.Exp.Med.Biol.* 525: 181-184 (2003).

332. Xu, X. et al., "Effect of the structure of natural sterols and sphingolipids on the formation of ordered sphingolipid/sterol domains (rafts). Comparison of cholesterol to plant, fungal, and disease-associated sterols and comparison of sphingomyelin, cerebrosides, and ceramide," *J.Biol.Chem.* 276 (36): 33540-33546 (2001).

333. Xu, X. X. and I. Tabas, "Sphingomyelinase enhances low density lipoprotein uptake and ability to induce cholesteryl ester accumulation in macrophages," *J.Biol.Chem.* 266 (36): 24849-24858 (1991).

334. Yang, C. F. et al., "Cadmium-induced oxidative cellular damage in human fetal lung fibroblasts (MRC-5 cells)," *Environ.Health Perspect.* 105 (7): 712-716 (1997).

335. Ye, G. et al., "Catalase protects cardiomyocyte function in models of type 1 and type 2 diabetes," *Diabetes* 53 (5): 1336-1343 (2004).

336. Yesner, L. M. et al., "Regulation of monocyte CD36 and thrombospondin-1 expression by soluble mediators," *Arterioscler.Thromb.Vasc.Biol.* 16 (8): 1019-1025 (1996).

337. Yla-Herttuala, S. et al., "Colocalization of 15-lipoxygenase mRNA and protein with epitopes of oxidized low density lipoprotein in macrophage-rich areas of atherosclerotic lesions," *Proc.Natl.Acad.Sci.U.S.A* 87 (18): 6959-6963 (1990).

338. Yla-Herttuala, S. et al., "Gene expression in macrophage-rich human

atherosclerotic lesions. 15-lipoxygenase and acetyl low density lipoprotein receptor messenger RNA colocalize with oxidation specific lipid-protein adducts," *J.Clin.Invest* 87 (4): 1146-1152 (1991).

339. Yokoyama, M., "Oxidant stress and atherosclerosis," *Curr.Opin.Pharmacol.* 4 (2): 110-115 (2004).

340. Yoshida, H. et al., "Minimally oxidized low-density lipoprotein increases expression of scavenger receptor A, CD36, and macrosialin in resident mouse peritoneal macrophages," *Arterioscler.Thromb.Vasc.Biol.* 18 (5): 794-802 (1998).

341. Zafari, A. M. et al., "Role of NADH/NADPH oxidase-derived H2O2 in angiotensin II-induced vascular hypertrophy," *Hypertension* 32 (3): 488-495 (1998).

342. Zeng, Y. et al., "Endocytosis of oxidized low density lipoprotein through scavenger receptor CD36 utilizes a lipid raft pathway that does not require caveolin-1," *J.Biol.Chem.* 278 (46): 45931-45936 (2003).

343. Zha, X. et al., "Sphingomyelinase treatment induces ATP-independent endocytosis," *J.Cell Biol.* 140 (1): 39-47 (1998).

344. Zhang, R. et al., "Myeloperoxidase functions as a major enzymatic catalyst for initiation of lipid peroxidation at sites of inflammation," *J.Biol.Chem.* 277 (48): 46116-46122 (2002).

345. Zhu, H. et al., "Oxidation pathways for the intracellular probe 2',7'-dichlorofluorescein," *Arch.Toxicol.* 68 (9): 582-587 (1994).

346. Zhu, H. et al., "Low density lipoprotein receptor-related

protein-mediated membrane translocation of 12/15-lipoxygenase is required for oxidation of low density lipoprotein by macrophages," *J.Biol.Chem.* 278 (15): 13350-13355 (2003).

347. Zuber, C. et al., "DS28-6, a temperature-sensitive mutant of Chinese hamster ovary cells, expresses key phenotypic changes associated with brefeldin A treatment," *Proc.Natl.Acad.Sci.U.S.A* 88 (21): 9818-9822 (1991).

Appendices

Cytotoxicity results.

1 Monocyte

Cells were suspended to 10^6cells/ml in serum free RPMI for 4hours prior to the treatment with different doses of C_2 ceramide with an incubation of 16 hours at 37°C in a humidified 5% CO_2 /95% air incubator. Cells (10^6 cells per sample) were harvested and washed in PBS. The cell pellet was resuspended in 1ml PI (25μg) in PBS/0.1% BSA with an incubation of 15minutes in dark at room temperature. Cells were immediately analyzed by flow cytometry. An ungated dual parameter histogram of FS versus Log FL3 (PI, red fluorescence, 560-590nm) was used to distinguish the cells to viable and dead population as described in method 2.2.12.1. As Fig 2.3 shows, C_2 ceramide does not cause cell death in monocytes.

Ceramide viability assay on monocyte by PI stain flow cytometry

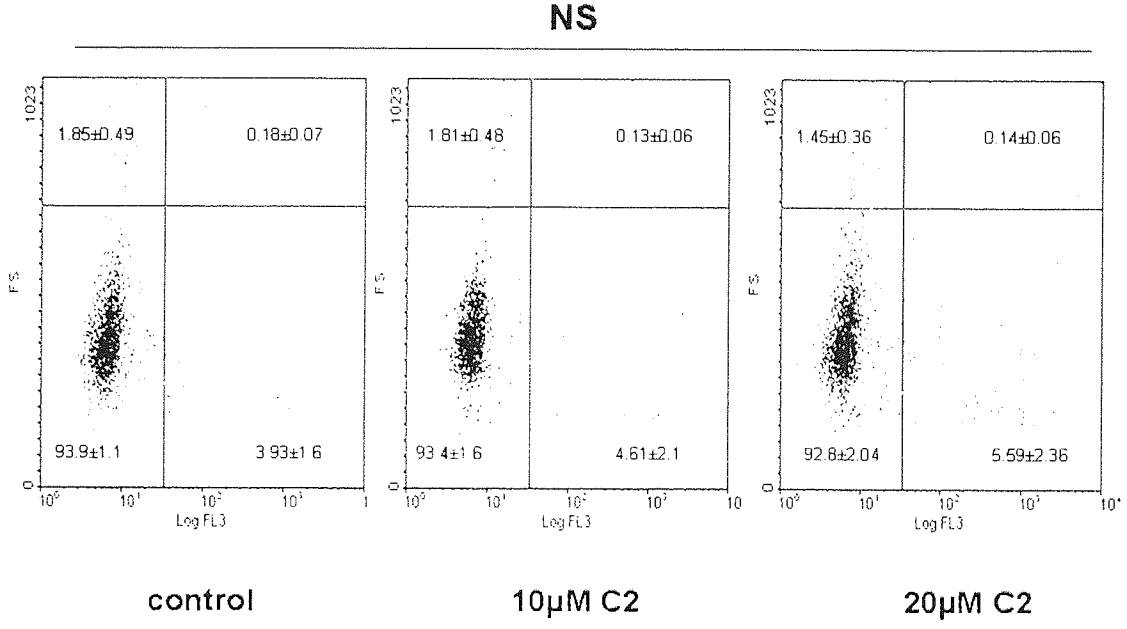

Fig 1 C_2 ceramide treatment does not affect cell viability in U937 monocyte.
Cells were suspended to 10^6cells/ml in serum free RPMI for 4hours prior to the treatment with different doses of C_2 ceramide with an incubation of 16 hours at 37°C in a humidified 5% CO_2 /95% air incubator. Cells (10^6 cells per sample) were harvested and washed in PBS. The cell pellet was resuspended in 1ml PI (25μg) in PBS/0.1% BSA with an incubation of 15minutes in dark at room temperature. Cells were immediately analyzed by flow cytometry. An ungated dual parameter histogram of FS versus Log FL3 (PI, red fluorescence, 560-590nm) was used to distinguish the cells to healthy and dead population as described in method 2.2.12.1. Flow cytometry histograms shown are representational of three individual experiments. Data are expressed as the percentage of cells in each quadrant as the Mean ± s.d of 3 individual experiments and test samples analyzed for statistical non- significance (NS) from control by one-way ANOVA followed by Dunnett's multiple comparison test.

2 Macrophage

Cells were resuspended in FBS % medium at 2 x 10^5/ml. 100nM PMA was added to cells with an incubation of 8 hrs prior to adding different dose of C_2 ceramide followed with 16 hrs incubation at 37°C in a humidified 5% CO_2 /95% air incubator. The MTT assay was used to test the cell viability as described in section 2.2.12.2.

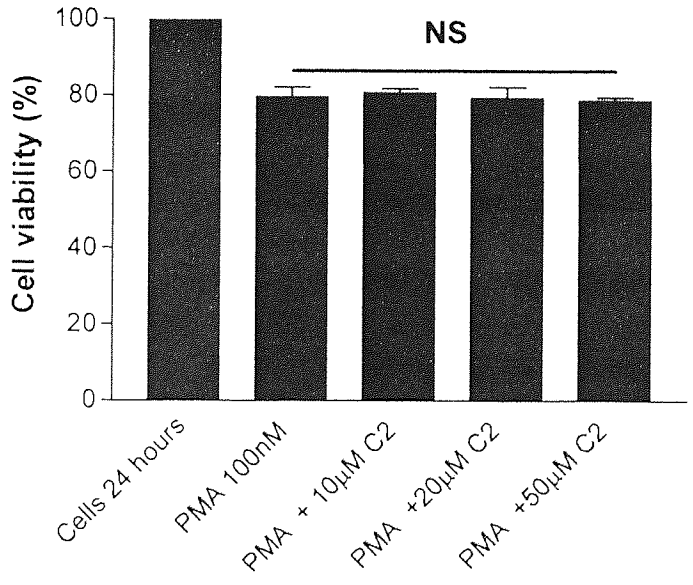

Fig 2 C_2 ceramide 16 hours treatment does not cause PMA differentiated cell death.

Cells were resuspended in FBS % medium at 2 x 10^5/ml. 100nM PMA was added to cells with an incubation of 8 hrs prior to adding different dose of C_2 ceramide followed with 16 hrs incubation at 37°C in a humidified 5% CO_2 /95% air incubator. MTT assay was used to test the cell viability as described in section 2.2.12.2. The histogram shown is representational of three individual experiments. The data are presented as the arithmetic mean ± SEM. All doses of C_2 ceramide data sets show non-significance (NS) compared to PMA 100nM by one-way ANOVA statistical analysis followed by Tukey's multiple comparison test.

From Fig 2.4, PMA differentiated cells show apparently lower viability which reflects less metabolism than control cells. This could be because PMA differentiation stops cells from growing. Therefore there were fewer cells after PMA differentiation. This hypothesis was confirmed by measuring total cell lysate protein concentration by the BCA assay. Briefly, cells were suspended in FBS 10% medium at $2.5x10^5$/ml and seeded 4ml per well in 6 well plate. Cells were treated with 100nM PMA for 8 hours prior to adding different dose of C_2 ceramide followed by 16 hours incubation at 37°C in a humidified 5% CO_2 /95% air incubator. Cells were harvested and washed in PBS. Cells were then lysed in 400 µl 5% Triton/PBS. The lysates were added back to the well with scraping with a cell scraper to lyse adherent cells. The protein concentration was measured by BCA assay (see section 2.2.9.4).

	Cell viability measured by MTT assay	Cell lysate protein concentration measured by BCA assay
Percentage of PMA differentiated cell / control cells ± STDEV	79.7 ± 4.37 %	78.9 ± 3.56 %

Table 1. PMA differentiation stops cells from growing.
Cells were resuspended in 10 %FBS medium at 2 x 10^5/ml. 100nM PMA was added to cells for differentiation over 24 hrs.

Cells were resuspended in 10% FBS medium at 2 x 10^5/ml. 100nM PMA and different doses of C_2 ceramide were added followed by 3days incubation at 37°C in a humidified 5% CO_2 /95% air incubator. MTT assay was used to test the cell viability as described in section 2.2.12.2.

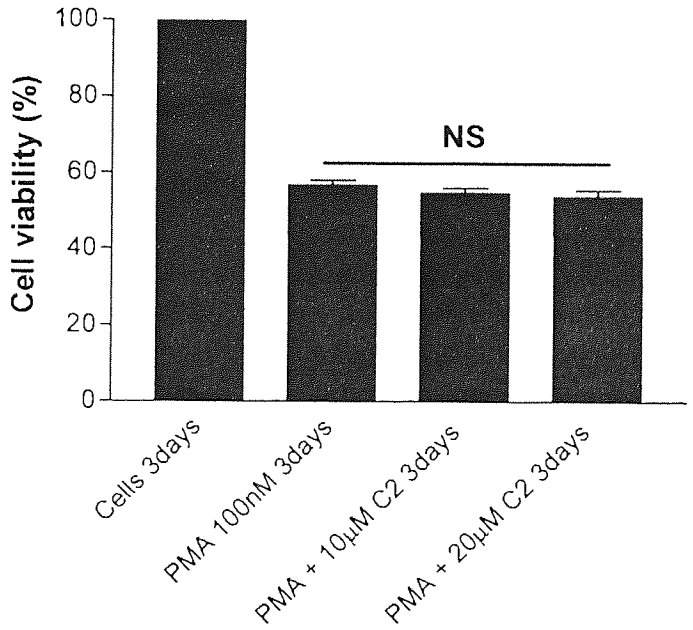

Fig 3 C_2 ceramide treatment does not cause PMA differentiated cell death over 3 days.

Cells were resuspended in 10% FBS medium at 2 x 10^5/ml. 100nM PMA and different dose of C_2 ceramide were added followed with 3days incubation at 37°C in a humidified 5% CO_2 /95% air incubator. The MTT assay was used to test the cell viability as described in section 2.2.12.2. The histogram shown is representational of three individual experiments. The data are presented as the arithmetic mean ± SEM. All dose of C_2 ceramide data sets show non-significance (NS) compared to PMA 100nM by one-way ANOVA statistical analysis followed by Tukey's multiple comparison test.